

**IMMUNOCHEMICAL DETECTION OF LYSERGIC ACID DIETHYLAMIDE  
USING A PHOTOCHEMICALLY LINKED IMMUNOGEN**

by

SARAH KERRIGAN

B.Sc. (Hons.), The University of Hull, England, 1992.

A THESIS SUBMITTED IN PARTIAL FULFILMENT OF  
THE REQUIREMENTS FOR THE DEGREE OF  
DOCTOR OF PHILOSOPHY

in

THE FACULTY OF GRADUATE STUDIES  
Department of Chemistry

We accept this thesis as conforming  
to the required standard

THE UNIVERSITY OF BRITISH COLUMBIA

December 1997

© Sarah Kerrigan, 1997

In presenting this thesis in partial fulfilment of the requirements for an advanced degree at the University of British Columbia, I agree that the Library shall make it freely available for reference and study. I further agree that permission for extensive copying of this thesis for scholarly purposes may be granted by the head of my department or by his or her representatives. It is understood that copying or publication of this thesis for financial gain shall not be allowed without my written permission.

Department of Chemistry

The University of British Columbia  
Vancouver, Canada

Date 6<sup>th</sup> December 1997

## Abstract.

A new immunogen was prepared in which lysergic acid diethylamide (LSD) was photochemically attached to keyhole limpet hemocyanin (KLH) using a heterobifunctional linker. Photoactivation of the aryl azide group in the linker produces a reactive nitrene, which facilitates the covalent attachment of LSD to the protein at a number of different sites on the drug. Multi-site attachment of the drug is advantageous, as this in principle facilitates epitope recognition, which therefore increases the antiserum sensitivity. Using this method, it was possible to attach an average of 35 LSD molecules to each KLH molecule, which is sufficient for immune recognition of the drug.

High affinity polyclonal antibodies to LSD were raised against the photochemically linked immunogen. The equilibrium association constant,  $K_a$ , was estimated to be  $1.3 \times 10^{10} \text{ M}^{-1}$  using a radiolabelled technique. Comparison of the new antiserum with commercial antibody preparations indicated it had the highest affinity, lowest dissociability and was the most sensitive antiserum by enzyme-linked immunosorbent assay (ELISA).

The new antiserum was used for drug detection and extraction purposes. A high affinity immunochromatographic support was prepared, which allowed sub-nanogram quantities of LSD to be selectively extracted from blood and urine with greater than 80% efficiency. An indirect ELISA was developed for the detection of LSD in human urine specimens. The limit of detection was 10 pg/mL when 50  $\mu\text{L}$  urine was used. Analytical recoveries of LSD were between 98 - 106 % and intra and inter-assay precision was good over a wide range of concentrations. Within-run and between-run CVs were 3.7% (n=4) and 6.3% (n=12) for a sample which contained 0.2 ng/mL LSD in urine. The upper and lower limits of quantification were between 7 ng/mL and 50 pg/mL, which is well within the region of forensic interest. The cross-reactivity of the new antiserum with the

major metabolite, nor-LSD, was 52%. Other derivatives of interest which cross-react with the antibody included lysergic acid methylpropylamide (34%) and 2-oxo-3-hydroxy-LSD (3.4%). The UBC ELISA, which offered improved sensitivity and precision compared to a number of commercial immunoassays, was used to detect LSD in non-urine matrices, including forensic case samples of post-mortem blood, urine, bile and vitreous fluid.

## Table of Contents.

<b>Abstract</b> .....	ii
<b>Table of contents</b> .....	iv
<b>List of Figures</b> .....	x
<b>List of Tables</b> .....	xiv
<b>List of abbreviations</b> .....	xvi
<b>Acknowledgements</b> .....	xviii

### Chapter 1. Introduction.

1.1. An overview of lysergic acid diethylamide.....	1
1.1.1. LSD past-present.....	1
1.1.2. Hallucinogens and the psychopharmacology of LSD.....	2
1.1.3. Toxicology of LSD.....	5
1.1.4. Chemistry of LSD.....	6
1.1.5. Structure-activity relationships.....	9
1.2. Antibodies: an overview.....	10
1.2.1. Immunogens, haptens and epitopes.....	10
1.2.2. The immune system.....	10
1.2.3. Immunoglobulin structure.....	12
1.2.4. Antibody-antigen binding.....	14
1.2.5. Antibody affinity.....	14
1.2.6. Experimental determination of antibody affinity.....	15
1.3. Immunochemical detection.....	17
1.3.1. Homogeneous vs. heterogeneous immunoassays.....	17
1.3.2. Assay design.....	19
1.3.3. ELISA methodology.....	20
1.3.4. Competitive vs. non-competitive immunoassays.....	23
1.3.5. Choice of immunoassay methodology for LSD and anti-LSD.....	25
1.3.5.1. Immunochemical detection of anti-LSD.....	25
1.3.5.2. Immunochemical detection of LSD.....	26
1.3.6. Immunochemical detection of drugs of abuse.....	28
1.3.6.1. Drugs of abuse testing in urine.....	28
1.3.6.2. Immunoassays for LSD.....	30
1.3.6.3. Existing immunoconjugates for LSD.....	31
1.4. Aims and objectives of the study.....	33
1.5. References.....	35

### Chapter 2. Synthesis of a New LSD Immunogen.

2.1. Introduction.....	39
2.1.1. Conjugate formation.....	39
2.1.2. Conjugate analysis.....	43
2.2. Materials and methods.....	47

2.2.1.	Preparation of KLH-SASD-LSD.....	48
2.2.1.1.	Availability of primary amines on KLH.....	48
2.2.1.2.	Derivatization of protein with SASD.....	48
2.2.1.3.	Photoactivation of SASD.....	49
2.2.1.4.	Synthesis of KLH-SASD-LSD.....	50
2.2.2.	Purification of immunogen.....	50
2.2.2.1.	Centrifugal filtration.....	51
2.2.2.2.	Size exclusion chromatography.....	51
2.2.2.3.	Dialysis.....	52
2.2.3.	Characterization of immunogen: Molar substitution ratio.....	53
2.2.3.1.	Radiolabeled LSD study.....	53
2.2.3.2.	Fluorescence and protein quantification.....	54
2.2.4.	Optimization of photocoupling conditions.....	55
2.2.5.	Control immunogen.....	56
2.2.5.1.	Preparation of KLH-LSD by the Mannich reaction.....	56
2.2.5.2.	Characterization of control immunogen.....	57
2.2.6.	Immunization and antibody production.....	57
2.3.	Results and discussion.....	59
2.3.1.	Conditions for the derivatization of KLH with SASD.....	59
2.3.2.	Conditions for the photoactivation of SASD.....	63
2.3.3.	Immunogen synthesis.....	64
2.3.3.1.	Theoretical considerations.....	65
2.3.4.	Purification of immunogen.....	72
2.3.5.	Characterization of immunogen.....	74
2.3.5.1.	Iodination of LSD.....	74
2.3.5.2.	Estimation of the MSR using KLH-SASD- <sup>125</sup> I-LSD.....	75
2.3.5.3.	Estimation of LSD incorporation by fluorescence.....	79
2.3.5.4.	Quantification of protein in KLH-SASD-LSD.....	80
2.3.6.	Optimization of the molar substitution ratio.....	83
2.3.6.1.	Ratio of LSD/KLH during photolysis.....	83
2.3.6.2.	Liquid and solid phase irradiation.....	85
2.3.6.3.	Preparation of KLH-SASD-LSD for immunization.....	85
2.3.6.4.	Reaction efficiencies.....	86
2.3.7.	Hapten density and immune response.....	89
2.3.8.	Control immunogen.....	90
2.4.	Conclusion.....	93
2.5.	References.....	95

### Chapter 3. Enzyme-Linked Immunosorbent Assay Development.

3.1.	Introduction.....	99
3.2.	Materials and methods.....	104
3.2.1.	Detection of LSD antibodies by ELISA.....	105
3.2.1.1.	Evaluation of blocking agents for microtitre plates.....	105
3.2.2.	Coating antigen preparation.....	106

3.2.2.1.	Covalent attachment of LSD to Nunc CovaLink.....	106
3.2.2.2.	Derivatization of BSA with LSD using a photoreactive linker.....	107
3.2.2.3.	Derivatization of PVA with LSD.....	107
3.2.2.4.	Derivatization of BSA with LSD by the Mannich reaction.....	108
3.2.3.	Immune response over time.....	109
3.2.3.1.	Measurement of antibody titres.....	109
3.2.3.2.	Thiocyanate elution and ELISA detection.....	109
3.2.4.	Detection of LSD by indirect ELISA.....	109
3.3.	Results in discussion.....	111
3.3.1.	Evaluation of blocking agents and detergents.....	112
3.3.2.	Performance of coating antigens in ELISA.....	112
3.3.2.1.	Nunc CovaLink LSD.....	112
3.3.2.2.	BSA-PFPA-LSD.....	120
3.3.2.3.	PVA-LSD.....	122
3.3.2.4.	BSA-LSD.....	125
3.3.3.	Immune response.....	129
3.3.3.1.	Antibody titres.....	129
3.3.3.2.	Functional antibody affinity.....	130
3.3.4.	Detection of LSD by ELISA.....	131
3.3.4.1.	Inhibition assay using free LSD.....	131
3.3.4.2.	Inhibition assay using BSA-LSD.....	133
3.4.	Conclusion.....	134
3.5.	References.....	136

## Chapter 4. Quantitative Enzyme-Linked Immunosorbent Assay for LSD in Urine.

4.1.	Introduction.....	138
4.2.	Materials and Methods.....	145
4.2.1.	Optimization of assay conditions.....	146
4.2.1.1.	Effect of human urine on ELISA.....	146
4.2.1.2.	Pre-incubation of sample with antibody.....	147
4.2.1.3.	Antibody concentration.....	148
4.2.1.4.	Antibody incubation conditions.....	148
4.2.1.5.	Coating antigen concentration.....	149
4.2.1.6.	Incubation with enzyme conjugate antibody.....	149
4.2.1.7.	Effect of TMB reaction time.....	149
4.2.2.	Evaluation of assay performance.....	150
4.2.2.1.	Limit of detection.....	150
4.2.2.2.	Limit of quantification.....	150
4.2.2.3.	Accuracy: Spike and recovery.....	151
4.2.2.4.	Inter and intra assay precision.....	151
4.2.3.	Amplification of ELISA signal with peroxidase anti peroxidase.....	151

4.2.3.1.	Optimization and assay performance.....	151
4.3.	Results and discussion.....	153
4.3.1.	Assay optimization.....	153
4.3.1.1.	Effect of urine on ELISA.....	153
4.3.1.2.	Pre-incubation of urine specimens.....	157
4.3.1.3.	Serum dilution.....	157
4.3.1.4.	Antibody incubation conditions.....	159
4.3.1.5.	Coating antigen concentration.....	161
4.3.1.6.	Conjugate antibody incubation.....	162
4.3.1.7.	TMB reaction time.....	163
4.3.1.8.	Summary of optimized ELISA conditions.....	164
4.3.2.	Performance parameters.....	164
4.3.2.1.	Limit of detection.....	166
4.3.2.2.	Limit of quantification.....	166
4.3.2.3.	Accuracy.....	167
4.3.2.4.	Precision.....	168
4.3.3.	Amplified LSD ELISA.....	171
4.3.3.1.	Optimization.....	171
4.3.3.2.	Assay performance.....	173
4.3.4.	Summary of assay performance.....	175
4.4.	Conclusion.....	179
4.5.	References.....	181

## Chapter 5. Characterization of Antibody: Specificity, Sensitivity and Affinity.

5.1.	Introduction.....	183
5.2.	Materials and methods.....	188
5.2.1.	Cross-reactivity Study.....	188
5.2.1.1.	Effect of organic solvent on antibody binding.....	189
5.2.1.2.	Antibody specificity by ELISA.....	191
5.2.2.	Calculation of affinity constant.....	192
5.2.2.1.	Hapten inhibition ELISA.....	192
5.2.2.2.	Radiolabelled Study.....	193
5.2.3.	Chaotropic elution with ELISA detection.....	194
5.2.3.1.	Thiocyanate elution at fixed antibody concentration.....	194
5.2.3.2.	Thiocyanate elution over a range of antibody concentrations.....	195
5.3.	Results and discussion.....	196
5.3.1.	Antibody specificity.....	196
5.3.1.1.	Photolinked antibody: structural insights.....	204
5.3.1.2.	Other antibodies: general observations.....	208
5.3.1.3.	Clinical specificity.....	211
5.3.2.	Affinity constant measurements.....	213
5.3.2.1.	ELISA method.....	213
5.3.2.2.	Radiolabelled study.....	222

5.3.3.	Antibody dissociability.....	226
5.3.3.1.	Antibody affinity profiles and distributions.....	227
5.3.3.2.	Antibody titration curves.....	229
5.3.4.	Affinity maturation of antibodies.....	232
5.3.5.	Affinity, dissociability and sensitivity.....	234
5.4.	Conclusion.....	238
5.5.	References.....	241

## **Chapter 6. Analysis of Forensic Case Samples and Immunoaffinity Extraction of LSD from Blood and Urine.**

6.1.	Introduction.....	244
6.2.	Materials and methods.....	248
6.2.1.	Detection of LSD in whole blood.....	248
6.2.1.1.	Effect of blood on ELISA signal.....	248
6.2.1.2.	Effect of whole blood on sensitivity and precision.....	249
6.2.1.3.	Calibration of LSD in blood.....	249
6.2.2.	Analysis of forensic case samples.....	249
6.2.2.1.	Sample preparation and storage.....	249
6.2.2.2.	Analysis of post-mortem urine.....	250
6.2.2.3.	Analysis of blood, bile, liver and vitreous fluid.....	250
6.2.3.	Immunoaffinity extraction of LSD from biological matrices.....	251
6.2.3.1.	Preparation of the affinity matrix.....	251
6.2.3.2.	Characterization of the affinity matrix.....	252
6.2.3.3.	Immunoaffinity extraction of LSD.....	252
6.3.	Results and discussion.....	254
6.3.1.	Detection of LSD in whole blood.....	254
6.3.1.1.	Effect of blood on ELISA signal.....	254
6.3.1.2.	Sample volume.....	255
6.3.1.3.	Calibration of LSD in whole blood.....	257
6.3.2.	Forensic case samples.....	261
6.3.2.1.	Quantification of LSD in post-mortem urine.....	261
6.3.2.2.	Quantification of LSD in blood, bile, liver and vitreous fluid.....	261
6.3.3.	Immunoaffinity extraction of LSD.....	266
6.3.3.1.	Characterization of the affinity matrix.....	266
6.3.3.2.	Immunoaffinity extraction of LSD from blood and urine.....	268
6.4.	Conclusion.....	275
6.5.	References.....	277

## **Chapter 7. Concluding Remarks and Further Study.**

7.1.	Summary of findings.....	279
7.2.	Future work and applications.....	282

7.3. References.....	286
<b>Appendix I.</b> Reagent mixtures.....	288
<b>Appendix II.</b> Optimized competitive binding ELISA for LSD.....	289
<b>Appendix III.</b> Structures of compounds used in the cross-reactivity study.....	290

## List of Figures.

	<i>Title</i>	<i>Page</i>
<b>Figure 1.1</b>	Structural similarities between hallucinogens of the indolylalkylamine and phenylalkylamine type.	4
<b>Figure 1.2</b>	Structural analogs of LSD.	8
<b>Figure 1.3</b>	Structure of an IgG molecule.	14
<b>Figure 1.4</b>	Common ELISA methodologies.	22
<b>Figure 1.5</b>	Competitive ELISA methodologies.	24
<b>Figure 1.6</b>	Immunochemical detection of anti-LSD antibodies in a test sample.	26
<b>Figure 1.7</b>	Immunochemical detection of LSD in a test sample.	28
<b>Figure 1.8</b>	Structures of some existing LSD immunogens.	32
<b>Figure 2.1</b>	Quantitative determination of primary amines using the fluorescamine assay.	60
<b>Figure 2.2 (a)</b>	Effect of pH on the availability of unprotonated lysine residues on KLH using the fluorescamine assay.	62
<b>Figure 2.2 (b)</b>	The effect of increasing pH on % lysines which are coupled with SASD.	62
<b>Figure 2.3</b>	Important reactions of aryl nitrenes.	67
<b>Figure 2.4</b>	Gel filtration separation of KLH and LSD standards on Sephadex G-25.	73
<b>Figure 2.5</b>	Purification of the radiolabelled immunogen by size exclusion chromatography.	77
<b>Figure 2.6</b>	Interference in colorimetric assays.	82
<b>Figure 2.7</b>	Effect of excess LSD on molar substitution ratio.	84
<b>Figure 2.8</b>	Quantitative determination of the primary amines in immunogenic carrier proteins using the fluorescamine assay.	88
<b>Figure 2.9</b>	Preparation of KLH-LSD by the Mannich reaction.	92
<b>Figure 3.1</b>	Immobilized secondary amine groups on Nunc CovaLink microtitre plates.	102

<b>Figure 3.2</b>	Non-specific binding of normal rabbit IgG to Corning polystyrene microtitre plates by ELISA.	112
<b>Figure 3.3</b>	Colorimetric detection of protein and LSD on CovaLink.	113
<b>Figure 3.4</b>	Titration of immune rabbit serum in the presence and absence of immobilized LSD using Nunc CovaLink.	115
<b>Figure 3.5</b>	Titration of immune and normal rabbit serum by ELISA on Nunc CovaLink microtitre plates derivatized with LSD.	115
<b>Figure 3.6</b>	Nunc CovaLink ELISA using BSA as the blocking agent during different incubations.	117
<b>Figure 3.7</b>	Masking effect of high molecular weight blocking proteins on Nunc CovaLink.	119
<b>Figure 3.8</b>	ELISA using BSA-PFPA-LSD as the coating antigen.	121
<b>Figure 3.9</b>	Schematic illustration of the displacement of BSA-PFPA-LSD coating antigen with IgG molecules in rabbit serum.	121
<b>Figure 3.10</b>	Reaction of <i>p</i> -dimethylaminobenzaldehyde with LSD under acidic conditions.	123
<b>Figure 3.11</b>	Performance of PVA antigens by ELISA.	125
<b>Figure 3.12</b>	Performance of difference coating antigens by ELISA.	127
<b>Figure 3.13</b>	Coating antigens used in ELISA.	128
<b>Figure 3.14</b>	Antibody titration curves for rabbits which were immunized with different immunoconjugates over four months.	130
<b>Figure 3.15</b>	Antibody affinity profiles for rabbits which were immunized with different LSD immunoconjugates.	131
<b>Figure 3.16</b>	Detection of LSD in PBS by indirect ELISA.	132
<b>Figure 3.17</b>	Inhibition of antibody binding using free drug and haptened protein.	133
<b>Figure 4.1</b>	Effect of urine on LSD calibration.	155
<b>Figure 4.2</b>	The effect of antibody concentration on LSD calibration by ELISA.	158
<b>Figure 4.3</b>	The effect of antibody-antigen incubation time on assay precision and sensitivity.	160
<b>Figure 4.4</b>	Calibration of LSD in urine.	166
<b>Figure 4.5</b>	Precision profile of the UBC LSD ELISA.	170

<b>Figure 4.6</b>	Mean response of quality control standards run in 12 assays over four months.	170
<b>Figure 4.7</b>	Calibration of LSD in urine using the amplified LSD ELISA.	174
<b>Figure 5.1</b>	Cross-reactivity of LSD antibodies with drug derivatives.	198
<b>Figure 5.2</b>	Effect of structural changes on photolinked antibody specificity.	205
<b>Figure 5.3</b>	Estimation of $K_{app}$ by hapten inhibition ELISA.	215
<b>Figure 5.4</b>	Affinity distribution of LSD antibodies measured by hapten inhibition ELISA.	219
<b>Figure 5.5</b>	Scatchard plot which described the binding of photolinked antibody to LSD.	224
<b>Figure 5.6</b>	Direct plot of photolinked antibody binding to LSD.	225
<b>Figure 5.7</b>	Antibody affinity profile measured by thiocyanate elution followed by ELISA detection.	228
<b>Figure 5.8</b>	Antibody titration and thiocyanate elution.	231
<b>Figure 5.9</b>	Affinity maturation of antibodies over a period of four months.	233
<b>Figure 5.10</b>	Calibration of LSD using four different polyclonal antisera to LSD.	235
<b>Figure 6.1</b>	Preparation of the immunoaffinity support.	245
<b>Figure 6.2</b>	Immunoaffinity extraction of LSD.	247
<b>Figure 6.3</b>	Effect of whole blood on ELISA.	255
<b>Figure 6.4</b>	Comparison of calibration curves obtained using 25 $\mu$ L whole blood and 50 $\mu$ L urine.	257
<b>Figure 6.5</b>	Calibration of LSD in blood by ELISA.	258
<b>Figure 6.6</b>	Calibration of LSD in blood using commercial and in-house immunoassays.	260
<b>Figure 6.7</b>	LSD calibration used for quantification of LSD in blood, bile, liver and vitreous fluid.	263
<b>Figure 6.8 (a)</b>	Immunoaffinity extraction of LSD from PBS using ethanol as the eluent.	270
<b>Figure 6.8 (b)</b>	Immunoaffinity extraction of LSD in PBS using 100 mM triethylamine as the eluent.	270

- Figure 6.9 (a)** Immunoaffinity extraction of 48 pg total LSD in 0.1 mL whole blood. 272
- Figure 6.9 (b)** Immunoaffinity extraction of 0.22 ng LSD from 1 mL buffered urine. 272

**List of Tables.**

	<i>Title</i>	<i>Page</i>
<b>Table 1.1</b>	Common hallucinogens and their properties.	4
<b>Table 2.1</b>	Conditions for the photoactivation of SASD.	64
<b>Table 2.2</b>	TLC separation of LSD and 2-iodo-LSD.	75
<b>Table 2.3</b>	Qualitative identification of fractions separated by gel filtration chromatography.	77
<b>Table 2.4</b>	Characterization of the immunoconjugate KLH-SASD-LSD used for immunization of rabbits.	87
<b>Table 2.5</b>	Comparison of epitope densities for KLH-SASD-LSD and other haptened proteins.	90
<b>Table 3.1</b>	ELISA using Nunc CovaLink in which the blocking agent (BSA) was introduced at different stages.	117
<b>Table 3.2</b>	Antibody titres for rabbits immunized with photolinked and Mannich immunogens.	129
<b>Table 4.1</b>	Effect of sample matrix on ELISA performance.	155
<b>Table 4.2</b>	Effect of serum dilution on assay performance.	158
<b>Table 4.3</b>	Effect of pH on ELISA signal.	161
<b>Table 4.4</b>	Effect of coating antigen on ELISA.	162
<b>Table 4.5</b>	The effect of TMB reaction time on assay performance.	164
<b>Table 4.6</b>	Summary of optimized ELISA conditions for the analysis of LSD in urine.	164
<b>Table 4.7</b>	Typical calibration data obtained by ELISA.	165
<b>Table 4.8</b>	Accuracy determination of LSD in urine by ELISA.	168
<b>Table 4.9</b>	Inter and intra-assay precision of LSD in urine by ELISA.	169
<b>Table 4.10</b>	Factors which affect assay sensitivity and precision in the amplified LSD ELISA.	172
<b>Table 4.11</b>	Determination of accuracy using the amplified LSD ELISA.	174
<b>Table 4.12</b>	Intra and inter-assay precision of the amplified LSD ELISA.	175

<b>Table 4.13</b>	Summary of amplified and un-amplified ELISA performance for the detection of LSD in human urine.	177
<b>Table 4.14</b>	Comparison of UBC LSD ELISA performance with other assays.	178
<b>Table 5.1</b>	Classification and solubility of compounds used in the specificity study.	190
<b>Table 5.2</b>	Source and description of five in-house and commercial antibodies to LSD used in characterization studies.	192
<b>Table 5.3</b>	Effect of organic solvents on ELISA signal.	196
<b>Table 5.4</b>	Specificity of the photolinked antibody.	202
<b>Table 5.5</b>	Specificity of commercial and in-house antibodies by ELISA.	203
<b>Table 5.6</b>	Calculation of the apparent affinity constant ( $K_{app}$ ) from hapten inhibition data.	214
<b>Table 5.7</b>	Affinity indices and antibody dissociabilities of polyclonal antisera to LSD.	229
<b>Table 5.8</b>	Correlation between affinity, dissociability and sensitivity parameters.	236
<b>Table 6.1</b>	Measurement of positive and negative blood specimens by ELISA.	256
<b>Table 6.2</b>	Precision of LSD spiked in whole blood.	259
<b>Table 6.3</b>	Calibration data using UBC and STC immunoassays for the detection of LSD in 25 $\mu$ L whole blood.	260
<b>Table 6.4</b>	Quantification of LSD and cross-reacting substances in forensic case samples.	262
<b>Table 6.5</b>	Summary of quantitative estimates of LSD and cross-reacting species in forensic case samples.	264
<b>Table 6.6</b>	Immunoaffinity extraction of LSD from blood, urine and buffer.	271

**List of abbreviations.**

BCA	bicinchoninic acid
BSA	bovine serum albumin
CEDIA	cloned enzyme donor immunoassay
CV	coefficient of variation or relative standard deviation
DMP	dimethyl pimelimidate
EC50	effective concentration that produces 50% inhibition
ELISA	enzyme-linked immunosorbent assay
EMIT	enzyme multiplied immunoassay technique
FL	fluorescence
FNPA	4-fluoro-3-nitrophenyl azide
GC-MS	gas chromatography - mass spectrometry
HPLC	high performance liquid chromatography
HRP	horseradish peroxidase
HSA	human serum albumin
IAE	immunoaffinity extraction
KIMS	kinetic interaction of microparticles in solution
KLH	keyhole limpet hemocyanin
LC	liquid chromatography
LLE	liquid-liquid extraction
LOD	limit of detection
LOQ	limit of quantification
LSD	lysergic acid diethylamide

MS-MS	tandem mass spectrometry
MSR	molar substitution ratio
MWCO	molecular weight cut-off
NSB	non-specific binding
OD	optical density
PBS	phosphate buffered saline
PFPA	polyfluorinated phenyl azide
PTG	porcine thyroglobulin
PVA	polyvinyl alcohol
RCMP	Royal Canadian Mounted Police
RIA	radioimmunoassay
SASD	sulfosuccinimidyl-2-( <i>p</i> -azidosalicylamido)ethyl-1,3'-dithiopropionate
SD	standard deviation
SM	skim milk
SM-PBS	skim milk (5%) in PBS
SPE	solid phase extraction
TMB	tetramethylbenzidine
TNBS	trinitrobenzenesulfonic acid

## **Acknowledgements.**

First and foremost I would like to thank my supervisor, Professor Donald. E. Brooks, for continued support, guidance and encouragement throughout this study. Many thanks are due to past and present students of the Brooks' laboratory for useful discussions and comradeship. In particular, special thanks to Dr. Johan Janzen, for endless patience and fearless problem solving and to Raymond Norris-Jones, who makes the Brooks lab a brighter place.

I am extremely grateful for the interest and support of members of the Royal Canadian Mounted Police Forensic Laboratories in Vancouver and Ottawa. In particular, Wayne Jeffery, who not only provided forensic case samples, but who also inspired the creation of this project. I appreciate the assistance of Dr. Haro Avdovich (Bureau of Drug Research, Health Canada, Ottawa, ON) who supplied a number of controlled substances and the National Institute on Drug Abuse (Rockville, MD), who provided a number of rare LSD derivatives through the Drug Supply Program.

Many thanks are also extended to Dr. Dana Devine and all members of the Devine laboratory, for resource sharing and useful discussions over a number of years. Financial support for this project was provided by The University of British Columbia (University Graduate Fellowship and Laird Fellowships) and by the Medical Research Council of Canada (Grant MT5759 to D.E.B.).

*For Ann and Brendan.*

*“Lead me from death to life,  
from falsehood to truth.*

*Lead me from despair to hope,  
from fear to trust.*

*Lead me from hate to love,  
From war to peace.*

*Let peace fill our hearts,  
Our world, our earth”.*

## Chapter 1.

### Introduction.

#### 1.1. Lysergic acid diethylamide.

##### 1.1.1. LSD past-present.

Lysergic acid diethylamide (LSD) is derived from ergot, a sugary excretion of the fungus *Claviceps purpurea* that grows on rye and other grains. Once the source of mass poisonings (ergotism) in the Middle ages, the medicinal properties of the ergot alkaloids have been recorded since the 16th Century, when it was used by European midwives to precipitate childbirth. Today, ergotamine is still used medicinally, as a treatment for migraine headaches.

Research on ergot alkaloids commenced in the early 1900's at Sandoz in Switzerland. It was not until 1943, when Albert Hofmann decided to repeat an earlier synthesis of lysergic acid diethylamide from ergonovine in the search for a new analeptic drug, that the unusual properties of LSD were discovered:

“The surroundings had changed in a strange way, and had become luminous, more expressive. I perceived an uninterrupted stream of fantastic pictures, with an intense kaleidoscope play of colours...”(1).

In 1947 Sandoz marketed LSD under the tradename Delysid. Initially it was foreseen that LSD would enhance our understanding of psychiatric illness, particularly schizophrenia, psychoses, neuroses and alcoholism. Inevitably the undisciplined use of the drug, particularly in the 1960's when its use was pandemic, became its most prominent feature. Despite this, LSD was used widely as a

therapeutic agent in psychotherapy up until 1965, when its use was restricted in the U.S. by an amendment of the Narcotics Act which went into effect the following year (2).

It has been suggested that the recreational use of LSD-like substances has taken place for more than 2,000 years. It is believed that *kykeon*, the holy potion of the Greek Goddess Eleusis, contained lysergic acid amide and lysergic acid hydroxyethylamide. The same species were found to occur in *ololiuqui*, a sacred drug of the Mexican Indians which contained seeds of *Convolvulaceae*, which is a plant of the morning glory family (1).

According to a 1995 survey of 50,000 12th-grade students in the United States, nearly 12% had tried LSD and these numbers have been steadily increasing since 1991 (3,4). Demographic data suggests that the typical LSD user is a middle-class Caucasian male, attending high school or college. It's use is more prevalent in the suburbs than in the inner city and tends to be quite regionalised; LSD is manufactured primarily on the West coast of North America where it remains popular. Other pockets of LSD use exist, particularly in regions where the "rave" scene is popular.

Synthetic LSD is usually sprayed onto blotting paper, which is dried, perforated and printed with colourful icons. A typical dose of about 100 µg costs between \$3 and \$5 (2), which provides a long-lasting effect for several hours when taken orally. The primary danger of LSD intoxication is from self-inflicted injury, suicide or unexpected flashbacks.

### **1.1.2. Hallucinogens and the psychopharmacology of LSD.**

Hallucinogen is derived from the Latin word *alucinari*, which means to wander in mind. In broad terms a hallucinogen is an agent which causes alterations in perception, cognition and mood as its primary actions in the presence of an otherwise clear sensorium (4). Classical hallucinogenic

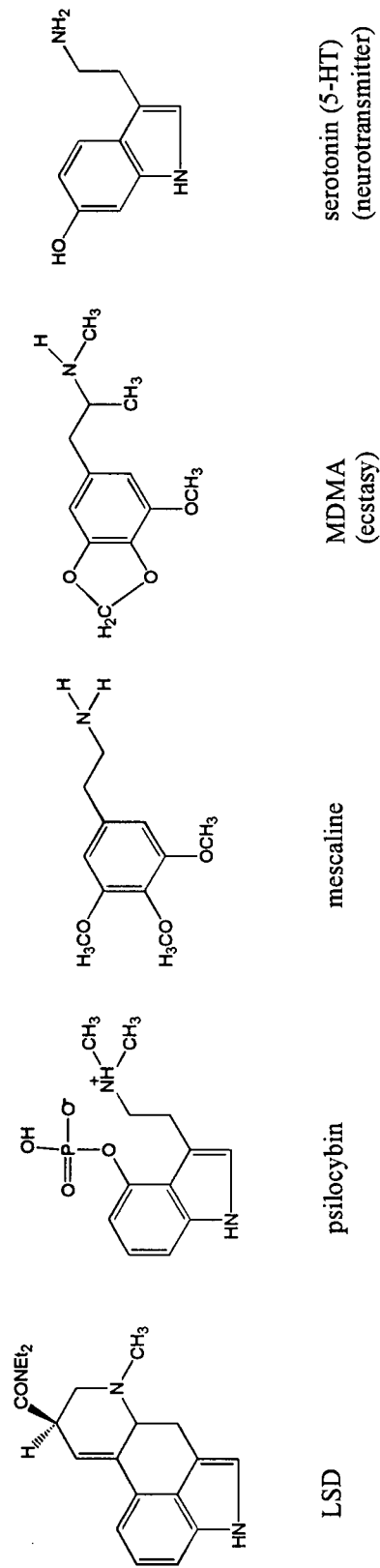
agents can be broadly sub-divided into two groups: indolylalkylamines and phenylalkylamines. Structural similarity exists between the indolylalkylamines, such as LSD or psilocybin, and the neurotransmitter serotonin (5-hydroxytryptamine or 5-HT). The properties of two common hallucinogens from each class (Table 1.1) indicate the high potency and duration of effects of LSD compared to other psychoactive substances (mescaline, psilocybin and ecstasy).

The precise mode of action of LSD is not fully understood and although it was widely believed to involve serotonin, its role has been hotly debated over the years. Experimental evidence suggests that hallucinogenic effect of LSD is due to its unique ability to interact as either an agonist, partial agonist or antagonist at a number of different 5-HT receptor sub-types (5). The cross-tolerance that exists between LSD and psilocybin or mescaline suggests that their mode of action is inter-related. Although LSD and similar psychedelic drugs have actions at multiple sites in the central nervous system it was generally believed that these drugs act as agonists at serotonin receptors of a particular sub-type (6). It is now known that there is a good correlation between hallucinogenic activity and the affinity of both indolylalkylamines and phenylalkylamines for 5-HT<sub>2</sub> receptors (7).

**Table 1.1.** Common hallucinogens and their properties (4).

Name	classification	source	common route	typical dose	duration of effects
lysergic acid diethylamide, (LSD)	indolylalkylamine	semi-synthetic, from fungus	oral	100 µg	6-12 hours
psilocybin	indolylalkylamine	mushrooms <i>psilocybe</i>	oral	4-6 mg (5-10 g dried mushrooms)	4-6 hours
mescaline	phenylalkylamine	Peyote cactus <i>L. Williamsii</i>	oral	200-400 mg (4-6 cactus buttons)	10-12 hours
methylene-dioxy-methamphetamine (MDMA, ecstasy)	phenylalkylamine	synthetic	oral	80-150 mg	4-6 hours

**Figure 1.1.** Structural similarities between hallucinogens of the indolylalkylamine and phenylalkylamine type.



### 1.1.3. Toxicology of LSD.

LSD is readily absorbed after oral administration, following which it undergoes rapid biotransformation in the liver to inactive metabolites (8). The LD<sub>50</sub> concentration for LSD administered to rabbits (iv) is 0.3 mg/kg. The toxicity of the drug is related to brain weight rather than body weight, which suggests that the LD<sub>50</sub> in humans might be around 0.2 mg/kg for an average adult male, which would be equivalent to about 140 typical LSD doses (2). Plasma concentrations greater than 1 ng/mL have been associated with toxic effects, although doses up to 10 mg have been administered with complete recovery (9). Despite reports to the contrary, there has been at least one reported death by LSD poisoning (10). However, this is the exception rather than the rule, as most LSD-related fatalities are the result of accidental death or suicide.

Although there is little convincing evidence of organic brain damage, as once suggested (11), there can be serious long-term disruption of the personality of LSD users. The incidence of LSD induced psychotic reactions, in which the user experiences symptoms similar to paranoid schizophrenia, has been debated. Reports of these types of reactions, which can occur following one time use, suggest that some individuals are particularly susceptible to the adverse effects of LSD, which is most usually explained by a pre-existing psychiatric disorder (4).

Somatic changes occur about half an hour after administration of LSD. These may include nausea, loss of appetite or vomiting. Higher doses can produce headache, dizziness, sweating and ataxia. Autonomic effects such as blurred vision, palpitations, increased blood pressure and pupillary dilation (mydriasis) often persist until after the perceptual effect of the hallucinogen have passed. Mydriasis is reported to be useful in estimating the intensity of the psychotropic influence (2). However, distinguishing between different hallucinogens in an emergency room setting is difficult as

many psychotropic drugs produce similar symptoms. Blood and urine toxicology can be used to confirm LSD use, but results are seldom available within the time frame of the intoxication. LSD overdoses or “bad trips” are treated conservatively in a medical setting, due to the relatively low toxicity of the drug. The best approach is often relaxation or “talking down” as opposed to drug therapy, which can, in some instances, intensify the experience of the user (4).

There are no withdrawal effects associated with LSD, although tolerance develops after 4-7 days of repeated drug use. Tolerance only lasts for about three days, after which the user experiences the effects of the drug at the normal dosage levels (4). The phenomenon of LSD flashbacks, now called *hallucinogen persisting perception disorder*, is not well understood despite reports of its frequent occurrence, particularly in those who have taken LSD more than about ten times (3). The mechanism of this phenomenon, whereby the user experiences the effects of LSD without ingesting the drug, is poorly understood although it is known not be caused by a persistence of LSD in the body.

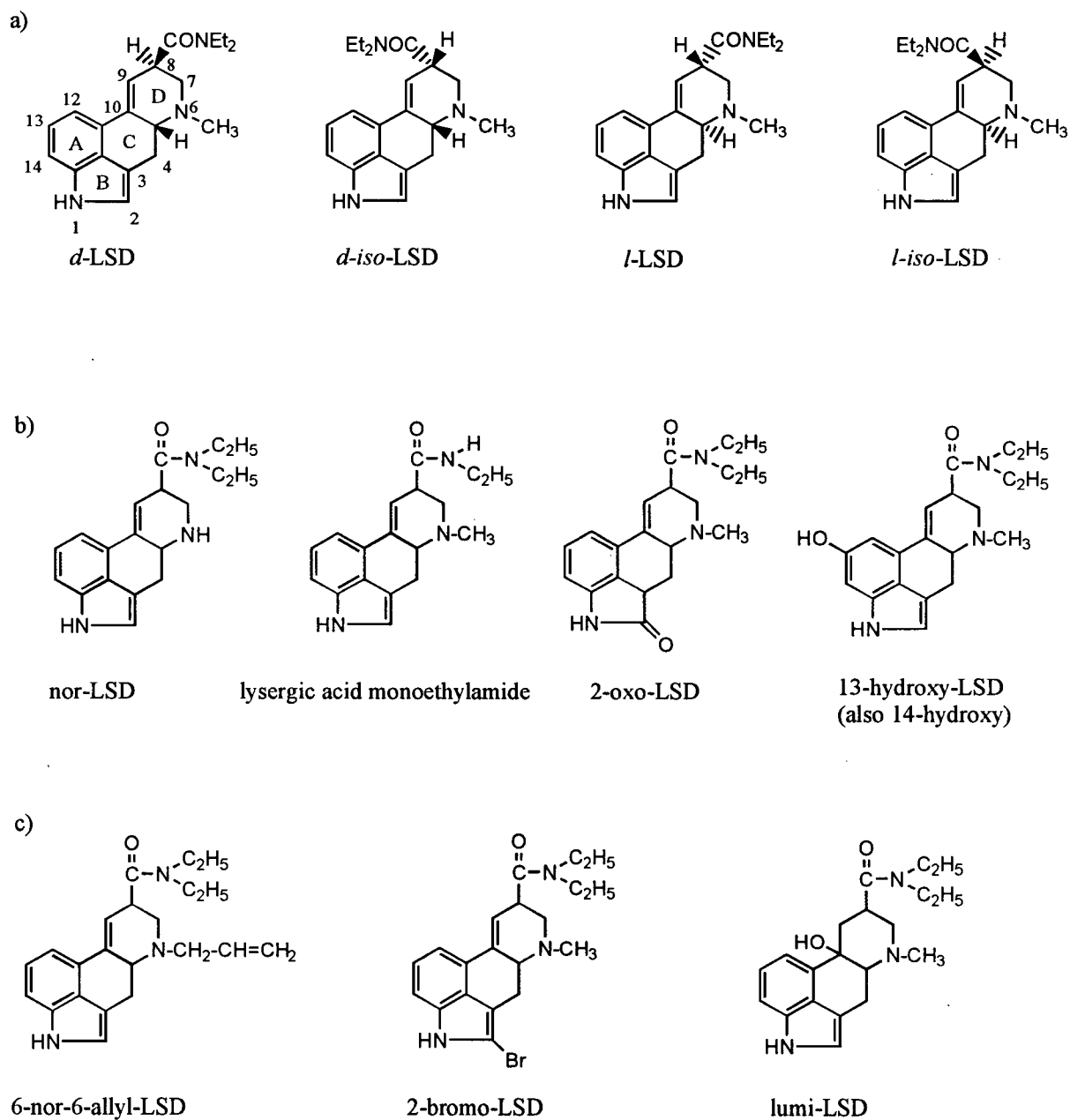
#### 1.1.4. Chemistry of LSD.

Lysergic acid diethylamide, like all ergot alkaloids, has a tetracyclic framework which includes the indole group. There are two asymmetric carbon centres in the drug at positions C5 and C8. Of the four stereoisomers of LSD, only *d*-LSD is a potent hallucinogen. Inversion of the stereochemistry at C5 (in *l*-LSD) or C8 (in *iso*-LSD) abolishes hallucinogenic activity (Figure 1.2). The use of LSD throughout the text refers exclusively to the hallucinogenic isomer (*d*-LSD). Besides variations in the spatial arrangement of the atoms, LSD has been modified by variation in the amide residue, saturation of the 9-10 double bond and substitutions in the ring system at positions 1, 2, 6, 8 and 12 (11-14).

Irradiation of LSD in acidic media results in the addition of water across the 9-10 bond to give lumi-LSD (15). The photodecomposition reaction is highly solvent dependent. Previous work has shown that in some solvents, no reaction occurs, whilst in others the photodecomposition occurs readily (16). Irradiation of the drug is only one prerequisite for the transformation of LSD to lumi-LSD; the reaction also necessitates the presence of a strongly polar species in sufficient quantity for photodecomposition to take place (17).

Chemical transformations of LSD occur *in vivo* during the rapid metabolism of the drug. To date, the only confirmed biotransformation is *N*-demethylation to give nor-LSD (18) although conversion to lysergic acid monoethylamide (19) and 2-oxo-LSD (20,21) are strongly implicated. Hydroxylated LSD derivatives (at positions 13 and 14) have been tentatively identified in animal and *in-vitro* studies, although these are believed to undergo glucuronidation prior to excretion (18,20-22).

**Figure 1.2.** Structural analogs of LSD including a) stereoisomers, b) suspected metabolites and c) other derivatives of interest.



### 1.1.5. Structure-activity relationships.

The hallucinogenic activity of LSD is exquisitely related to its structure; replacement of groups, such as substituents on the amide nitrogen, can decrease the psychoactivity to a fraction of its original potency. Structure-activity relationships between different LSD-like drugs have been investigated by a number of authors (12,24) and is still on-going (6,23). Structural alterations which affect hallucinogenic properties are explained by the nature of the drug-receptor interaction. LSD binds to a receptor, which is defined by a three dimensional array of amino acids. A change in either the amino acid sequence of the receptor binding protein or a structural alteration of the drug itself, is likely to affect the affinity of the drug-receptor interaction, in manner analogous to antibody-antigen binding.

Hallucinogenic activity of LSD is affected by substitutions at the indole nitrogen (N1), C2, C8 and by reduction of the 9-10 double bond (6). Stereochemistry at positions C5 and C8 also play an important role; both *l*-LSD and iso-derivatives are inactive (12). Despite reports that LSD is the most potent hallucinogen known, this is not strictly true. Drug discrimination studies using rats have shown that substitution of certain groups in the N6 position increased hallucinogenic activity, with 6-nor-6-allyl-LSD having the most pronounced effect. The measured increase in potency was accompanied by an approximate three-fold increase in binding affinity of the 6-nor-6-allyl-LSD towards the 5-HT receptor (6). Substitution in the C2 position has also produced some interesting results; 2-bromo-LSD, which is inactive as a hallucinogen, acts as a serotonin antagonist. Surprisingly however, its antagonistic effect actually prevents subsequently administered LSD from binding to 5-HT receptors (6,11).

## **1.2. Antibodies: an overview.**

### **1.2.1. Immunogens, haptens and epitopes.**

An immunogen or antigen is any substance which is capable of eliciting an immune response. The ability of a given substance to be immunogenic is largely dependent on its size and complexity of structure. Antibodies can be raised against an immunogen, which could be a protein or complex macromolecule which is foreign to the host. However, low molecular weight species (below about 5000) are not very effective as immunogens. A small molecule such as LSD, which is not capable of eliciting an immune response but can bind to an antibody is called a hapten. Antibodies can be raised against a particular hapten by coupling it to a large complex carrier molecule. Bovine serum albumin (BSA) and keyhole limpet hemocyanin (KLH) are frequently used for this purpose (25). The specific regions of the antigen or hapten which are directly involved in binding to the antibody are called epitopes or antigenic determinants. The part of the antibody which binds to the antigenic determinant is called the antigen-combining site or paratope (which is complementary to the epitope). If a particular region of the hapten is known to contain an epitope or a number of epitopes, it is sometimes called the immunodominant region. For example, antibody binding studies have shown that the immunodominant region of LSD are the C and D rings (Figure 1.2) (26-28).

### **1.2.2. The immune system.**

Stimulation of the immune system results in an elaborate humoral and cell-mediated response. Antibodies are produced and circulated in the body along with specialised cells, which can react with antigen on the cell surface and destroy it. There are essentially two types of lymphocytes found in the blood, lymph and lymphoid tissue which are responsible for this response; T cells, which are

developed in the thymus for cell mediated immunity and B cells, developed independent of the thymus, which are responsible for the production of antibodies.

Once B cells are stimulated, they divide rapidly to produce sufficient cells to protect the host. Each activated B cell secretes one type (class) of antibody; all of the antibody which is produced from the same cell has the same specificity. T cells, which can directly attack the incoming agent, are also responsible for regulating the activity of B cells and determining the class of antibody which is produced (29).

The immune system can recognize many thousands of different antigens. Each lymphocyte however, can only recognize one epitope which means that, of the thousands of different antigens available, lymphocytes which recognize a particular antigen are a very small proportion of the total. The way in which a successful immune response is mounted from a small number of lymphocytes is explained by clonal selection (29). Both T and B cells are committed to react with a specific antigen even before it has been exposed to it. Surface receptor proteins which fit the antigen activate the cell to multiply. Therefore, the foreign antigen selectively stimulates cells which have complementary antigen specific receptors whereby all cells of the same clone have the same antigenic specificity.

Injection of an immunogen results in the activation of B and T cell clones, each of which has a different binding affinity with respect to the antigenic determinant. Activation of many clones is called a polyclonal response, in which the antibodies which are produced are of a heterogeneous nature. Monoclonal antibodies, which are comprised of a homogeneous antibody population, are selected from only one population of cells.

Repeated exposure of the host animal to a particular antigen over a period of time stimulates the immune system to produce antibodies which have a complementary structure which allows it to

bind to the antigen and “deactivate” it. These antibodies, which are circulated in the host animal, can be found in the serum (called the antiserum). The immunogenic response can be increased by injection of an adjuvant at the same time as the immunogen. Freund's complete adjuvant, which has been widely used for this purpose, contains heat killed *Mycobacterium tuberculosis* in paraffin oil. Stimulation of the immune system using an adjuvant can increase the production of antibodies which are raised against a particular immunogen (30,31).

### 1.2.3. Immunoglobulin structure.

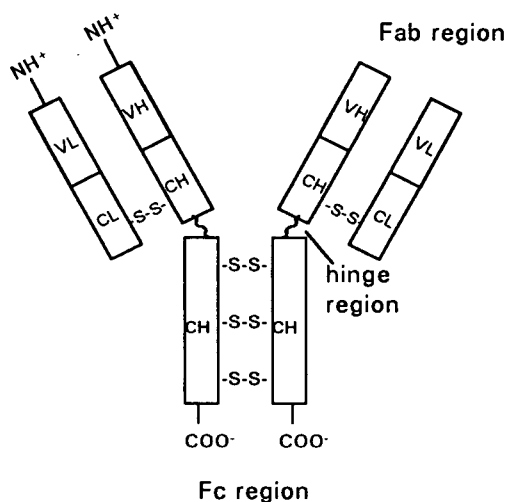
Antibodies belong to a class of proteins called immunoglobulins (Ig) which are designed to bind antigens and activate specific reactions. Immunoglobulins consist of two parts; antigen binding sites on one part of the molecule have a structure which is complementary to the antigen, while receptors on the other end control effector function and biological activity. There are a number of distinct classes and sub-classes of immunoglobulin which differ from each other with respect to their size, amino acid composition and carbohydrate content.

The basic Ig molecule consists of two identical light (L) polypeptide chains and two identical heavy (H) chains, which are linked together by disulfide bonds (29). There are five types of heavy chain,  $\alpha$ ,  $\delta$ ,  $\epsilon$ ,  $\gamma$  and  $\mu$  which are responsible for the five main classes of immunoglobulins, IgA, IgD, IgE, IgG and IgM respectively. Each heavy chain, of approximately 440 amino acid (AA) residues, is attached to the corresponding light chain (220 AA's) by non-covalent association and a disulfide bridge. For IgG (Figure 1.3), each pair of heavy and light chains is linked by disulfide bonds between the heavy chains to give a Y shaped molecule. Other classes and sub-classes of immunoglobulins differ with respect to the disulfide bridges between the heavy chains and the number of light and

heavy chain pairs. IgA and IgM have dimeric and pentameric structures, which are capable of binding up to 4 or 10 epitopes respectively. IgM is the first type of antibody which is produced on exposure to an immunogenic substance. Repeated exposure to the same immunogen results in mostly an IgG response which is circulated in the blood. The concentration of IgG in human serum is 8-16 mg/mL, compared to < 4 mg/mL for IgM or IgA and even lower ( $\mu\text{g/mL}$ ) for IgD and IgE (32,33).

In the *N*-terminal region, the sequence of amino acids in the polypeptide chain varies greatly from one molecule to the next, unlike the heavy and light chains of the *C*-terminal region. Both light and heavy chains have variable (V) and constant (C) regions. In the light chain, the variable and constant regions make up about 110 amino acids each, whereas the heavy chain is composed of about 110 and 330 residues in the variable and constant regions respectively. The antigen binding site is comprised of both heavy and light chains in the *N*-terminal ends (called the Fab regions). Only a small part of this region is actually involved in antigen binding (approximately 20 - 30 amino acids). The heterogeneity of amino acid sequences within the variable regions of both these chains accounts for the diversity of antigen binding among antibody molecules. In contrast, it is the constant region of the *C*-terminal end (called the Fc region) that controls the effector functions which are common to each class of immunoglobulin.

**Figure 1.3.** Structure of an IgG molecule.



#### 1.2.4. Antibody-antigen binding.

There are two identical antigen combining sites on each IgG molecule which suggests that, one molecule of antibody can bind two molecules of hapten, or antigen (depending on its size). In general, repeated exposure to the immunogen improves the ability of the antibody to recognize the antigen. This is demonstrated by improved antibody-antigen interactions, three dimensional fit and epitope recognition. The overall specificity is largely dependent on the construction of the paratope on the antibody. Antibody-antigen binding is dependent on a number of non-covalent associations, such as electrostatic, hydrogen bonds, van der Waals and hydrophobic interactions. It is the goodness of fit between the epitope on the antigen and the paratope on the antibody that creates the environment in which these attractive forces can be maintained.

#### 1.2.5. Antibody affinity.

The affinity, or the binding energy between an antibody and the antigen is the sum of the

attractive and repulsive forces between the interacting regions of both species. A perfect fit between the epitope and the paratope is more likely to result in a high affinity association. If there is a poor complementary nature between the two, fewer non-covalent associations will be established within the complex and the overall affinity will be reduced. In general, a polyclonal response produces a mixture of both high and low affinity antibodies. Repeated exposure to the antigen over time can improve epitope recognition which results in a higher affinity response.

Multi-valent immunoglobulins may be able to form more than one attachment to the antigen, depending on its size. Therefore, an antibody with low overall affinity can still bind strongly if it does so with more than one epitope at the same time (33). The strength of multi-valent antibody or antigen attachments are referred to as avidity (34). However, the interaction between an antibody and a hapten such as LSD, is a function of the affinity rather than avidity, because it is not possible for the antibody to bind to LSD at more than one epitope, due to the small size of the molecule. The term *intrinsic affinity* is often used to describe the interaction of a monovalent hapten with a corresponding antibody, whereas *functional affinity* is used to describe the interaction of the antibody combining sites on the antibody with antigenic determinants on an antigen (34).

#### 1.2.6. Experimental determination of antibody affinity.

Antibody affinity can be determined experimentally from the simple binding reaction which occurs between one molecule of antibody (Ab) and one molecule of antigen (Ag) to give an antibody-antigen complex (AbAg),



The equilibrium association constant,  $K_a$ , is given by,

$$K_a = [AbAg] / [Ab] [Ag] \quad [1]$$

where square brackets indicate the concentration of each species at equilibrium. Scatchard analysis of the antibody-antigen binding reaction allows both the equilibrium association constant,  $K_a$  and the number of antibody binding sites to be determined (35). During the reaction, the total amount of antibody,  $[Ab]_T$ , is the sum of the unoccupied and occupied fraction of antibody (which is complexed with antigen),

$$[Ab]_T = [Ab] + [AbAg]. \quad [2]$$

Replacement of the term  $[Ab]$  in equation [1] gives,

$$K_a = [AbAg] / ([Ag] \cdot ([Ab]_T - [AbAg])) \quad [3]$$

which can be rearranged to give,

$$[AbAg] / [Ag] = -K_a [AbAg] + K_a [Ab]_T \quad [4]$$

Which is of the form  $y = mx + c$ , given that the total concentration of antibody,  $[Ab]_T$ , remains constant. Assuming that all antibodies have the same affinity for the antigen, in the absence of cooperativity, a plot of  $[AbAg] / [Ag]$  against  $[AbAg]$  should give a straight line with a gradient of  $-K_a$  and an intercept on the  $[AbAg]$  axis of  $[Ab]_T$ , the total concentration of binding sites. In practice, Scatchard plots are often non-linear, especially when they are used to calculate the affinity of polyclonal antisera, which contain a heterogeneous mixture of antibodies with different  $K_a$  values. This treatment assumes a monovalent interaction between one molecule of hapten and the an antigen binding site on IgG. However, when larger antigens are used, such as a drug-protein conjugate on the surface of a microtitre plate, the bivalency of IgG can contribute to the antibody-antigen interaction. Alternative mathematical treatments allow the intrinsic affinity of these interactions to be estimated, in situations where it is possible for both antigen binding sites to attach to the same

molecule of haptened protein (34,35). Experimental determination of the equilibrium concentration of free and bound antigen is most frequently obtained using a radiolabelled antigen. The antibody affinity is usually reported as the  $K_a$  value, which has the units  $M^{-1}$ . It is this value which largely determines the sensitivity of the test, particularly for competitive-type immunoassays (32).

### **1.3. Immunochemical detection.**

An immunoassay is a technique for detecting the presence of either an antibody or antigen by its immunological reaction. The method is among the most widely used of all analytical techniques, which can be applied to an extensive range of substances, from large molecules such as viruses to small drugs and toxins. Multiple variations of immunoassay methodology have evolved over time and there is not a strict universal classification or terminology for the different types. However, the fundamental principle is based on the reaction which occurs between an antibody and an antigen, which may be used either qualitatively or quantitatively with respect to either one of the immunoreactants. A variety of immunoassay methodologies have been described, which involve numerous different antibody-antigen reactions, separation methods and detection systems, which are broadly discussed below.

#### **1.3.1. Homogeneous vs. heterogeneous immunoassays.**

Immunoassays can be either heterogeneous (separation required) or homogeneous (no separation). The advantage of homogeneous immunoassay formats are their speed, simplicity and ease of automation. The majority of separation-free methods involve either enzyme or fluorescent detection systems, the most successful of which have been FPIA (fluorescence polarization

immunoassay), EMIT (enzyme multiplied immunoassay technique) and more recently, CEDIA (cloned enzyme donor immunoassay). Using these methods it is possible to measure the species of interest without a separation step. For example, using an enzyme labelled method, such as EMIT, it is possible to measure the concentration of a hapten based on antibody-mediated changes in enzyme activity, i.e. the decreased enzymic activity of a drug-enzyme conjugate once it has been bound to an antibody. Homogeneous immunoassays typically suffer from high non-specific interferences, which can limit their sensitivity in certain applications.

Heterogeneous assays however, involve the separation of free and bound fractions, wherein it is assumed that the antibody is effectively irreversibly bound. In contrast to homogeneous immunoassays, the antibody or antigen which may be linked to an enzyme, retains its enzymatic activity once it is complexed. The incorporation of a separation step can enhance specificity and precision, which in turn improves assay sensitivity. The separation technique should be performed effectively without disturbing the overall equilibrium or introducing non-specific interferences. The two most frequently used methods of separation are precipitation and solid-phase immobilization methods. The latter is advantageous in terms of its simplicity, whereby free (un-bound) reactants can be washed off the surface. This method can also reduce non-specific binding, by removing weakly bound species which contribute to the background signal.

The attachment of either antigen or antibody to a solid-phase support is usually achieved by either covalent or passive adsorption to particulate material, tubes, beads, disks or microtitre plates. The addition of a complementary enzyme labelled species, which should have high activity and be readily available in purified form can be used to detect the immobilized species. Subsequently, a substrate reaction which yields an intensely coloured product can be used to spectrophotometrically

detect the amount of enzyme labelled species which is immobilized. Horseradish peroxidase and alkaline phosphatase are among the most frequently used enzyme labels for enzyme-linked immunosorbent assay (ELISA). The chromogenic substrate used for ELISA should be colourless initially, but strongly coloured after reaction with the enzyme. Tetramethylbenzidine (TMB) is a good chromogen for peroxidase labelled reagents, due to its sensitivity and comparative safety, relative to other chromogens which are known to have mutagenic properties (36).

### **1.3.2. Assay design.**

The selection of an appropriate methodology is the first step in assay design. Factors such as the concentration range of the analyte, molecular size and required specificity predetermine to some degree, the type of test which can be used. For example, sandwich immunoassays (see later) which employ two antibodies, are potentially more sensitive (and specific) than many other immunoassays but are not readily adapted for the analysis of small molecules using conventional reagents (37). Similarly, precipitation-type methods, which have limited sensitivity, are best suited to large antigens, with multiple epitopes which facilitate the formation of multi-valent precipitation complexes. The overall assay specificity, which is largely predetermined by the antibody reagent, is also reflected in the assay methodology. For example, fluorescence-based tests may be poorly suited to the analysis of biological specimens, particularly in some homogenous immunoassays, which tend to suffer from high background interferences.

The selection of reagents which are used in a given immunoassay largely determines its success or failure. The antibody equilibrium constant,  $K_a$ , is of particular importance in determining assay sensitivity of competitive-type immunoassays; antibodies which have higher  $K_a$  values can be

used to develop more sensitive tests than antibodies of lower affinity. The specificity also plays an important role in determining the usefulness of an immunoassay. Antibody-antigen interactions which occur with compounds other than the target molecule of interest are called cross-reactions. Extensive cross-reactivity towards other antigens is characteristic of a poorly specific antiserum. However, this feature can be exploited for screening groups of drugs which have similar structures eg. barbiturates, tricyclic antidepressants and benzodiazepines.

The type of label which is used for the detection of free and bound fractions may also affect the sensitivity range of the assay. Perhaps the most widely used detector labels have been radioisotopes and enzymes due to their widespread availability and relative ease of use. The disadvantage of radioimmunoassay (RIA) procedures includes the legislative requirements for the use of radioisotopes and the relatively short shelf-life of the reagents. The virtues of ELISA, which include its relative low cost, reagent stability, sensitivity and safety, have been responsible for its widespread diagnostic use in almost all the major disciplines.

The use of fluorescent and chemiluminescent metal-ligand complexes has been shown to improve the sensitivity of non-competitive immunoassays down to sub-picomolar concentrations (38-41). Even more recently, immunosensor-based detection techniques have been used to measure femtomolar concentrations of antigen in competitive binding immunoassays (42).

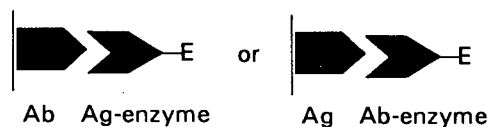
### **1.3.3. ELISA methodology.**

A number of formats have been used for the detection of either antibody or antigen by heterogeneous enzyme-linked immunosorbent assays. Different methodologies for the determination of either antibody or antigen by ELISA are summarized in Figure 1.4 and will not be discussed in

detail here. In general, immunoreagents are added in a step-wise fashion, separated by incubation periods followed by washing steps. The usefulness and widespread use of ELISA is due to the relative ease with which antibodies or antigens can be passively adsorbed onto solid surfaces such as 96 well microtitre plates, which are commercially available in a number of different plastics. The separation of free from bound reagents is achieved by rinsing the microtitre plate and the use of an enzyme labelled reagent and substrate colour reaction can be measured using a multichannel spectrophotometric plate reader.

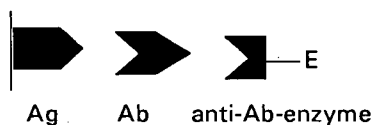
**Figure 1.4.** Common ELISA methodologies.

**DIRECT**



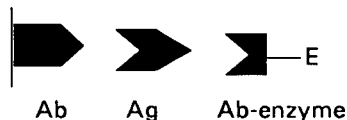
*Direct labelled Ag or Ab, analogous to many RIA methods; can form the basis of other techniques such as competition assays.*

**INDIRECT**



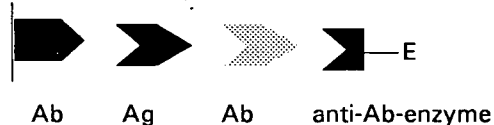
*Extensively used for the detection or titration of specific antibodies in serum samples. Advantageous over the direct method in that a single anti-species enzyme conjugate can be used to measure antisera to many different antigens.*

**SANDWICH**



*Using two antibodies which can bind antigen increases overall specificity; one is used for antigen "capture", the other for detection purposes. Antigens must have at least two epitopes. Disadvantageous for low molecular weight antigens or where antigenic sites are concentrated in one part of the molecule.*

**INDIRECT SANDWICH**



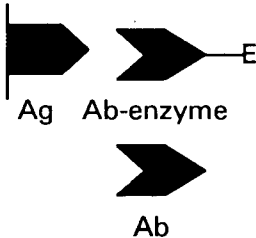
*Advantage is that the specific antibody need not be conjugated to the enzyme label; a single enzyme conjugate antibody can be used to detect antibodies raised against a number of different antigens.*

#### **1.3.4. Competitive vs. non-competitive immunoassays.**

Competitive immunoassays involve two immunoreactants, both of which can bind to a third species. True competition assays involve the simultaneous addition of competing species to the reaction mixture, whereas inhibition assays allow one of the reactants to be incubated before the second competitor is added. However, in the literature, inhibition and competition are often used synonymously to describe both types of assay. Non-competitive immunoassays are generally performed under conditions of reagent excess. Sometimes called an immunometric assay, this type of test can be potentially more sensitive than the competitive-type. The theoretical limitations of non-competitive assay sensitivity are that they are dependent on the type of labelling used and its detection, as opposed to competitive-type immunoassays, which is largely dependent on the affinity of the antibody (41). Many variations of this approach can be used to detect either antigen or antibody. In an indirect ELISA, a second enzyme labelled antibody (sometimes called conjugate antibody) is used to detect the amount of specific antibody which is bound. Using this method, using a different host animal, an anti-immunoglobulin antibody is raised against IgG from the same host as is used to raise the specific antibody, which is then enzyme labelled. One of the advantages of this approach is that it avoids labelling the specific antibody, which may affect its ability to bind the antigen or may be in short supply. However, it is possible to avoid a second antibody incubation step by direct labelling of the specific antibody. A number of alternative approaches for competitive binding ELISA's are summarized in Figure 1.5.

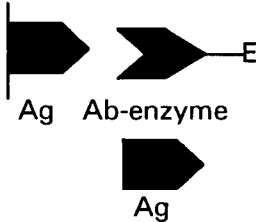
**Figure 1.5.** Competitive ELISA methodologies.

**DIRECT ANTIBODY COMPETITION**



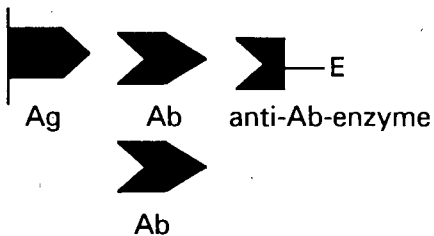
*The specific antibody must be enzyme labelled; can inhibit antibody binding using serum from any species. Colour decreases with increasing concentration of antibody (as with all competitive ELISA formats listed here).*

**DIRECT ANTIGEN COMPETITION**



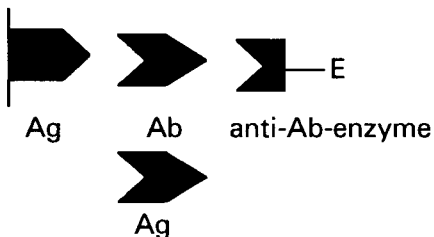
*Free antigen in the sample can react with enzyme labelled antibody to prevent it binding to the solid phase. Can be used to quantify antigen or to measure the relative affinity of different antigens towards the same antibody.*

**INDIRECT ANTIBODY COMPETITION**



*Essentially the same as the indirect ELISA except that a competing antibody is added to the solid phase antigen with the specific antibody; competing antibody must be from a different species or the enzyme labelled antibody will react with both.*

**INDIRECT ANTIGEN COMPETITION**



*Similar to the indirect antibody competition assay except that it is antigen which inhibits antibody binding to the solid phase. Can measure the concentration of antigen using one specific antibody and a conjugate antibody which is raised against the immunoglobulin of the specific antibody.*

### **1.3.5. Choice of immunoassay methodology for LSD and anti-LSD.**

Each ELISA format has associated with it relative advantages and disadvantages which restrict its use, sensitivity and performance qualities. The indirect ELISA was the most appropriate immunoassay for the detection of anti-LSD and LSD in samples for a number of reasons. The versatility of this approach allows the detection of both high molecular mass antibody to LSD and low molecular mass drug. The sensitivity of indirect ELISA measurements can equal that of a radioimmunoassay, providing the quality of the immunoreagents is high. Finally, relatively low concentrations of specific antibody are needed, particularly if a secondary enzyme labelled conjugate is used. The indirect approach, in which specific and secondary antibody incubations are performed in a step-wise fashion, separated by washing, minimizes the risk that proteases or enzyme inhibitors, which may be present in the test sample (urine, blood or other biological fluid), will affect the activity of the enzyme label.

#### **1.3.5.1. Immunochemical detection of anti-LSD.**

Indirect microtitre plate ELISA's are frequently used for the detection of antibody in a test sample. Figure 1.6 shows a schematic of the immunoassay, which is essentially a two-step process. LSD is immobilized on the surface of the microtitre plate by either passive adsorption of a protein-LSD conjugate, or by covalent attachment of the drug. Excess or weakly bound LSD is removed by washing, after which the test sample (rabbit serum) which contains antibody to LSD is allowed to react. After an appropriate incubation period and removal of excess reagent by washing, peroxidase labelled anti-rabbit IgG is added, which attaches to rabbit anti-LSD which is bound to the surface. Once more, after incubation and removal of unbound material by washing, tetramethylbenzidine

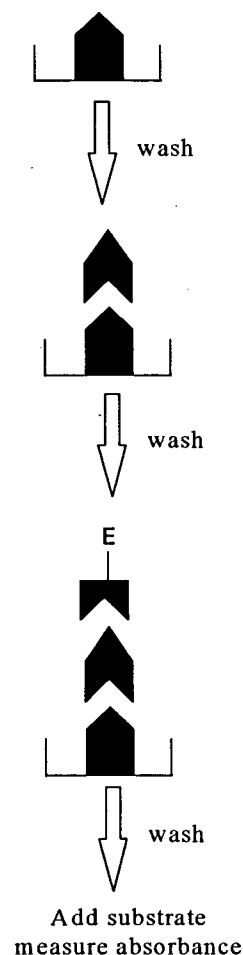
(TMB) substrate solution is added. After a fixed length of time, the colour reaction is stopped by the addition of acid after which the absorbance is measured at 450 nm using 620 nm as the reference.

**Figure 1.6.** Immunochemical detection of anti-LSD antibodies present in a test sample (rabbit serum) by indirect ELISA.

*LSD is immobilized on the surface of a microtitre plate.*

*Test sample is added (which may contain antibodies to LSD). If antibodies to the drug are present they will bind to immobilized LSD on the surface of the plate.*

*An enzyme conjugate antibody is added, which is raised against rabbit IgG (eg. goat anti-rabbit IgG peroxidase). This binds to rabbit IgG immobilized on the surface of the plate. The amount of specific antibody bound is estimated indirectly from the colour reaction between the substrate solution and the peroxidase labelled conjugate antibody.*



### 1.3.5.2. Immunochemical detection of LSD.

The presence of free haptens during the serum incubation step will inhibit antibody binding to the solid phase. This is exploited in the assay of LSD by competitive indirect ELISA (Figure 1.7).

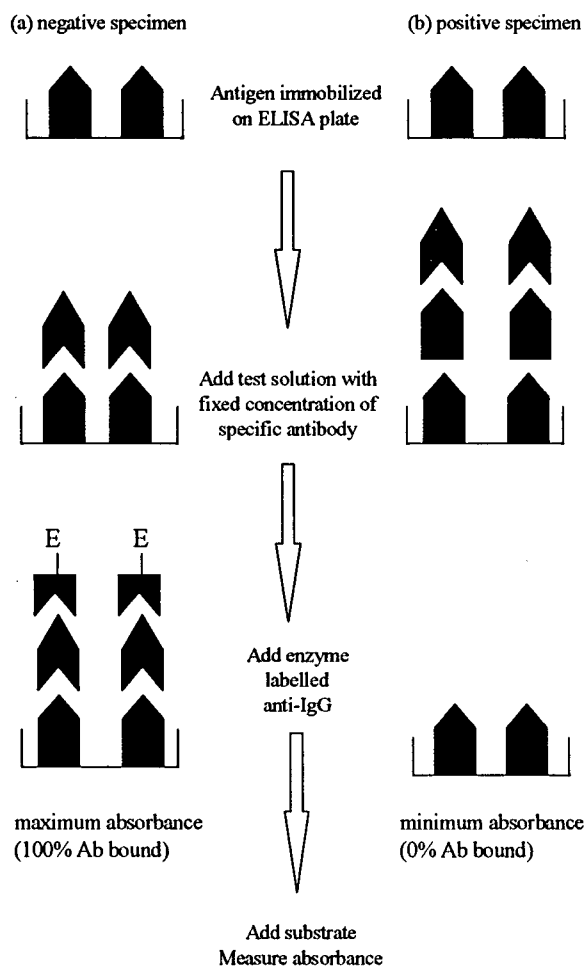
In this example, the test solution (eg. urine) is added to LSD coated microtitre wells with a fixed concentration of rabbit serum which contains antibodies to LSD. If the test sample contains no LSD, the antibody binds to the solid phase uninhibited. Under these conditions, the measured absorbance of the "blank" sample (or zero calibrator) is at a maximum ( $A_{\text{blank}}$ ). However, if LSD is present in the test sample, both free and immobilized LSD will compete for a limited amount of specific antibody. The fraction of antibody which is bound to the solid phase can be determined by incubation with peroxidase labelled anti-rabbit IgG and TMB substrate solution as previously described. Under these conditions, the presence of LSD in the test sample is indicated by a decrease in absorbance relative to the blank sample ( $A_{\text{test}}$ ). The inverse relationship between the measured signal and the concentration of LSD in the test sample results in high absorbance readings for low concentrations of drug and vice versa. The percentage of the absorbance measured for the test sample relative to the blank ( $100 \times A_{\text{test}}/A_{\text{blank}}$ ) represents the percent of antibody which is bound to the solid phase over a range of concentrations. A calibration graph, sometimes referred to as a dose-response curve, is obtained by plotting the percent of antibody bound against the concentration of LSD in a known test sample.

**Figure 1.7.** Immunochemical detection of LSD in a test sample, for example urine.

*LSD is immobilized on the surface of a microtitre plate.*

*A fixed concentration of diluted antibody to LSD and the test solution (eg. urine) which is suspected to contain LSD is added. If the test sample contains no drug, then antibody will bind uninhibited, as in (a). However, if LSD is present in the test solution, it will compete with immobilized LSD for a limited amount of antibody, which results in less antibody bound to the solid phase (b).*

*A peroxidase labelled anti-rabbit IgG conjugate antibody is used to detect the number of specific drug antibodies which are bound to the solid phase.*



### 1.3.6. Immunochemical detection of drugs of abuse.

#### 1.3.6.1. Drugs of abuse testing in urine.

Recommended guidelines for drugs of abuse testing in urine stipulate that a sensitive immunoassay, which is specific to a particular drug or class of drugs, should be used to screen negative specimens from presumptive positive specimens. Thereafter, a highly specific technique, such

as GC-MS, should be used to confirm presumptive positive results (43). The preferred specimen for commercial immunoassays is urine, although testing in medical or forensic settings often necessitate the use of other fluids or tissues. The immunoassay screening procedure is essential for high-volume testing as this can often be performed in a matter of minutes rather than hours. A recent evaluation of common drug screening tests for marijuana and cocaine reported that a selection of homogeneous immunoassays, which take between 4 and 7 minutes to run, cost between \$9 - 13 per test, compared with mass spectrometric confirmation, which takes approximately 2 hours, and costs about \$15 per test (44). The importance of immunoassay screening procedures for drugs of abuse should not be underestimated; they not only reduce analyst time, but are the first step in identifying presumptive positive specimens. As such, the quality and reliability of the screening technique ultimately determines the success in confirming the presence of an illicit substance.

The concentration of drug in any biological fluid is affected by the dose, route of administration, pattern of drug use as well as the distribution, metabolism and excretion. The analysis of urine is made more complicated by factors such as urinary flow and pH. Therefore, interpretation of quantitative drug estimates obtained from urine are hard to interpret from a forensic standpoint. A change in urinary flow rate will change the concentration of drug in the urine. Creatinine, which is endogenous in urine, is neither absorbed or secreted and can therefore be used as a marker to correct for changes in urine flow rate (45).

Quantitative drug estimates which are based on immunoassays usually produce higher concentrations than more rigorous confirmation procedures, such as GC-MS. The antibody reagent which is used is not absolutely specific for the compound of interest; cross-reactions with structurally related compounds such as selected metabolites is common. There are often differences between

different immunoassays for this reason too, especially if they employ antibody reagents with different specificity characteristics (46). In general, only those immunoassays which utilize antibodies which are raised from structurally related immunogens are likely to give similar results. As such, quantitative estimates from immunoassays must be viewed in the context of antibody specificity, which is rarely absolute.

#### **1.3.6.2. Immunoassays for LSD.**

Prior to the completion of this work, commercially available immunoassays to LSD were restricted to either RIA, eg. Abuscreen (Roche Diagnostic Systems, Somerville, NJ) and Coat-a-Count (Diagnostic Products Corp., Los Angeles, CA) or EMIT (Behring Diagnostics, San Jose, CA). However, renewed interest in LSD as well as the trend towards faster and non-isotopic methods has resulted in some new homogeneous screening technologies which have recently become available. These include Abuscreen OnLine for LSD (Roche Diagnostic Systems) (47) which is a latex agglutination inhibition assay, based on the kinetic interaction of microparticles in solution (KIMS) (44,48) and CEDIA (cloned enzyme donor immunoassay) for LSD (Boehringer Mannheim Corp., Indianapolis, IN) (49).

In general, homogeneous drug screening techniques such as KIMS, CEDIA and EMIT require the use of large and expensive automated analysers which are not always available in smaller drug testing facilities. High volume screening for LSD use is not normally done outside of the U.S. Military, therefore small-scale testing is still useful, especially in forensic settings. For this reason, an ELISA for LSD (STC Diagnostics, Bethlehem, PA) (50) recently became available, nearing the completion of this work.

### 1.3.6.3. Existing immunoconjugates for LSD.

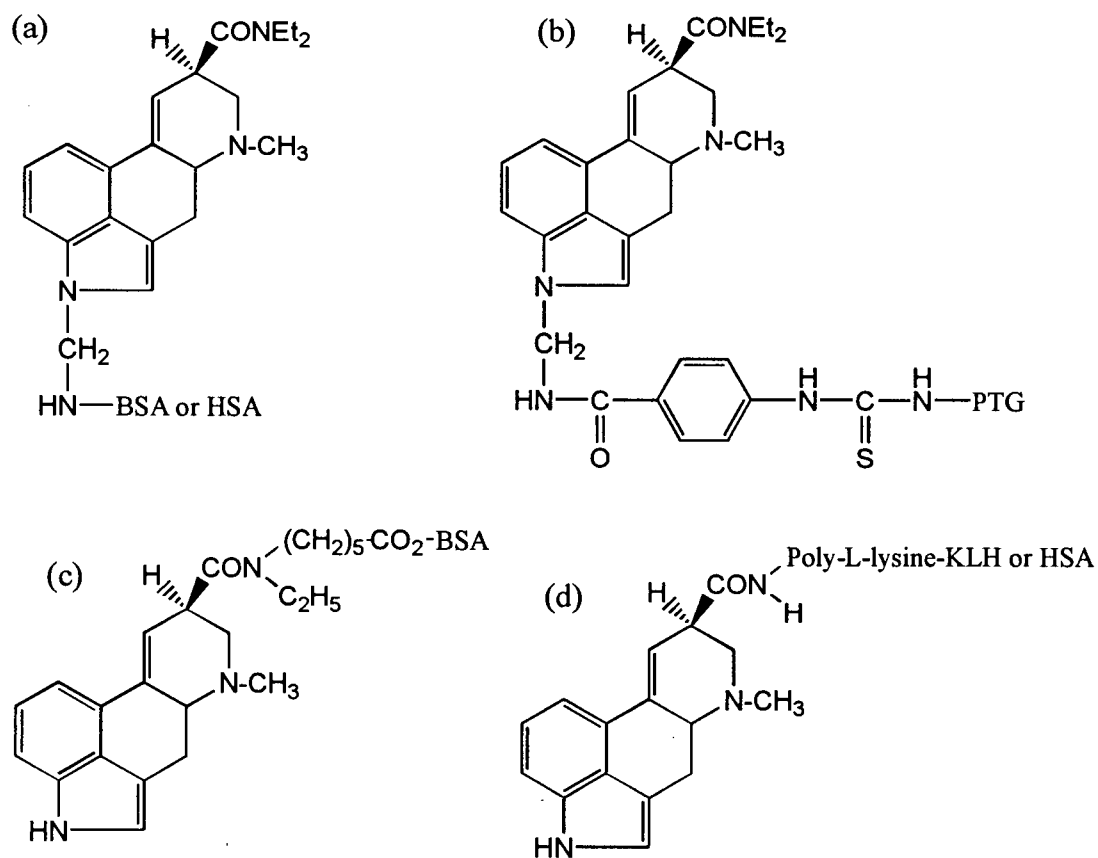
LSD has been coupled to large carrier proteins for the purpose of raising antibodies by relatively few methods. The most common approach has been to couple the drug at either the indole nitrogen of LSD using the Mannich reaction (51,52) or by carbodiimide mediated linkage at the carboxylic acid group of lysergic acid (52-54). Immunoconjugates which utilize spacer arms, which hold the drug a small distance away from the protein have been described (47,52) but these too were coupled at positions already mentioned. A summary of existing LSD immunogens which have been described in the literature over the last 25 years is shown in Figure 1.8.

The selection of the site of attachment between the drug and the carrier protein is a fundamental feature of immunogen design, as is the nature of the coupling reaction. The coupling technique which is used to prepare the immunoconjugate affects the overall characteristics of the antibody, including its inherent sensitivity and specificity (55,56). Therefore, it is the immunogen design which largely determines the characteristics of the immunoassay and its subsequent success or failure.

Theoretically, a superior antiserum is obtained if the carrier protein is attached to drug molecules at a number of different sites on the molecule (57). Antibody formation is sterically guided by the site at which the drug is coupled to the protein; generally the epitope is contained in a region of the molecule which is not close to the site of attachment. Therefore, if chemical linkages can be made at a number of different sites, it may be possible to enhance epitope recognition and subsequently improve the quality of the antiserum. The attachment of LSD via a number of different sites may be difficult using conventional methods due to the complex chemistry of LSD and the limited number of reactive sites. In theory, the use of a linking reagent which can react non-

specifically with neighbouring molecules could be used for multi-site attachment of LSD to a carrier molecule. This non-conventional approach to LSD immunogen synthesis is described in detail in the following chapters.

**Figure 1.8.** Structures of some existing LSD immunogens. LSD is attached via the indole nitrogen (N1) to either human serum albumin (HSA) or bovine serum albumin (BSA) in a) (28,51,52,58) or to porcine thyroglobulin (PTG) via a spacer arm in b) (47). Alternatively, derivatives of lysergic acid were coupled to either BSA in c) (52) and HSA or poly-L-lysine-KLH in d) (53,54) via the carboxylic acid group attached to C8.



#### **1.4. Aims and objectives of the study.**

The purpose of this study was to prepare an LSD immunogen using a unique chemical linkage which had not been described elsewhere for this purpose. In theory, multi-site attachment of a hapten to a carrier molecule should enhance epitope recognition and increase the sensitivity of the antiserum. Immunoassays for LSD require the use of very sensitive antibodies to the drug in order to detect very low concentrations in biological specimens. The overall objectives of this study were to:

- 1.) Prepare a new LSD immunogen in which LSD is attached to a carrier protein at a number of different sites which should maximize epitope recognition.
  
- 2.) Raise a polyclonal antiserum against the immunogen and characterize it in terms of its specificity, sensitivity and affinity towards the parent drug, LSD.
  
- 3.) Determine the usefulness of the antibody in an immunoassay for the detection of LSD in body fluids, select an appropriate immunoassay methodology and optimize the test conditions.
  
- 4.) Validate the immunoassay in terms of its sensitivity, specificity, precision, accuracy etc.
  
- 5.) Explore the potential of the immunoassay for the analysis of other

specimens, which might be encountered in a forensic setting eg. blood.

6.) Finally, illustrate how the antiserum can be used as a tool for the selective extraction of LSD from a complex biological fluid using immunoaffinity chromatography.

### 1.5. References.

1. Hofmann, A. 1994. 50 Years of LSD. A. Pletscher and D. Ladewig, Eds., pp. 7-16. Parthenon Publishing Group, New York.
2. Blum, K. 1984. Handbook of Abusable Drugs, Gardner Press, New York.
3. Schwartz, R.H. 1995. *Pediatr. Clin. N. Am.* 42: 403-410.
4. Abraham, H.D., Aldridge, A.M., and Gogia, P. 1996. *Neuropsychopharmacology* 14(4): 285-298.
5. Peroutka, S.J. 1994. 50 Years of LSD. A. Pletscher and D. Ladewig, Eds., pp. 19-26. Parthenon Publishing Group, New York.
6. Glennon, R.A. 1994. Hallucinogens: An Update. G.C. Lin and R.A. Glennon, Eds., pp. 4-73. National Institute on Drug Abuse, Rockville, MD.
7. Aghajanian, G.K. 1994. 50 Years of LSD. A. Pletscher and D. Ladewig, Eds., pp. 27-41. Parthenon Publishing Group, New York.
8. Axelrod, J., Brady, R.O., Witkop, B., and Evarts, E.V. 1956. *Ann. NY. Acad. Sci* 66: 435-444.
9. Moffat, A.C. 1986. Clarke's Isolation and Identification of Drugs, p. 716. The Pharmaceutical Press, London.
10. Fysh, R.R., Oon, M.C.H., Robinson, R.N., Smith, R.N., White, P.C., and Whitehouse, M.J. 1985. *Forens. Sci. Intl.* 28: 109-113.
11. Sankar, D.V.S. 1975. LSD - A Total Study, PJD Publications, Westbury, NY.
12. Isbell, H., Miner, E.J., and Logan, C.R. 1959. *Psychopharmacologia* 1: 20-28.
13. Troxler, F. and Hofmann, A. 1957. *Helvetica Chimica Acta* 1957: 1706-1720.
14. Troxler, F. and Hofmann, A. 1957. *Helvetica Chimica Acta* 40(7): 2160-2170.
15. Blake, E.T., Cashman, P.J., and Thornton, J.I. 1973. *Anal. Chem.* 45(2): 394-395.
16. Niwaguchi, T. and Inoue, T. 1971. *Proc. Japan. Acad.* 47: 747-750.
17. Hellberg, H. 1957. *Acta Chem. Scand.* 2: 219-229.
18. Lim, H.K., Andrenyak, D., Francom, P., and Foltz, R.L. 1988. *Anal. Chem.* 60: 1420-1425.

19. Cai, J. and Henion, J. 1996. *J. Anal. Toxicol.* 20: 27-37.
20. Siddik, Z.H., Barnes, R.D., Dring, L.G., Smith, R.L., and Williams, R.T. 1975. *Biochem. Soc. Trans* 3(2): 290-292.
21. Siddik, Z.H., Barnes, R.D., Dring, L.G., Smith, R.L., and Williams, R.T. 1979. *Biochemical Pharmacology* 28: 3081-3091.
22. Niwaguchi, T., Inoue, T., and Nakahara, Y. 1974. *Biochemical Pharmacology* 23: 1073-1078.
23. Nicols, D.E., Monte, A., Huang, X., and Marona-Lewicka, D. 1996. *Behavioural Brain Research* 73: 117-119.
24. Snyder, S.H. and Richelson, E. 1968. *Proc. Nat. Acad. Sci.* 60: 206-213.
25. Pierce Chemical Company, Rockford, IL. 1994. Inject Carrier Proteins, *package insert*.
26. Lopatin, D.E. and Voss, E.D. 1974. *Immunochemistry* 11: 285-293.
27. Huang, X., Marona-Lewicka, D., Pfaff, R.C., and Nichols, D.E. 1994. *Pharm. Biochem. Behaviour* 47(3): 667-673.
28. Berde, B. and Schild, H.O. 1978. Ergot Alkaloids and Related Compounds, Springer-Verlag, New York.
29. Alberts, B., Bray, D., Lewis, J., Raff, M., Roberts, K., and Watson, J. 1983. Molecular Biology of the Cell, pp. 952-1008. Garland Publishing Inc, New York.
30. Bollen, L.S., Crowley, A., Stodulski, G., and Hau, J. 1996. *J. Immunol. Methods* 191: 113-120.
31. Smith, D.E., O'Brien, M.E., Palmer, V.J., and Sadowski, J.A. 1992. *Laboratory Animal Science* 42(6): 599-601.
32. Edwards, R. 1996. Immunoassays. Essential Data, John Wiley and Sons, Chichester, UK.
33. Kemeny, D.M. 1991. A Practical Guide to ELISA, Pergamon Press, New York.
34. Steward, M.W. and Steensgaard, J. 1983. Antibody Affinity: Thermodynamic Aspects and Biological Significance, pp. 59-94. CRC Press, Boca Raton.
35. Steward, M.W. and Steensgaard, J. 1983. Antibody Affinity: Thermodynamic Aspects and Biological Significance, pp. 1-56. CRC Press, Boca Raton.
36. Bos, E.S., van der Doelen, A.A., van Rooy, N., and Schuurs, A.H.W.M. 1981. *Journal of*

*Immunoassay* 2(3/4): 187-204.

37. Winger, L.A., Dessi, J.L., and Self, C.H. 1996. *J. Immunol. Methods* 199: 185-191.
38. Kricka, L.J. 1994. *Clin. Chem.* 40(3): 347-357.
39. Dong, L. and Martin, M.T. 1996. *Anal. Biochem.* 236: 344-347.
40. Terpetschnig, E., Szmecinski, H., and Lakowicz, J.R. 1996. *Anal. Biochem.* 240: 54-59.
41. Jackson, T.M. and Ekins, R.P. 1986. *J. Immunol. Methods* 87: 13-20.
42. Helmersen, K., Kishore, R., Phillips, W.D., and Weetall, H.H. 1997. *Clin. Chem.* 443(2): 379-383.
43. Department of Health and Human Services 1986. Urine Testing for Drugs of Abuse. NIDA Research Monograph Series 73, National Institute on Drug Abuse, Rockville, MD.
44. Schwartz, J.G., Zollars, P.R., Carnahan, J.J., Wallace, J.E., and Briggs, J.E. 1991. *Am. J. Emerg. Med.* 9(2): 166-170.
45. Luceri, F., Godi, F., and Messeri, G. 1997. *J. Anal. Toxicol.* 21: 244-245.
46. Wu, A.H.B., Feng, Y., Pajor, A., Gornet, T.G., Wong, S.S., Forte, E., and Brown, J. 1997. *J. Anal. Toxicol.* 21: 181-184.
47. McNally, A.J., Goc-Szcutnicka, K., Li, Z., Pilcher, I., Polakowski, S., and Salamone, S.J. 1996. *J. Anal. Toxicol.* 20: 404-408.
48. Armbruster, D.A., Schwarzhoff, R.H., Hubster, E.C., and Liserio, M.K. 1993. *Clin. Chem.* 39(10): 2137-2146.
49. Boehringer Mannheim Corp., Concord, CA. 1996. CEDIA DAU for LSD, *product brochure*.
50. Cassels, N.P., Craston, D.H., Hand, C.W., and Baldwin, D. 1996. *J. Anal. Toxicol.* 20: 409-415.
51. Taunton-Rigby, A., Sher, S.E., and Kelley, P.R. 1973. *Science* 181: 165-166.
52. Ratcliffe, W.A., Fletcher, S.M., Moffat, A.C., Ratcliffe, J.G., Harland, W.A., and Levitt, T.E. 1977. *Clin. Chem.* 23(2): 169-174.
53. Van Vunakis, H., Farrow, J.T., Gjika, H.B., and Levine, L.L. 1971. *Proc. Natl. Acad. Sci. USA* 68(7): 1483-1487.

54. Loeffler, L.J. and Pierce, J.V. 1973. *J. Pharm. Sci.* 62(11): 1817-1820.
55. Adamczyk, M., Fishpaugh, J., Harrington, C., Hartter, D., Johnson, D., and Vanderbilt, A. 1993. *J. Immunol. Methods* 162: 47-58.
56. Adamczyk, M., Grote, J., Douglas, J., Dubler, R., and Harrington, C. 1997. *Bioconjugate Chem.* 8: 281-288.
57. Strahilevitz, M. 1986. *United States Patent Number 4,620,977*.
58. Castro, A., Grette, D.P., Bartos, F., and Bartos, D. 1973. *Research Communications in Chemical Pathology and Pharmacology* 6(3): 879-886.

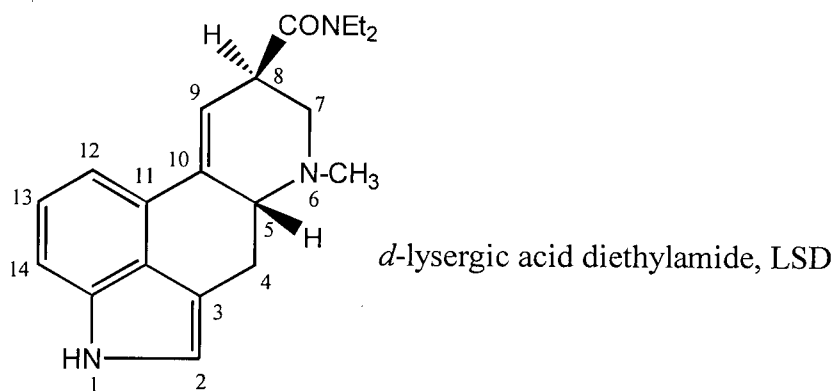
## Chapter 2.

### Synthesis of a New LSD Immunogen.

#### 2.1. Introduction.

##### 2.1.1. Conjugate formation.

Antisera to LSD are raised from conjugates in which drug is coupled to a carrier protein in order to elicit an immune response. There have been relatively few developments in terms of the type of chemical linkage that is used to covalently attach drug to protein. The most successful approach in the past has been to couple the protein to the indole nitrogen of LSD by the Mannich condensation (1,2) which was first reported over 20 years ago. Other conjugates have been



prepared directly by coupling the carboxyl group of lysergic acid to protein using carbodiimide (3,4). This approach however leads to poorly specific antisera, although the introduction of a four carbon spacer was shown to improve this (5). Recently an LSD immunogen was prepared in which protein was coupled to drug via an extended spacer arm which was attached at the indole nitrogen

(6). The use of a spacer arm between drug and protein in theory facilitates immune recognition at the site of attachment which in turn enhances specificity. There are no known reports in the literature which describe the conjugation of protein to LSD at positions other than the C8 side chain or the indole nitrogen.

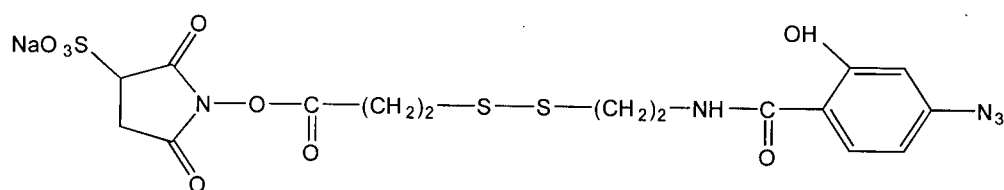
The chemical modification of drug which takes place during protein conjugation influences the immune response at the T-cell level (7). Immunogen design therefore has a profound effect, not only on specificity, but also on the affinity and overall characteristics of the antiserum (8). In addition to the chemistry of the linkage, the hapten density of the conjugate affects both the intensity and the character of the immune response. The immunogenic properties of the hapten-protein conjugate are also determined by the nature of the carrier molecule and the number of haptenic determinants.

The primary goal was to synthesize a new LSD immunoconjugate that would increase antiserum sensitivity. In theory LSD could be attached to an immunogenic carrier molecule, such as keyhole limpet hemocyanin (KLH), at a number of different sites on the drug using a photoreactive heterobifunctional crosslinker. Using this approach the reaction yields a number of products with different points of attachment to the carrier. This reduces the risk that epitopes at the site of attachment will not be recognized by the immune system therefore making more epitopes available and in principle, enhancing sensitivity. Additionally the use of a photolinker with an adequate spacer arm allows the hapten to be held away from the carrier increasing the chance that lymphocytes can distinguish the antigenic determinant at the point of attachment and therefore maintain good specificity.

The last 15 years has seen an explosion in the area of bioconjugate chemistry. New and improved photoreactive crosslinking reagents are frequently used for the covalent attachment of

two macromolecular species. There have been only two literature reports in which small drug molecules were conjugated to carrier proteins using photoreactive probes. Gentamicin and quinidine were coupled to BSA using an aryl azide containing heterobifunctional crosslinker (9). Although conjugates were not characterized, low titre immune sera raised in rabbits illustrated that drug had been successfully coupled to protein. Metoclopramide was coupled to BSA in a similar fashion using an aryl azide spacer arm (10). The photolinked conjugate was used to raise high affinity antibodies in rabbits.

Photoreactive heterobifunctional linkers contain a photoreactive group which is chemically inert but becomes reactive when exposed to UV light. Aryl azides, which are used most extensively for this purpose, are photolyzed to produce nitrogen and reactive aryl nitrenes, which are capable of nonselective reactions to form covalent bonds with neighbouring molecules. The high reactivity of the nitrene allows the formation of conjugates which would not be possible using group specific chemical reagents. Sulfosuccinimidyl-2-(*p*-azidosalicylamido)ethyl-1,3'-dithiopropionate (SASD) is a cleavable, photoreactive heterobifunctional crosslinker which contains an amine reactive *N*-hydroxysuccinimide (NHS) ester and a photoreactive aryl azide separated by a spacer arm of 19 Å. Immunogen synthesis proceeds via a two step conjugation in which the most labile group, the NHS ester, is reacted with the primary amines on the protein after which excess linker is removed. Protein derivatized with aryl azide is then photolyzed in the presence of hapten whereby relatively nonselective covalent bonds are formed between the azide and neighbouring molecules. The spacer arm of SASD should in theory enhance the specificity of the antiserum but also improve the likelihood of a reaction with LSD by holding the aryl azide away from the protein surface.



sulfosuccinimidyl-2-(*p*-azidosalicylamido)ethyl-1,3'-dithiopropionate  
(SASD)

The lifetime of a reactive nitrene is about  $10^{-4}$  seconds (11) although this depends on the substituent groups attached to the aryl ring (12). Aryl nitrenes or their intermediates are reported to react with C-H, N-H and aryl groups, which are present in the LSD molecule. The nitrene is one of the few reactive species that can react with C-H by abstraction and insertion therefore allowing covalent attachment in the absence of any particular functional group. The species is particularly reactive towards nucleophilic groups which are abundant in protein surfaces. It is therefore likely that in the case of KLH-SASD-LSD, a large part of the nitrene reactivity will be directed towards neighbouring protein. Linking reagents with short spacer arms result in greater intramolecular crosslinking whereas extended spacer arms increase the likelihood of a bimolecular reaction (12). An inherent disadvantage of the photocoupling technique is its low efficiency compared to many other bioconjugation methods. Yields resulting from photoreactive linking of unsubstituted aryl azide are generally low and efficiencies  $< 10\%$  are considered acceptable (13). Efficient coupling requires not only a reactive nitrene but also a favourable orientation towards the target molecule. To partly compensate for this it is necessary to use a large excess of LSD to improve the probability that the reactive nitrene is in proximity to a drug molecule. A measure of the overall efficiency is obtained by calculating the number of moles of LSD attached to one mole of KLH, which is called the molar substitution ratio (MSR).

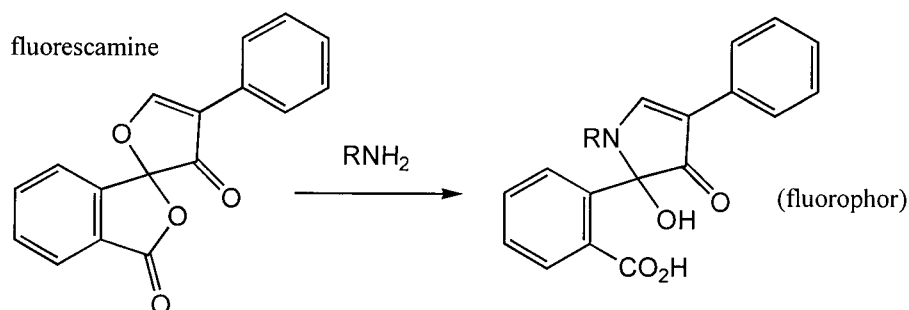
### 2.1.2. Conjugate analysis.

The most frequently used method for determining the degree of protein derivatization is direct UV spectroscopy. This however can only be used when the chromophore of the hapten is distinct from the protein in the absence of any overlapping species. Indirect spectroscopic techniques, such as the use of trinitrobenzene sulfonic acid (TNBS) allow the colorimetric determination of unreacted amino groups. Radiolabelled haptens can be used to measure the extent of coupling directly, by measuring the associated radioactivity of the conjugate. Mass spectrometry, particularly ESI (electrospray ionization) and MALDI (matrix assisted laser desorption) techniques have become increasingly useful for the characterization of conjugates with relatively high degrees of substitution. Other methods include sodium dodecyl sulfate polyacrylamide gel electrophoresis (SDS-PAGE), isoelectric focussing and amino acid analysis, which are primarily used for the characterization of protein-protein conjugates. In practice however, there are often few options available for analysis. Characterization of multi-component immunoconjugates is frequently hampered by poor solubility, interferences and severe limitations based on the relative size of hapten and carrier and the degree of substitution.

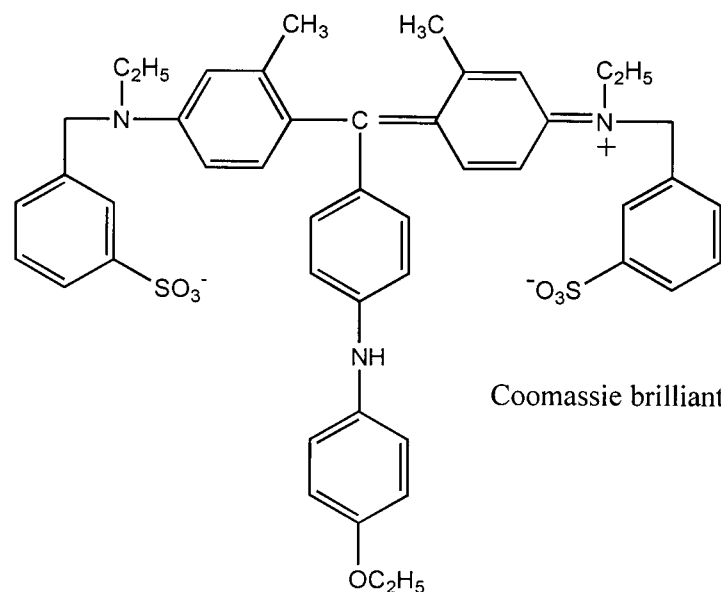
Keyhole limpet hemocyanin is one of the most commonly used protein carriers capable of imparting immunogenicity to covalently coupled haptens. KLH, which is isolated from the Californian giant keyhole limpet, *Megathura crenulata*, has a molecular weight range of 450,000 - 13,000,000 (14). Hemocyanins are copper containing respiratory proteins found in the blood of certain molluscs and arthropods. KLH has complex architecture and exists in a number of aggregation states, which can dissociate into smaller subunits, each housing a binuclear copper centre which is capable of binding an oxygen molecule (15,16). Despite rather poor solubility characteristics, KLH remains a popular carrier protein due to its large size and immunogenic

character.

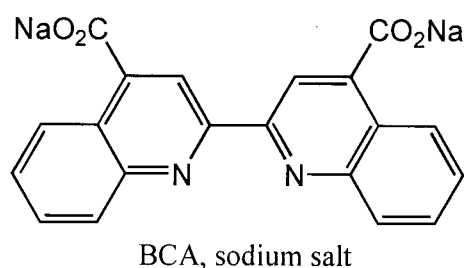
Fluorescamine can be used for the quantitative determination of primary amino groups in proteins, the main source of which is lysine (17). At neutral to alkaline pH, fluorescamine reacts with primary amines to produce a highly fluorescent species. The reagent and hydrolysis products are non-fluorescent which allows sensitive and specific analysis of proteins at the nanogram level. In this way, it is possible to determine the extent of modification of protein by the decrease in the number of lysines. Other less sensitive reagents, such as TNBS, are routinely used for this type of analysis.



The Coomassie Brilliant Blue protein assay (18), also known as the Bradford assay, has remained popular for over 20 years due to its relative speed, sensitivity and specificity towards protein species. At low pH, a blue protein-dye complex is formed which has an absorption maximum of 595 nm. The complex interactions are chiefly between dye and arginine in the protein as opposed to primary amino groups which was previously suggested (19). Some basic (His, Lys) and aromatic residues (Try, Tyr, Phe) give a slight response. The interactions between dye and protein are comprised of electrostatic, van der Waals forces and hydrophobic interactions. The main disadvantage of the Bradford dye binding assay is its tendency to produce slightly non linear calibration graphs, as is well documented in the literature (19-21).

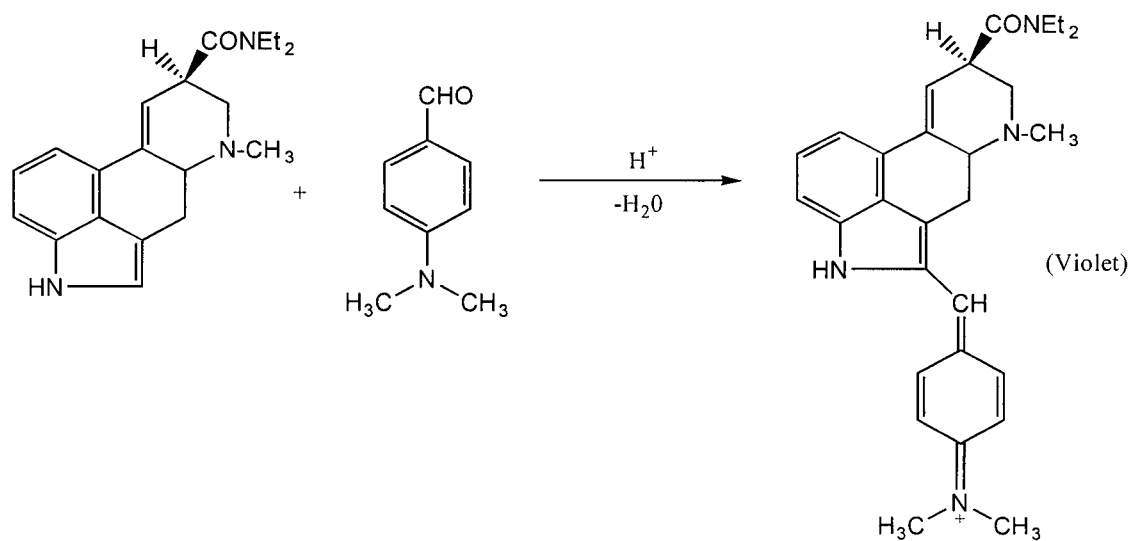


The Pierce BCA protein assay is a detection reagent for Cu (I). Proteins reduce Cu(II) in alkaline medium to Cu(I), which subsequently reacts with bicinchoninic acid (BCA) to give a purple complex with an absorption maximum at 562 nm. Cysteine, cystine, tryptophan and tyrosine are known to react with BCA reagent. A disadvantage of this technique is that any group that reduces copper will give a positive reaction which can result in unwanted interferences.



The Van Urk reagent has been used for qualitative identification of unsaturated indoles. Under acidic conditions these compounds react with *p*-dimethylaminobenzaldehyde to give a violet condensation product in the presence of excess reagent (22). It has been used extensively for on-the-spot testing of confiscated LSD and for visualization of ergot alkaloids by TLC. It does

however give a positive reaction with any indole, such as tryptophan, and is not specific for LSD alone.



## 2.2. Materials and methods.

Keyhole limpet hemocyanin, sulfosuccinimidyl-2-(*p*-azidosalicylamido)ethyl-1,3'-dithiopropionate and bicinchoninic acid reagent were obtained from Pierce (Rockford, IL). Lysergic acid diethylamide tartarate was kindly supplied by Dr. H. Avdovich of the Bureau of Drug Research, Health and Welfare Canada (Ottawa, ON). Freund's complete and incomplete adjuvant was from Difco (Detroit, MI) and Coomassie Brilliant Blue G-250 was supplied by Eastman Kodak (Rochester, NY). Fluorescamine (4-phenylspiro[furan-2(3H),1'-phthalan]-3,3'-dione) and chloramine-T were obtained from Sigma (St. Louis, MO). Inorganic salts, acids, organic solvents, formaldehyde and hydrogen peroxide supplied from Fisher Scientific were certified ACS grade. Glycine (tissue culture grade), *p*-dimethylaminobenzaldehyde and Whatman PE SIL G 250  $\mu\text{m}$  silica TLC plates were purchased from Fisher Scientific (Edmonton, AB).  $\text{Na}^{125}\text{I}$  (98 mCi/mL) was from Amersham (UK) and Sephadex G-25 was supplied by Pharmacia Biotech (Quebec, Canada).

Quantitative determination of primary amines was routinely performed using fluorescamine as described previously (23). A sample containing primary amines (1.5 mL) was vortex mixed with 0.5 mL fluorescamine in acetone (0.3 mg/mL). After ten minutes the fluorescence was measured using a Turner Model 430 Spectrofluorometer at excitation and emission wavelengths 395 and 475 nm respectively. Glycine was routinely used as the standard to compensate for changes in fluorescence intensity over a range of pH.

## **2.2.1. Preparation of KLH-SASD-LSD.**

### **2.2.1.1. Availability of primary amines on KLH.**

The number of lysines in KLH was estimated using glycine as the standard. Quantitative determination of the number of amines in KLH (0 - 25  $\mu\text{g}$ ) and glycine (0 - 1.5  $\mu\text{g}$ ) in 1.5 mL phosphate buffer (100 mM, pH 8.0) was performed using fluorescamine. A solution containing fluorescamine, buffer and no protein was used as the blank. The effect of pH on amine availability was estimated by measuring the fluorescence of KLH (25  $\mu\text{g}$ ) relative to glycine in 100 mM phosphate or carbonate buffer between pH 6.0 and 9.0. After 10 minutes the fluorescence was measured relative to the blank, which contained fluorescamine, buffer and no protein.

### **2.2.1.2. Derivatization of protein with SASD.**

The reaction efficiency of SASD with protein at different pH's was estimated by measuring the decrease in the number of amines before and after the reaction. The photoreactive group was removed from the derivatized protein prior to analysis by cleaving the disulfide bond in SASD with the reducing agent dithiothreitol (DTT). BSA was used in place of KLH to minimize solubility problems.

In the absence of light, 100  $\mu\text{g}$  BSA was reacted with SASD (0.14 mg in dry DMSO) for 2 hours in 50 mM phosphate or carbonate buffer between pH 7 and 9.5. Samples containing BSA in the absence of SASD were run in parallel for use as the blanks. DTT (0.06 mg in deionized water) was added to each sample and reacted for one hour after which excess linker and the photoreactive end were removed by centrifugal filtration (Section 2.2.2.1). The number of lysines present was determined using fluorescamine in the presence of light. The percent of lysines which

were coupled to SASD was estimated from the ratio of fluorescence measurements with and without reaction with SASD at different pH.

The coupling efficiency of SASD with KLH was estimated using at least a 20-fold molar excess of linker relative to the number of amines at optimal pH. In the absence of light, KLH (0, 25, 35, 50  $\mu\text{g}$ ) and SASD (0.25 mg in DMSO) in 50 mM phosphate buffer, pH 8.0 were stirred for 2 hours. The photoreactive end of the linker was removed using DTT and the high molecular weight fraction of interest was isolated by centrifugal filtration as described above. The number of lysines present in the retentate was quantitatively determined using fluorescamine. For comparison, samples were treated as described above in the absence of SASD (0% reaction). The percent derivatization was estimated from the ratio of the slopes before and after reaction with SASD at pH 8.0.

### **2.2.1.3. Photoactivation of SASD.**

Photolysis of the aryl azide in SASD results in a measurable decrease in the absorption maximum using an HP 8450A UV/VIS spectrophotometer. The conditions required for photoactivation were determined by exposing SASD (0.05  $\mu\text{mol/mL}$  in 50 mM pH 8.0 phosphate buffer, 1% DMSO) to different light sources. These included visible light in the laboratory, camera flashes and irradiation under long and short wave UV in a Chromato-Vue C3 (Ultraviolet Products Inc., San Gabriel, CA). The sample was placed 10 cm from 2 long wave (General Electric G15T8, 15W germicidal lamp) and 2 short wave (Sylvania Blacklite F15T8-BL, 15 Watt) phosphor coated lamps, which emit light at 254 and 365 nm. The decrease in absorbance was measured after each consecutive exposure which was used to determine conditions necessary for

the photoactivation of the aryl azide.

#### **2.2.1.4. Synthesis of KLH-SASD-LSD.**

The *N*-hydroxysuccinimide ester of SASD was coupled to the carrier protein KLH by nucleophilic substitution. All steps preceding photolysis were performed in complete darkness or in the presence of a red safety light. KLH was dissolved in 1.5 mL 100 mM pH 8.0 phosphate buffer in a 2 mL Pierce Reacti-Vial. SASD in dry DMSO was added dropwise to the protein with gentle stirring and the reaction was allowed to proceed for 2 hours in a light-tight box. A 20-fold molar excess of linker relative to the number of lysines was routinely used to compensate for hydrolysis of the ester. Derivatized KLH was separated from excess linker in the dark by either centrifugal filtration, size exclusion chromatography or dialysis (Section 2.2.2). LSD tartarate was added to purified KLH-SASD and mixed thoroughly. After freeze drying overnight, the sample was placed at a distance of 10 cm from long and short wave UV lamps for 20 minutes. Photodecomposition of LSD under these conditions was monitored by TLC on silica using a mobile phase of chloroform/methanol (9:1) (24). Thin layer chromatograms were visualized using fluorescence under UV light and by the Van Urk reagent (22).

#### **2.2.2. Purification of immunogen.**

Two purification steps are necessary during immunogen synthesis: The first, after derivatization with SASD, removes excess linker and the second, after photolysis with LSD, removes unbound drug. The requirements of the purification method are that,

- 1.) it can be performed in the absence of light in step one,
- 2.) it is effective in the presence of poorly soluble immunogen,
- 3.) it can be performed fairly rapidly.

A number of purification methods were evaluated including centrifugal filtration, size exclusion chromatography and dialysis.

#### **2.2.2.1. Centrifugal filtration.**

Centricon-10 centrifugal filtration devices (Amicon, Oakville, Ontario) were used to isolate the KLH containing species from reaction mixtures. The microconcentrator contains a 10,000 molecular weight cut off (MWCO) membrane which allows small species such as SASD and LSD to pass through. Samples containing immunogen or derivatized KLH (1.5 mL) were added to the sample reservoir and centrifuged for 40 minutes at 6000 rpm. After 3 or 4 successive cycles of washing with buffer and centrifugation, the high molecular weight retentate was removed according to the manufacturers instructions.

#### **2.2.2.2. Size exclusion chromatography.**

Sephadex-G25 was swollen overnight at 4 °C in 50 mM pH 8 phosphate buffer. A 15 x 0.7 (id) cm column was packed with Sephadex and equilibrated with buffer at a flow rate of approximately 1 mL/min. KLH (100 µg) and LSD (0.7 mg) were dissolved in 0.2 mL of buffer and 0.1 mL of this mixture was loaded on the column. A total of 45 fractions were collected in eppendorf tubes (1.5 mins/fraction). Fractions were monitored by fluorescence, Pierce BCA

protein reagent and Van Urk reagent. For fluorescence, excitation and emission wavelengths were set at 322 and 412 nm respectively and buffer eluent was used as the blank. Pierce BCA reagents A and B were mixed (50:1) according to the manufacturers instructions. In a microtitre plate 150  $\mu\text{L}$  BCA reagent and 150  $\mu\text{L}$  of each fraction were reacted at room temperature for 30 minutes before the absorbance at 550 nm was measured. The same procedure was used to separate excess linker and drug during the two step synthesis. Approximately 1 mL of immunogen or derivatized protein was separated on Sephadex G-25 as outlined above.

#### **2.2.2.3. Dialysis.**

Pierce Slide-A-Lyzer dialysis cassettes were used to separate excess linker and drug from immunogen. Small volume cassettes (0.1 to 3 mL) are available with 10,000 MWCO membranes. Sample is introduced using an 18 gauge needle through a self sealing silicone injection port and the device mounted on a buoy and placed in a stirred beaker of deionized water. This method was used for the removal of excess SASD prior to irradiation. Following reaction of KLH with SASD, sample was injected into the cassette in the dark and the dialysis performed in a light tight box. Exchange of water every 30 minutes enabled dialysis to be completed in 2 hours. The removal of excess LSD after photolysis was performed over 24 hours prior to characterization and immunization.

### 2.2.3. Characterization of immunogen: Molar substitution ratio.

#### 2.2.3.1. Radiolabelled LSD study.

The use of radiolabelled drug theoretically allows the degree of substitution to be calculated directly from the associated radioactivity of the immunoconjugate. Synthesis of 2- $^{125}\text{I}$ iodo-LSD was performed in accordance with established methods from the literature (25-27). At first, preparation, purification and characterization were performed using cold NaI.

Using freshly prepared solutions, the following were mixed in order in an eppendorf tube and heated for 15 minutes at 65 °C:

LSD tartarate, 50  $\mu\text{g}$  in 10  $\mu\text{L}$  (13.5 mM HCl/methanol, 1:1)

potassium phosphate buffer, 20  $\mu\text{L}$  (0.3 M, pH 7.2)

NaI, 20  $\mu\text{L}$  (6.3  $\mu\text{g}/\text{mL}$  in 0.1 M NaOH)

chloramine-T, 20  $\mu\text{L}$  (0.34 mg/mL)

After heating, the reaction was stopped by the addition of 300  $\mu\text{L}$   $\text{Na}_2\text{S}_2\text{O}_3$  (1 mg/mL). Alkaloids were extracted with 2 x 300  $\mu\text{L}$  volumes of 0.01% phenolic ethyl acetate and evaporated under nitrogen. Thin layer chromatography on silica using a mobile phase of chloroform/methanol (9:1) was used to separate the extracts which were visualized with iodine, UV light and Van Urk reagent. Preparative TLC was used to separate 2-iodo-LSD from LSD. Bands of silica were excised and extracted with mobile phase after which the UV and fluorescence spectra were used to confirm the presence of iodinated drug.

Isotope labelled 2- $^{125}\text{I}$ iodo-LSD was prepared as above except that 5  $\mu\text{L}$  of 2 mCi  $\text{Na}^{125}\text{I}$  in 0.1 M NaOH (98.0 mCi/mL) was used in place of unlabelled NaI. Alkaloids were extracted with 4 x 300  $\mu\text{L}$  volumes of 0.01% phenolic ethyl acetate and separated by preparative TLC as

outlined above. After evaporation of the ethyl acetate under nitrogen, the residue was redissolved in methanol and stored in a lead chamber at  $-20^{\circ}\text{C}$ . The activity of purified 2- $^{125}\text{I}$ iodo-LSD was measured in an LKB Model 1282 gamma counter (Wallac LKB, Turku, Finland) and the concentration of labelled material was calculated from the specific activity of  $^{125}\text{I}$  (2175 Ci/mmol) (26).

KLH-SASD- $^{125}\text{I}$ -LSD was prepared using a mixture of labelled and unlabelled LSD during synthesis. Immunogen (100  $\mu\text{g}$ ) was prepared in the usual way (Section 2.2.1.4) except that excess SASD was not removed prior to irradiation. Unlabelled LSD (8.5 mg) and  $^{125}\text{I}$ -LSD ( $6.7 \times 10^5$  cpm) were added to the mixture and photolyzed in the usual manner. The high molecular weight fraction of interest was separated on a Sephadex G-25 column, 15 x 0.7 (id) cm, equilibrated with 100 mM pH 8 phosphate buffer. Fractions were identified using Bradford dye binding reagent and by  $\gamma$ -counting.

#### 2.2.3.2. Fluorescence and protein quantification.

Concentrations of LSD and KLH in the antigen were estimated using spectrofluorometry and colorimetric protein assays respectively. The purified KLH-SASD-LSD immunogen was poorly soluble so antigen preparations were allowed to stand overnight at  $4^{\circ}\text{C}$  after which the clear supernatant layer containing soluble fraction (typically  $< 10 \mu\text{g}/\text{mL}$ ) was removed for analysis.

The fluorescence of LSD between 0 - 50 ng/mL in deionized water was measured using a Turner Model 430 Spectrofluorometer. Wavelengths of excitation and emission were set at 322 nm and 412 nm respectively corresponding to fluorescence characteristics of LSD. The

fluorescence of soluble antigen was measured along with appropriate blanks and the concentration of LSD was interpolated directly from the calibration graph. Quantitative estimation of LSD in KLH-SASD-LSD in this manner assumes no change in fluorescence characteristics due to coupling. The fluorescence spectrum of the soluble immunogen indicated the excitation and emission wavelengths were unchanged. However, it is not known whether the intensity of the LSD fluorescence changes once the drug is bound.

The concentration of KLH in the soluble antigen was estimated by the Bradford method (18) in which the volumes were modified to allow measurements to be made in a microtitre plate. Bradford dye binding reagent (Appendix I) (200  $\mu$ L) and sample (100  $\mu$ L) were mixed and the absorbance of the protein-dye complex was measured using an SLT microtitre plate reader EAR 400 AT (SLT-Labinstruments, Austria) at 550 nm relative to the blank, which contained no protein. KLH calibration standards were typically in the 0 - 25  $\mu$ g range. The Pierce BCA protein assay was also used according to the manufacturers instructions (59).

#### **2.2.4. Optimization of photocoupling conditions.**

Molar substitution ratios (MSRs) were used to describe the efficiency of the photocoupling step. Of particular interest were,

- 1.) the ratio of LSD to KLH present in the reaction mixture during photolysis,
- 2.) photolysis performed on liquid and solid phase matrices,
- 3.) the effect of buffer components in the reaction mixture.

KLH-SASD was prepared as in Section 2.2.1.4. and purified by gel filtration in the absence of

light. Samples containing varying excesses of LSD to KLH (w/w) were photolyzed as a dry matrix and purified by gel filtration. The molar substitution ratios of soluble antigen fractions was determined using LSD fluorescence and Bradford dye binding measurements. Immunogen was prepared as outlined above except that gel filtration purification was replaced by dialysis against deionized water. Using this method, photolysis was performed in the absence of any buffer components.

The efficiency of liquid and solid phase photolysis was investigated. KLH-SASD prepared in the usual way (Section 2.2.1.4) was purified by gel filtration. LSD was added and the sample divided in two; one portion was freeze dried, the other left in buffer solution. Solid and liquid phase reaction mixtures were photolyzed and purified by gel filtration. Molar substitution ratios were determined in the usual way.

#### **2.2.5. Control immunogen.**

In order to evaluate any improvement in antisera quality obtained using the novel immunogen (KLH-SASD-LSD), an LSD conjugate was synthesised using conventional coupling chemistry. The Mannich reaction is the most common method for direct linkage of the indole nitrogen of LSD to amine groups in the protein (1,5,28,29). However, it was necessary to prepare KLH-LSD with a molar substitution ratio of approximately 35, so that hapten densities in both conventional (Mannich) and novel (photolinked) conjugates were comparable.

##### **2.2.5.1. Preparation of KLH-LSD by the Mannich reaction.**

The method of Taunton-Rigby (1) was modified to facilitate coupling of LSD to KLH at

a pre-specified level. Concentrations of LSD and formaldehyde were varied in order to obtain conjugates with different degrees of substitution. The following procedure was used to prepare KLH-LSD with an MSR of 37. In a 1 mL Pierce Reacti-Vial, 200  $\mu$ L 2M sodium acetate was added to 1 mg KLH. With gentle stirring, 40  $\mu$ L formaldehyde (38%) was added dropwise. After 5 minutes stirring, 0.5 mg LSD in 100  $\mu$ L of deionized water was added dropwise. The reaction was allowed to proceed for 2 hours after which excess LSD was removed by dialysis over 24 hours. The immunogen was freeze dried and stored at -20 °C until required for immunization.

#### **2.2.5.2. Characterization of control immunogen.**

The molar substitution ratio in purified control immunogen was estimated in two ways. First, by fluorescence spectroscopy and Bradford dye binding (Section 2.2.3.2) which was routinely used for characterization of the photolinked immunogen. The only difference was that KLH-LSD prepared by the Mannich reaction was more soluble than KLH-SASD-LSD and did not require overnight clearing. The degree of substitution was also determined using UV absorption spectroscopy (1). The characteristic absorption wavelengths of protein and drug at 280 and 310 nm respectively were used to estimate the amount of LSD bound to KLH as previously described (1,30,31).

#### **2.2.6. Immunization and antibody production.**

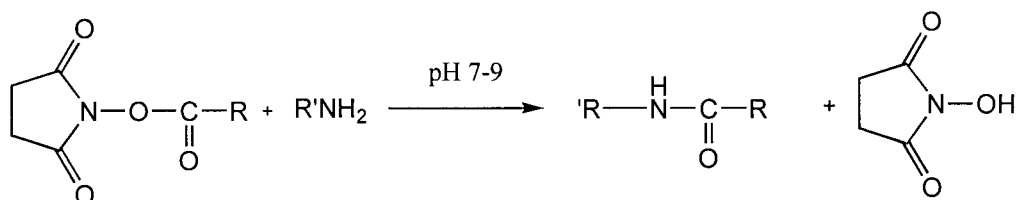
Two female New Zealand White rabbits were immunized with the KLH-SASD-LSD (photolinked) immunogen and two received the control (Mannich) immunogen KLH-LSD. Each rabbit received a prime injection and three boosts of emulsified antigen using Freund's adjuvant.

The prime injection consisted of 150  $\mu\text{g}$  antigen per rabbit in a 1:1 mixture of aqueous antigen and Freund's Complete Adjuvant (FCA). A total volume of 2 mL was injected sub-cutaneously over 6 sites on the neck. Boosts were prepared with 150  $\mu\text{g}$  antigen per rabbit in a 1:1 mixture of aqueous antigen and Freund's Incomplete Adjuvant (FIA). The total volume was 1 mL which was injected intra-muscularly at two sites in the thigh muscle. Blood was collected from the femoral vein 10 - 14 days after the booster injections. Serum was aliquoted into small volumes and stored at  $-70\text{ }^{\circ}\text{C}$  for further use.

## 2.3. Results and discussion.

### 2.3.1. Conditions for the derivatization of KLH with SASD.

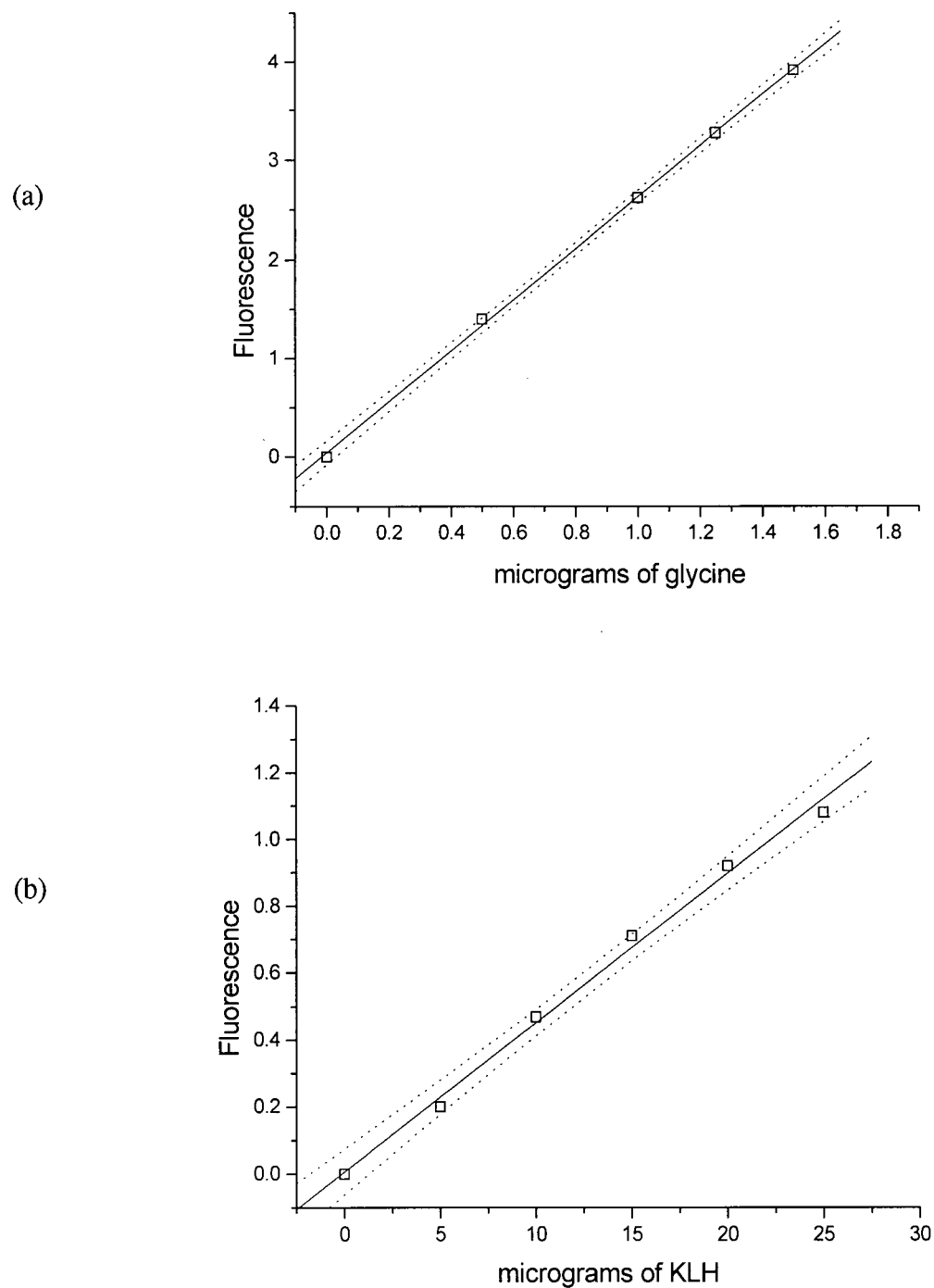
NHS esters are reactive towards the  $\epsilon$ -amine of lysine which is available on most protein surfaces. Whilst a number of other amino acids have nitrogen in their side chain, only lysines react significantly under neutral to alkaline conditions to form a stable amide bond as shown below.



Reactions with other side chains are possible, but proceed with very poor efficiency (13,30). Therefore the number and availability of primary amines on KLH is a performance limiting factor during immunogen synthesis. A high degree of substitution of SASD on KLH is necessary for the subsequent covalent attachment of LSD and to increase the immunogenicity of the antigen.

The linear relationship between fluorescence and primary amines detected by fluorescamine is shown in Figure 2.1. The number of lysines in KLH at pH 8.0 was determined using fluorescamine which reacts with primary amines to yield highly fluorescent species (17,23). Linear regression analysis for glycine and KLH gave the equation of the lines to be  $y = 2.59 \times 10^{-1}x + 4.03 \times 10^{-3}$  ( $r = 0.999$ ,  $n = 5$ ) and  $y = 4.46 \times 10^{-3}x + 6.19 \times 10^{-4}$  ( $r = 0.997$ ,  $n = 6$ ) respectively, where the units of the  $x$  and  $y$  axes are  $\mu\text{g}$  of substrate and arbitrary fluorescence.

**Figure 2.1** Quantitative determination of primary amines using the fluorescamine assay, (a) glycine, (b) KLH. Dotted lines represent 95% confidence limits. Comparison of the slopes predicts there to be  $689 \pm 34$  lysines on one KLH assuming a molecular mass of  $3 \times 10^6$  (32).



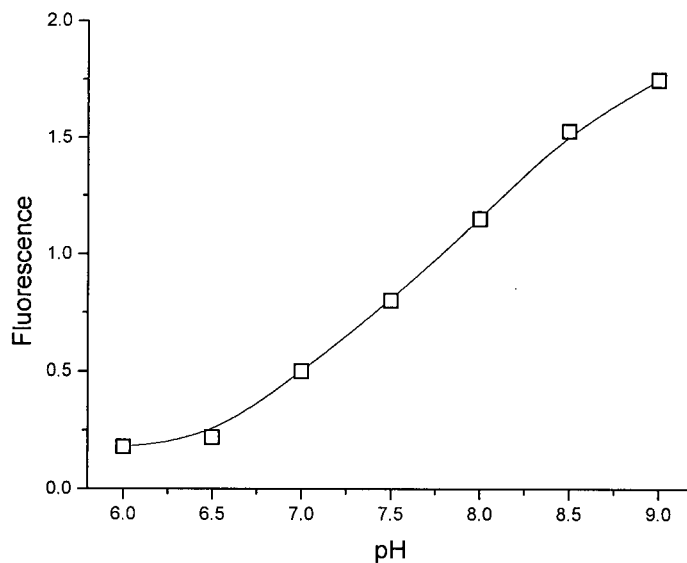
A comparison of the slopes predicts there to be  $2.3 \times 10^4$  ( $\pm 5\%$ ) lysines per gram of KLH, corresponding to a total of  $689 \pm 34$  lysines on one KLH molecule assuming a molecular mass of  $3 \times 10^6$ . Despite poor characterization of the protein due to its large size, amino acid analysis of KLH suggests that there are about 879 lysine residues assuming the same molecular mass (32).

Only unprotonated amines are reactive towards NHS esters, therefore it is necessary to use a pH at which a significant number of amines are uncharged. Fluorescamine was also used to determine the pH conditions under which the concentration of unprotonated amines at the time of the reaction was maximised (Figure 2.2(a)). A shift in pH from neutral to alkaline more than triples the fluorescence, which is linearly related to the number of primary amines. This is in accordance with the increased number of unprotonated  $\epsilon$ -amines in lysine at alkaline pH.

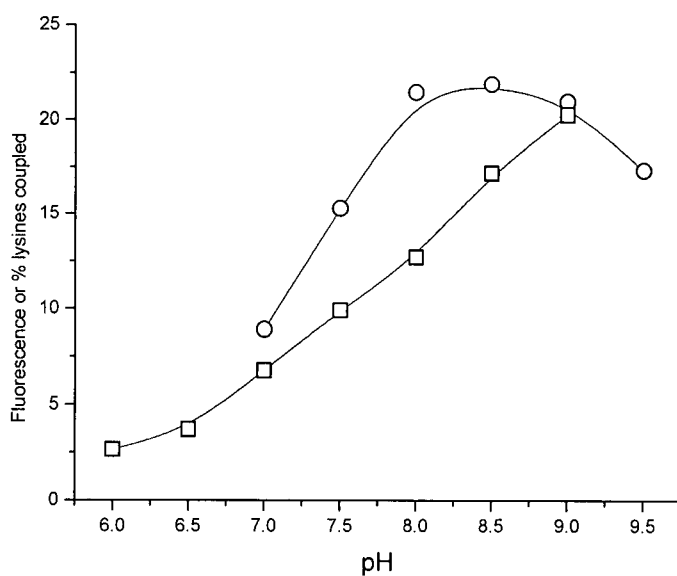
Fluorescence measurements before and after reaction with SASD at varying pH were used to estimate the number of lysines which had been derivatized with SASD. Figure 2.2(b) illustrates the delicate balance between competing aminolysis and hydrolysis reactions. Increasing stoichiometry with increasing pH is the result of deprotonation of amine groups whereas the decrease in reaction efficiency at elevated pH is the result of hydrolysis of the active ester. A shift of one pH unit from 7 to 8 increased the derivatization of lysines on BSA from 9% to 22%. Therefore, a pH of 8.0 was chosen as a compromise between the number of available amines and the lability of the ester. The ester moiety of SASD although stable at acid pH, hydrolyses to *p*-azidosalicylamido-1,3'-dithiopropionate (ASD) and *N*-hydroxysuccinimide (NHS) under alkaline conditions. The half life of NHS-esters at pH 9, 7.5 and 5 is reported to be 1, 14 and >90 minutes respectively (33). Optimum substitution is achieved when a large molar excess of linker is used to overcome inefficiencies due to hydrolysis (13). Molar excess of 200 or more are not uncommon (10,32).

**Figure 2.2 (a)**

Effect of pH on the availability of unprotonated lysine residues on KLH using the fluorescamine assay.

**Figure 2.2 (b)**

The effect of increasing pH on % lysines which are coupled with SASD. The percent of lysines which were coupled at different reaction pH (circles) is shown with the availability of primary amines on the protein at different pH (squares).



The reaction efficiency of SASD with KLH was estimated by the decrease in fluorescence after different amounts of protein were coupled to a large molar excess of NHS ester at pH 8.0. Linear regression analysis of the results gave the equations of the lines for derivatized and underivatized KLH to be  $y = (8.3 \pm 0.9) \times 10^{-4} x + 1.7 \times 10^{-4}$  ( $r=0.989$ ) and  $y=(1.85 \pm 0.3) \times 10^{-3} x + 5.5 \times 10^{-4}$  ( $r = 0.975$ ), where the units of  $x$  and  $y$  were  $\mu\text{g}$  KLH and fluorescence respectively. The relative change in fluorescence per  $\mu\text{g}$  of protein suggests that the  $45\% \pm 13\%$  of the lysines on KLH were derivatized with SASD which is comparable to other reports (34). This corresponds to about 310 SASD moieties covalently linked to one molecule of KLH.

It should be noted that although SASD has a sulfonate group which increases its solubility in water, it is recommended that the linker be dissolved in DMSO first. Solubility problems are frequently encountered, indicated by turbidity. Incorporation of a co-solvent such as DMSO or DMF up to 20 - 30% has been suggested to reduce precipitation (30). The KLH-SASD conjugate is less soluble than native KLH partly due to the electrostatic changes caused by the replacement of positively charged amino groups with neutral amides. This may upset the natural folding of the molecule and cause the conjugate to be less stable and liable to precipitate. The reduction in the surface charge on the protein after reaction with the active ester is reported to decrease the solubility of some conjugates up to 30-fold in some instances (35).

### **2.3.2. Conditions for the photoactivation of SASD.**

Conditions for coupling LSD to KLH-SASD were a balance between activating the linker and preventing photodegradation of LSD. According to the literature, the  $\lambda_{\text{max}}$  of phenyl azides decreases on UV irradiation (34,36) and complete photolysis results in a 40% decrease in the absorption maximum (37). As such, the change in absorption maximum for SASD was measured

by spectrophotometry. The photolysis of aryl azide-containing heterobifunctional linkers has been reported to be insignificant during scanning (38). The  $\lambda_{\text{max}}$  of SASD was 267 nm in pH 8 phosphate buffer (1% DMSO) and the extinction coefficient ( $\epsilon_{267}$ ) was  $3.16 \times 10^4 \text{ M}^{-1} \text{ cm}^{-1}$ . The percent decrease in  $A_{267}$  with increased exposure to light is shown in Table 2.1. Measurement of SASD absorption at 267 nm showed that 20 minutes irradiation was sufficient for activation and more prolonged irradiation had little effect on efficiency. These conditions were routinely employed for the activation of KLH-SASD with LSD. Complete reaction of the aryl azide resulted in a  $\Delta\epsilon_{267}$  of  $1.4 \times 10^4 \text{ M}^{-1} \text{ cm}^{-1}$  (45%) which is in accordance with literature reports (34,39,40).

**Table 2.1.** Conditions for the photoactivation of SASD.

Irradiation conditions	$A_{267}$	% decrease in $A_{267}$
None	1.58	0
10 minutes on bench top	1.58	0
6 camera flashes	1.58	0
10 minutes under long and short UV lamps	1.04	34
20 minutes under long and short UV lamps	0.90	43
30 minutes under long and short UV lamps	0.87	45

### 2.3.3. Immunogen synthesis.

As expected, the new LSD immunogen was poorly soluble in the solvents used. KLH-SASD-LSD tends to precipitate, particularly during the final purification step following UV photolysis. When pure immunogen was allowed to stand overnight at 4 °C, sedimentation resulted in a clear supernatant of soluble immunogen, typically around 5  $\mu\text{g}/\text{mL}$ . Concentration of this fraction resulted in further precipitation which indicates that KLH-SASD-LSD is several orders

of magnitude less soluble than the native protein.

One disadvantage of the photolabelling method is that aryl azide and protein have overlapping UV absorption wavelengths. Fortunately, the linker has higher molar absorptivity (of the order  $10^4$ ) such that photolysis can be completed before appreciable photolytic damage occurs. In our case, denaturation of the protein is not important as this is unlikely to reduce the immunogenicity of the conjugate. However, the effect of UV photolysis on the drug is of much greater importance. Irradiation of LSD in aqueous acidic media results in the addition of water across the C9-10 double bond to give lumi-LSD (41). Thin layer chromatography has been used to study a number of uncharacterized LSD photodegradation products which can be identified by the Van Urk reagent, or by fluorescence, which is sensitive to about  $0.05 \mu\text{g}$  (24,42,43). Lumi-LSD, which is not fluorescent, can be readily identified by TLC using the Van Urk reagent down to  $10 \mu\text{g}$  (44). When 1 mg LSD was irradiated in the dry immunogen matrix, TLC revealed only one fluorescent species with an  $R_F$  value corresponding to LSD. This indicated that photodecomposition, if any, following immunogen synthesis was less than 1%. This favourable outcome may be related to photolysis taking place in the absence of bulk water, as it is understood that the photodegradation of LSD is heavily solvent dependent (24). For example, a solution of LSD in chloroform photodecomposes readily under UV light, whereas the drug can be irradiated in benzene for several hours with virtually no photodecomposition of the molecule (45).

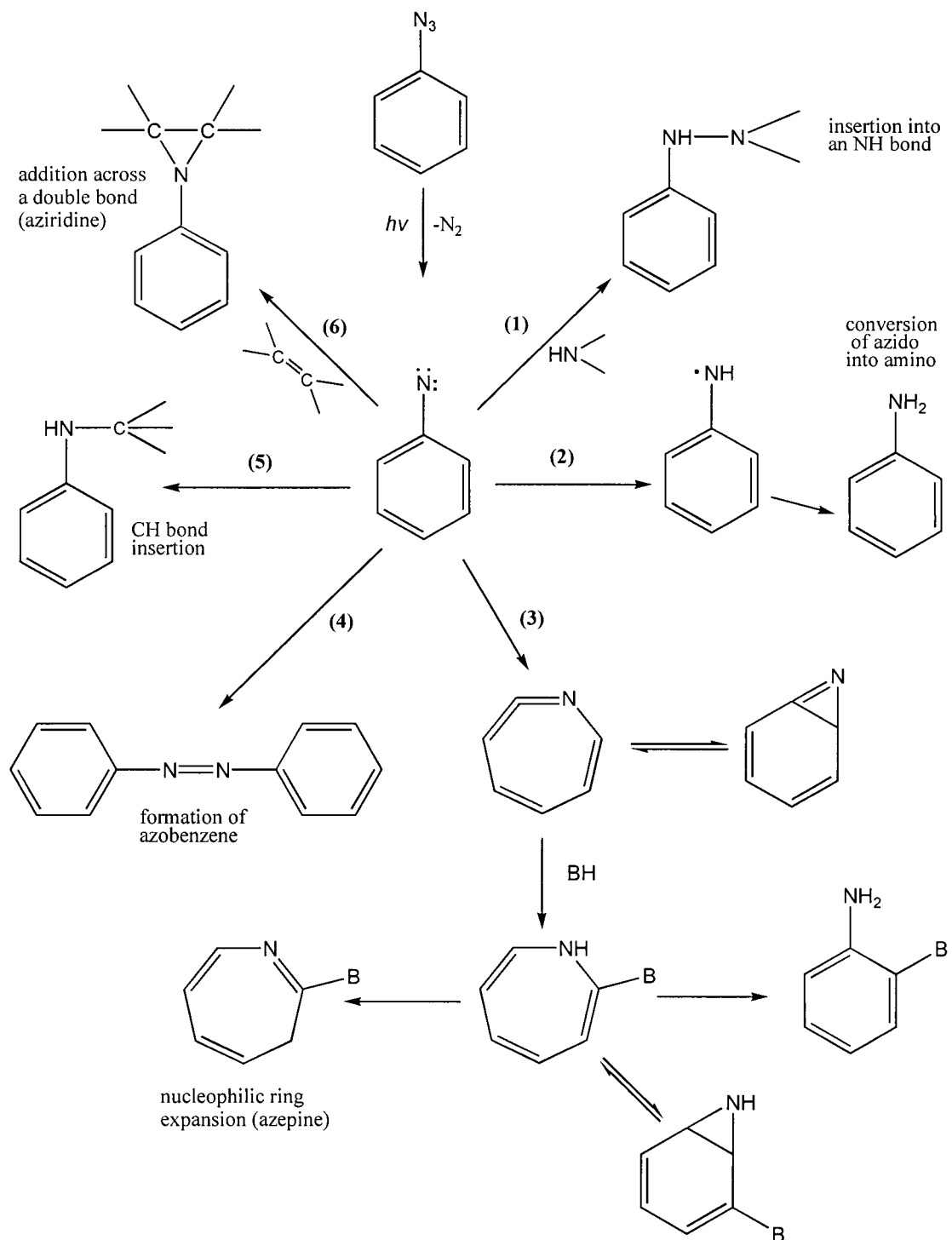
#### **2.3.3.1. Theoretical considerations.**

Insertion of aryl azides in model systems such as cyclohexane or diethylamine is well documented, although investigation of protein conjugates is rarely attempted. The relationship between insertion characteristics of the nitrene in a model system compared to a macromolecule

is extraordinarily difficult due to the variety of functional groups and environments in the protein (40). Aryl azide chemistry has been studied for many years although a number of important details are incompletely understood. The photochemistry involves 3 excited states and at least 6 short lived ground state intermediates. There is still some confusion regarding the role of these species in the photochemistry of aryl azides, which has been described as a wonderfully complex system (46). Photolysis of phenyl azides usually results in multiple reaction pathways of highly amorphous products which makes interpretation and identification often difficult. To complicate things further, the products are highly variable, depending on reaction conditions such as an inert or reactive solvent systems and the characteristics of the light source as well as substituent groups on the aryl azide ring. However, in simplified terms, some important reactions of aryl azides are shown in Figure 2.3. which can be summarized as follows:

- (1) Insertion into an NH bond.
- (2) Reduction of azido to an amino group.
- (3) Ring expansion and reaction with a nucleophile.
- (4) Formation of azobenzene.
- (5) Insertion into a CH bond.
- (6) Addition across a double bond.

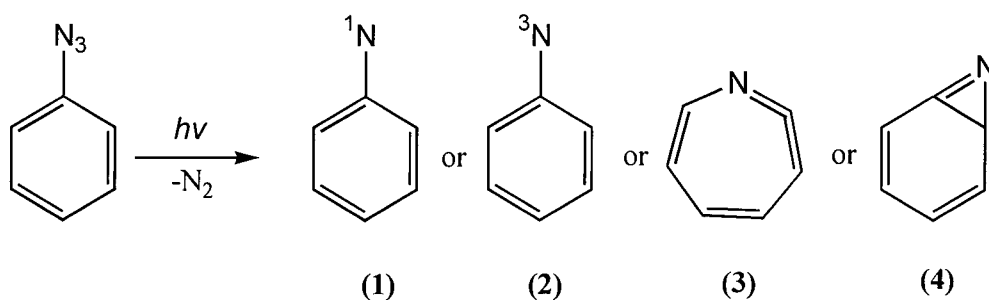
Figure 2.3. Important reactions of aryl azides.



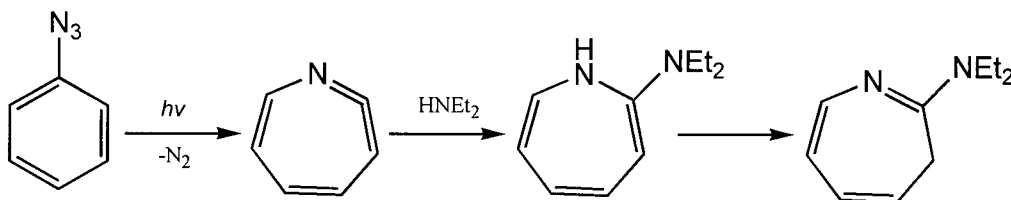
It should be noted however that the most favourable reaction pathways are primarily dependent on the electrophilic character of the nitrene and its environment. CH insertion products are produced using very strongly electrophilic nitrenes, such as polyfluorinated phenyl azides. Strong electron withdrawing groups increase the reactivity of the nitrene towards CH bond insertion. Aryl azides without such substituents are more likely to react with other groups, such as nucleophiles, especially if they are embedded in a nucleophilic environment, such as a protein molecule.

The photochemistry of aryl azides in the presence of nucleophilic species is almost exclusively described in the literature using diethylamine. The reactivity of the nitrene is heavily environment dependent, so a comparison of reactivities between diethylamine and the immunogen, which has an abundance of nucleophilic groups, is highly tentative. However, it likely provides some useful information regarding the possible sites of attachment of KLH-SASD on LSD.

Photolysis of parent phenyl azide leads to fragmentation to molecular nitrogen and reactive intermediate  $C_6H_5N$ . The structure of  $C_6H_5N$  is a singlet phenyl nitrene (1), or triplet phenyl nitrene (2), which rearranges to a ketenimine (also called azacycloheptatetraene or dehydroazepine) (3) or benzazirine (4):



It has been suggested that the dehydroazepine is the major trappable species (47), which, in the absence of amines can polymerize. In non-nucleophilic solvents, the major products are aniline, azobenzene and tar. However, in the presence of diethylamine, ring expansion followed by nucleophilic reaction occurs to form an azepine:



Triplet sensitization was shown to increase the yields of azobenzene and aniline, which supports the proposal that these products are the result of the triplet phenyl nitrene whereas azepines and related nucleophilic incorporation products are the result of the singlet species. The substituents on the phenyl azide ring can change the mechanism of the reaction greatly eg. pentafluorophenylazides produce triplet nitrenes exclusively (46).

Perhaps the most important difference between the literature reports of phenyl nitrene chemistry and the system we describe is the use of a solid matrix for photoactivation. There have been relatively few reports of the effect of temperature and phase on aromatic nitrene chemistry. Although these simple systems do not resemble KLH-SASD in the presence of LSD, a number of interesting observations have been made. A study using polyfluorinated phenyl azide and frozen toluene in a crystalline matrix gave near quantitative yields of CH insertion products via radical recombination. Dimerization to form azo compounds was retarded as a result of matrix conditions (48). It has been suggested elsewhere that in a restricted environment, such as solid state or ligand bound to macromolecule, that radical coupling predominates due to restricted movement of the

reactive species (49). The increase in CH insertion products via radical recombination as a result of a "rigid" matrix, was used to suggest that the trapping of aryl azide in the hydrogenic crevices of the protein results in higher protein labelling efficiencies (40).

The photoactivation of KLH-SASD in the presence of LSD could result in any number of possible reactions given the complexity of the matrix and the menagerie of functional groups present. This results in a mixture of both favourable and unfavourable reaction products of high molecular weight in the immunogenic mixture.

The most desirable reactions are between KLH-SASD and LSD, of which there are a number of hypothetical products. Azepine type conjugates may result from the reaction between the electrophilic nitrene and nucleophilic substituents on LSD. Lone pairs on nitrogen in amines and other nucleophiles are known to attack the nitrene. The nitrogen in the 6 position is strongly basic due to the presence of three electron donating alkyl groups. The indole nitrogen, which is less basic due to the aromaticity of the indole ring, could also react with a nitrene to form an azepine. Addition across double bonds could also occur at a number of sites on the LSD molecule, although there are very few reports of stable aziridine products from such reactions (50). Singlet nitrenes can insert into CH bonds with varying efficiencies depending on the CH bond strength. The possible site for this reaction could be the hydrogen in the 2 position, which would lead to formation of an amine. Phenyl azides are also capable of NH insertion reactions which could take place at the indole nitrogen to produce a hydrazine product. In summary, there are more than half a dozen hypothetical reaction sites on LSD which would result in covalent attachment of the drug to the modified protein.

However, there are a greater number of undesirable reactions which might occur in the reaction matrix. Perhaps the most likely of these is the reaction between aryl azide and

neighbouring amino acids. The reactivity of phenyl nitrenes with functional groups found in biological molecules is unquestionable. In particular, reactivity with aryl (Phe, Tyr, Trp, His), N-H (Lys, His, *N*-termini), O-H (Ser, Thr, Try) and S-H (Cys) has been suggested (51). In one report photolysis of  $^{125}\text{I}$ -SASD in the presence of BSA indicated incorporation of radiolabel into His, Thr, Lys, Cys, Glu and Asp (52). It is quite likely that the bulk of the nitrene reactivity is towards these groups and not the target molecule LSD. For this reason, it is necessary to use a large excess of drug during photolysis to increase the chance that SASD reacts with a drug molecule. In this way, we are using LSD as a "scavenger". In conventional photoaffinity labelling, scavengers are used to preferentially react with photogenerated intermediates at places other than the ligand binding site between protein and receptor. Nucleophilic molecules such as tris and *p*-aminobenzoic acid have been used for this purpose (12). In a sense, LSD which contains some of the same groups which are reactive with electrophilic nitrenes, is being used as a scavenger to bind non-specifically with photolabelled protein.

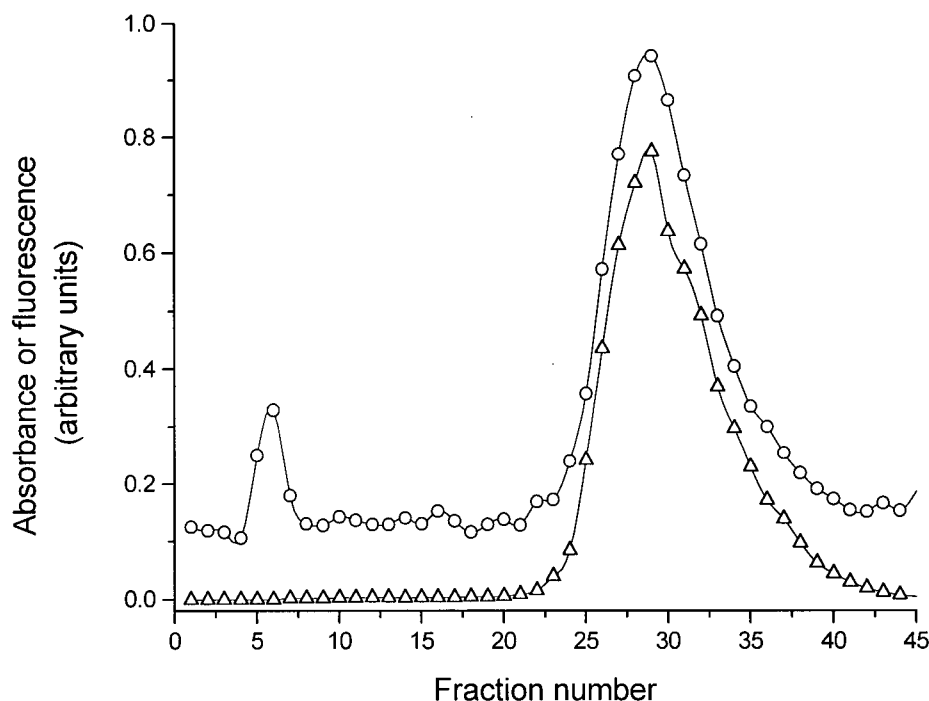
Additional unwanted reactions can occur between the aryl azide and water or buffer components in the mixture. This has been blamed for the poor efficiencies of many photoreactive conjugation processes (12). Other unwanted reactions might involve the formation of aniline or azobenzene type products. In the latter case, the reaction between two aryl azide moieties in the immunogen is unlikely due to the low concentration of KLH-SASD and the restricted mobility of the derivatized protein. However, intramolecular crosslinking can occur in the same protein molecule if the two aryl azide groups are in close enough proximity.

#### 2.3.4. Purification of immunogen.

Centrifugal filtration was explored for purification purposes. Recovery of underivatized KLH from such a process was 70% but when the same method was used for milligram quantities of derivatized protein, recoveries were poor. Immunogen precipitated out during centrifugation and adhered to the membrane which resulted in incomplete separation and sample loss. Centricon-10 filtration devices were only suitable for very dilute solutions ( $\mu\text{g/mL}$ ) of derivatized protein or immunogen.

Size exclusion chromatography was used to separate high and low molecular weight species. Figure 2.4 shows the elution profile of uncoupled KLH and LSD on Sephadex G-25. BCA reagent allows both KLH and LSD to be identified simultaneously in fractions 6 and 30 respectively. Fluorescence was the only selective test for the identification of fractions containing LSD. Purification of KLH-SASD-LSD by gel filtration resulted in very poor recoveries. This was due to the low solubility of KLH-SASD-LSD which resulted in significant sample loss, sometimes greater than 80%. In order to pool sufficient conjugate to immunize rabbits, an alternative method of purification was required.

**Figure 2.4.** Gel filtration separation of KLH and LSD standards on Sephadex G-25. BCA reagent (open circles) and Fluorescence,  $\lambda_{ex}$  and  $\lambda_{em}$  322 and 412 nm (open triangles).



Dialysis using a Pierce Slide-A-Lyzer provided the most effective means of immunogen purification in terms of recovery, efficiency and solubility. UV absorption of dialysate indicated that excess SASD was removed from KLH-SASD in 2 hours with half hourly water changes. Fluorescence of dialysate during removal of LSD showed that after 2, 3 and 20 hours dialysis 0.72, 0.04 and 0% total LSD remained. The recovery of KLH after 24 hours of dialysis was 56%. Measurement of protein concentration over time revealed that sample loss occurs in the first 2 hours, which suggests this is due to adsorption of protein on the membrane. Less precipitation occurred during dialysis than with other purification methods which not only minimized sample loss, but also aids solubilization of immunogen for characterization purposes.

### 2.3.5. Characterization of immunogen.

The difficulty in identifying and characterizing crosslinked aryl azide conjugates which generate a number of products has been noted (53). The conjugate matrix likely contains a mixture of species with varying degrees of substitution (30). However, it is generally necessary to make an estimate of the average number of haptens coupled to carrier as a measure of the success or failure of the coupling procedure. In this instance, characterization of the purified immunogen was necessary primarily to confirm that covalent attachment of drug had taken place, and secondly to determine the most favourable conditions for optimum substitution.

A number of established techniques for the determination of molar substitution ratios were not applicable for the novel KLH-SASD-LSD immunogen. Mass spectrometric determinations require the antigen to be soluble at 0.3 mg/mL or greater (54,55). In our case the antigen was only soluble up to about 5  $\mu\text{g/mL}$  which was below the detection limit of the technique. Direct spectroscopic determination of the MSR was not possible because SASD overlaps with the wavelengths of interest for both protein and drug in the immunogen.

#### 2.3.5.1. Iodination of LSD.

A modified procedure based on existing methods was used to prepare 2-iodo-LSD from LSD using unlabelled sodium iodide. TLC revealed two spots of interest with  $R_f$  values  $> 0$  as outlined in Table 2.2.

**Table 2.2.** TLC separation of LSD and 2-iodo-LSD. (Mobile phase  $\text{CHCl}_3/\text{MeOH}$ , 9:1).

$R_F$ value	0.23	0.52
visualization in iodine	strong	weak
visualization under UV light	strongly fluorescent	weakly fluorescent
Van Urk reagent	blue (positive)	no colour (negative)
Inference	LSD	2-iodo-LSD

The Van Urk reagent, which contains *p*-dimethylaminobenzaldehyde, is specific for unsaturated indoles (22). Therefore it produces a characteristic blue colour with LSD but not with iodinated counterpart, which is substituted in the 2-position. Preparative TLC was used to separate the mixture and a UV spectrum in methanol revealed characteristic absorption maxima at 242, 310 nm (LSD) and 227, 285 nm (2-iodo-LSD) respectively, which confirmed the TLC observations. The fluorescence spectrum of 2-iodo-LSD in methanol revealed the maximum emission wavelength to be 420 nm when the excitation wavelength was 340 nm which is in agreement with the literature (25). The total activity of purified 2- $^{125}\text{I}$ iodo-LSD was  $4.4 \times 10^7$  dpm (20  $\mu\text{Ci}$ ) and the specific activity was  $2.175 \times 10^6$  Ci/mol, assuming that all  $\gamma$ -counts were due to  $^{125}\text{I}$  and that only one iodine is attached to each LSD.

### 2.3.5.2. Estimation of the MSR using KLH-SASD- $^{125}\text{I}$ -LSD.

Although size exclusion chromatography was not suitable for purification on a preparative scale, it did provide qualitative information regarding the composition of the immunogen reaction mixture. The elution profile in Figure 2.5 which indicates 3 major peaks bears striking resemblance to Sephadex G-25 chromatography of a BSA-metoclopramide derivative prepared

using a heterobifunctional aryl azide linker (10). The Bradford reagent indicates there to be one major protein containing peak which also contains  $^{125}\text{I}$ . The two low molecular weight peaks identified by  $\gamma$ -counting were tentatively identified as free 2- $^{125}\text{I}$ iodo-LSD and 2- $^{125}\text{I}$ iodo-LSD-SASD using TLC and UV absorption spectroscopy (Table 2.3).

**Figure 2.5.** Purification of the radiolabelled immunogen by size exclusion chromatography. Bradford dye binding reagent for proteins (open triangles) and radioactive counts per minute (closed circles).

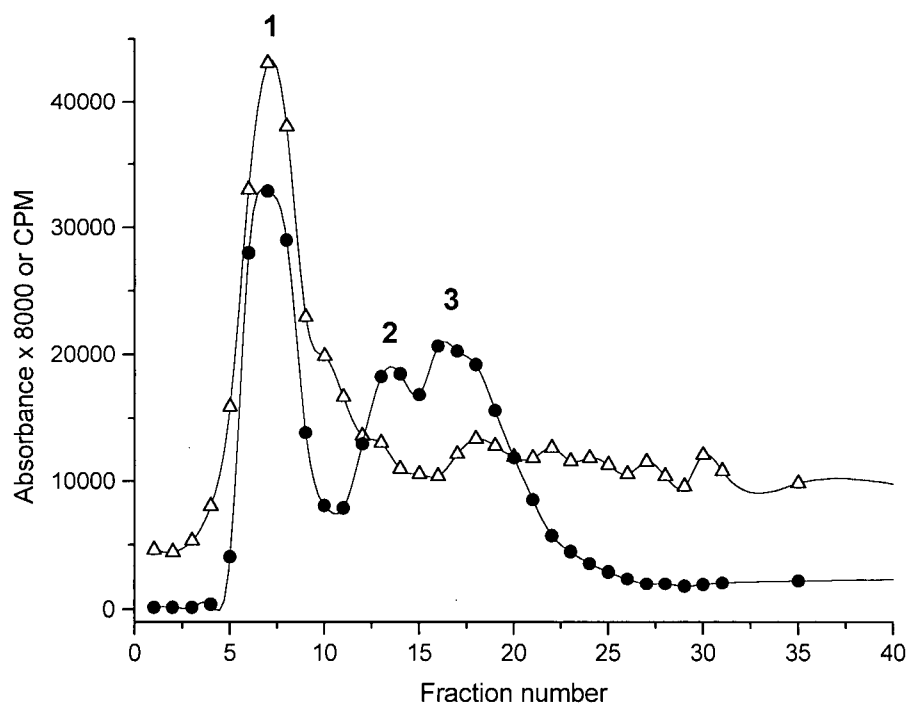


**Table 2.3.** Qualitative identification of fractions separated by gel filtration chromatography.

Peak #	Observation	Inference
1 (KLH-SASD-LSD)	Positive Bradford colour test (blue) TLC (benzene/chloroform/ethyl acetate/acetic acid) 1:1:1:0.1 $R_F=0$ ( $I_2$ ) UV absorption spectrum $\lambda_{max}$ 267 nm above background $\gamma$ count	contains KLH no unbound SASD  characteristic of SASD contains 2-[ $^{125}$ I]iodo-LSD
2 (SASD-LSD)	Negative Bradford test UV absorption $\lambda_{max}$ 267 and 315 nm TLC (MeOH) $R_F=0.38$ (FL) above background $\gamma$ count	no KLH characteristic of SASD contains LSD contains 2-[ $^{125}$ I]iodo-LSD
3 (LSD)	TLC (methanol) $R_F=0.58$ & 0.38 (FL) UV absorption $\lambda_{max}$ 309 nm (no 267 nm) above background $\gamma$ count	2-[ $^{125}$ I]iodo-LSD & LSD characteristic of LSD contains 2-[ $^{125}$ I]iodo-LSD

The activity of pooled protein fractions was  $5.3 \times 10^4$  cpm which indicates that 7.9% of the total counts added were incorporated into KLH. Assuming that during photolysis LSD and 2- $^{125}\text{I}$ iodo-LSD react with SASD to the same degree then  $2.1 \times 10^{-6}$  moles LSD are bound to 100  $\mu\text{g}$  KLH. This corresponds to a substitution ratio of the order  $10^4$  LSD molecules attached to one KLH, which is extremely high. At best, assuming that LSD is coupled only via the SASD linker arm attached to lysines on the protein, the maximum number of LSD molecules which can be coupled to one KLH is around 689. Although SASD can react with other groups on the protein, it does so with poor efficiency and this could not explain the difference. A possible explanation could be a non covalent association of drug on KLH. Thin layer chromatography of the purified immunogen on silica using a mobile phase of chloroform/methanol (9:1) showed that this was not the case. However, it did reveal a non-protein spot with an  $R_F$  value which did not correspond with either LSD or its iodinated counterpart. The spot was not fluorescent but  $\gamma$ -counting showed that it contained significant amounts of  $^{125}\text{I}$ . Attempts to separate this radioactive impurity from the protein were unsuccessful and although the substance could not be identified, it contributes to the excessively high MSR obtained by this method.

$^{125}\text{I}$  labelled tracers are frequently used to determine coupling efficiencies in photoaffinity labelling techniques (52). However, there are reports of photodeiodination (56) and in one instance, as much as 50% of the iodine was released during photolysis and incorporated into surrounding macromolecules in a non-specific manner (39). The photo-dissociation of iodine from  $^{125}\text{I}$ -LSD into surrounding KLH may be a possible explanation of the magnitude of error in the MSR. Another area of concern is the possible C-I bond fission which has been reported to occur in radiolabelled hormones which were photolyzed with UV light (57). This not only results in incorporation of radiolabel into neighbouring amino acids, it might also pose a potential safety

risk. The use of radiolabelled analogues for characterization of bioconjugates prepared using conventional chemical coupling is unquestionable. However, reports of label transfers during the preparation of photolinked conjugates, which is sometimes referred to as “dark labelling”, casts some doubt on the reliability of the method in this instance.

### **2.3.5.3. Estimation of LSD incorporation by fluorescence.**

LSD has a high fluorescence quantum yield which allows spectrofluorometric detection in the sub ng/mL region. KLH and SASD do not fluoresce detectably at concentrations found in soluble immunogen which permits the selective determination of LSD in the antigen. By comparison with standard solutions the concentration of LSD in the immunogen was interpolated. Linear regression analysis gave the equation of the line to be  $y = 2.81 \times 10^4 x + 3.71 \times 10^{-2}$  ( $r = 0.999$ ,  $n = 6$ ) where the units for the  $x$  and  $y$  axis were concentration in ng/mL and fluorescence. The limit of detection by fluorescence was  $2.6 \times 10^{-10}$  g/mL LSD calculated from the mean blank reading plus three standard deviations. By this method, the amount of LSD in KLH-SASD-<sup>125</sup>I-LSD (Section 2.2.3.1) was determined to be  $2.16 \times 10^{-9}$  moles on 100  $\mu$ g KLH. This corresponds to a molar substitution ratio of 65 compared to  $6 \times 10^4$  by radiolabelled studies (Section 2.3.5.2) which represents a more realistic estimation of the coupling efficiency.

This method provides only an approximation of the LSD content in the soluble immunogen fraction since it depends on a number of assumptions. The photolytic approach to immunogen synthesis likely results in a number of KLH-SASD-LSD products with varying degrees of substitution. The first assumption is that the LSD content of the soluble fraction is representative of the entire sample which might not be true. Solubility is likely to decrease with increasing

substitution of protein which might result in the least soluble complexes (which have higher MSRs) precipitating out. Secondly, although the fluorescence spectra of free and bound LSD have the same maximum emission wavelength, the effect of fluorescence intensity after LSD is bound to KLH is not known. Finally, there is also a possibility that some of the KLH-SASD-LSD products are not fluorescent.

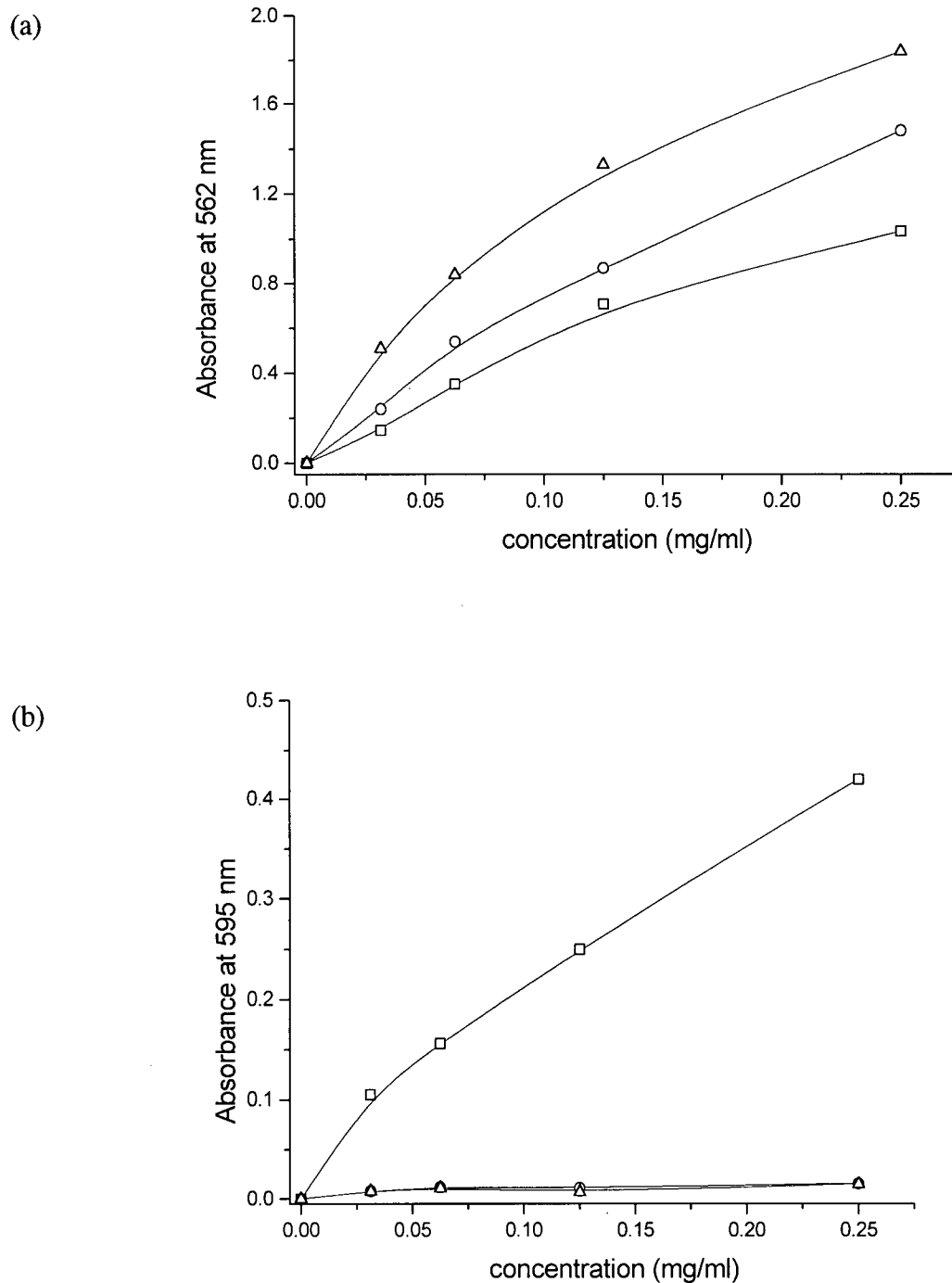
Characterization of KLH-SASD-LSD in which relatively few drug molecules are attached to a protein with a molecular weight of several million is not an easy task. Conventional methods for bioconjugate analysis are unsuitable due to the large size and low solubility of the conjugate. The fluorescence technique was the only method suitable for sensitive and specific estimation of LSD bound to KLH in the immunocomplex.

#### **2.3.5.4. Quantification of protein in KLH-SASD-LSD.**

Quantitative analysis of protein in the antigen presented a different problem. The Pierce BCA protein reagent was not suitable due to interferences with other species present in the immunogen. BCA reagent reacted with the non-protein species present more readily than with the protein itself (Figure 2.6 a). This reagent, which is known to have wide ranging reactivity, reacts with cystine, tryptophan and tyrosine to give a purple complex. LSD and SASD contain some of the same functional groups which are known to give a positive reaction, thus it is no surprise that they too react with BCA reagent. In contrast, the Bradford reagent was subject to minimal interference by SASD or LSD even at relatively high concentrations (Figure 2.6 b). This method gave the best approximation of KLH concentration in the immunogen. Since, the interaction between Bradford dye binding reagent chiefly occurs with arginine residues in the protein (19), covalent modification of lysine groups should have no significant effect on the Bradford dye

binding response (58). When used in the microtitre format (0 - 25  $\mu\text{g}/\text{mL}$  KLH), the linear regression of the line was  $y = 2.96 \times 10^{-3} x + 4.00 \times 10^{-4}$  ( $r = 0.998$ ,  $n = 4$ ) where the units of the  $x$  and  $y$  axis are concentration in  $\mu\text{g}/\text{mL}$  and absorbance at 550 nm. The detection limit based on the mean of the blank plus three standard deviations was 1.8  $\mu\text{g}/\text{mL}$  KLH.

**Figure 2.6.** Interference in colorimetric assays. KLH (squares), SASD (circles) and LSD (triangles) in neutral buffer were assayed with (a) Pierce BCA protein assay (59) and (b) Bradford dye binding assay (18).



### 2.3.6. Optimization of the molar substitution ratio.

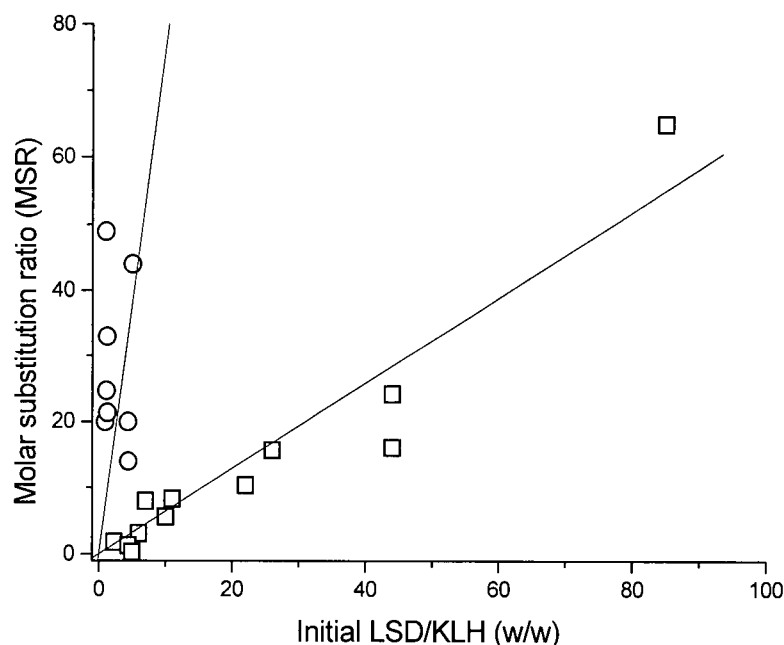
As expected, an important factor affecting reaction efficiency is the presence of excess SASD during photolysis. Molar substitution ratios fell by 50% or more when conjugates were prepared without removal of excess linker prior to photolysis. This is most likely explained by the reaction of uncoupled SASD with free LSD which makes it unavailable for reaction with KLH-SASD. As a general rule, due to the random nature of the reaction, optimum coupling conditions should be met when excess LSD surrounds KLH-SASD in the absence of all other species.

#### 2.3.6.1 Ratio of LSD/KLH during photolysis.

Covalent attachment of aryl azides with surrounding molecules is non-specific. To increase the chances of reaction with LSD, a large excess of drug should be used. Figure 2.7 summarizes the results of twelve immunogen preparations performed over a number of weeks in which reaction conditions were identical with the exception of the ratio of LSD to KLH employed during photolysis. All samples were purified by gel filtration which result in dried buffer components being present in the reaction matrix during irradiation. The initial ratio of LSD/KLH employed during photolysis determines the degree of substitution in the immunogen. There is a clear correlation between increased concentration of LSD during photolysis and increase molar substitution ratio. A linearized fit of the scattered data through the origin indicates that the MSR is approximately 65% of the initial LSD/KLH (w/w) ratio (correlation coefficient,  $r = 0.958$ ). The use of large excesses of drug during photolysis is a definite drawback considering that LSD is a controlled substance which is available in limited quantities. Reaction conditions which give the highest MSR's could not be reproduced on a preparative scale for immunization of rabbits

because the quantity of drug required would be too large.

**Figure 2.7.** Effect of excess LSD on molar substitution ratio. Open squares represent samples which were purified by gel filtration, lyophilized and irradiated in the presence of dried buffer components. Open circles represent samples dialysed against water, lyophilized and irradiated in the absence of buffer components.



However, when KLH-SASD is purified by dialysis against deionized water instead of gel filtration the results are quite different. Characterization of immunogens prepared in this way reveals a dramatic increase in reaction efficiency when buffer components are removed prior to irradiation (Figure 2.7). By this method, molar substitution ratios of 20 - 40 are attainable using only slight excesses of drug. This indicates that dried buffer components compete with LSD for reactive nitrenes. In the absence of buffer, approximately equal amounts of KLH and LSD by

weight react to give about 30 LSD's per KLH.

#### **2.3.6.2. Liquid and solid phase irradiation.**

Liquid phase photolysis decreased the substitution of drug on protein. Irradiation of KLH-SASD and LSD in liquid buffer following gel filtration resulted in a 70% decrease in substitution compared to dried samples. When photolysis was performed wet and dry after dialysis, in which there was no buffer, there was more than a 40% decrease in efficiency. Removal of water from the reaction mixture is favourable as the nitrene can react with water to form hydroxylamine (50) which may account for lower substitution. Despite reports of poor reaction efficiencies due to photolysis in aqueous solvent (40) there are no known reports of dry photolysis for conjugation in the literature.

#### **2.3.6.3. Preparation of KLH-SASD-LSD for immunization.**

Factors such as excess linker, reaction pH, irradiation of dry matrix in the absence of buffer and ratio of LSD to KLH used during photolysis were shown to have pronounced effects on the quality of the immunogen. An improvement in the overall yield was observed when the first conjugation step was performed directly in the dialysis cassette. This obviates the need for sample transfer after the reaction. The same cassette was rinsed and re-used for dialysis in the second conjugation step to reduce additional sample loss due to absorption on the membrane.

All steps preceding photolysis were performed in complete darkness or in the presence of a red safety light. SASD (5.0 mg) was dissolved in 50  $\mu$ L of DMSO which had been dried over molecular sieves. KLH (2.0 mg) dissolved in 1.5 mL 100 mM pH 8.0 phosphate buffer was

injected into a 3 mL Side-A-Lyzer dialysis cassette. SASD in DMSO was injected through a second port into the cassette with gentle agitation. A small air bubble (0.5 mL) was injected to facilitate mixing and the cassette was taped to an oscillating table and allowed to react for 2 hours in the dark. The cassette was then mounted on a flotation device and dialysed against deionized water in the dark for 2.5 hours with frequent water changes to remove the excess unreacted linker and its hydrolysis products. Purified KLH-SASD solution was removed from the dialysis cassette and LSD (2.2 mg) was added. The sample was mixed thoroughly and freeze dried overnight. Dry KLH-SASD in the presence of LSD was then placed at a distance of 10 cm from long and short wave UV lamps for 20 minutes. After photolysis, the irradiated sample was taken up in water and reintroduced into the Side-A-Lyzer for further dialysis (24 hours).

#### **2.3.6.4. Reaction efficiencies.**

A combination of drug and protein measurements by fluorescence and Bradford reagent was used to give approximate values for the molar substitution ratio of LSD to KLH which ranged between 20 - 65 under optimum conditions. The best of these were pooled for immunization so that the average MSR of the injected antigen was 35 (Table 2.4). The efficiency of the reaction was calculated from the percentage of lysine residues on KLH that were eventually coupled to LSD. The average two-step reaction efficiency for the injected immunogen was 5.1% (assuming 689 lysines per KLH). It was estimated that only about 45% of the total lysines on KLH were derivatized with SASD. Therefore, the reaction efficiency of the photolysis step towards LSD using optimized conditions was approximately 11%, which is quite favourable considering the non-selective nature of the photochemical coupling. This is likely the result of solvent and buffer

removal prior to photolysis and the presence of nucleophilic groups on LSD which are attractive to the electrophilic nitrene. Typical efficiencies of photoreactive linkers towards high molecular weight species are moderate to low due to the non-specific nature of the reaction. Reaction efficiencies of 15% using conventional phenyl azide photoprobes such as SASD are considered good (60).

Reaction efficiencies vary greatly, depending on the type of linker used. The recent introduction of polyfluorinated phenyl azide heterobifunctional linkers, which generate strongly electrophilic nitrenes, result in greater efficiencies (30,61) typically reported between 20 - 60% (62). Efficiencies of greater than 80% were measured using fluorinated probes for the conjugation of human serum albumin to immunoglobulin (40).

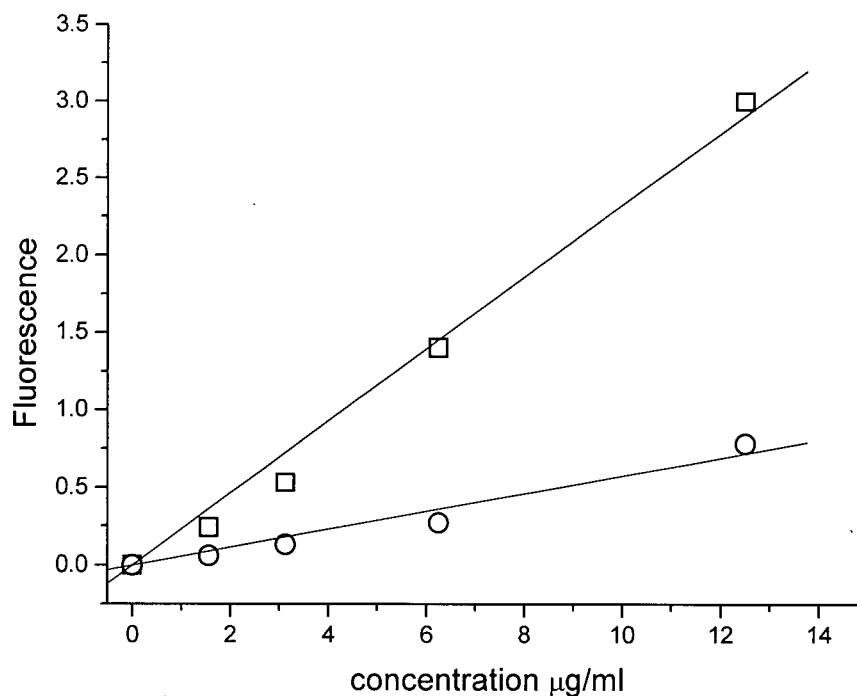
**Table 2.4.** Characterization of the immunoconjugate KLH-SASD-LSD used for immunization of rabbits. Efficiencies are calculated assuming 689 lysines per KLH (assuming a molecular mass of  $3 \times 10^6$ ).

Mean immunizing antigen composition		Efficiency (%)
number of SASD's coupled to KLH	310	45
concentration of LSD (soluble fraction)	20 ng/mL	11
concentration of KLH (soluble fraction)	5.3 $\mu$ g/mL	
number of LSD's coupled to KLH (MSR)	35	
<b>Overall reaction efficiency</b>		<b>5.1</b>

It has been suggested that KLH is rich in lysine residues, which is advantageous for conjugation purposes (63) but this is not strictly true. The primary amine density in BSA is  $8.9 \times 10^{-4}$  lysines per g (assuming 59 lysines per molecule and a molecular mass of 66,000) compared

with  $2.3 \times 10^4$  lysines per g for KLH (assuming 689 lysines per molecule and a molecular mass of  $3 \times 10^6$ , Section 2.3.1). This would indicate that KLH contains only about 25% of the total lysines found in BSA by weight. The availability of lysines on these two proteins was determined using the fluorescamine assay and is shown in Figure 2.8. A direct comparison of the slopes for BSA ( $0.233 \pm 0.009$ ,  $r = 0.997$ ) and KLH ( $0.057 \pm 0.004$ ,  $r = 0.987$ ) show that KLH has only  $24.7 \pm 2.9$  % of the total lysines on BSA by weight which confirms the theoretical prediction. This finding suggests that overall higher reaction efficiencies might be achieved using albumin.

**Figure 2.8.** Quantitative determination of the primary amines in immunogenic carrier proteins using the fluorescamine assay. BSA (squares) and KLH (circles).



### 2.3.7. Hapten density and immune response.

Previous investigations into epitope density and immune response indicate that optimum molar substitution ratios were between 5.8 and 14 for haptenated BSA immunogens (64). The report of epitope density as a mole ratio can be misleading when a very large carrier such as KLH is used however. For this reason the density of LSD on KLH is reported in LSD per gram KLH and % weight of hapten, which takes this into account.

The effect of epitope density on immunogenicity has been investigated using BSA derivatized with dopamine (DA) (64) and dinitrophenyl groups (DNP) (65). Hapten densities are reported for these immunogens and some typical LSD conjugates (Table 2.5). This shows that in KLH-SASD-LSD the amount of drug per g of carrier is more than 7 times lower than the lowest density for optimum immunogenicity (BSA-DA<sub>5.8</sub>) and 5 times lower than any other LSD immunogen. However, it should be noted that the cited literature measures optimum response in terms of the antiserum titre, which is a measure of the concentration rather than the quality of the antibody. Although the very low hapten density is a disadvantage, it is known that very few molecules of hapten are required on the surface of the antigen to illicit an immune response. Above optimum substitution results in an IgM response which exceeds that of IgG and produces antibodies of lower affinity. A low hapten density induces a slower immune response that usually yields smaller amounts of high affinity antibody (64-66).

**Table 2.5.** Comparison of epitope densities for KLH-SASD-LSD and other haptened proteins.

Immunogen	Epitope Density		
	MSR	hapten / g carrier	% hapten (w/w)
KLH-SASD-LSD <sup>1</sup>	35	$1.2 \times 10^{-5}$	0.4
KLH-LSD <sup>2</sup>	37	$1.2 \times 10^{-5}$	0.4
BSA-DA (64)	5.8	$8.8 \times 10^{-5}$	1.3
Poly-L-lysine-LSD (4)	6	$6.3 \times 10^{-5}$	2.0
BSA-DA (64)	14	$2.2 \times 10^{-4}$	3.2
BSA-LSD (5)	12	$1.8 \times 10^{-4}$	5.9
HSA-LSD (1)	10	$1.5 \times 10^{-4}$	4.9
BSA-LSD (29)	40	$6.1 \times 10^{-4}$	19.6
Poly-L-lysine-LSD (67)	65	$6.8 \times 10^{-4}$	22.0
Poly-L-lysine-LSD (68)	58	$6.8 \times 10^{-4}$	22.0
HSA-LSD (3)	50	$7.6 \times 10^{-4}$	24.5

<sup>1</sup> photolinked immunizing antigen.

<sup>2</sup> Mannich immunizing antigen.

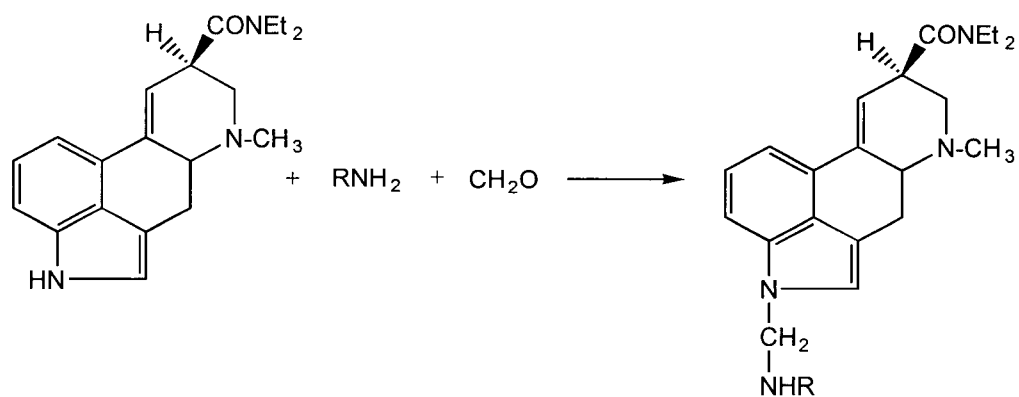
### 2.3.8. Control immunogen

KLH-LSD prepared by the Mannich reaction resulted in a slightly opaque immunogen which was largely water soluble, unlike KLH-SASD-LSD. Improved solubility resulted in good recoveries (60 - 80%) and facilitated characterization. The Mannich reaction is much simpler and proceeds with greater efficiency than the photolinked chemistry. Molar substitution ratios of purified KLH-LSD conjugates were between 18 and 104, depending on the concentration of formaldehyde and LSD

which was used during the reaction. However, in order to compare antisera quality, it was necessary to prepare KLH-LSD with a molar substitution ratio which was comparable to KLH-SASD-LSD which was 35. The MSR of the Mannich antigen which was used for immunization of rabbits was 35 (Table 2.5). Typical concentrations of KLH and LSD in soluble Mannich antigen were around 0.3 mg/mL and 1.5  $\mu\text{g/mL}$  respectively, compared to about 5  $\mu\text{g/mL}$  and 20 ng/mL in the photolinked immunogen. It was estimated that the solubility of KLH-SASD-LSD was about 60 times lower than that of KLH-LSD prepared by the Mannich reaction.

Amines on KLH react with formaldehyde to produce reactive iminium ions which in turn couple with the indole nitrogen on LSD (Figure 2.9). The degree of linking was controlled by varying the amount of formaldehyde, in order to produce a low MSR which was comparable to photolinked immunogen. The improved solubility of the Mannich coupled immunogen and the absence of interfering absorption bands allowed the MSR to be estimated by UV spectroscopy (1) which was in good agreement with fluorescence and Bradford dye binding results (Section 3.3.2.4).

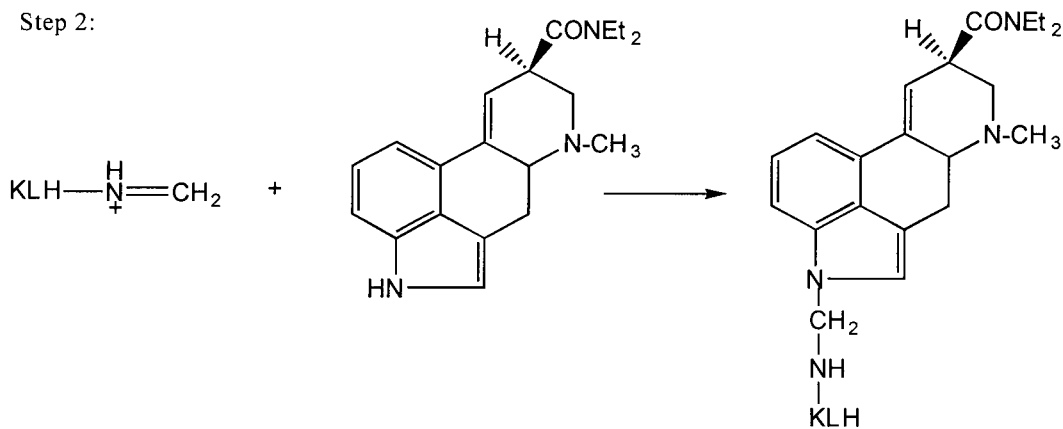
**Figure 2.9.** Preparation of KLH-LSD by the Mannich reaction.



Step 1:



Step 2:



#### 2.4. Conclusion.

A new LSD immunogen was prepared in which drug was coupled to the immunogenic carrier protein, KLH using a unique chemical linkage. The photoreactive heterobifunctional linker, SASD which contains an *N*-hydroxysuccinimide ester and a photoreactive aryl azide was used to covalently attach LSD to KLH using a two step conjugation procedure. During the first step, lysine residues on the protein surface react with the amine reactive end of the linker to form a stable amide bond. After removal of excess SASD, the derivatized protein is photoactivated under UV light in the presence of LSD, which results in covalent attachment of drug to protein. High molecular weight immunoconjugates were purified by dialysis and characterized by fluorescence and protein quantification. Special attention was paid to the molar substitution ratio, which is not only a measure of the reaction efficiency, but also controls the characteristics of the immune response.

The modification of lysines on KLH with SASD is heavily dependent on the pH of the reaction. Quantitative analysis of primary amines using fluorescamine was used to determine the effect of pH on the availability of reactive lysines on KLH and the extent of derivatization with SASD. Reaction conditions are a balance between the increased availability of amino groups with increasing pH and the ester hydrolysis which occurs readily under alkaline conditions. When a large molar excess of linker was employed, 45% of the lysines on KLH were derivatized with SASD. This corresponds to about 310 aryl azide moieties attached to one molecule of protein. The reaction efficiency between the photoreactive end of SASD with LSD was determined by the ratio of LSD to KLH in the reaction mixture and the presence of both water and buffer components during photolysis. An increase in the LSD/KLH (w/w) ratio during irradiation resulted in a linear increase in the molar substitution ratio, and the removal of both water and buffer salts prior to photolysis

resulted in an overall increase in reaction efficiency. The overall efficiency of the two step conjugation was estimated from the percent of lysines on KLH which are finally derivatized with LSD. On average, 35 molecules of LSD were attached to one KLH molecule, which represents an overall efficiency of 5.1%. The efficiency of the photocoupling step was approximately 11%, which is considered acceptable for photoreactive linking (60).

Photoactivation of the aryl azide results in the formation of a highly reactive nitrene which can react non-specifically with neighbouring molecules. Some of these nitrenes react with LSD which results in the covalent attachment of drug to carrier protein. Theoretically, the nitrene could attach at any one of several positions on the drug. Conjugation at different positions is advantageous because this, in principle, makes more epitopes available for recognition and therefore increases antiserum sensitivity. However, the electrophilic nitrene is most likely to attach at the N6 or the indole nitrogen, both of which have lone pairs, although reactions could also occur at the 2 position, or at any C=C double bond or C-H bond.

A second immunogen was synthesized using conventional coupling chemistry. LSD was conjugated to KLH at the indole nitrogen using the Mannich condensation. The Mannich immunogen was prepared with the same molar substitution ratio as the photolinked immunogen so that the immune signal was independent of hapten density. Rabbits were immunized with either photolinked or Mannich immunogen in order to assess any change in antibody characteristics as a result of the type of chemical linkage utilized in the immunoconjugate.

## 2.5. References.

1. Taunton-Rigby, A., Sher, S.E., and Kelley, P.R. 1973. *Science* 181: 165-166.
2. Twitchett, P.J., Fletcheer, S.M., Sullivan, A.T., and Moffat, A.C. 1978. *J. Chromatog.* 150: 73-84.
3. Loeffler, L.J. and Pierce, J.V. 1973. *J. Pharm. Sci.* 62(11): 1817-1820.
4. Van Vunakis, H., Farrow, T.T., Gjika, H.B., and Levine, L. 1971. *Proc. Nat. Acad. Sci. USA* 68(7): 1483-1487.
5. Ratcliffe, W.A., Fletcher, S.M., Moffat, A.C., Ratcliffe, J.G., Harland, W.A., and Levitt, T.E. 1977. *Clin. Chem.* 23(2): 169-174.
6. McNally, A.J., Goc-Szkutnicka, K., Li, Z., Pilcher, I., Polakowski, S., and Salamone, S.J. 1996. *J. Anal. Toxicol.* 20: 404-408.
7. Delmas, A., Brack, A., and Trudelle, Y. 1992. *Bioconjugate Chem.* 3: 80-84.
8. Berde, B. and Schild, H.O. 1978. *Ergot Alkaloids and Related Compounds*, Springer-Verlag, New York.
9. Regan, C.M. 1986. *J. Pharm. Pharmac.* 38: 834-836.
10. De-Villiers, M., Parkin, D., Van Jaarrsveld, P., and Van der Walt, B. 1987. *J. Immunol. Methods* 103: 33-39.
11. Wilson, D.F., Miyata, Y., Ericiniska, M., and Vanderkooi, J.M. 1975. *Arch. Biochem. Biophys.* 171: 104-107.
12. Das, M. and Fox, C.F. 1979. *Ann. Rev. Biophys. Bioeng.* 8: 165-193.
13. Mattson, G., Conklin, E., Desai, S., Nielander, G., Savage, M.D., and Morgensen, S. 1993. *Molecular Biology Reports* 17: 167-183.
14. van Brugen, E.F.J. 1980. *Trends Biochem. Sci.* 5: 185-188.
15. Herskovits, T.T. 1988. *Comp. Biochem. Physiol.* 91B(4): 597-611.
16. Harris, J.R. and Markl, J. 1992. *Cell Tissue Res.* 269: 411-420.
17. Udenfriend, S., Stein, S., Bohlen, P., Dairman, W., Leimgruber, W., and Weigele, M. 1972. *Science* 178: 871-872.

18. Bradford, M.M. 1976. *Anal. Biochem.* 72: 248-254.
19. Compton, S.J. and Jones, C.G. 1985. *Anal. Biochem.* 151: 369-374.
20. Zor, T. and Selinger, Z. 1996. *Anal. Biochem.* 236: 302-308.
21. Splittgerber, G. and Sohl, J. 1989. *Anal. Biochem.* 179: 198-201.
22. Look, J. 1967. *J. Pharm. Sci.* 56(11): 1526-1527.
23. Stocks, S.J., Jones, J.M., Ramey, C.W., and Brooks, D.E. 1986. *Anal. Biochem.* 154: 232-234.
24. Stoney, D.A. and Thornton, J.I. 1979. *Anal. Chem.* 51(8): 1341-1343.
25. Moretti-Rojas, I., Ezrailson, E.G., Birnbaumer, L., Entman, M.L., and Garber, A.J. 1983. *J. Biol. Chem.* 258(20): 12499-12508.
26. Engel, G., Muller-Schweinitzer, E., and Palacios, J.M. 1984. *Naunyn-Schmiedeberg's Arch. Pharmacol.* 325: 328-336.
27. Stead, A.H., Watton, J., Goddard, C.P., Patel, A.C., and Moffat, A.C. 1986. *Forens. Sci. Intl.* 32: 49-60.
28. Smith, R.N. and Robinson, K. 1985. *Forens. Sci. Intl.* 28: 229-237.
29. Castro, A., Grette, D.P., Bartos, F., and Bartos, D. 1973. *Research Communications in Chemical Pathology and Pharmacology* 6(3): 879-886.
30. Brinkley, M. 1992. *Bioconjugate Chem.* 3: 2-13.
31. Adamczyk, M., Gebler, J.C., and Mattingly, P.G. 1996. *Bioconjugate Chem.* 7: 475-481.
32. Shuler, K.R., Dunham, R.G., and Kanda, P. 1992. *J. Immunol. Methods* 156: 137-149.
33. Carlsson, J., Drevin, H., and Axen, R. 1978. *Biochem. J.* 173: 723-737.
34. Wollenweber, H.W. and Morrison, D.C. 1985. *J. Biol. Chem.* 260(28): 15068-15074.
35. Shanahan, M.F., Wadzinski, B.E., Lowndes, J.M., and Ruoho, A.E. 1985. *J. Biol. Chem.* 260(20): 10897-10900.
36. Ji, T.H. 1977. *J. Biol. Chem.* 252(5): 1566-1570.
37. Shephard, E.G., De-Beer, F.C., Von-Holt, C., and Hapgood, J. 1988. *Anal. Biochem.* 168:

306-313.

38. Vanin, E.F. and Ji, T.H. 1981. *Biochem.* 20(24): 6754-6760.
39. Koch, T., Suenson, E., Korsholm, B., Henriksen, U., and Buchardt, O. 1994. *Bioconjugate Chem.* 5: 205-212.
40. Pandurangi, R.S., Karra, S.R., Kuntz, R.R., and Volkert, W.A. 1995. *Bioconjugate Chem.* 6: 630-634.
41. Urich, B.W., Bowerman, D.L., Wittenberg, P.H., McGaha, B.L., Schisler, D.K., Anderson, J.A., Levisky, J.A., and Pflug, J.L. 1975. *Anal. Chem.* 47(3): 581-583.
42. Andersen, D.L. 1969. *J. Chromatog.* 41: 491-492.
43. Genest, K. and Farmilo, C.G. 1963. *J. Pharm. Pharmac.* 16: 250-257.
44. Blake, E.T., Cashman, P.J., and Thornton, J.I. 1973. *Anal. Chem.* 45(2): 394-395.
45. Niwaguchi, T. and Inoue, T. 1971. *Proc. Japan. Acad.* 47: 747-750.
46. Schrock, A.K. and Schuster, G.B. 1984. *Journal of the American Chemical Society* 106: 5228-5234.
47. Soundarajan, N. and Platz, M.S. 1990. *J. Org. Chem.* 55: 2034-2044.
48. Leyva, E., Young, M.J., and Platz, M.S. 1986. *Journal of the American Chemical Society* 108: 8307-8309.
49. Keana, J.F.W. and Cai, S. 1990. *J. Org. Chem.* 55: 3640-3647.
50. Patai, S. 1971. *The Chemistry of the Azido Group*, Interscience, New York.
51. Bayley, H. and Staros, J.V. 1984. *Azides and Nitrenes. Reactivity and Utility*. E.F.V. Scriven, Ed., pp. 439-460. Academic Press, Orlando.
52. Ueno, H., Masuko, T., Wang, J., and Hashimoto, Y. 1994. *J. Biochem.* 115: 1119-1127.
53. Phadke, A.S., Aggler, R., Keana, J.F.W., and Capaldi, R.A. 1994. *Biochemical and Biophysical Research Communications* 201(2): 635-641.
54. Straub, K.M. and Levy, M.J. 1994. *Bioconjugate Chem.* 5: 194-198.
55. Adamczyk, M., Buko, A., Chen, Y., Fishpaugh, J.R., Gebler, J.C., and Johnson, D.D. 1994.

*Bioconjugate Chem.* 5: 631-635.

56. Cai, S., Glenn, D.J., and Keana, J.F.W. 1992. *J. Org. Chem.* 57: 1299-1304.
57. Van der Walt, B., Nikodem, V.M., and Cahnmann, H.J. 1982. *Biochem.* 79: 3508-3512.
58. Ahmad, H. and Saleemuddin, M. 1985. *Anal. Biochem.* 148: 533-541.
59. Pierce Chemical Company, Rockford, IL. 1992. BCA Protein Assay, *package insert*.
60. Thevenin, B.J.M., Shahrokh, Z., Williard, R.L., Fujimoto, E.K., Kang, J.J., Ikemoto, N., and Shoheit, S.B. 1992. *European Journal of Biochemistry* 206: 471-477.
61. Yan, M., Cai, S.X., Wybourne, M.N., and Keana, F.W. 1994. *Bioconjugate Chem.* 5: 151-157.
62. Kym, P.R., Carlson, K.E., and Katzenellenbogen, J.A. 1995. *Bioconjugate Chem.* 6: 115-122.
63. Pierce Chemical Company, Rockford, IL. 1994. Imject Carrier Proteins, *package insert*.
64. Malaitsev, V.V. and Azhipa, O.Y. 1993. *Bull. Exp. Biol. Med* 115(6): 726-728.
65. Klaus, G.G.B. and Cross, A.M. 1974. *Cell. Immunol.* 14: 226-241.
66. Portmann, A.J., Levison, S.A., and Dandliker, W.B. 1975. *Immunochemistry* 12: 461-466.
67. Van Vunakis, H., Farrow, J.T., Gjika, H.B., and Levine, L.L. 1971. *Proc. Natl. Acad. Sci. USA* 68(7): 1483-1487.
68. Lopatin, D.E. and Voss, E.D. 1974. *Immunochemistry* 11: 285-293.

## Chapter 3.

### Enzyme-Linked Immunosorbent Assay Development.

#### 3.1. Introduction.

Essential reagents for the development of an indirect enzyme-linked immunosorbent assay (ELISA) for LSD include antibodies to the drug and an LSD conjugate for immobilization to the ELISA plate. Aside from the characteristics of the antibody, which are discussed in detail in Chapter 5, the success of antibody binding to immobilized LSD depends on the presentation of epitopes on the solid phase. This is achieved by either passively adsorbing a drug conjugate to the microtitre surface, or by covalently attaching it to the surface.

Structural aspects of the layer can restrict antibody binding due to steric hindrance or overcrowding. It is generally accepted that for small molecules, attachment of the hapten to a carrier molecule via a spacer arm is preferable, to minimize the likelihood that the hapten is embedded in the macromolecule. Just as the immunogen described in Chapter 2 was prepared to maximize epitope recognition by multi-site attachment, the coupling chemistry used to prepare the drug conjugate (or coating antigen) significantly influences the ELISA. It has been shown that heterologous immunoassays which employ immunogen and plate coating antigen prepared using different carrier and hapten linkages, are more sensitive (1). This is of particular importance when developing immunoassays for small molecules such as LSD. Under these circumstances, antibody is also raised against all or part of the linker arm. This can result in the antibody recognizing the conjugated hapten

more efficiently than the free drug. If a highly immunogenic linker is used, there may be little or no reactivity towards the drug itself (1). Utilization of the same chemical linker in the immunogen and the coating antigen, can reduce the specificity of the immunoassay by introducing cross-reactivity towards the linker moiety. It has been further suggested that for small molecules, hapten-protein coupling should involve different amino acid residues (2). In this way, antibodies which are directed towards a hapten coupled to a particular amino acid on the protein, do not compromise the overall specificity of the assay.

Drug conjugates were prepared using different chemical linkages and carrier molecules. The suitability of different coating antigens is dependent on high specific antibody binding and low non-specific binding by ELISA. It is also important that the conjugate, which must cross-react with the antibody, does not bind with greater affinity than the free drug, which would result in decreased sensitivity. The following drug conjugates were investigated:

- 1.) LSD coupled to microtitre plates by stable covalent linkage.
- 2.) LSD coupled to BSA using a photoreactive linker.
- 3.) LSD coupled to PVA with and without a photoreactive linker.
- 4.) LSD coupled to BSA directly, with no spacer arm.

Passive adsorption involves multiple interactions between the protein and the solid surface which can interfere with the structure and activity of the antigen. The strength of antigen adsorption to the solid phase is dependent on the number of interactions between the molecule and the interface. As a general rule, larger molecules, with potentially more sites of attachment adsorb more strongly than smaller molecules which will have fewer interactions. Not all proteins adsorb readily to polystyrene microtitre plates, but the introduction of polar groups on the polymer surface can

increase the antigen binding capacity towards water soluble proteins in some cases. This is attributed to the introduction of hydrophilic groups on the solid phase, often achieved by gamma irradiation of microtitre plates, which can potentially contribute to electrostatic and hydrogen bonding interactions (3-5).

Protein adsorption is essentially irreversible in the absence of other macromolecules (6,7). This is because only one site on the molecule needs to attach for the protein to become bound to the surface, after which complete adsorption results in multiple sites of attachment between the protein and the surface. For desorption to occur, all sites of attachment must be lost simultaneously, which is unlikely in an unperturbed system. However, desorption of some antigen during ELISA incubation and washing steps is common (8). The hydrophobic, hydrogen bonding, electrostatic and van der Waals forces which are responsible for protein adsorption may be too weak to maintain adherence, particularly in the presence of non-ionic detergents, such as Tween, or other proteins which might adsorb more favourably. Desorption of the antigen affects both sensitivity and precision of ELISA measurements, so it is important that the antigen density is maintained constant throughout the assay.

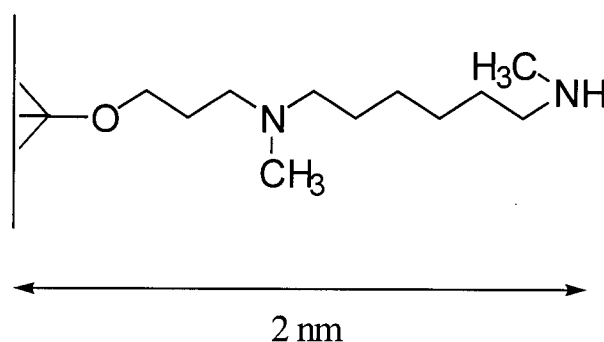
The interactions responsible for antigen binding can also result in non-specific binding of other protein components which can adsorb to the surface during the assay. This is minimized by treating the remaining surface with a blocking agent after the plate has been coated with antigen. Typically, non-interacting macromolecules are used, which are large enough to adsorb to the surface, but small enough to fit easily between the immuno-reactants.

Detergents are also used to wash off loosely or non-specifically bound proteins. They can also be used to block excess polystyrene surface after coating with protein, to avoid non-specific immobilization of subsequent reactants. Incorporation of a detergent into the ELISA washing

solution can break unstable hydrophobic interactions between the protein and surface, or non-specific interactions between macromolecules.

Desorption of surface immobilized antigen can be reduced by covalent attachment, which in some instances can facilitate specific orientation of the molecule on the solid phase. The presentation of antigen in a more readily defined manner can increase the likelihood that epitopes on the antigen are unhindered and free to interact with the antibody. Introduction of reactive functional groups onto the solid surface allows antigen to be covalently attached using conventional coupling chemistries. However, the introduction of these groups on polystyrene surfaces usually involves severe chemical treatment (9,10). Polystyrene microtitre plates with amino groups on the surface are commercially available from Nunc (Roskilde, Denmark). CovaLink microtitre plates contain secondary amino groups that can extend 20 Å from the polystyrene surface via a spacer arm (Figure 3.1). There are approximately  $10^{14}$  active groups per  $\text{cm}^2$  which corresponds to about 0.5 nmol/well (11,12). These plates are frequently used to attach protein or peptide antigens to microtitre plates using activated *N*-hydroxysuccinimide (NHS) esters or carbodiimide mediated linkage (13).

**Figure 3.1.** Immobilized secondary amine groups on Nunc CovaLink microtitre plates.



Successful immobilization of LSD was necessary for the detection of both antibody and hapten by ELISA. The amount of specific antibody directed towards LSD was measured by indirect ELISA during the course of immunizations. Free LSD was detected by a competitive binding assay, in which drug in solution competes with immobilized drug for a fixed amount of antibody. The percent of antibody which is bound is detected using an anti-rabbit IgG peroxidase labelled conjugate and subsequent colour reaction using tetramethylbenzidine (TMB). The methodology of the ELISA which is used for the detection of both anti-LSD in rabbit serum and LSD in a test sample was described in detail in Section 1.3.5.

### 3.2. Materials and methods.

Disposable 96 well polystyrene plates were obtained from Corning (New York). Lysergic acid diethylamide tartarate was kindly supplied by Dr. Haro Avdovich of the Bureau of Drug Research, Health Canada (Ottawa, ON). Goat anti-rabbit IgG horseradish peroxidase, bovine serum albumin and 3, 3', 5, 5'-tetramethylbenzidine (TMB) were purchased from Sigma (St. Lois, MO) as were Tween 20 and Triton X-100. Polyvinyl alcohol (molecular mass approximately 15,000) was purchased from Fluka Chemie (Germany), polyethylene glycol 6000 was from J.T. Baker (Phillipsburg, NJ) and Pluronic 10R8 and Tetronic 50R4 detergents were from BASF (Wyandotte, MI). The 4-fluoro-3-nitrophenyl azide and the succinimide ester of 4-azido-2,3,5,6-tetrafluorobenzoic acid were purchased from Molecular Probes (Eugene, OR). A solution of Carnation non-fat dry skim milk powder in 150 mM phosphate buffered saline, pH 7.4 (PBS) was routinely used as a blocking agent. Inorganic salts, H<sub>2</sub>O<sub>2</sub>, acids, formaldehyde (37%) and dimethyl sulfoxide supplied by Fisher Scientific (Edmonton, AB) were certified ACS grade. Antibodies to LSD were produced in rabbits immunized with KLH-SASD-LSD as described earlier (Section 2.2.6).

### **3.2.1. Detection of LSD antibodies by ELISA.**

Blood was collected from the femoral vein of rabbits approximately 10 - 14 days after each booster injection. Serum was prepared by clotting blood at 37 °C for 30 minutes in polypropylene tubes and refrigeration overnight at 4 °C. Serum was removed and stored at -20 °C, or -70 °C for long term use.

Microtitre plates with LSD immobilized on the surface (Section 3.2.2) were used to detect drug antibodies by indirect ELISA as previously outlined (Figure 1.6). Uncovered sites on the polystyrene plates were treated with blocking agent (150 µL/well) for 30 minutes at 37 °C to reduce non-specific binding. A solution of 5% (w/v) skim milk powder in PBS (SM-PBS) was routinely used as the blocking solution unless otherwise indicated. Microtitre plates were washed four times with PBS (250 µL/well) between subsequent incubation steps. Rabbit serum diluted in blocking solution (100 µL/well) was incubated at 37 °C for one hour to allow the anti-LSD to bind to the plate. After washing, goat anti-rabbit IgG peroxidase (100 µL/well) diluted 1:1000 in blocking solution was incubated for 30 minutes at 37 °C. After the final plate wash, TMB substrate solution (100 µL/well) was added. The colour reaction was stopped by the addition of 1M sulfuric acid (50 µL/well), after which the absorbance was measured at 450 nm with a 620 nm reference filter using an SLT EAR 400AT microtitre plate reader (SLT Labinstruments, Austria).

#### **3.2.1.1. Evaluation of blocking agents for polystyrene microtitre plates.**

Corning polystyrene microtitre plates were used to measure the non-specific binding of normal rabbit serum by ELISA. Microtitre plates were incubated with blocking solution (100 µL/well) for 30 minutes at 37 °C. Normal rabbit serum, diluted 1:10 in the same blocking solution

was incubated for 30 minutes at 37 °C and thoroughly rinsed with PBS. Immobilized antibody was detected using goat anti-rabbit IgG peroxidase (100 µL/well), diluted 1:1000 in blocking solution. After incubation for 30 minutes at 37 °C, plates were washed, TMB substrate solution was added and the absorbance was measured as described earlier (Section 3.2.1). Replicate measurements (n=6) over a range of concentrations (0.03 to 3% by weight) were made using each of the following agents in PBS, in place of the blocking solution:

Skim milk powder (SM)	Bovine serum albumin (BSA)
Polyvinyl alcohol (PVA)	Pluronic 10R8
polyethylene glycol 6000 (PEG)	Tetronic 50R4
Tween 20	PBS only

### **3.2.2. Coating antigen preparation.**

#### **3.2.2.1. Covalent attachment of LSD to Nunc CovaLink.**

Secondary amino groups on the surface of Nunc CovaLink were derivatized with LSD using a heterobifunctional linker which had photoreactive and NHS ester moieties. The amine reactive end of the linker was coupled to microtitre plates according to the manufacturers recommendations (14), after which the aryl azide end was photoactivated in the presence of LSD. In the absence of light, a freshly prepared stock solution of 4-azido-2,3,5,6-tetrafluorobenzoic succinimide ester (PFPA) in dry DMSO was diluted to 2 mM in PBS. The linker was immediately dispensed into Nunc CovaLink microtitre plates (100 µL/well), covered and incubated overnight at room temperature in a light tight box. Plates were washed four times with PBS and tapped dry. LSD (0.2 mg/mL) in deionized water was added to microtitre plates (100 µL/well) and irradiated approximately 10 cm from long and short

wave UV lamps for 30 minutes. After the photoreaction, the plates were washed with PBS and used in the ELISA described in Section 3.2.1. A number of blocking agents and detergents were used to reduce non-specific binding. PBS, PBS/Tween (0.05%) and CovaBuffer (a high salt washing buffer recommended by the manufacturer) were used to wash ELISA plates between incubation steps. CovaBuffer was prepared by adding NaCl (116.9 g),  $\text{MgSO}_4 \cdot 7\text{H}_2\text{O}$  (10.0 g) and Tween 20 (0.5 mL) to 1 L of freshly prepared PBS.

### **3.2.2.2. Derivatization of BSA with LSD using a photoreactive linker.**

A heterobifunctional linker was used to covalently couple LSD to BSA. The succinimidyl ester of 4-azido-2,3,5,6-tetrafluorobenzoic acid (PFPA) was used in place of SASD for the stepwise modification of amine groups on BSA and subsequent photoreaction with LSD as earlier described (Section 2.3.6.3). In this way, the polyfluorinated phenyl azide (PFPA) is used to bridge LSD and the carrier molecule in BSA-PFPA-LSD, which is analogous to the immunizing antigen, KLH-SASD-LSD. The former was used to coat polystyrene microtitre plates for use in ELISA.

### **3.2.2.3. Derivatization of PVA with LSD.**

Attempts were made to covalently attach LSD to PVA in different ways. First, LSD was coupled using the polyfluorinated phenyl azide (PFPA) linker, which was attached to PVA via cyanogen bromide activation and amination (15). Cyanogen bromide (0.1 g) was added to 2 mL PVA (3% in deionized water). The pH of the reaction was maintained at about 11 by the dropwise addition of 20% NaOH. After 10 minutes, 3 mL of concentrated ammonia solution was added. PVA was isolated and washed by acetone precipitation and dissolved in water. PFPA (0.4 mg) in a small

volume of dry DMSO was added to the PVA in solution, which was reacted for one hour in the dark. After acetone precipitation of PVA-PFPA, LSD (0.5 mg) in 2 drops of deionized water was added and photolyzed for 30 minutes under long and short wave UV lamps. The final product was dialysed in a Pierce Slide-A-Lyzer against deionized water to remove unbound LSD from PVA-PFPA-LSD.

A second photoreactive agent, 4-fluoro-3-nitrophenyl azide (FNPA), was used to couple LSD to PVA. FNPA (0.5 mg) in dry DMSO was added to 1.0 mL PVA (3%) in deionized water. The reaction was allowed to proceed for one hour in the absence of light. Excess linker was removed by precipitation of PVA with acetone. LSD (0.25 mg) in approximately two drops of water was added to derivatized PVA and irradiated in the usual way. Excess drug was removed from PVA-FNPA-LSD by dialysis. PVA, which contains a number of active carbonyls as impurities, was also mixed directly with LSD. Approximately 0.3 mL sulfuric acid (1 M) was added to a stirred solution of LSD (0.8 mg) and PVA (0.15 g) in deionized water. After 30 minutes, LSD was removed by dialysis.

#### **3.2.2.4. Derivatization of BSA with LSD by the Mannich reaction.**

An existing method was used to couple LSD to BSA by the Mannich reaction (16). BSA (8 mg) dissolved in 0.5 mL deionized water was added to 1 mL sodium acetate (3 M) in a Pierce Reacti-Vial. A solution of 37% formaldehyde (0.2 mL) was added dropwise and allowed to stir gently for 5 minutes. LSD (1 mg) dissolved in 0.5 mL deionized water was added dropwise and the reaction was allowed to proceed for 2 hours at room temperature. Excess drug was removed by dialysis using a Pierce Slide-A-Lyzer in the usual way.

### **3.2.3. Immune response over time.**

#### **3.2.3.1. Measurement of antibody titres.**

Polystyrene microtitre plates were coated with 5  $\mu\text{g/mL}$  BSA-LSD in PBS overnight at 4 °C. The ELISA described in Section 3.2.1. was used to measure the amount of antibody present in the serum of four rabbits, which had been immunized with either photolinked (KLH-SASD-LSD) or Mannich (KLH-LSD) immunogen (Section 2.2.6). The antibody titre was taken to be the dilution of antiserum that resulted in half maximum absorbance.

#### **3.2.3.2. Thiocyanate elution and ELISA detection.**

The functional affinity of anti-LSD in rabbit serum was evaluated by chaotropic salt elution and ELISA detection, which is discussed in detail in Chapter 5. A fixed dilution of serum from each rabbit was used in the ELISA described in Section 3.2.1. This time, ammonium thiocyanate, diluted in PBS (0 - 8.3 M) was added to microtitre wells (100  $\mu\text{L}$ ) for 15 minutes at room temperature in between the serum and conjugate antibody incubations. Serum from each rabbit was diluted to give an absorbance reading of approximately 1 in the absence of thiocyanate ions. The absorbance of wells which were treated with thiocyanate was plotted as a percentage (relative to no thiocyanate added) against the concentration of chaotropic eluent which was used.

#### **3.2.4. Detection of LSD by indirect ELISA.**

The detection of LSD by ELISA depends on the ability of free LSD in solution to compete with immobilized drug for a limited number of antibody molecules. The inhibitory effect of LSD on antibody binding was demonstrated in the following ELISA, which was outlined schematically in

Chapter 1 (Figure 1.7). Polystyrene microtitre plates were coated with the BSA-LSD (5  $\mu\text{g}/\text{mL}$ ) in PBS overnight at 4 °C. Equal volumes of LSD (diluted in PBS between 1  $\mu\text{g}/\text{mL}$  and 1  $\text{pg}/\text{mL}$ ) and a fixed concentration of antibody in 10% SM-PBS were mixed to give a final serum dilution of 1:50. Samples were incubated at 37 °C, concurrently with the pre-blocking step for 30 minutes. After washing the plate, pre-incubated samples (100  $\mu\text{L}/\text{well}$ ) were added to the microtitre plate and incubated for a further 60 minutes at 37 °C. After washing the plate four times with PBS, goat anti-rabbit peroxidase (1:1000) in SM-PBS was incubated for 30 minutes at 37 °C. After a final plate wash, TMB substrate solution was added and the absorbance was measured in the usual way. The percent of antibody which was bound was calculated relative to the absorbance of samples which contained no LSD. Replicate measurements ( $n=5$ ) were made for each concentration of LSD tested and normal rabbit serum was run in the same assay to assess the degree of non-specific binding.

### 3.3. Results and discussion.

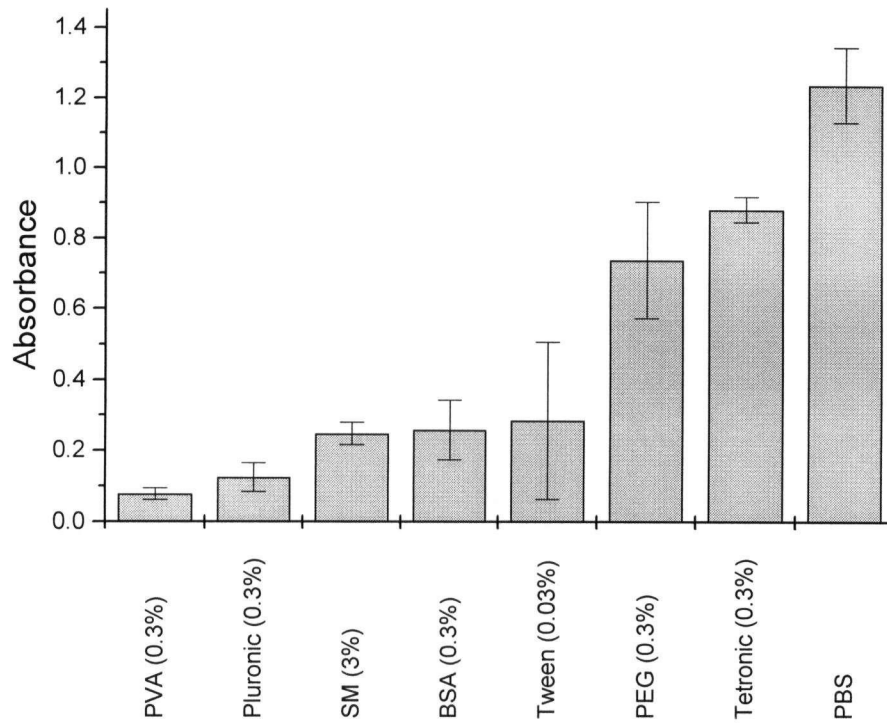
#### 3.3.1. Evaluation of blocking agents and detergents.

The non-specific binding which was associated with the indirect ELISA was measured using a number blocking proteins and detergents. The average signal ( $n=6$ ) obtained using 1:10 diluted normal rabbit serum was used to rank reagents in order of increasing non-specific interference (Figure 3.2). When no blocking agent was used the non-specific signal was  $1.24 \pm 0.11$  (SD). Results showed that both high and low molecular weight agents were able to reduce non-specific binding; non-ionic detergents Tetronic 50R4, Tween 20 and Pluronic 10R8 decreased the average signal to 0.88, 0.28, and 0.13 respectively. As expected, the commonly used blocking proteins BSA and skim milk also decreased non-specific binding, but by far the best blocking agent was PVA which had a non-specific signal of only 0.08 absorbance units when used with 1:10 diluted normal serum. The five most effective agents for reducing non-specific binding of immunoglobulins to Corning polystyrene microtitre plates were, in decreasing order, PVA (0.3%) > Pluronic 10R8 (0.3%) > SM (3%) > BSA (0.3%) > Tween (0.03%). The concentration of agent as a w/w % is given in brackets.

It is possible for detergents to increase non-specific interferences by introducing hydrophilic groups to the hydrophobic surface. Increasing the hydrophilicity of the surface can increase protein binding and therefore the non-specific signal (3,4). Routinely, it was found that the addition of Tween 20 during serum and conjugate antibody incubations increased the non-specific signal, particularly when antigens were passively adsorbed. When BSA-LSD (Section 3.2.2.4) was used to coat microtitre plates, the non-specific signal using both SM-PBS and 0.5% BSA blocking solutions increased more than 5-fold in the presence of 0.03% Tween. This may be caused by the displacement

of antigen from the surface by the detergent and the subsequent non-specific binding of IgG in these unprotected sites. In general, detergents were not used unless absolutely necessary.

**Figure 3.2.** Non-specific binding of normal rabbit IgG to Corning polystyrene microtitre plates by ELISA.



### 3.3.2. Performance of coating antigens in ELISA.

#### 3.3.2.1. Nunc CovaLink LSD.

Preliminary efforts to utilize microtitre plates to which LSD was covalently attached, employed SM-PBS as the blocking solution, as recommended by the manufacturer (14). Titration of antisera obtained from rabbits immunized with KLH-SASD-LSD by ELISA indicated decreased

absorbance with increased serum dilution. However, an identical titration performed in Nunc CovaLink wells which had not been derivatized with LSD showed the same results, which suggested that perhaps no LSD was bound (Figure 3.4). Pierce BCA reagent (17) is known to react with protein, LSD and the heterobifunctional linker SASD (Section 2.3.5.4). When 100  $\mu\text{L}$  of BCA reagent was added to microtitre wells which had been derivatized with PFPA and LSD, a positive colour reaction and the absorbance at 550 nm suggested that modification had taken place (Figure 3.3) (12).

**Figure 3.3.** Colorimetric detection of protein and LSD on CovaLink. A) covalently attached LSD, B) covalently attached BSA, C) passively adsorbed BSA, D) un-modified. Plates were washed with PBS/Tween (0.05%) after treatment. BCA reagent (100  $\mu\text{L}$ ) was incubated for one hour at room temperature and the absorbance measured at 550 nm.

CovaLink treatment		Absorbance
 PFPA-LSD	A	1.0
 PFPA-BSA	B	0.3
 BSA	C	0.2
	D	0.0

When SM-PBS used in the ELISA was replaced with 0.05% Tween 20 in PBS, the results were quite different (Figure 3.5). The increased absorbance of immune serum relative to normal serum indicated that antibodies to LSD were present in the serum. However, under these conditions there was significant non-specific binding, indicated by the premature binding plateau of immune

serum at about 0.6 OD and the unacceptably high signal obtained from normal rabbit serum (0.4 - 0.7).

**Figure 3.4.** Titration of immune rabbit serum in the presence and absence of immobilized LSD using Nunc CovaLink. SM-PBS was used as the blocking agent in ELISA.

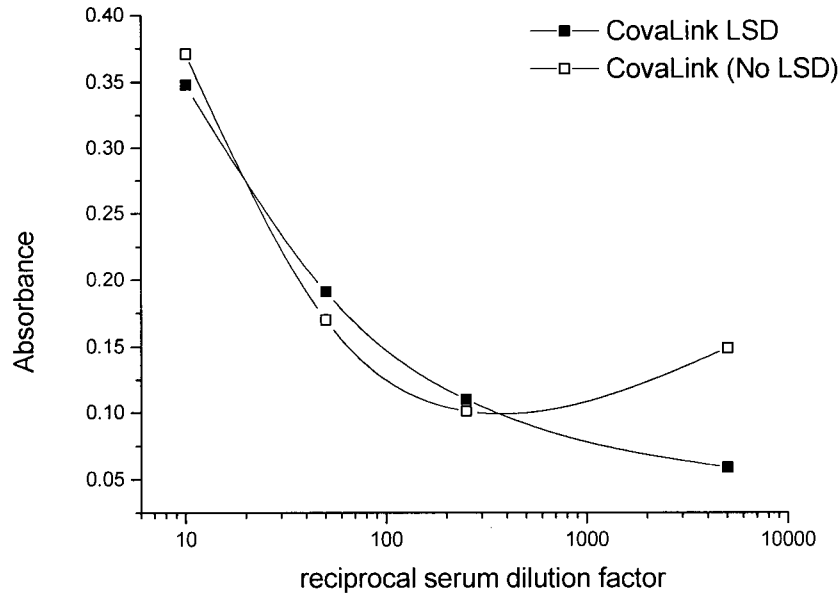
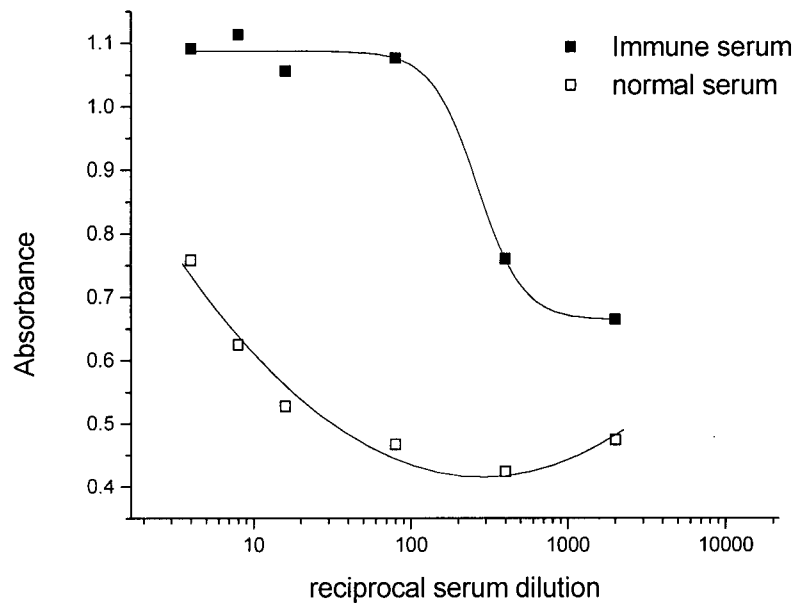


**Figure 3.5.** Titration of immune and normal rabbit serum by ELISA on Nunc CovaLink microtitre plates derivatized with LSD. Tween 20 (0.1%) in PBS was used in place of SM-PBS blocking solution.



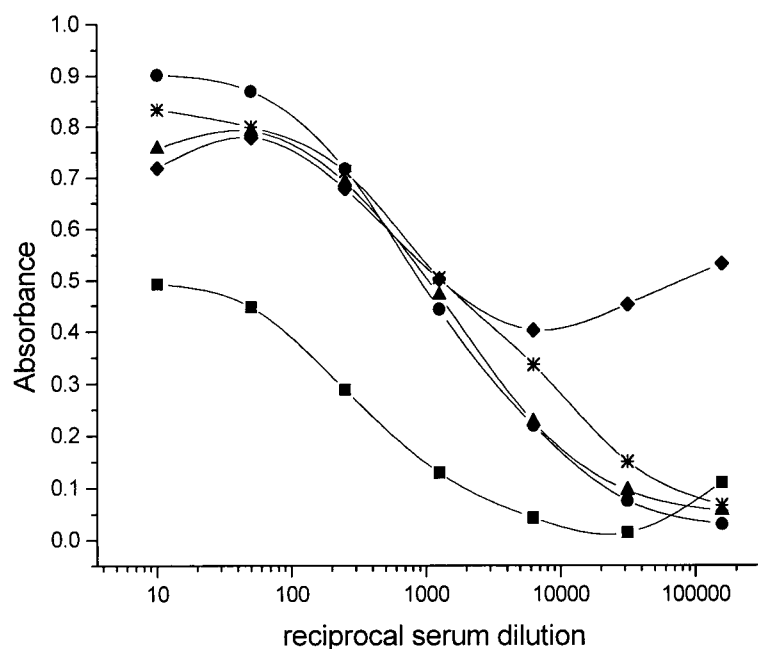
Nunc CovaLink plates which were derivatized with LSD, were used in the ELISA described in Section 3.2.1 using the blocking conditions outlined in Table 3.1. Titration of immune rabbit serum showed that the use of BSA blocking solution during serum, conjugate or both incubation steps gave similar results (Figure 3.6). However, the inclusion of a pre-blocking step (condition A), significantly decreased the absorbance of immune rabbit serum relative to all other conditions. This effect was not the result of decreased non-specific binding, which was estimated to be 50% using normal rabbit serum. When non-specific binding was subtracted from the immune signal, for ELISAs performed with and without pre-blocking, there was a noticeable decrease in the absorbance (Figure 3.7).

The disproportionate decrease in specific antibody binding using Nunc CovaLink was observed for other high molecular weight blocking proteins, particularly SM-PBS. A possible explanation is that due to the small size of the hapten, immunologic detection is masked to some degree by the smothering effect of the relatively large blocking protein on the derivatized surface, which is particularly noticeable when a pre-blocking step is used. Similar results have been reported in the literature, in which skim milk was shown to have the most pronounced effect (18) which may be the result of large spherical casein micelles, which make up 80% of the total protein in milk (19). Under these circumstances, it is quite likely that the decrease in specific antibody signal is due to steric hindrance caused by the blocking agent, which is a particular problem with small antigens (9).

**Table 3.1.** ELISA using Nunc CovaLink in which the blocking agent (BSA) was introduced at different stages. Incubations which were performed in the absence of blocking agent were diluted in 0.05% Tween in PBS. Plates were washed four times with Nunc CovaBuffer in between each of the incubation steps.

	Pre-block 30 mins, 37 °C	Serum incubation 30 mins, 37 °C	Conjugate incubation 30 mins, 37 °C
	Blocker ? (Y/N) (0.5% BSA in PBS)	Blocker ? (Y/N) (0.5% BSA in PBS, 0.05% Tween)	Blocker ? (Y/N) (0.5% BSA in PBS, 0.05% Tween).
A	Y	Y	Y
B	N	Y	Y
C	N	Y	N
D	N	N	Y
E	N	N	N

**Figure 3.6.** Nunc CovaLink ELISA using BSA as the blocking agent during different incubations. See Table 3.1 for a description of the conditions used in A (squares), B (circles), C (triangles), D (stars) and E (diamonds).



Pierce BCA protein reagent was used to confirm that BSA was attached to the surface during pre-blocking (Figure 3.3). When BSA was photolinked onto CovaLink plates, in place of LSD, the absorbance was slightly higher, perhaps indicating that more protein was bound. More importantly however, when these wells were incubated with 1:10 diluted normal serum, the non-specific ELISA signal was five times lower after covalent attachment of BSA. Two conclusions were drawn from these results. First, that passively adsorbed BSA is weakly attached to CovaLink, being readily replaced by IgG molecules. Second, that covalent attachment of a macromolecule, such as BSA affords greater protection from non-specific binding compared to a small molecule like LSD.

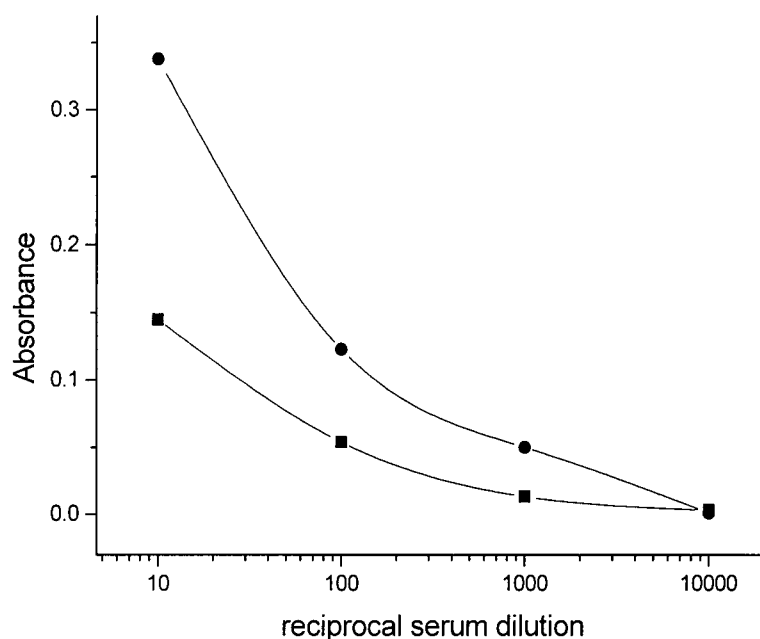
More than 8 different blocking agents were used on Nunc CovaLink plates derivatized with LSD. These included proteins, non-ionic detergents and polymers which are known to adsorb to polystyrene surfaces, none of which gave satisfactory results. The problems experienced could be categorized into the following:

- 1.) A masking effect of high molecular weight blocking agents, which inhibit antibody binding to immobilized LSD for steric reasons eg. skim milk, BSA, human serum.
- 2.) Distinguishable immune signal but very high non-specific binding when blocking agents are replaced with low molecular weight detergents. eg. Tween, Triton-X, Pluronic.

The problem of increased non-specific binding when using aminated polystyrene plates is generally attributed to increased hydrophilicity of the surface (20). Reports indicate that Nunc CovaLink microtitre plates result in considerably higher non-specific binding compared to unmodified polystyrene plates, by as much as 8 times in one instance (11,13,14). In most

applications, CovaLink plates are used to detect fairly large antigens such as proteins or peptides which, when attached to the surface, minimise non-specific binding. PVA and other agents shown to reduce non-specific binding on polystyrene plates (Section 3.3.1) did not perform well on Nunc CovaLink, and the incorporation of high salt, detergent, or both in washing buffers offered no improvement. Other workers have overcome the high non-specific binding of Nunc CovaLink by using harsh washing solutions eg. 250 mM carbonate buffer, pH 11.25 (12) which is undesirable in an immunoassay.

**Figure 3.7.** Masking effect of high molecular weight blocking proteins on Nunc CovaLink. Titration of immune sera (minus non-specific binding) in the absence (circles) and presence (squares) of a pre-blocking step with a high molecular weight blocking protein (0.5% BSA in PBS).



### 3.3.2.2. BSA-PFPA-LSD.

LSD which was coupled to BSA using a photoreactive linker was poorly suited to ELISA. Polystyrene microtitre plates were coated with BSA-PFPA-LSD overnight at 4 °C and skim milk (5%), BSA (0.5%) or PVA (0.3%) in PBS was used to pre-block the remaining surface. Titration of immune and normal sera on BSA-PFPA-LSD coated plates indicated that similar amounts of IgG were bound over a range of dilutions (Figure 3.8) whereas pre-blocked plates, which were not coated with antigen, had negligible non-specific signal (<0.05 for PVA). Preferential displacement of BSA-PFPA-LSD by the blocking agent would have resulted in a similar low background signal, which was not the case. This suggested that although BSA-PFPA-LSD remained intact after the pre-blocking step, the antigen was preferentially displaced by IgG molecules during the serum incubation (Figure 3.9).

Irreversible adsorption of the antigen is essential; antigen which becomes detached during the serum incubation can increase the non-specific binding and will compete with immobilized antigen for antibody. BSA-PFPA-LSD, which had a molar substitution ratio of 50, was poorly adsorbed to microtitre plates over a range of concentrations, ionic strengths and pH. Very little could be done to improve this property, which is probably the result of the electrostatic changes which take place in BSA during photochemical linking.

**Figure 3.8.** ELISA using BSA-PFPA-LSD as the coating antigen. PVA (0.3% in PBS) was used as the blocking agent.

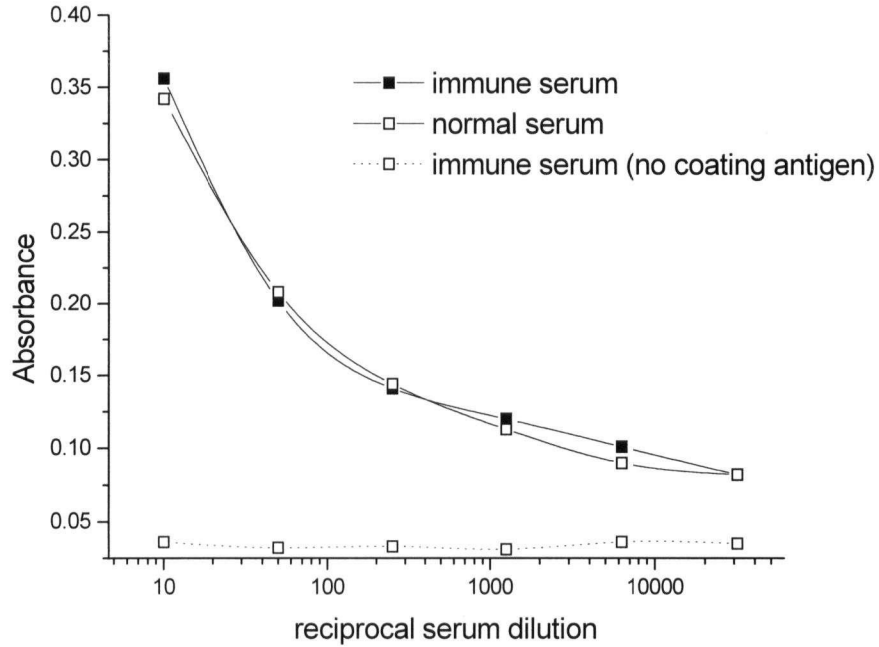
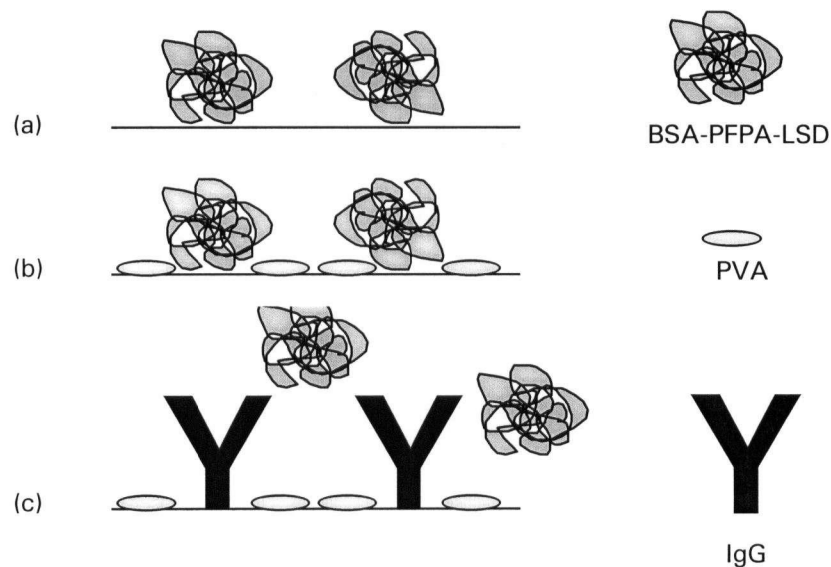


**Figure 3.9.** Schematic illustration of the displacement of BSA-PFPA-LSD coating antigen with IgG molecules in rabbit serum. The surface is coated with antigen, BSA-PFPA-LSD in a), PVA is added to block the remaining sites on the surface in b) and rabbit serum, which contains IgG is added in c).

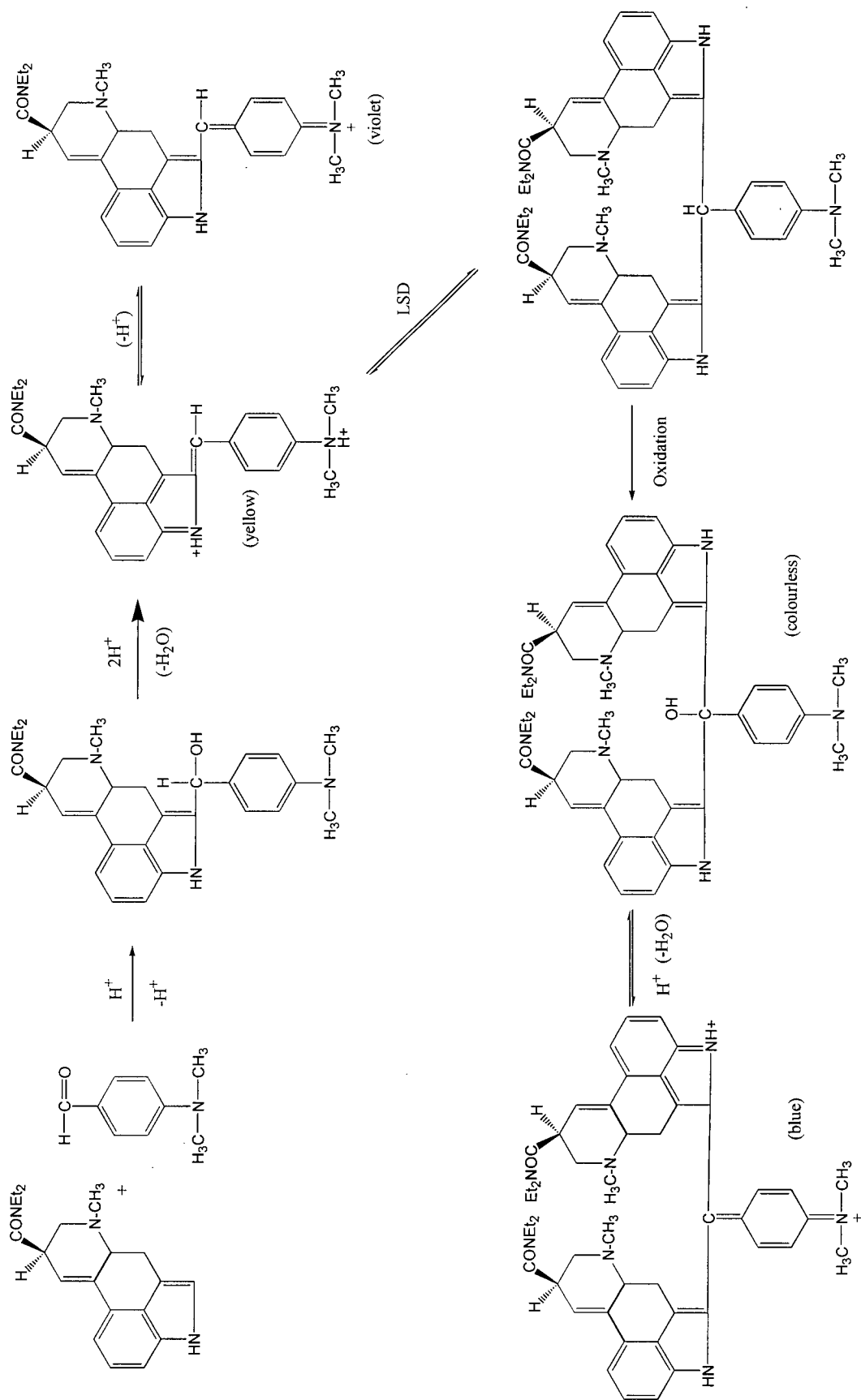


### 3.3.2.3. PVA-LSD.

PVA, which adsorbs well to polystyrene microtitre plates, was used as a carrier molecule for the LSD coating antigen. A variety of methods were used to try to covalently attach LSD to the polymer in such a way that the antibody would recognize the drug and the polymer would not lose its adsorptive properties.

TLC revealed that PVA-PFPA-LSD and PVA-FNPA-LSD contained significant amounts of unbound LSD after photochemical linking, whereas the PVA-LSD reaction mixture surprisingly contained none. The absorption spectrum of dialysed PVA-PFPA-LSD, which was the only visibly fluorescent conjugate, revealed a shift in absorbance maximum from 279 nm (PVA) to 255 nm (PVA-PFPA-LSD), which was consistent with the incorporation of PFPA. TLC results and a shift in the absorption maximum of dialysed PVA-LSD from 279 to 268 nm indicated that a reaction had taken place between the drug and polymer at low pH. PVA contains a number of carbonyl groups which are present as impurities (21) which are present in sufficient quantity to be visible in the UV absorption spectrum (22). It is suggested that LSD could react with these groups in a manner similar to the aldehyde group in the Van Urk reagent, which forms a number of condensation-type products with LSD in the 2-position (23) (Figure 3.10).

**Figure 3.10.** Reaction of *p*-dimethylaminobenzaldehyde with LSD under acidic conditions.



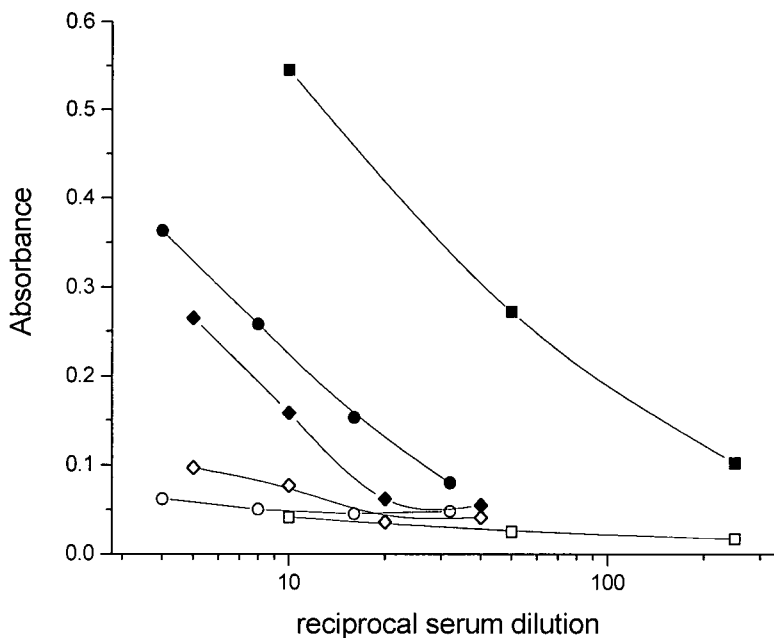
PVA-PFPA-LSD, PVA-FNPA-LSD and PVA-LSD were used to coat polystyrene microtitre plates for ELISA. The success of reaction was measured by titration against immune rabbit serum, using normal rabbit serum as the blank. An immune signal significantly above background indicated that LSD was bound to PVA. Titration data indicated that the specific antibody signal was above background for all PVA antigens tested, which suggests that all three PVA derivatives contained some LSD (Figure 3.11). Once more, all PVA derivatives retained their native affinity to polystyrene, which resulted in low non-specific binding. Subtraction of the non-specific signal from the immune signal was used to rank PVA antigens in the order,

$$\text{PVA-PFPA-LSD} > \text{PVA-FNPA-LSD} > \text{PVA-LSD}.$$

Interestingly, both conjugates prepared using photoreactive linkers (PFPA and FNPA) gave the best results. This may be the result of the aromatic ring between the polymer chain and LSD which makes the drug slightly more accessible to the antibody. Neither of the linkers have extended spacer arms between the two reactive ends, as does SASD in the immunogen. In this respect, one would not necessarily attribute the increased immune signal to cross-reactivity with the SASD moiety of the immunogen, given the structural dissimilarity.

PVA-PFPA-LSD was a better coating antigen than PVA-FNPA-LSD, which was similar in structure. The former, which utilizes a polyfluorinated phenyl azide, is reported to undergo more efficient chemical crosslinking (24,25). A higher incorporation rate of LSD on PVA as a result of the polyfluorinated phenyl azide, might explain the observed increase in specific antibody signal.

**Figure 3.11.** Performance of PVA antigens by ELISA. Closed symbols represent the immune signal and empty symbols show the non-specific signal obtained using normal rabbit serum. The following PVA antigens were used, PVA-PFPA-LSD (squares), PVA-FNPA-LSD (circles) and PVA-LSD (diamonds).



#### 3.3.2.4. BSA-LSD.

LSD which was covalently attached to BSA using the Mannich reaction gave the best overall performance as a coating antigen for ELISA. This soluble conjugate resulted in good specific antibody binding and low non-specific binding. Derivatization of BSA with the drug did not significantly decrease its adsorption to the polystyrene surface; when SM-PBS was used as the blocking solution, normal serum binding indicated that BSA-LSD was not desorbed from the surface, as was the photochemically coupled antigen, BSA-PFPA-LSD.

BSA-LSD was characterized by fluorescence and Bradford dye binding as outlined previously (Section 2.2.3.2). Characteristic absorption maxima for LSD and BSA at 310 nm ( $\epsilon =$

8800 M<sup>-1</sup> cm<sup>-1</sup>) and 280 nm ( $\epsilon = 46200 \text{ M}^{-1} \text{ cm}^{-1}$ ) were used to calculate the molar substitution ratio by UV spectrophotometry for comparison (16). The molar substitution ratios for three conjugate preparations were 2.23 (2.53), 2.3 (2.9) and 4.58 (4.13) by fluorescence/Bradford dye binding and UV spectrophotometry (in brackets), which were in good agreement.

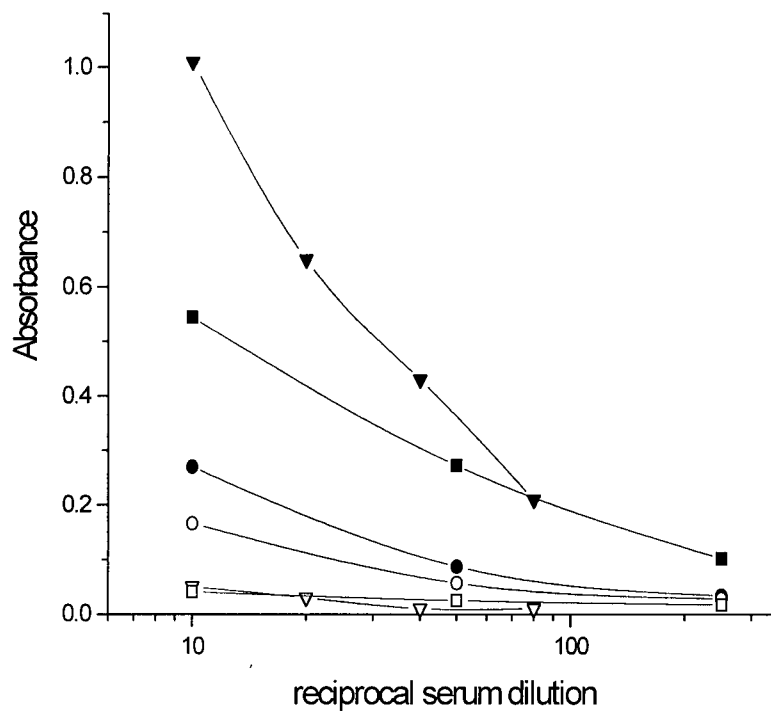
The degree of substitution of LSD on BSA was varied by changing reaction conditions (Section 2.2.5.1). BSA-LSD prepared with molar substitution ratios between 1 and 40 were used as coating antigens for ELISA. Conjugates with high substitution ratios (eg. 40) did not adsorb onto polystyrene microtitre plates; non-specific binding increased with increased molar substitution ratio due to decreased adherence of the conjugate. BSA-LSD with a molar substitution ratio between one and five gave the best results. The specific antibody signal did not increase with increasing epitope density over this range, which suggests that even low substitution ratios provide sufficient LSD coverage. Assuming that about 0.5  $\mu\text{g}$  of antigen is bound to the surface of each microtitre well, the total number of LSD molecules bound per well is of the order  $10^{13}$ .

Figure 3.12 summarizes the performance of different coating antigens by ELISA. The overall trend, in order of decreasing performance was,

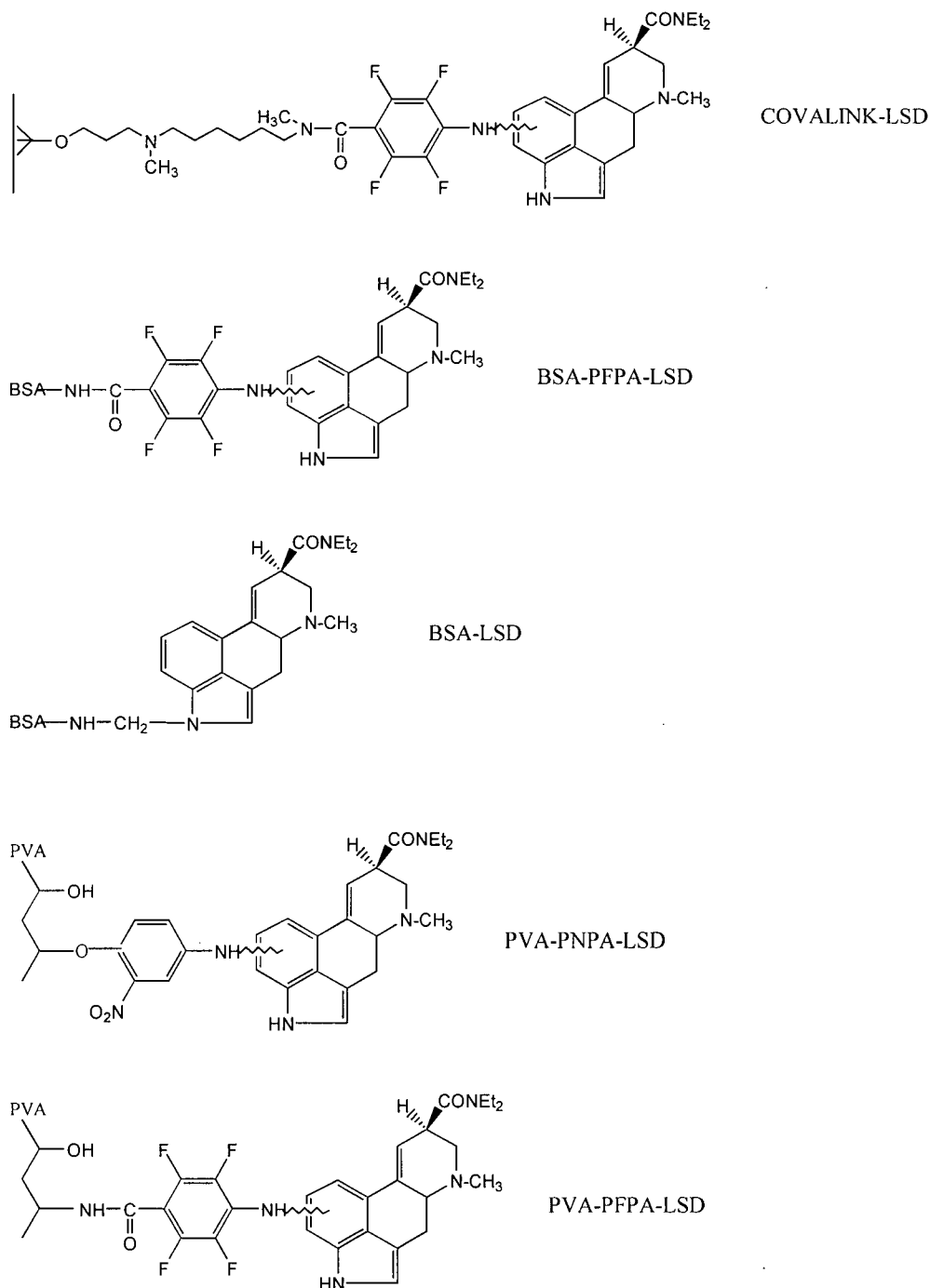
BSA-LSD > PVA-PFPA-LSD > Nunc CovaLink

The structures of these and other drug conjugates which were evaluated by ELISA are shown in Figure 3.13. BSA-LSD prepared by the Mannich reaction was the coating antigen of choice because it gave the highest signal and was prepared and characterized more readily than other derivatives. Mannich coating antigen was used in all subsequent immunoassays (5 - 10  $\mu\text{g}/\text{mL}$  in PBS) unless otherwise stated.

**Figure 3.12.** Performance of different coating antigens by ELISA. Closed symbols represent the immune signal and empty symbols show the non-specific signal obtained using normal rabbit serum. LSD was immobilized on polystyrene wells by covalent attachment on Nunc CovaLink (circles), Mannich reaction between LSD and BSA (triangles), and PVA derivatized with LSD using a photoreactive linker (squares).



**Figure 3.13.** Coating antigens used in ELISA. LSD was coupled to PVA, BSA or directly to microtitre plates using different chemical linkages. The site at which the aryl azide attaches to LSD is not known, although cross-reactivity data suggests it could be at positions 1 (indole nitrogen), 2 or 6 (Chapter 5).



### 3.3.3. Immune response.

#### 3.3.3.1. Antibody titres.

The two rabbits which were immunized with the photolinked immunogen (KLH-SASD-LSD) had lower antibody titres than rabbits which received the Mannich immunogen (KLH-LSD), which was run as a control antibody. Table 3.2 summarizes the antibody titres for both immunogens over a period of four months. Exsanguination of rabbits receiving the photolinked immunogen was performed after four months due to the decrease in antibody titre, whilst those rabbits receiving the Mannich antigen received three more booster injections.

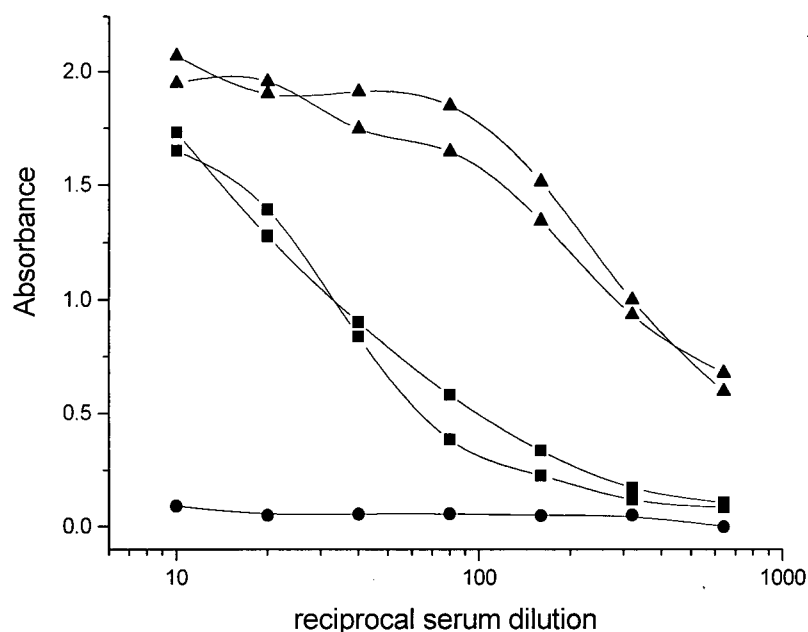
**Table 3.2.** Antibody titres for rabbits immunized with photolinked and Mannich immunogens.

		titre range	highest titre	final titre <sup>1</sup>
photolinked	Rabbit 1	20 - 100	day 40	30
	Rabbit 2	20 - 70	day 63	30
Mannich	Rabbit 1	80 - 300	day 90	300
	Rabbit 2	80 - 300	day 90	300

<sup>1</sup> after four months.

Although photolinked and Mannich immunogens gave very different antibody responses, rabbits which received the same immunogen gave similar results. Figure 3.14 shows antibody titration curves for both immunogens after four months. The comparatively low antibody titres observed are probably due to the very low epitope density of the immunogens (Section 2.3.7).

**Figure 3.14.** Antibody titration curves for rabbits which were immunized with different immunoconjugates over four months. Two rabbits received the photolinked immunogen, KLH-SASD-LSD (squares) and two received the Mannich immunogen, KLH-LSD as a control (triangles). The response of pre-immune (normal) sera is also shown (circles).

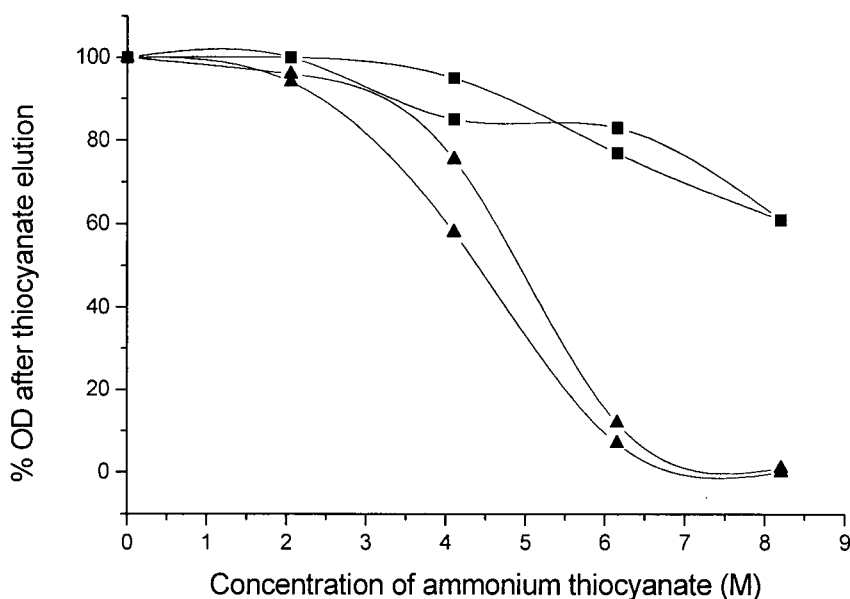


### 3.3.3.2. Functional antibody affinity.

Ammonium thiocyanate was titrated against a fixed antiserum dilution, to assess the functional affinity of the antibody; resistance towards chaotropic thiocyanate ions, which disrupt antibody-antigen bonds, is related to the affinity of the antibody (26). Antibody affinity profiles are shown for both rabbits receiving photolinked and Mannich immunogens over four months (Figure 3.15). The absorbance which remains after treatment with thiocyanate is plotted as a percentage (relative to no thiocyanate) against the concentration of chaotropic ions used. Clearly, antibodies to LSD which were produced in rabbits immunized with the photolinked immunogen were more

resistant to chaotropic ion elution than those immunized with the Mannich immunogen. Once again, both rabbits which were immunized with the same immunogen appear to have similar characteristics, which suggest that the overall immune response, in terms of both antibody affinity and titre may be related to the immunogen design, which is discussed in detail in Chapter 5.

**Figure 3.15.** Antibody affinity profiles for rabbits which were immunized with different LSD immunoconjugates. Two rabbits received the photolinked immunogen, KLH-SASD-LSD (squares) and two received the Mannich immunogen, KLH-LSD (triangles).



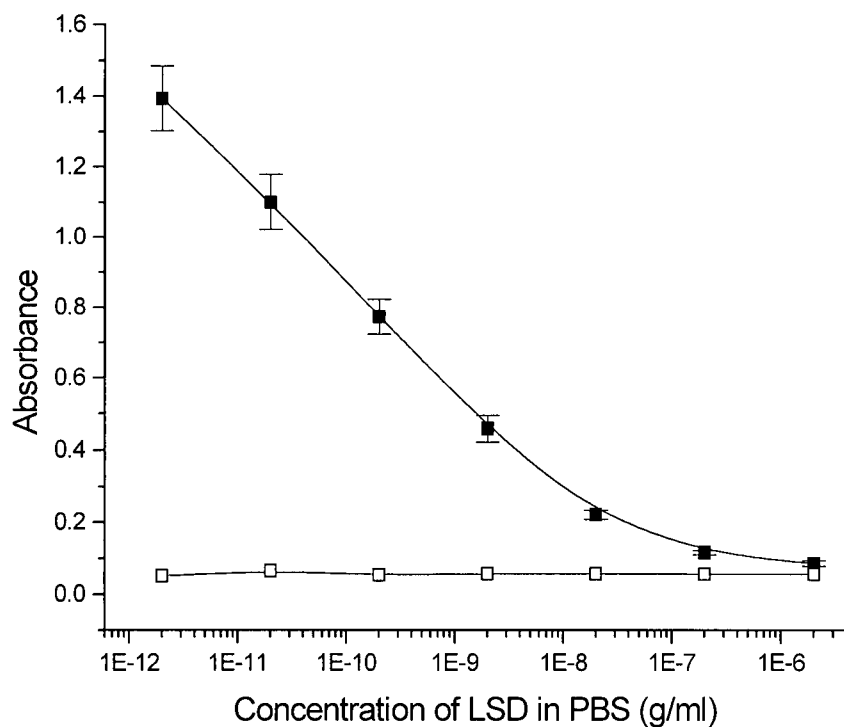
### 3.3.4. Detection of LSD by ELISA.

#### 3.3.4.1. Inhibition assay using free LSD.

The inhibitory effect of free LSD on antibody binding was measured by indirect ELISA (Figure 3.16). The mean blank signal, which contained no LSD was  $1.77 \pm 0.017$  (SD,  $n=5$ ). Clearly, concentrations as low as 1 pg/mL in PBS were detectable by this method in which the serum from

a rabbit immunized with the photolinked LSD immunogen was used with the BSA-LSD coating antigen. This suggests that despite the low titre response, the antibodies raised against the photolinked immunogen were sensitive enough to allow LSD determinations in the sub-ng/mL region of forensic interest.

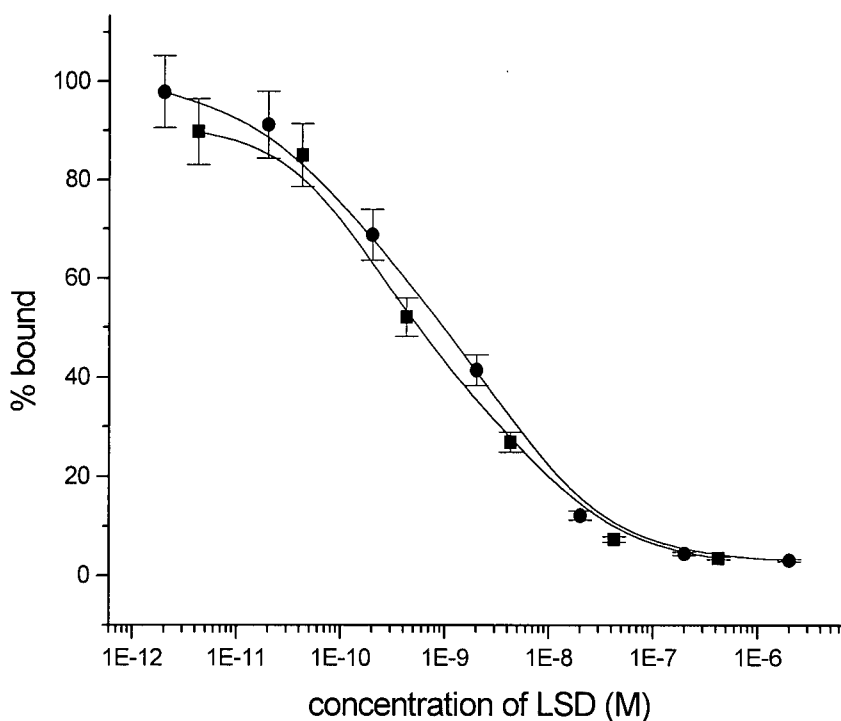
**Figure 3.16.** Detection of LSD in PBS by indirect ELISA. Immune serum (closed squares), normal serum (open squares). Data represents the mean of 5 replicate measurements  $\pm$  1 SD. The absorbance of the blank was  $1.7 \pm 0.017$ .



### 3.3.4.1. Inhibition assay using BSA-LSD.

When free LSD in the above inhibition assay was replaced with BSA-LSD coating antigen, results suggested that the antibodies raised against the photolinked immunogen had similar affinity to both free and conjugated LSD. Assuming the molar substitution ratio of the coating antigen was 1.4 (determined by fluorescence and Bradford dye binding reagents), the molar concentration of LSD at each inhibition concentration of BSA-LSD was calculated. Inhibition curves obtained for both free LSD and LSD in BSA-LSD were very similar (Figure 3.17). Assuming that the molar substitution ratio is correct, these results suggest that the cross-reactivity of the Mannich coating antigen is approximately 100%.

**Figure 3.17.** Inhibition of antibody binding using free drug and haptened protein. Data represents the mean of duplicate measurements  $\pm$  1 SD using either free LSD (circles) or the coating antigen, BSA-LSD (squares).



### 3.4. Conclusion.

LSD was immobilized on the surface of polystyrene microtitre plates using a variety of methods. Each conjugate was evaluated by ELISA in terms of its adsorption to the solid phase, specific antibody signal and non-specific binding. Covalent attachment of LSD to aminated microtitre plates using a heterobifunctional linker was unsuccessful due to high non-specific binding and steric effects. Coating antigens for passive adsorption were prepared by derivatization of BSA and PVA with LSD by direct linkage or via a photoreactive linker.

The best coating antigen for ELISA was BSA-LSD which was derivatized using the Mannich reaction. Surprisingly this conjugate performed better than coating antigens prepared using heterobifunctional linkers, which are expected to facilitate antibody recognition by holding the hapten away from the carrier molecule. In general, coating antigens which were prepared by photochemical linking exhibited poor solubility, desorbed from the polystyrene surface, or produced a low specific antibody signal.

Conversely, the conjugate prepared by the Mannich reaction resulted in the highest specific antibody signal, low non-specific binding and was readily adsorbed onto polystyrene microtitre plates. An inhibition ELISA suggested that the cross-reactivity of the coating antigen was about 100% relative to LSD. In other words, the affinity of the antibody raised against the photolinked immunogen was approximately the same for both free LSD and BSA-LSD.

Antibodies to LSD were detected in the serum of rabbits immunized with the photolinked immunogen described in Chapter 2. A low titre immune response was measured, which was likely the result of the very low epitope density of the immunizing antigen. However, these antibodies were highly resistant to dissociation during ELISA, which suggested that a high affinity antibody might

be present.

Antibodies raised against the photolinked immunogen were used in an inhibition ELISA, whereby free LSD in solution competes with LSD immobilized on the surface of the microtitre well for a limited number of antibody molecules. Using this method, it was possible to inhibit antibody binding using ng/mL to pg/mL concentrations of LSD, which was a good indication that such a test might be useful for the determination of LSD in the sub-ng/mL region of forensic interest.

### 3.5. References.

1. Rose, B.G., Kamps-Holtzapfle, C., and Stanker, L.H. 1995. *Bioconjugate Chem.* 6: 529-535.
2. Danilova, N.P. 1994. *J. Immunol. Methods* 173: 111-117.
3. Zouali, M. and Stollar, B.D. 1986. *J. Immunol. Methods* 90: 105-110.
4. Boudet, F., Theze, J., and Zouali, M. 1991. *J. Immunol. Methods* 142: 73-82.
5. Buchardt, O., Jorgensen, A.W., Henriksen, U., Rasmussen, M., Lohse, C., Lovborg, U., Bjerrum, O., and Nielsen, P.E. 1993. *Biotechnol. Appl. Biochem.* 17: 223-237.
6. Nygren, H. and Stenberg, M. 1989. *Immunology* 66: 321-327.
7. Ansari, A.A., Hattikudur, N.S., Joshi, S.R., and Medeira, M.A. 1985. *J. Immunol. Methods* 84: 117-124.
8. Lehtonen, O.P. and Viljanen, M.K. 1980. *J. Immunol. Methods* 34: 61-70.
9. Hobbs, R.N. 1989. *J. Immunol. Methods* 117: 257-266.
10. Zammateo, N., Girardeaux, C., Delforge, D., Pireaux, J., and Remacle, J. 1996. *Anal. Biochem.* 236: 85-94.
11. Sondergard, J., Lauritzen, E., Lind, K., and Holm, A. 1990. *J. Immunol. Methods* 131: 99-104.
12. Nunc, Roskilde, Denmark. 1993. Colorimetric Determination of Amino Groups of Covalink NH Microwells, *Nunc Bulletin Number 11*.
13. Rasmussen, S.E. 1990. *Annales de Biologie Clinique* 48: 647-650.
14. Nunc, Roskilde, Denmark. 1990. CovaLink, *User Manual*.
15. Hermanson, G.T., Mallia, A.K., and Smith, P.K. 1992. Immobilized Affinity Ligand Techniques, Academic Press, San Diego.
16. Taunton-Rigby, A., Sher, S.E., and Kelley, P.R. 1973. *Science* 181: 165-166.
17. Pierce Chemical Company, Rockford, IL. 1992. BCA Protein Assay, *package insert*.
18. Spinola, S.M. and Cannon, J.G. 1985. *J. Immunol. Methods* 81: 161-165.
19. Jakubke, H.D. 1983. Concise Encyclopedia of Biochemistry, Walter de Gruyter, Berlin.

20. Neurath, A.R. and Strick, N. 1981. *Journal of Virological Methods* 3: 155-165.
21. Molyneux, P. 1984. *Water Soluble Synthetic Polymers: Properties and Behaviour*, Volume I, CRC Press, Boca Raton.
22. Lloyd, D.G. 1959. *Journal of Applied Polymer Science* 1(1): 70-72.
23. Look, J. 1967. *J. Pharm. Sci.* 56(11): 1526-1527.
24. Brinkley, M. 1992. *Bioconjugate Chem.* 3: 2-13.
25. Yan, M., Cai, S.X., Wybourne, M.N., and Keana, F.W. 1994. *Bioconjugate Chem.* 5: 151-157.
26. Ferreira, M.U. and Karzin, A.M. 1995. *J. Immunol. Methods* 187: 297-305.

## Chapter 4.

### Quantitative Enzyme-Linked Immunosorbent Assay for LSD in Urine.

#### 4.1. Introduction.

The continued use of lysergic acid diethylamide (LSD) for recreational drug use has persisted for over 30 years. LSD ingestion frequently causes hallucinations, delusions, panic reactions and other abnormal behaviour. In an emergency room setting it can be difficult to differentiate LSD intoxication from stimulant drug overdose or psychosis. Due to its high potency as a psychedelic drug, LSD is ingested orally in relatively small doses, typically about 100  $\mu\text{g}$ . This, along with the rapid biotransformation of LSD, necessitates the use of highly sensitive techniques for the detection and quantification of drug in biological fluids. It was reported that the maximum urinary concentration of parent drug in 2 human subjects was 0.9 and 1.6 ng/mL, which was detected 2 and 4 hours after administration of a typical LSD dose (1). However, the concentration of LSD in urine can drop to sub-ng/mL within a few hours after ingestion, which provides a considerable analytical challenge for law enforcement and drug detection agencies (2,3).

*N*-demethyl-LSD (nor-LSD) is the only confirmed human metabolite in vivo although a number of other substances have been tentatively identified. Only about 0.9% of the total LSD ingested is excreted in the urine, with a half life of elimination of 3.6 hours (4). Approximately

1.2% of the drug is excreted as the nor-LSD metabolite in urine which has an increased biological half life of 10.0 hours. The increased persistence of the metabolite in urine can allow recent drug use to be detected, even after the concentration of unmetabolized LSD has dropped below the detection limit of the technique. Animal studies have shown that LSD undergoes *N*-demethylation, *N*-deethylation, aromatic hydroxylation and oxidation in the 2 position, among other biotransformations to give, as yet, unidentified metabolites (5). A metabolic study using isolated perfused rat liver indicated that the highest concentrations of drug and metabolites were found in the bile and liver, mostly as hydroxylated glucuronide conjugates (6). Using human liver, in-vitro metabolites have been identified as lysergic acid ethylamide and 2-oxo-LSD (7). However, a substantial portion of the administered dose is not accounted for by our current understanding of LSD biotransformation in humans. As such, analytical techniques are primarily focussed on the detection of parent drug, confirmed metabolite (nor-LSD) and other ergot alkaloids which may be present in an illicit LSD sample (eg. *iso*-LSD).

The most frequently used techniques for the detection of LSD in urine and biological matrices are thin layer chromatography (TLC), radioimmunoassay (RIA), high performance liquid chromatography - fluorescence (HPLC-FL) and gas chromatography-mass spectrometry (GC-MS). As a general rule, the latter methods require large sample volumes, are technically demanding and are poorly suited for high sample throughput. Immunoassays are advantageous in terms of their potential sensitivity, small sample volume requirement and large sample capacity. In general an immunoassay is the first test in the routine investigation of biological specimens for drugs of abuse according to recognized guidelines (8). However, the positive identification of LSD based on an immunoassay results is not considered conclusive for legal purposes due to low assay specificity. It is quite common for antibodies raised against the parent drug to undergo cross-reactions with

structurally similar molecules including metabolites, some of which are as yet unidentified. Those samples which screen positive must be confirmed using a more rigorous technique which has both adequate sensitivity and specificity.

The most frequently used screening technique for LSD has been radioimmunoassay, of which there are a number of commercially available kits in both Europe and North America. The sensitivity of different radioimmunoassays for LSD are reported in the literature as 0.2, 0.4, 1.0 and 5 ng/mL (9-12). The cut-off concentration recommended by the manufacturer, above which a sample is considered positive, is usually 0.5 ng/mL to avoid the possibility of false positives. However, forensic case samples are often below this cut-off concentration which frequently results in the test being used at concentrations lower than recommended, eg. 0.1 ng/mL (13). This is because, following a typical dose, the concentration of LSD can fall below the cut-off concentration within 24 hours (1). Ideally, the cut-off value should be set at a reasonable concentration that reflects the urinary elimination of the drug (8). However, it must also reflect the sensitivity which is attainable using current analytical techniques.

The need for a highly sensitive immunoassay for LSD is probably the result of increasingly sensitive confirmatory procedures, the relatively short detection time of the drug and the renewed interest in LSD, due to a resurgence of abuse among young people (14). The main advantage of radioimmunoassay is its inherent sensitivity when it is used with a radiolabelled drug which has a high specific activity. However, recent trends have been towards non-isotopic procedures which are safer, have longer shelf-lives and do not need special disposal and laboratory facilities. A number of recent advances have been made regarding immunoassay screening technologies for LSD drug use, some of which can be used in a quantitative mode. These include the OnLine latex based aggregation assay (Roche Diagnostic Systems, Somerville, NJ) (15), cloned enzyme donor

immunoassay, or CEDIA (Boehringer Mannheim Corp., Concord, CA) (16) and the enzyme multiplied immunoassay technique, EMIT II (Behring Diagnostics, San Jose, CA). The disadvantage is that these methods require the use of large and expensive automated analysers. Recently however, an enzyme linked immunosorbent assay was made available (STC, Bethlehem, PA) which is reported to be sensitive down to 0.085 ng/mL LSD in urine (17).

Confirmatory analysis using techniques such as HPLC-FL and GC-MS in the past has suffered from relatively poor sensitivity, typically around 0.5 ng/mL in urine (1,2,13,18,19). This is the result of normal background interference observed with biological specimens, the need for prior extraction, derivatization, as well as thermal instability, low volatility and the tendency of the drug to undergo absorptive losses during chromatographic procedures. However, recent advances in mass spectrometry, particularly MS-MS coupled procedures, have resulted in significant improvement of confirmatory analysis. There are an increasing number of reports which describe mass spectrometric confirmation of LSD with sensitivities between 10 - 50 pg/mL (3,4,7,18,20,21).

The aim of this work was to develop an enzyme-linked immunosorbent assay for LSD in urine which was as sensitive as the emerging confirmatory techniques. A competitive binding assay which utilizes a novel polyclonal drug antibody is used to quantify LSD in urine. Free drug in the urine specimen and immobilized drug on the surface of a polystyrene well compete for a limited number of antibody binding sites. Antibody which is bound to immobilized antigen is detected using peroxidase labelled anti-IgG and subsequent tetramethylbenzidine colour reaction in which the absorbance is inversely proportional to the concentration of drug in the sample (Section 1.3.5.2). The primary objective was to develop and optimize conditions for the detection of LSD in urine and characterize immunoassay performance in terms of precision, accuracy,

sensitivity and assay range. It should be noted that quantitative estimates of LSD in biological fluids are typically higher by immunoassay compared to confirmatory techniques, which is attributed to the cross-reactivity of the antibody with drug metabolites present in urine (11,22,23). Therefore quantitative estimates obtained by immunoassay more closely represent the concentration of LSD and related compounds in the urine, depending on the specificity of the immunoreagent (investigated in Chapter 5). For the purpose of this study, the sensitivity of the immunoassay is described exclusively with respect to the parent drug, LSD. Drug-free urine samples used in the study were spiked with a pure standard of *d*-LSD tartarate and were therefore free of metabolites or related LSD-like substances which might be present in the urine of someone who had taken LSD.

The assay sensitivity is the lowest concentration of drug determinable, below which the test is no longer considered reliable. The minimum detectable concentration is determined by the physical and chemical properties of the immunoassay constituents and by the mathematical formulae used to calculate it. There are essentially three analytical regions, consisting of unreliable detection, qualitative analysis and quantitative analysis. The limit of detection (LOD) is the lowest analyte concentration that is considered acceptable for qualitative analysis. This value is calculated from the mean response of the zero calibrator (blank) minus 3 standard deviations (SD). The limit of quantification (LOQ) is the lowest analyte concentration that is considered reliable for quantitative purposes. This value is defined as the mean negative response from a number of drug-free individuals minus 3 SDs. This value reflects the variation in assay sensitivity between individuals of different age, sex, diet, metabolism etc.

The accuracy is dependent on a number of analytical variables ranging from assay configuration to pipetting technique. Good precision is necessary to discriminate a positive from

a negative sample when the analyte concentration is near the sensitivity limit of the assay. Spike and recovery methods are commonly used for the evaluation of assay accuracy. LSD is spiked into drug-free urine over the concentration range of interest. Calibration standards are used to construct a dose-response curve (or calibration curve) and the spiked LSD samples are interpolated from the calibration graph. Assay precision is estimated from the coefficient of variation (CV) of replicate analyses. Within run (intra-assay) and between run (inter-assay) CVs are used to estimate the precision of measurements over the concentration range of interest.

Calibration curves are non linear due to the hyperbolic nature of the binding reaction and the heterogeneous nature of the polyclonal antibody. Four parameter logistic equations most frequently satisfy the need for flexibility of shape and position for immunoassay dose-response relationships (24-26). Four parameter curve fits were calculated using Microcal Origin (Northampton, MA) according to the equation,

$$y = \frac{A_1 - A_2}{1 + (x / x_0)^p} + A_2$$

Where,  $y$  is the response (or signal)

$A_1$  is the response at the high asymptote (zero dose)

$A_2$  is the response at the low asymptote (high dose)

$x_0$  is the midpoint of the curve

$p$  is the slope factor (or gradient at the midpoint of the curve).

Finally, the use of an amplifying system was investigated to increase the overall signal due to the low titre response of the antibody used in the assay. The peroxidase-anti-peroxidase (PAP)

complex was chosen due to its simplicity and the need for only one additional incubation step. In this system an anti-rabbit IgG molecule serves as a bridge between the drug antibody and the PAP complex, which is available commercially. Anti-peroxidase antibodies are raised in the same host animal as the antibody to drug. When peroxidase is added to anti-peroxidase antibodies, the immune complex facilitates an amplified absorbance reading due to the increased amount of peroxidase which is attached to one IgG molecule.

## 4.2. Materials and methods.

Disposable 96 well polystyrene plates were obtained from Corning (New York, NY). Lysergic acid diethylamide tartarate was kindly supplied by Dr. Haro Avdovich of the Bureau of Drug Research, Health Canada (Ottawa, ONT). The LSD working standard, which was used to prepare calibration standards, was prepared daily for quantitative analysis. Goat anti-rabbit IgG horseradish peroxidase, goat anti-rabbit IgG, rabbit peroxidase-anti peroxidase and 3, 3', 5, 5'-tetramethylbenzidine (TMB) were purchased from Sigma (St. Lois, MO). A 5% solution of Carnation non fat skim milk powder in 150 mM phosphate buffered saline, pH 7.4, (PBS) was routinely used as the blocking agent (SM-PBS). Inorganic salts, hydrogen peroxide and acids supplied by Fisher Scientific (Edmonton, AB) were certified ACS grade. Anti-LSD serum was obtained from rabbits immunized with the LSD immunogen, KLH-SASD-LSD.

As outlined in Chapter 3, the concentration of LSD in a sample can be determined by indirect ELISA whereby free drug in the sample competes with immobilized drug on the surface of a polystyrene microtitre plate for a limited number of binding sites on drug specific antibodies. The general procedure for the competitive binding ELISA was as follows. Microtitre plates were coated overnight at 4 °C with 100  $\mu$ L of BSA-LSD coating antigen (10  $\mu$ g/mL in PBS) which was prepared by the Mannich reaction (9,10,27,28). Uncoated sites were pre-blocked with 175  $\mu$ L SM-PBS for 0.5 hours at 37 °C. Plates were washed 5 times with PBS between each of the following incubation steps. LSD was diluted in neat drug-free urine over the concentration range of interest (typically  $10^{-12}$  to  $10^{-7}$  g/mL) and 50  $\mu$ L was added to the plate. Anti-LSD rabbit serum in double strength blocking solution was added to the urine to give an overall serum dilution of 1:50 and a total volume of 100  $\mu$ L. Normal serum from pre-immune rabbits was used to estimate the non-specific binding. After gentle mixing, the plate was incubated at 37 °C for a specified time. After

washing the plate; 100  $\mu\text{L}$  of diluted goat anti-rabbit IgG horseradish peroxidase (1:1000) in blocking solution was added and incubated for 30 minutes at 37 °C. The colour reaction was initiated with 100  $\mu\text{L}$  of TMB substrate solution followed by 50  $\mu\text{L}$  1M sulfuric acid to stop the reaction 5 minutes later. Optical densities were measured at 450 nm, using 620 nm as the reference using an SLT EAR 400AT plate reader (SLT Lab-Instruments, Austria).

#### **4.2.1. Optimization of assay conditions.**

Optimum assay performance was investigated using an empirical approach to experimental conditions. In general, LSD calibration data was generated by changing one variable at a time (eg. incubation time) due to the restriction in the number of samples which could be run in one plate, and the need for replicates for reliable comparisons. Detector antibodies, such as anti-rabbit IgG peroxidase and rabbit PAP were used at dilutions which gave the highest background subtracted signal. Assay optimization was performed during the immunization of rabbits in which different sera were used over time. As one set of conditions indicated optimum assay performance, these conditions were routinely employed in subsequent assays. This step by step approach to assay optimization using different serum batches allows the comparison of assay characteristics within experiments but not between them, as the quality of the antiserum changed over time.

##### **4.2.1.1. Effect of human urine on ELISA.**

The first step in the investigation of assay conditions was to investigate the effect of human urine on the ELISA with respect to absorbance, non-specific signal, precision and calibration characteristics. Polystyrene microtitre plates were coated with 100  $\mu\text{L}$  BSA-LSD conjugate (10

$\mu\text{g/mL}$ ) in PBS overnight at  $4^\circ\text{C}$ . Remaining protein binding sites on the surface of the wells were pre-blocked with  $150\ \mu\text{L}$  of SM-PBS for 30 minutes at  $37^\circ\text{C}$ . After rinsing the plate with PBS (5 times),  $85\ \mu\text{L}$  of solution containing LSD over a range of concentration was added to the plate. LSD was made up in blocking solution, neat urine and a 1:1 mixture of urine and blocking solution. Each concentration of LSD was measured in triplicate over the calibration range for each sample matrix. Diluted LSD antiserum ( $15\ \mu\text{L}$ ) in blocking solution was added to each well and allowed to incubate at  $37^\circ\text{C}$  for 1.5 hours. Normal rabbit serum at the same dilution was added to wells to estimate the degree of non-specific signal. After the plate was washed again with PBS, goat anti-rabbit IgG peroxidase labelled conjugate antibody (1:1000) in blocking solution was added ( $100\ \mu\text{L}$ ) and incubated at  $37^\circ\text{C}$  for 45 minutes. After a final plate wash,  $100\ \mu\text{L}$  of TMB substrate solution was added for 3 minutes before the reaction was stopped with acid. The absorbance was measured at  $450\ \text{nm}$  using  $620\ \text{nm}$  as the reference in the usual way. In other assays, the amount of skim milk powder in blocking agent mixed with urine was increased and the relative volumes of urine and diluted antibody were varied.

#### 4.2.1.2. Pre-incubation of sample with antibody.

An ELISA similar to that described in section 4.2.1.1. was used to investigate the effect of pre-incubation of urine sample with antibody prior to incubation in the microtitre plate. Equal volumes of LSD in urine and diluted antibody in double strength blocking solution were pre-incubated for 30 minutes at  $37^\circ\text{C}$  after which  $100\ \mu\text{L}$  was added to the ELISA plate and incubated for 1.5 hours at  $37^\circ\text{C}$ . LSD calibration data prepared in this way was compared with drug and antibody which was not pre-incubated, but added directly to the plate in a 1:1 mixture. Peroxidase labelled conjugate antibody and the TMB colour reaction was used to detect the percent of

antibody bound at each concentration of LSD in the usual way.

#### **4.2.1.3. Antibody concentration.**

LSD calibrators in urine were run in the ELISA as outlined previously. Urine containing drug and diluted antibody in double strength blocking solution mixed in a 1:1 ratio were incubated directly in microtitre plates which had been coated with BSA-LSD and pre-blocked with SM-PBS (Section 4.2.1.1). Different dilutions (1:20, 1:50 and 1:100) of rabbit serum were used to measure the effect of antibody concentration on the ELISA. Replicates (n=4) of each LSD calibrator over the concentration range of interest were run for each of the three antibody dilutions.

#### **4.2.1.4. Antibody incubation conditions.**

LSD calibration data was obtained from experiments in which the antibody-antigen incubation time was varied (0.5 to 2.0 hours). Replicate measurements of each LSD calibrator were performed in urine (n=4) under the same conditions. Normal rabbit serum was used to estimate the degree of non-specific binding in the assay.

The effects of pH and ionic strength were investigated with respect to the absorbance of the background subtracted signal. Replicate measurements (n=4) were made with urine and antibody diluted in blocking solution at pH 9.4, 8.5, 8.0 and 7.4 using the indirect ELISA described previously. LSD was calibrated using 1:1 mixtures of urine and 10% skim milk in 150 to 400 mM PBS to measure the effect of ionic strength on antibody binding characteristics.

#### **4.2.1.5. Coating antigen concentration.**

The effect of coating antigen concentration on ELISA was investigated by sensitizing microtitre plates overnight with different concentrations of BSA-LSD conjugate. LSD in urine was calibrated between 1 pg/mL and 10 ng/mL using ELISA plates which were coated with 5 - 0.5  $\mu\text{g/mL}$  of drug conjugate in PBS. Calibration data obtained under these conditions was compared with respect to changes in sensitivity, precision and non-specific binding.

#### **4.2.1.6. Incubation with enzyme conjugate antibody.**

The dilution of goat anti-rabbit IgG peroxidase was determined for each antibody lot purchased. Dilutions were used which gave the maximum background subtracted signal. The effect of incubation time was investigated between 0.5 and 2 hours over a range of conjugate antibody concentrations (1:500 to 1:10,000) by checker-board titration, in which incubation time was varied in one direction across the microtitre plate and dilution was varied across the other.

#### **4.2.1.7. TMB reaction time.**

LSD was calibrated in urine in the usual way, this time allowing different reaction times for colour development. The colour reaction was allowed to proceed for a given time before 1 M sulfuric acid was added to stop the reaction. The absorbance was measured at 450 nm, using 620 nm as the reference, as outlined previously.

#### **4.4.2. Evaluation of assay performance.**

##### **4.2.2.1. Limit of detection.**

The optimized competitive binding ELISA described in Appendix II was used to construct a calibration graph for LSD in urine ( $2 \times 10^{-12}$  -  $2 \times 10^{-8}$  g/mL). LSD standards and the zero calibrator (blank) were run in quadruplicate. Normal rabbit serum was also run in the assay to estimate the degree of non-specific binding, which was subtracted from subsequent data. The percent of antibody bound was calculated relative to the blank, which contained no LSD (100% bound). The limit of detection was calculated from the mean - 3 standard deviations of the blank.

##### **4.2.2.2. Limit of quantification.**

Drug-free urine specimens were stored without preservative at  $-20^{\circ}\text{C}$  for 1 to 6 weeks prior to use. The optimized LSD ELISA described in Appendix II was used to measure LSD calibration standards ( $2 \times 10^{-12}$  -  $2 \times 10^{-8}$  g/mL) in urine and the blank ( $n=4$ ). Urine specimens obtained from 24 drug-free volunteers was used to estimate the spread of the negative response from one individual to the next. Non-specific binding, which was estimated using normal rabbit serum was subtracted from absorbance readings. The percent of antibody bound was calculated for each inhibitor concentration relative to the blank, which contained no LSD. The lower limit of quantification was calculated from the mean negative response minus 3 standard deviations. The upper limit of quantification, which determines the maximum quantifiable concentration of drug, was calculated from the background signal plus 3 standard deviations.

#### **4.2.2.3. Accuracy: spike and recovery.**

Urine specimens were spiked with LSD to give final concentrations of 10.0, 1.0 and 0.1 ng/mL. Replicate measurements (n=8) were used to interpolate the concentration from the calibration curve using a four parameter logistic equation. The analytical recovery of drug, 95% confidence limits and coefficients of variation were calculated for each sample.

#### **4.2.2.4. Intra and inter-assay precision.**

The intra-assay (within run) precision was estimated from the coefficient of variation (CV) of calibration standards (n=4) over a range of concentrations. The inter-assay CV (between run precision) was estimated from calibration standards run in 12 assays performed over 4 months. Three standards (2.00, 0.20 and 0.02 ng/mL LSD in urine) were run in every assay to serve as quality control markers. Results were plotted in chart form over a period of months to assess the repeatability of quantitative measurements and to record any differences due to reagent changes.

### **4.2.3. Amplification of ELISA signal using peroxidase-anti-peroxidase.**

#### **4.2.3.1. Optimization and assay performance.**

The peroxidase-anti-peroxidase amplification system was used to increase the overall absorbance of ELISA measurements. In general, after incubation of the sample with rabbit anti-LSD antibodies, anti-rabbit IgG was added to the plate, followed by rabbit peroxidase-anti-peroxidase (PAP). Finally, TMB substrate solution is used to detect the amplified signal in the usual way. The general procedure for the amplified ELISA was as follows. Polystyrene microtitre plates were coated with 100  $\mu$ L BSA-LSD conjugate (10  $\mu$ g/mL) in PBS overnight at 4 °C.

Remaining protein binding sites on the surface of the wells were pre-blocked with 150  $\mu\text{L}$  of SM-PBS for 30 minutes at 37 °C. After rinsing the plate with PBS (5 times), 50  $\mu\text{L}$  of urine containing LSD was added to the plate. LSD antiserum diluted in 10% SM-PBS (50  $\mu\text{L}$ ) was added to each well and allowed to incubate at 37 °C for a given time. Normal rabbit serum at the same dilution was added to wells to estimate the degree of non-specific signal. After the plate was washed with PBS, either goat anti-rabbit IgG or goat anti-rabbit IgG peroxidase diluted in SM-PBS was added (100  $\mu\text{L}$ ) and incubated at 37 °C for a specified time. After washing the plate, rabbit peroxidase-anti-peroxidase diluted in blocking solution was added. After a final plate wash, 100  $\mu\text{L}$  of TMB substrate solution was added for 5 minutes before the reaction was stopped with acid. The absorbance was measured at 450 nm, using 620 nm as the reference in the usual way.

Assay conditions were optimized with respect to antibody-antigen incubation time, coating antigen concentration, serum dilution and detector antibody incubation times and dilutions as outlined in section 4.2.1. Particular attention was paid to the effect of assay conditions on precision, sensitivity and non-specific binding. Once suitable conditions were found, the overall assay performance was evaluated as described in section 4.2.2.

### 4.3. Results and discussion.

#### 4.3.1. Assay optimization.

##### 4.3.1.1. Effect of urine on ELISA.

The effect of different sample matrices on the LSD calibration by ELISA is shown in Figure 4.1. When 5% SM-PBS is replaced with a 1:1 mixture of urine and blocking solution or neat urine, assay performance gradually worsens; the slope of the calibration curve decreases, sensitivity decreases, precision of individual measurements decreases and the non-specific signal increases (Table 4.1). The numerical evaluation of the steepness of the slope was estimated from the calculated  $p$  value obtained from a four parameter logistic equation; as the curve steepens,  $p$  increases numerically. The value of  $p$  is numerically derived from the gradient at the midpoint of the calibration, at which the dose-response relationship is approximately linear. The steepness of the calibration curve is a good indication of assay sensitivity and precision. An increase in  $p$  indicates a large change in signal for a small change in concentration, increasing assay precision. Although the steepness of the curve is largely pre-determined by the affinity of the antibody (26,29), it is also affected by ELISA conditions and matrix effects.

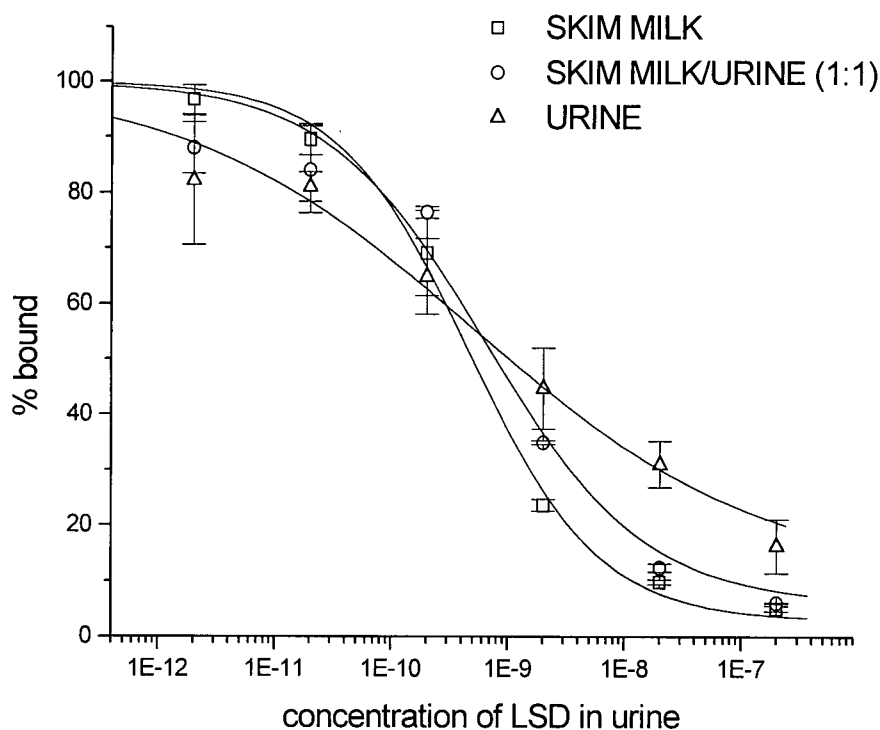
An indication of assay sensitivity is also obtained from the concentration of drug which results in 50% antibody binding (EC<sub>50</sub>) which can be used to measure a positional shift in the calibration curve to the left (increased sensitivity) or the right (decreased sensitivity). The overall CV, which was averaged for all calibration standards increases over the entire range from around 4% in buffer to 12% in neat urine. This represents a substantial decrease in assay precision, which is evident from the increased size of the error bars ( $\pm 1$  SD) for individual LSD calibrators (Figure

4.1). The absolute absorbance decreased by 25% when a 1:1 mixture of blocking solution and urine was used. However, the increased absorbance using neat urine was largely the effect of non-specific binding (NSB), which increased steadily with increased urine content from 2.9% to 5.5% to 10.4% in neat urine.

**Table 4.1.** Effect of sample matrix on ELISA performance. LSD calibration curves were generated in 5% SM-PBS, neat urine and a 1:1 mixture of the two.

	5% skim milk	5% skim milk/urine (1:1)	neat urine
steepness of slope, $p$	0.78	0.64	0.35
EC50 (g/mL)	$4.9 \times 10^{-10}$	$7.8 \times 10^{-10}$	$1.0 \times 10^{-9}$
overall % CV (n=3)	4.2	3.7	12.5
Maximum OD (blank)	0.81	0.60	0.74
% NSB	2.9	5.5	10.4

**Figure 4.1.** Effect of urine on LSD calibration. Skim milk blocking solution (5%), a mixture of 5% skim milk and urine (1:1) and neat urine. Data is represented by the mean % of antibody bound (n=3)  $\pm$  1 SD. Calibration curves indicate the decreased precision and increased non-specific signal when urine is used instead of blocking solution.



In order to measure LSD in urine under conditions which closely resemble the ideal buffered system (5% SM-PBS), urine and diluted antibody were varied in volume and composition and evaluated using the above criteria. Optimum conditions were obtained when equal volumes of LSD in urine and diluted antibody in double strength blocking solution (10% SM-PBS) were used. Under these conditions, the calibration curve obtained using LSD in the urine matrix closely resembled that of buffer. The steepness of the calibration curve and precision of replicate blank measurements ( $CV_{\text{blank}} = 5.3$  and  $4.7\%$  in buffer and diluted urine respectively,  $n=4$ ) was not compromised. The dose-response curve obtained from urine calibrators increased the 50% binding concentration from  $4.8 \times 10^{-10}$  (in buffer) to  $6.8 \times 10^{-10}$  g/mL. However, the absorbance of the urine matrix was not lowered, relative to buffer measurements and the non-specific signal was within acceptable limits ( $<5\%$ ).

Improved precision was observed when the volume of LSD in urine and antibody in skim milk were equal ( $50 \mu\text{L}$  each) rather than  $85$  and  $15 \mu\text{L}$  respectively. The overall CV of the LSD calibrators decreased from  $10.3$  to  $7.5$  ( $n=4$ ) which was accompanied by a decrease in the CV of the blank ( $CV_{\text{blank}}$ ). Increased precision is merely an effect of the decreased volumetric error when  $50 \mu\text{L}$  aliquots of drug and antibody are pipetted. This also decreases the overall sample requirement of the assay from  $85$  to  $50 \mu\text{L}$ , which is preferable.

#### 4.3.1.2. Pre-incubation of urine specimens.

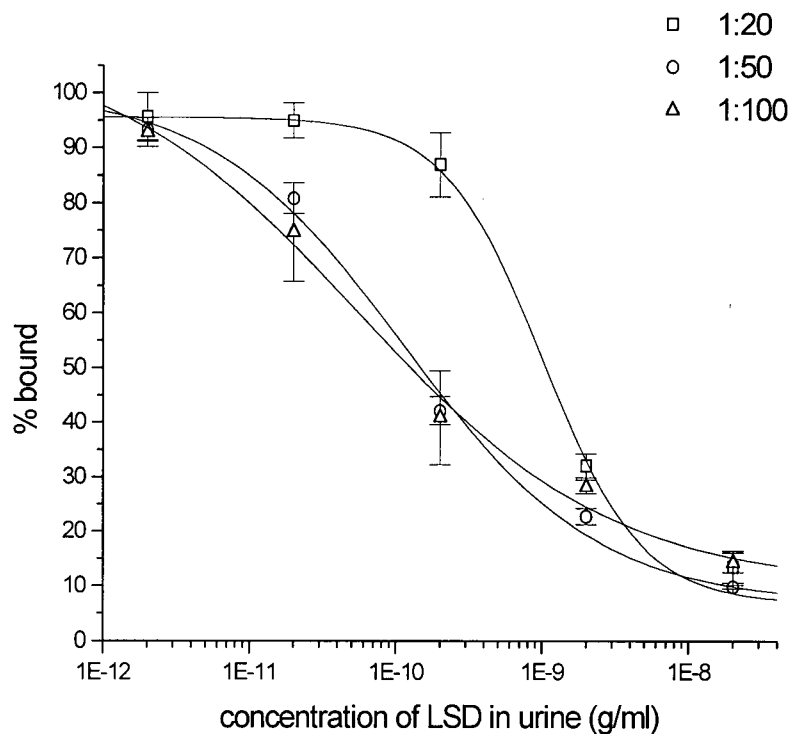
Pre-incubation of the test solution with the antibody prior to the ELISA had no effect on the assay calibration. However, the overall precision of pre-incubated samples was decreased due to the increased number of volumetric steps. Pre-incubation of the specimen with antibody in the absence of labelled antigen, or in our case, immobilized antigen (BSA-LSD) can sometimes improve immunoassay sensitivity (29). However, in this instance, no improvement was evident and direct incubation of drug and antibody in the microtitre plate gave satisfactory results.

#### 4.3.1.3. Serum dilution.

Sensitivity, assay range and precision were affected by the concentration of antibody which was used in the assay (Figure 4.2). Lower concentrations of antibody result in more sensitive 50% binding concentrations (EC<sub>50</sub>), shallower calibration curves and decreased precision. Decreasing the serum dilution from 1:20 to 1:50 decreases the EC<sub>50</sub> by almost an order of magnitude. Although calibration curves obtained using 1:50 and 1:100 diluted antiserum look very similar, individual precision measurements indicate the latter to be inferior (Table 4.2). There is a substantial increase in the CV of replicate measurements when the serum dilution is increased from 1:50 to 1:100. The overall decrease in precision with decreasing antibody concentration is a factor of both decreased overall signal and a shallowing in the calibration curve. A 1:50 dilution of antiserum provided the best compromise in terms of assay range, sensitivity and precision.

**Table 4.2.** Effect of serum dilution on assay performance.

		Serum dilution		
		1:20	1:50	1:100
Steepness of curve, $p$		1.285	0.653	0.497
EC50 (g/mL)		$1.1 \times 10^{-9}$	$1.5 \times 10^{-10}$	$1.3 \times 10^{-10}$
CV <sub>blank</sub> (n=4)		1.5	3.9	11.5
Precision	LSD (ng/mL)	CV (n=4)	CV (n=4)	CV (n=4)
	$2 \times 10^{-9}$	6.7	6.7	4.4
	$2 \times 10^{-10}$	6.6	6.1	21.0
	$2 \times 10^{-11}$	3.4	3.5	12.0
	$2 \times 10^{-12}$	4.5	2.3	10.9

**Figure 4.2.** The effect of antibody concentration on LSD calibration by ELISA.

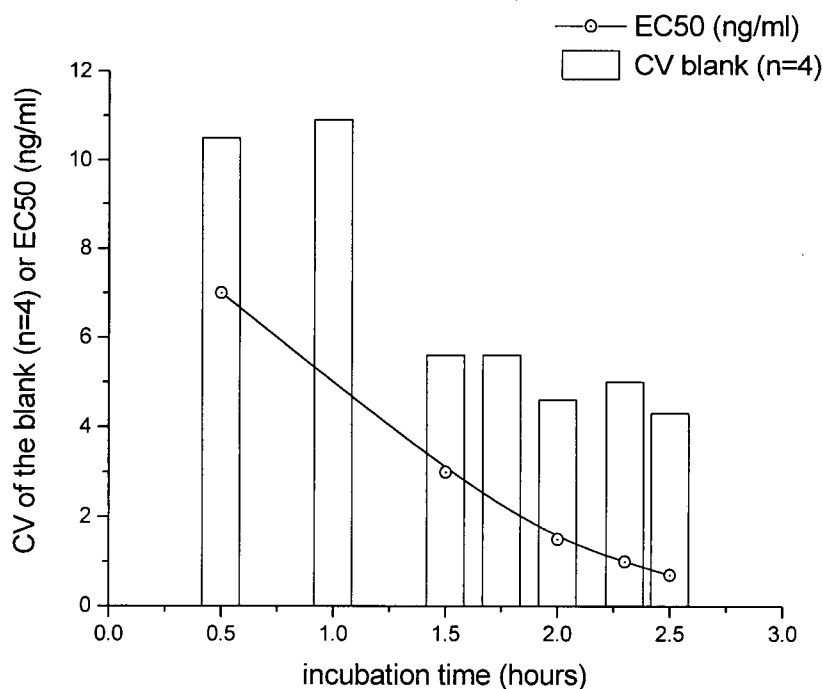
#### 4.3.1.4. Antibody incubation conditions.

When short antibody-antigen incubation times are used, small differences in incubation time can cause large changes in signal, which increase the inter-assay variation. Ideally ELISA incubations should be continued for sufficient time to allow an approach to equilibrium, usually achieved within two hours or so (29), depending on the incubation temperature. As a general rule, lower incubation temperatures minimize non-specific binding but decrease the rate of reaction. Incubations were performed at 37 °C to increase the rate of reaction of LSD with antibody, which is present at very low concentration. No significant increase in non-specific binding was measured when antibody and antigen were reacted at 37 °C as opposed to room temperature.

Similar ELISA conditions were used to measure the effect of antibody incubation time using the same antiserum batch. Figure 4.3 shows the effect of increased incubation time on both precision and sensitivity. Using the CV of blank urine (n=4) as the precision marker, it is clear that precision increases with increasing incubation time, which is likely the result of increased signal. The data clearly indicate that an incubation time greater than 1.5 hours was necessary to minimize imprecision. Increase in non-specific binding was negligible over the range of incubation times tested; the non-specific signal obtained from normal rabbit serum increased from OD 0.013 to 0.016 when incubation time was increased from 1.5 to 2.5 hours. The position of the calibration curve shifts towards greater sensitivity when the incubation time is extended, as indicated by the 50% binding concentration. An extension of the incubation time from 0.5 to 2.5 hours results in a ten-fold increase in sensitivity, the latter of which was routinely used in subsequent ELISA's. The antibody reaction time depends on the temperature and concentration of reagents in the system. High concentrations of antibody result in increased reaction rates but may decrease overall assay performance (Section 4.3.1.3). This assay utilizes a very low concentration of specific drug

antibody, in a low titre antiserum, which is why a long incubation time was used.

**Figure 4.3.** The effect of antibody-antigen incubation time on assay precision and sensitivity.



When the pH of the anti-LSD incubation step was varied, absorbance measurements indicated that optimal antibody-antigen binding occurred at near neutral pH. Table 4.3 shows that the background subtracted signal for blank urine at pH 7.4 was nearly twice that at pH 9.4. Decreased signal with increasing pH accompanied a general decrease in precision. Phosphate buffered saline at pH 7.4 was routinely used in ELISA. Changes in the ionic strength, which was tested using PBS up to 0.4 M, (before dilution with the urine sample) did not affect the absorbance or the non-specific binding.

**Table 4.3.** Effect of pH on ELISA signal. Background subtracted absorbance measurements are given for antibody which was incubated with blank urine (no LSD).

pH	absorbance $\pm$ SD	% CV (n=4)
9.4	0.87 $\pm$ 0.13	14.3
8.5	1.40 $\pm$ 0.16	11.6
8.0	1.48 $\pm$ 0.14	9.2
7.4	1.70 $\pm$ 0.10	5.9

#### 4.3.1.5. Coating antigen concentration.

Decreasing the concentration of drug conjugate which was used to sensitize microtitre plates decreased the amount of immobilized LSD, which increased assay sensitivity for two reasons. Firstly, a decrease in the concentration of LSD which is bound to the plate increases the chance that antibody will react with free LSD in the sample. Secondly, when the concentration of immobilized antigen is limiting in the presence of a fixed amount of antiserum, the highest affinity antibodies will preferentially bind to antigen (30). Table 4.4 compares urinary LSD calibration data obtained using wells which were coated with different concentrations of BSA-LSD conjugate. There is clearly a shift in sensitivity, indicated by the decrease in EC<sub>50</sub>, when coating antigen conditions are below saturation (0.5  $\mu$ g/mL). Each calibration standard was run in duplicate and the blanks were run in quadruplicate. It is clear from both the CV of the blank and the overall CV of calibration standards across the concentration range that precision is severely compromised at very low coating antigen concentration. The overall increase in CV is likely the result of the decrease in absorbance which accompanies the decrease in coating antigen concentration. This

shift in precision parallels the change towards increased sensitivity when unsaturated conditions are employed. It is also apparent that the coating antigen concentration also affects the degree of non-specific signal, which increases with decreasing concentration of conjugate, as might be expected. Conditions were chosen such that sensitivity was somewhat reduced in order to achieve good precision; 5 - 10  $\mu\text{g/mL}$  of BSA-LSD conjugate was routinely used to coat microtitre plates. High concentrations of conjugate should be avoided as proteins have a tendency to form multi-layers at elevated concentrations rather than monolayers on the polystyrene surface (29).

**Table 4.4.** Effect of coating antigen concentration on ELISA.

	coating antigen concentration ( $\mu\text{g/mL}$ )	
	5	0.5
$\text{CV}_{\text{blank}}$ (n=4)	1.1	5.6
Mean CV (n=2)	2.4	12.9
EC50 (g/mL)	$7.4 \times 10^{-10}$	$4.6 \times 10^{-11}$
Non-specific signal	0.025	0.061

#### 4.3.1.6. Conjugate antibody incubation.

Immobilized rabbit IgG molecules were detected on the surface of ELISA plates using peroxidase labelled anti-rabbit IgG. The optimum dilution for maximum background subtracted signal was 1:1000 in most cases. The conjugate antibody incubation conditions have very little effect on assay performance in comparison to the competitive antibody-antigen incubation step performed previously. Most of the binding occurred within the first 20 minutes and the use of extended incubation times (> 1 hour) decreased overall precision. A 30 minute incubation was

routinely used for ELISA measurements. The difference in reaction times which are used for the first (2.5 hours) and second (0.5 hour) antibody incubations can be explained in terms of the differences in the rate of reaction. The second antibody incubation, in which anti-rabbit IgG peroxidase binds to drug specific IgG bound to the microtitre plate, occurs with relative speed for two reasons. Firstly, due to the high concentration of affinity purified peroxidase-labelled antibody in solution and secondly, due to the high local density of drug specific antibody on the polystyrene surface. By comparison, the first reaction, between drug specific antibody and LSD occurs in both fluid and solid phases at relatively low antibody concentration.

#### **4.3.1.7. TMB reaction time.**

Assay sensitivity was independent of the TMB reaction time. There was no shift in the calibration curve over the range of reaction times studied (2.5 to 15 minutes). The OD dependence of assay precision was illustrated by changing the length of the TMB reaction. Short development times result in lower absorbance readings which, under the conditions described, give rise to decreased precision. Table 4.5 shows the difference in non-specific binding and precision when 2.5 and 5 minute TMB reaction times were used. Elevated non-specific binding was due to the low absorbance of the specific antibody signal when a 2.5 minute reaction time was used. Further reaction for another 2.5 minutes, decreased the non-specific binding by more than half. This is reflected also in the CV of the blank (n=4) which decreased for the same reason. Extended reaction times (> 5 minutes) increased the frequency of outliers and tended to produce higher non-specific binding. A TMB reaction time of 5 minutes was routinely employed in ELISA.

**Table 4.5.** The effect of TMB reaction time on assay performance.

	TMB reaction time (minutes)	
	2.5	5.0
CV blank (n=4)	10.6	4.1
% non-specific binding	12.0	4.9
OD maximum (blank urine)	0.56	0.93

**4.3.1.8. Summary of optimized ELISA conditions.**

Conditions which result in optimum assay performance are summarized in Table 4.6 below. The detailed ELISA procedure is given in full in Appendix II.

**Table 4.6.** Summary of optimized ELISA conditions for the analysis of LSD in urine.

coating antigen	5 - 10 $\mu\text{g/mL}$ BSA-LSD in PBS, overnight at 4 °C
matrix dilution	1:1 mixture of sample (urine) and rabbit serum diluted in 10% SM-PBS
antibody-antigen incubation	2.5 hours at 37 °C
antibody dilution	1:50 in skim milk/urine matrix
detector antibody incubation	0.5 hours at 37 °C
TMB reaction time	5.0 minutes

**4.3.2. Performance parameters.****4.3.2.1. Limit of detection.**

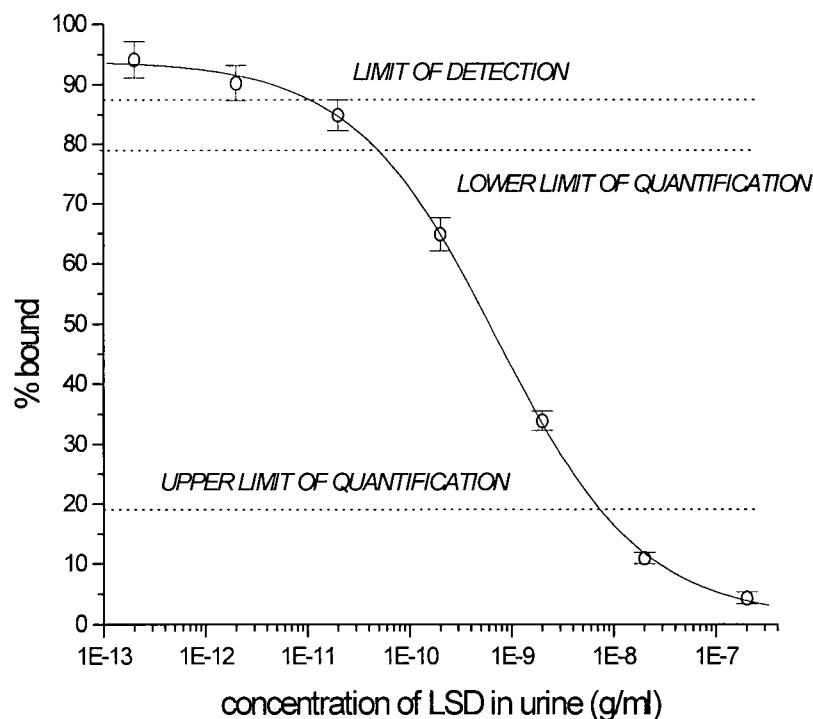
The limit of detection was calculated from the mean absorbance - 3 SD of the zero calibrator (n=4). Table 4.7 shows the raw data for a typical calculation, in which calibration

standards and the blank were run in quadruplicate. The same data is represented graphically in Figure 4.4. After subtraction of the non-specific signal, interpolation from the calibration suggests the limit of detection is 12 pg/mL LSD in urine. The limit of detection was determined in a number of assays over a period of several months to assess any variation in sensitivity as a result of reagent changes. The average limit of detection was 8 pg/mL (n=10) which is an order of magnitude more sensitive than the commercial ELISA which reports a detection limit of 80 pg/mL by extrapolation (31). The limit of detection using the optimized UBC ELISA described in Appendix II also compares favourably with other immunoassays for LSD which report sensitivities of 1.0 (11), 0.4 (10), 0.2 (9), and <0.2 ng/mL (15) towards parent drug.

**Table 4.7.** Typical calibration data obtained by ELISA. LSD calibrators and the blank (n=4) were run in the assay described in Appendix II.

LSD (ng/mL)	Immune sera						Normal sera
	1	2	3	4	mean	SD	
20.000	0.049	0.056	0.046	0.048	0.050	0.004	0.017
2.000	0.161	0.160	0.146	0.151	0.155	0.007	0.016
0.200	0.304	0.309	0.287	0.283	0.296	0.013	0.017
0.020	0.395	0.396	0.370	0.387	0.387	0.012	0.014
0.002	0.423	0.422	0.396	0.405	0.412	0.013	0.014
0.000	0.469	0.481	0.442	0.432	0.456	0.023	0.015

**Figure 4.4.** Calibration of LSD in urine. Data represent the mean of 4 calibration standards  $\pm 1$  SD (error bars).



#### 4.3.2.2. Limit of quantification.

Calibration data used for the calculation of the limit of quantification is shown in Figure 4.4. The percent of antibody bound was calculated relative to the mean blank response which was  $0.456 \pm 0.023$  (SD,  $n=4$ ). The mean negative response of 24 negative urine samples was  $0.432 \pm 0.025$ . Interpolation from the calibration graph indicated that the lower limit of quantification was 50 pg/mL based on the mean negative response minus 3 standard deviations. The maximum quantifiable concentration of LSD, estimated from the non-specific binding plus 3 standard deviations, was 7 ng/mL. Therefore the quantitative range of the immunoassay was between 50 pg/mL and 7 ng/mL LSD in urine. The degree of non-specific binding, which was estimated using

pre-immune sera was 3.3%.

#### 4.3.2.3. Accuracy

A four parameter logistical curve fit was calculated according to the following equation,

$$y = \frac{A_1 - A_2}{1 + (x / x_0)^p} + A_2$$

Where  $A_1 = 97.6$ ,  $A_2 = 1.8$ ,  $x_0 = 7.9 \times 10^{-10}$ ,  $p = 0.618$  and  $x$  and  $y$  are concentration of LSD in urine in g/mL and % binding respectively. The analytical recovery of LSD from urine ranged from 98 to 106% over three orders of magnitude (Table 4.8). Interpolated concentrations of LSD were 10.3, 0.98 and 0.11 ng/mL for 10.0, 1.00, and 0.10 ng/mL respectively. The indirect nature of the assay which results in increased absorbance with decreased concentration of drug in the urine is reflected in the precision of replicate measurements. The coefficient of variation for 10.0, 1.0 and 0.1 ng/mL LSD in urine (n=8) was 5.1, 2.5 and 2.4% respectively. This compared favourably with the commercial ELISA which reports a CV of 6% for 0.5 ng/mL LSD in urine (17). Using the UBC ELISA the analytical recovery of 0.1 ng/mL LSD in urine was 106% and the CV was only 2.4% (n=4). This illustrates that even in the sub-ng/mL range of forensic interest, precision and accuracy is not compromised.

**Table 4.8.** Accuracy determination of LSD in urine by ELISA. LSD was spiked in normal human urine and at 10.000, 1.000 and 0.100 ng/mL (n=8). Calibration standards (n=4) were used to interpolate concentrations directly from the graph using a four parameter logistical equation.

Expected concentration (ng/mL)	Interpolated concentration $\pm$ 95%CL (ng/mL)	Recovery (%)	%CV (n=8)
10.000	10.30 $\pm$ 2.00	103	5.1
1.000	0.98 $\pm$ 0.15	98	2.5
0.100	0.11 $\pm$ 0.02	106	2.4

#### 4.3.2.4. Precision.

Intra-assay precision was estimated from the coefficients of variation of calibration standards which were run in the same assay. As expected, the overall precision decreases as concentration of analyte increases due to the indirect nature of the assay. Table 4.9 shows precision measurements over a wide range of LSD concentrations. Figure 4.5 illustrates a precision profile for the optimized LSD ELISA whereby the intra-assay CV is plotted against the concentration of drug. This clearly shows that optimum precision is achieved at sub-ng/mL concentrations of LSD in urine. Table 4.8 also shows the inter-assay precision of calibration standards run in different assays over 4 months (n=12). The precision profile indicates the same overall trend for between and within run CVs, the former of which are somewhat more exaggerated, as expected. Once more, optimum inter-assay precision is achieved in the sub-ng/mL range.

Concentrations greater than 4 ng/mL result in significantly decreased precision (> 15% inter-assay CV), of which acceptable limits are usually between 10 - 20 % (29). Figure 4.6

indicates the results of the quality control standards (2.00, 0.20, 0.02 ng/mL LSD in urine) which were run in each assay over 4 months (n=12). These standards reflect assay reproducibility at concentrations approaching the upper and lower limits of the assay. Reagent changes such as new BSA-LSD coating antigen, TMB stock solution or enzyme conjugate antibody did not adversely affect the data.

**Table 4.9.** Inter and intra-assay precision of LSD in urine by ELISA. The coefficient of variation is shown for LSD calibration standards run in the same assay (n=4) and in different assays (n=12).

Concentration of LSD in urine (ng/mL)	Intra-assay CV (%) (n=4)	Inter-assay CV (%) (n=12)
20	7.57	22.59
2	4.05	11.30
0.2	3.71	6.25
0.02	2.69	4.10
0.002	2.78	4.64

**Figure 4.5.** Precision profile of the UBC LSD ELISA. The intra-assay CV is shown for each concentration of LSD tested (n=4). Optimum precision is achieved in the sub-ng/mL region of forensic interest.

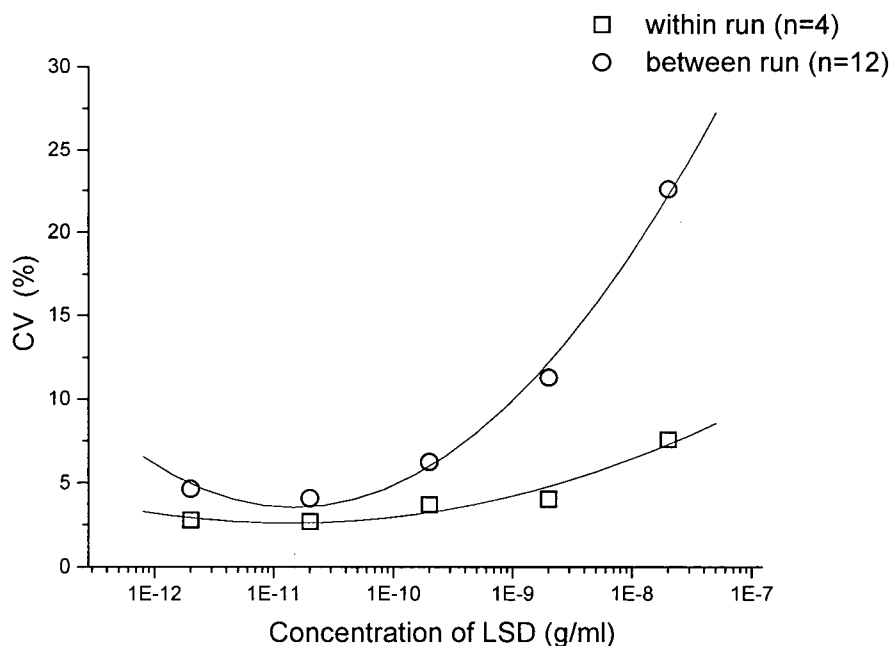
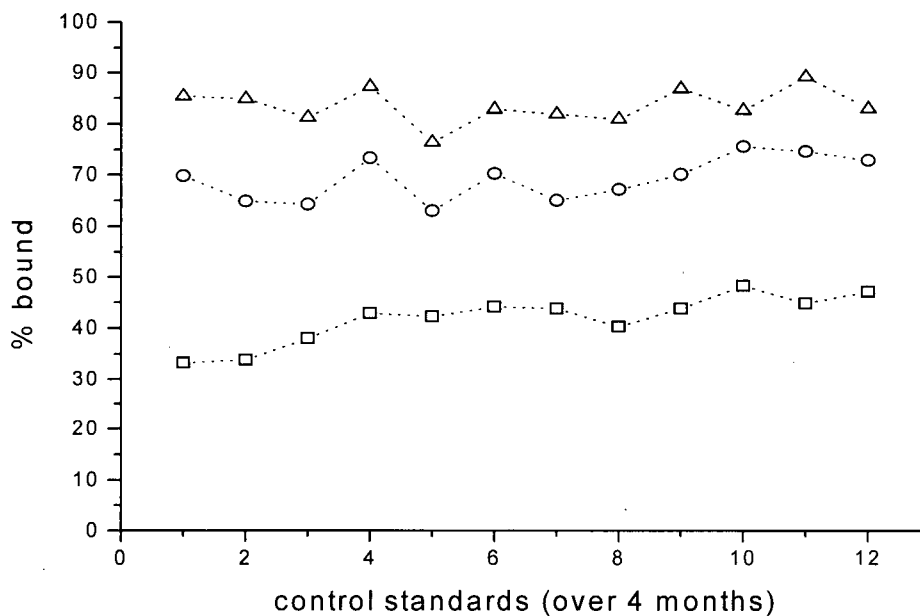


**Figure 4.6.** Mean response of quality control standards, which were run in 12 assays, performed over 4 months. Three standards were run in each assay at 2.0 ng/mL (squares), 0.2 ng/mL (circles) and 0.02 ng/mL (triangles).



### **4.3.3. Amplified LSD ELISA.**

#### **4.3.3.1. Optimization.**

Table 4.10 summarizes the effects of assay conditions on the performance of the amplified ELISA. Antibody-antigen incubation time, coating antigen concentration and anti-LSD serum dilution affected assay sensitivity, which is seen as a change in the 50% binding concentration (EC<sub>50</sub>). Factors such as incubation time and dilution of detector antibodies (goat anti-rabbit IgG peroxidase and rabbit peroxidase-anti-peroxidase) primarily affected the assay precision, which was measured using the %CV of replicate measurements. In summary, optimum conditions for the amplified ELISA was achieved using ELISA plates which were saturated with BSA-LSD, a 2.5 hour antibody-antigen incubation, 1:50 diluted anti-LSD serum and 0.5 hour incubations of both goat anti-rabbit IgG peroxidase (1:1000) and rabbit peroxidase-anti-peroxidase (1:500).

**Table 4.10.** Factors which affect assay sensitivity and precision in the amplified LSD ELISA. Antibody-antigen incubation time, coating antigen concentration and anti-LSD serum dilution affect sensitivity. Detector antibodies, goat anti-rabbit IgG peroxidase (HRP) and rabbit peroxidase-anti-peroxidase (PAP) affect assay precision.

		EC50 (ng/mL)	CV (n=4)	CV <sub>blank</sub> (n=4)	% NSB	OD blank
antibody-antigen incubation time (hours)	2.5	0.35	3.7	5.5	2.9	-
	1.5	0.90	5.6	6.8	4.7	-
coating antigen concentration ( $\mu\text{g/mL}$ )	0.78	0.3	6.5	7.2	10.5	0.38
	2.50	0.4	5.5	5.9	6.4	0.5
	5.00	0.5	4.3	4.8	5.0	0.64
	25.00	0.8	3.1	4.6	5.1	0.66
dilution of detector antibody (anti-rabbit IgG peroxidase)	1:250	-	-	5.6	4.7	0.53
	1:500	-	-	4.8	5.3	0.42
	1:1000	-	-	3.7	4.6	0.42
	1:2000	-	-	1.4	4.5	0.41
dilution of anti-LSD	1:20	1.2	5.7	1.5	3.3	2.1
	1:50	0.5	3.8	5.6	2.8	1.2
	1:100	0.3	5.0	7.8	3.4	0.7
detector antibody incubation time (hours)	HRP	PAP	-	-	-	-
	0.5	0.5	0.5	9.7	-	6.5
	0.5	1.0	0.5	14.0	-	6.2
	1.0	0.5	0.5	13.0	-	4.2
	1.0	1.0	0.5	11.0	-	5.2

#### 4.3.2.2. Assay performance.

The performance characteristics of the amplified LSD ELISA was evaluated as outlined in Section 4.3.3.1. Typical calibration data obtained from LSD spiked in human urine is shown in Figure 4.7. The limit of detection, calculated from the zero calibrator - 3 SDs (n=4) was 20 pg/mL. The upper and lower limits of quantification, estimated from the mean negative response of 24 drug-free urine samples  $\pm$  3 SDs, was 8 ng/mL and 50 pg/mL respectively. Non-specific binding, estimated from the signal obtained using pre-immune rabbit serum was 4.6%.

Accuracy was determined using traditional spike and recovery methods described in section 4.2.2.3. Urine which was spiked with LSD at 10.0, 1.0 and 0.1 ng/mL was recovered at concentrations 9.58, 1.10 and 0.09 ng/mL as shown in table 4.11. Once again, at the sub-ng/mL region of interest, 0.1 ng/mL LSD was recovered in urine at 99% with a CV of 3.0% (n=8). Intra and inter-assay precision of LSD spiked in urine over a range of concentrations is shown in Table 4.12. Optimum precision is achieved at sub-ng/mL concentrations of LSD in urine.

**Table 4.11.** Determination of accuracy using the amplified LSD ELISA in urine. LSD was spiked in normal human urine and at 10.000, 1.000 and 0.100 ng/mL (n=8). Calibration standards (n=4) were used to interpolate concentrations directly from the graph using a four parameter logistical equation.

Expected concentration (ng/mL)	Interpolated concentration $\pm$ 95%CL (ng/mL)	Recovery (%)	%CV (n=8)
10.000	9.58 $\pm$ 0.39	96	6.0
1.000	1.09 $\pm$ 0.02	109	1.7
0.100	0.10 $\pm$ 0.02	99	3.0

**Figure 4.7.** Calibration of LSD in urine using the amplified LSD ELISA. Each calibrator represents the mean of 4 measurements  $\pm$  1 SD. The limit of detection was 20 pg/mL and the upper and lower limits of quantification were 8 ng/mL and 50 pg/mL respectively.

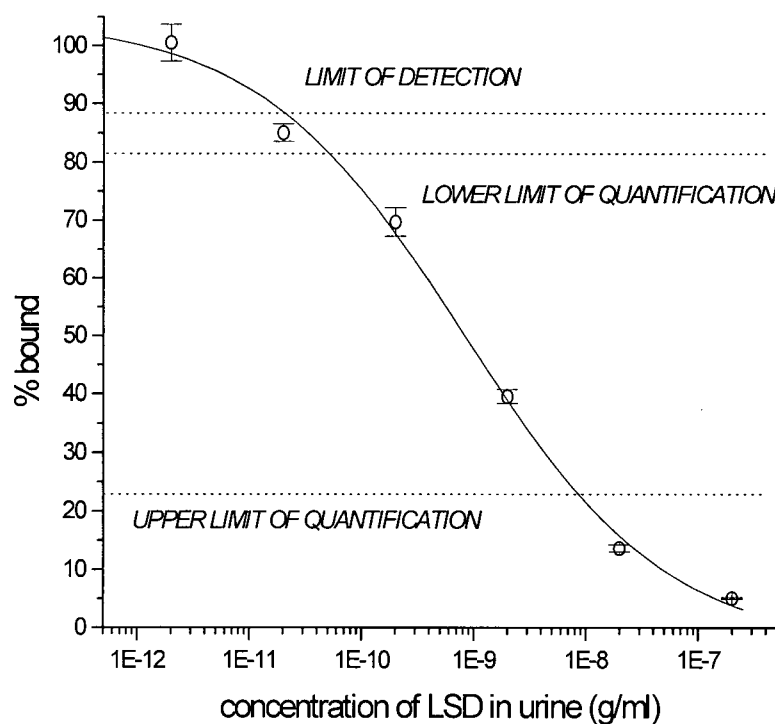


**Table 4.12.** Intra and inter-assay precision of the amplified LSD ELISA. Coefficients of variation were calculated for LSD calibrators run in the same assay (n=4) and different assays (n=12).

Concentration of LSD in urine (ng/mL)	Intra-assay CV (%) (n=4)	Inter-assay CV (%) (n=12)
20	11.1	10.27
2	3.90	7.32
0.2	4.20	6.98
0.02	4.25	5.10
0.002	4.30	6.39

#### 4.3.4. Summary of assay performance.

Table 4.13 summarizes the performance of the amplified LSD ELISA with its unamplified counterpart. The regular ELISA has increased sensitivity, lower non-specific binding and improved precision at low concentrations. The amplified ELISA, despite having increased overall absorbance, exhibits decreased sensitivity and increased non-specific binding. The slight positional shift in the calibration curve towards decreased sensitivity does however result in some increased precision at high concentrations of LSD in urine. It was concluded therefore that the un-amplified ELISA, despite having a lower than ideal absorbance range, outperformed the amplified ELISA in terms of both sensitivity and precision for the detection of low concentrations of LSD in urine.

Table 4.14 summarizes the sensitivity and precision of some commercial LSD immunoassays. The UBC ELISA compares favourably in terms of sensitivity towards parent drug, compared to other assays. Probably, the most sensitive commercial immunoassay for LSD is the Roche Abuscreen RIA, which has a limit of detection of 25 pg/mL (32). By comparison, the UBC

ELISA allows LSD to be detected in urine down to 10 pg/mL, without the need for radioisotopes. Performance characteristics of the commercial STC ELISA with the UBC ELISA indicates the latter to be superior in terms of both sensitivity and precision at the sub-ng/mL region of forensic interest.

**Table 4.13.** Summary of amplified and un-amplified ELISA performance for the detection of LSD in human urine.

		LSD ELISA			amplified LSD ELISA		
limit of detection		10 pg/mL			20 pg/mL		
lower limit of quantification		50 pg/mL			50 pg/mL		
upper limit of quantification		7 ng/mL			8 ng/mL		
precision cut-off range:							
intra-assay CV < 5%		10 pg/mL - 2 ng/mL			20 pg/mL - 20 ng/mL		
inter-assay CV < 15%		10 pg/mL - 4 ng/mL			20 pg/mL - 20 ng/mL		
non-specific binding		3.3%			4.6%		
OD range		0 - 0.5			0 - 1.0		
Mean EC50		0.61 ng/mL			0.83 ng/mL		
Accuracy	Actual (ng/mL)	Found (ng/mL)	recovery (%)	%CV (n=8)	Found (ng/mL)	recovery (%)	%CV (n=8)
	10.0	10.30	103	5.1	9.58	96	3.0
	1.0	0.98	98	2.5	1.10	110	1.7
	0.1	0.11	106	2.4	0.10	99	6.0
Precision  %CV	(ng/mL)	intra/inter-assay (n=4,12)			intra/inter-assay (n=4,12)		
	20	7.6 / 22.6			11.1 / 10.3		
	2	4.0 / 11.3			3.9 / 7.3		
	0.2	3.7 / 6.3			4.2 / 7.0		
	0.02	2.7 / 4.1			4.3 / 5.1		
	0.002	2.8 / 4.6			4.3 / 6.4		

**Table 4.14.** Comparison of UBC LSD ELISA performance with other assays.

Technique	Sensitivity	Precision					
		Inter-assay			Intra-assay		
		ng/mL	% CV	ng/mL	ng/mL	% CV	% CV
UBC LSD ELISA	LOD = 0.010 ng/mL LOQ = 0.050 ng/mL	2.00	4.0 (n=12)	2.00	2.00	11.3 (n=4)	
		0.20	3.7 (n=12)	0.20	0.20	6.3 (n=4)	
		0.02	2.7 (n=12)	0.02	0.02	4.1 (n=4)	
UBC AMPLIFIED LSD ELISA	LOD = 0.020 ng/mL LOQ = 0.050 ng/mL	2.00	3.9 (n=12)	2.00	2.00	7.3 (n=4)	
		0.20	4.2 (n=12)	0.20	0.20	7.0 (n=4)	
		0.02	4.3 (n=12)	0.02	0.02	5.1 (n=4)	
STC ELISA (17)	LOD = 0.085 ng/mL	5.00	6.5 (n=24)	5.00	5.00	6.6 (n=24)	
		0.50	6.0 (n=24)	0.50	0.50	7.1 (n=24)	
		0.25	5.2 (n=24)	0.25	0.25	6.9 (n=24)	
BOEHRINGER MANNHEIM CEDIA (23)	LOD = 0.066	0.30	10.9 (n=20)	0.30	0.30	13.8 (n=89)	
		0.70	12.2 (n=20)	0.70	0.70	22.8 (n=89)	
SYVA EMIT II (33)	not known	0.25	0.6 (n=240)	0.25	0.25	0.6 (n=240)	
		0.50	0.6 (n=240)	0.50	0.50	0.6 (n=240)	
		1.00	0.5 (n=240)	1.00	1.00	0.5 (n=240)	
ROCHE ONLINE (15)	LOD = 0.060 ng/mL	no data in quantitative mode					
ROCHE ABUSCREEN (32)	LOD = 0.025 ng/mL						
OTHER RIA'S	LOD = 0.2, 1.0, 0.4 ng/mL (9-11)						

#### 4.4. Conclusion

A new LSD antibody was used to develop a novel indirect ELISA for the quantitative estimation of drug in urine. Free LSD in the urine specimen and immobilized LSD on the surface of a polystyrene well compete for a limited quantity of drug antibody. Antibody bound to the well is detected using peroxidase-labelled antibody and subsequent colour reaction in which the absorbance is inversely proportional to the concentration of drug in the sample. A low concentration of high affinity antibody was used in the assay, which allows detection of parent drug in the pg/mL range. Assay optimization indicated that variation of both antibody concentration and incubation time with the sample were effective in achieving maximum sensitivity. A modification of the ELISA which utilized the peroxidase-anti-peroxidase amplification system to increase overall absorbance did not improve the assay.

Evaluation of the new assay against the commercially available LSD ELISA (STC Diagnostics, Bethlehem, PA) shows improved performance. Our test requires 50  $\mu$ L of urine which is used to measure concentrations of drug in the ng/mL to pg/mL range. The limit of detection was 10 pg/mL compared to 80 pg/mL in the commercial assay (31) and analytical recoveries were between 98 - 106%. Comparison of precision measurements for the new and existing assay showed the present test to be superior. Using the UBC ELISA, 0.1 ng/mL of LSD in urine could be detected with an intra-assay CV of 2.4% (n=8) compared with 6.0% for a 0.5 ng/mL sample in the commercial assay (n=20) (17). The calibration range which gave inter-assay CVs below the threshold level of 15% was 10 pg/mL to 4 ng/mL. The lower limit of quantification, determined using urine from 24 healthy drug-free individuals was 50 pg/mL and the non-specific binding was < 5%. This new method for the determination of LSD in urine offers both improved sensitivity and precision compared to the commercial ELISA assay, which

facilitates the detection of LSD in urine at lower concentrations with a much greater degree of certainty.

#### 4.5. References.

1. Francom, P., Andrenyak, D., Lim, H., Bridges, R.R., Foltz, R.L., and Jones, R.T. 1988. *J. Anal. Toxicol.* 12: 1-8.
2. Webb, K.S., Baker, P.B., Cassels, N.P., Francis, J.M., Johnson, D.E., Lancaster, S.L., Minty, P.S., Reed, G.D., and White, S.A. 1996. *J. Forens. Sci.* 41(6): 938-946.
3. Nelson, C.C. and Foltz, R.L. 1992. *Anal. Chem.* 64: 1578-1585.
4. Lim, H.K., Andrenyak, D., Francom, P., and Foltz, R.L. 1988. *Anal. Chem.* 60: 1420-1425.
5. Siddik, Z.H., Barnes, R.D., Dring, L.G., Smith, R.L., and Williams, R.T. 1975. *Biochem. Soc. Trans* 3(2): 290-292.
6. Siddik, Z.H., Barnes, R.D., Dring, L.G., Smith, R.L., and Williams, R.T. 1979. *Biochemical Pharmacology* 28: 3081-3091.
7. Cai, J. and Henion, J. 1996. *J. Anal. Toxicol.* 20: 27-37.
8. Department of Health and Human Services 1986. Urine Testing for Drugs of Abuse. NIDA Research Monograph Series 73, National Institute on Drug Abuse, Rockville, MD.
9. Taunton-Rigby, A., Sher, S.E., and Kelley, P.R. 1973. *Science* 181: 165-166.
10. Ratcliffe, W.A., Fletcher, S.M., Moffat, A.C., Ratcliffe, J.G., Harland, W.A., and Levitt, T.E. 1977. *Clin. Chem.* 23(2): 169-174.
11. Twitchett, P.J., Fletcheer, S.M., Sullivan, A.T., and Moffat, A.C. 1978. *J. Chromatog.* 150: 73-84.
12. Loeffler, L.J. and Pierce, J.V. 1973. *J. Pharm. Sci.* 62(11): 1817-1820.
13. McCarron, M.M., Walberg, C.B., and Baselt, R.C. 1990. *J. Anal. Toxicol.* 14: 165-167.
14. Schwartz, R.H. 1995. *Pediatr. Clin. N. Am.* 42: 403-410.
15. McNally, A.J., Goc-Szkutnicka, K., Li, Z., Pilcher, I., Polakowski, S., and Salamone, S.J. 1996. *J. Anal. Toxicol.* 20: 404-408.
16. Boehringer Mannheim Corp., Concord, CA. 1996. CEDIA DAU LSD Assay, *product brochure*.
17. STC Diagnostics, Bethlehem, PA. 1996. STC LSD Micro-Plate EIA, *package insert*.

18. Nelson, C.C. and Foltz, R.L. 1992. *J. Chromatog.* 580: 97-109.
19. White, S.A., Catterick, T., Harrison, M.E., Johnston, D.E., Reed, G.D., and Webb, K.S. 1997. *J. Chromatog. B* 689: 335-340.
20. Paul, B.D., Mitchel, J.M., Burbage, R., Moy, M., and Sroka, R. 1990. *J. Chromatog.* 529: 103-112.
21. Cai, J. and Henion, J. 1996. *Anal. Chem.* 68: 72-78.
22. Fysh, R.R., Oon, M.C.H., Robinson, R.N., Smith, R.N., White, P.C., and Whitehouse, M.J. 1985. *Forens. Sci. Intl.* 28: 109-113.
23. Wu, A.H.B., Feng, Y., Pajor, A., Gornet, T.G., Wong, S.S., Forte, E., and Brown, J. 1997. *J. Anal. Toxicol.* 21: 181-184.
24. Brown, E.N., McDermott, T.J., Bloch, K.J., and McCollom, A.D. 1996. *Clin. Chem.* 42(6): 893-903.
25. Robinson-Cox, J.F. 1995. *J. Immunol. Methods* 186: 79-88.
26. Shindelman, J.E., Brown, J.L., Motton, D.D., Weingarten, P.W., Vistica, C.A., Crenshaw, M.C., Harris, D.G., Bellet, N.F., Coty, W.A., Khanna, P.L., and Sigler, G.F. 1996. *J. Anal. Toxicol.* 20: 73
27. Smith, R.N. and Robinson, K. 1985. *Forens. Sci. Intl.* 28: 229-237.
28. Castro, A., Grettle, D.P., Bartos, F., and Bartos, D. 1973. *Research Communications in Chemical Pathology and Pharmacology* 6(3): 879-886.
29. Kemeny, D.M. 1991. *A Practical Guide to ELISA*, Pergamon Press, New York.
30. Nieto, A., Gaya, A., Jansa, M., Moreno, C., and Vives, J. 1984. *Mol. Immunol.* 21(6): 537-543.
31. Cassels, N.P., Craston, D.H., Hand, C.W., and Baldwin, D. 1996. *J. Anal. Toxicol.* 20: 409-415.
32. Roche Diagnostic Systems, Somerville, NJ. 1993. Abuscreen Radioimmunoassay for LSD, *package insert*.
33. Behring Diagnostics Inc., San Jose, CA. 1996. EMIT II LSD Assay, *product brochure*.

## Chapter 5.

### Characterization of Antibody: Specificity, Sensitivity and Affinity

#### 5.1. Introduction

The specificity and sensitivity of Ab-Ag reactions has made the use of antibodies as analytical probes an important part of diagnostics and biotechnology. These factors are crucial in determining the usefulness of an antibody in an immunodiagnostic test. Some assays require low specificity immunoreagents to give effective broad spectrum screening for a particular class of drugs eg. benzodiazepines, whereas others require a more specific antibody with less cross-reactivity to detect primarily the parent drug and selected metabolites eg. lysergic acid diethylamide. In the case of LSD, immunodiagnosis requires a very sensitive antibody in order to reliably detect sub ng/mL quantities of drug in biological specimens. The sensitivity of the assay is largely dependent on the affinity of the antibody used, which is frequently the performance limiting reagent. A highly specific and sensitive antibody to LSD has greater discriminating ability, enabling it to detect very low levels of parent drug in the presence of structurally similar interfering compounds.

The influence of antibody affinity on immunoassay performance has been investigated using a number of techniques including RIA, ELISA and precipitation methods. It has been suggested that below a certain affinity plateau, immunoassay sensitivity is progressively diminished (1). Polyclonal antisera contain a heterogeneous population of antibodies which vary in class, concentration and affinity. The effect of affinity on immunoassay performance is reflected

in the continuing interest in the measurement of antibody affinity. For a polyclonal antiserum, this value is usually reported as an average affinity, which is estimated from a distribution of affinities in the entire antibody population.

The binding constant in an Ab-Ag complex is a measure of the strength of interaction between antibody and antigen. This value depends on the size of the antigen, its environment and the rate at which antibody and antigen associate and dissociate. Equilibrium association constant measurements have been made using radiolabelled species or other physical properties, such as fluorescence, which allow free and bound fractions to be calculated at equilibrium. Published methods include equilibrium dialysis, precipitation methods, agglutination, electrophoresis, gel filtration, affinity chromatography, RIA and ultracentrifugation (2). More recently the trend has been towards the use of ELISA-based methods for affinity determinations (3-12). The advantage of this approach includes the ease of separation of solid and liquid phases and the lack of requirement for labelling either antibody or antigen, since this can have an unpredictable effect on binding. Although this approach is fast, there are a number of drawbacks which usually necessitate that a more rigorous technique, such as equilibrium dialysis or a radiochemical method, is used for comparison. The latter techniques, which are labour intensive, are still subject to several drawbacks when the affinity measurements are attempted for polyclonal antibody preparations. These include problems with experimental methods, determining the amount of antibody present, the affinity heterogeneity and shortcomings of the mathematical assumptions used to treat the data. However, the use of hybridoma technology for the production of monoclonal antibodies has made it possible to estimate affinity measurements less ambiguously and assess the relative importance of some of these problems.

Calculation of antibody association constants from ELISA-based methods provides an estimate of the functional affinity of an antibody rather than its intrinsic affinity. The most cited drawback of this approach is the influence of solid phase antigen density on calculated affinity, particularly in the case of the polyclonal antisera. The method of Nieto et al. (10) not only takes this in to account but utilizes the effect of antigen density on sensitivity to calculate an affinity distribution for the antiserum. By this method it is possible to estimate the affinities of antibody subpopulations and their relative abundance in complex mixtures. It has been claimed that overall apparent association constants determined by this method are in close agreement with intrinsic affinity constants measured using fluorescence quenching and other methods (10).

In the Nieto (10) method, the concentration of antigen coated on the surface is decreased to below saturation and different amounts of antigen are immobilized. Using a fixed concentration of diluted antibody in a hapten inhibition ELISA, different subpopulations are detected by a change in concentration of antigen on the surface. When the microtitre plate is saturated with antigen, both high and low affinity antibodies are bound. However, when the concentration of immobilized antigen is low, high affinity antibodies are preferentially bound to the surface.

Thiocyanate elution has been suggested as an alternative method for the rapid relative assessment of affinity distributions of polyclonal antisera. The proportion of antigen-specific antibodies dissociated by increasing concentrations of chaotropic agent can be measured by ELISA and the results presented as an antibody affinity distribution. A simple titration can be used to assess the functional affinity of antibodies by increasing the concentration of thiocyanate and measuring the resistance of antibody dissociation. This tolerance is a measure of the strength of the Ab-Ag interaction (13) and as such, the tolerance distribution represents a relative affinity

distribution within the heterogeneous antibody population. One advantage of this approach is that the concentration of specific antibody required is much lower than in conventional affinity assays (14). Chaotropic ion elution and ELISA detection have been used extensively to measure affinity distributions in sera from patients exposed to viral encephalitis, multiple sclerosis (15), rotavirus (16), *Rubella* (17), *Moxarella catarrhalis* (18), *Plasmodium falciparum* (13) and *Toxoplasma gondii* (19).

Estimates of functional affinity by this method involve the addition of a reagent such as guanidine hydrochloride, thiocyanate, diethylamine or urea after Ab-Ag binding has taken place. The exact properties of some of these reagents are not well understood although guanidine hydrochloride is known to be a protein denaturant (16) and the dissociation of antibody with diethylamine is thought to be a pH effect (18). Thiocyanate ions probably affect the fine structure of the antibody combining site, which weakens the association by creating a "loose fit" which results in easier dissociation. This disruption of the Ab-Ag complex is independent of pH and likely occurs as a result of protein unfolding through the breaking of hydrophobic interactions. Because of this, it has been concluded that thiocyanate elution in combination with hapten inhibition are the preferred solid phase methods for the assessment of functional affinity (18).

The primary aim of the specificity study was to determine whether the antibody to the photolinked immunogen was suitable for the detection of LSD in body fluids. The secondary objective was to obtain some structural insight into immunogen linkage, in particular the possible site or sites of attachment of carrier protein on LSD. Further characterization involved investigation of the Ab-Ag interaction by a number of approaches. These include estimates of,

- 1.) apparent affinity constants obtained by ELISA, which give a measure of functional affinity,
- 2.) the equilibrium association constant obtained using radiolabelled drug, which measures the intrinsic antibody affinity,
- 3.) dissociation of the Ab-Ag complex by chaotropic elution with thiocyanate followed by ELISA detection,
- 4.) the sensitivity of the antibody towards parent drug by ELISA.

The characterization of four polyclonal antisera to LSD, which were raised against different immunogens, is discussed with respect to these variables and the correlation among antibody affinity, dissociability and sensitivity is explored.

## 5.2. Materials and methods.

LSD which was tritiated in the *N*-methyl position ( $[^3\text{H}_3]$ -LSD, 0.25 mCi) and Atomlight scintillation fluid were obtained from DuPont NEN (Mississauga, ON). The specific activity of tritiated LSD was 71.5 Ci/mmol. *Iso*-LSD and (+)2-bromo-LSD hydrogen tartarate were supplied by Dr. Kevin Gormley through the National Institute on Drug Abuse (NIDA) Drug Supply Program (Rockville, MD). Dr. Haro Avdovich of the Bureau of Drug Research (BDR), Health Canada, (Ottawa, ON) supplied additional controlled substances. These included dimethyltryptamine, *l*-amphetamine sulfate, *d*-lysergic acid, *d*-lysergic acid amide, mescaline and psilocin. Coramine, (+)6-nor-6-allyl-lysergic acid diethylamide tartarate, 5-hydroxytryptamine,  $\alpha$ -ergocryptine, ergonovine maleate, ergotamine tartarate, hordenine hemisulfate, *l*-tryptophan, *d*-lysergic acid diallylamide tartarate, lysergol, and *N*-demethyl-LSD (nor-LSD) were purchased from Sigma (St. Lois, MO). Research Biochemicals Inc. (Natick, MA) supplied ergocornine, ergocryptine, methylergonovine maleate and methysergide maleate. Finally, 2-oxo-3-hydroxy-LSD was purchased from Radian International (Austin, TX). LSD and the reagents used for ELISA are given in Chapter 4. Commercial LSD antibodies were kindly provided by Dr. Sal Salamone, Roche Diagnostic Systems (Somerville, NJ) and Dr. Bill Coty, Boehringer Mannheim Corporation (Concord, CA).

### 5.2.1. Cross-reactivity Study.

LSD derivatives and controlled substances supplied by U.S. and Canadian Government agencies were investigated for their cross-reactivity with drug antibody. In total 27 compounds of interest from these and other sources were obtained and classified as follows:

<i>Class I compounds</i>	potential cross-reacting substances which differ from LSD in one position only, eg. <i>d</i> -lysergic acid.
<i>Class II compounds</i>	potential cross-reacting substances which differ from LSD in two positions, eg. methysergide.
<i>Class III compounds</i>	potential cross-reacting substances which differ from LSD at three positions or more, eg. tryptophan.

Classification, solubility and structural information of compounds used in the study are listed in Table 5.1. and their structures are shown in Appendix III. In total, 15 class I compounds were obtained in which derivatives contained the 4 ring structure (ABCD) of LSD with only one structural alteration. In order to carry out the study, it was necessary to determine whether derivatives could be solubilized in organic solvents and used in ELISA without affecting antibody binding.

#### **5.2.1.1. Effect of organic solvent on antibody binding.**

Some derivatives chosen for the cross-reactivity study were only soluble in ethanol, methanol or acetonitrile. It was therefore necessary to measure the effect of these solvents on antibody binding in the ELISA. This was done using the optimized competitive binding ELISA described in Appendix II. After plates had been coated and pre-blocked, 150 mM phosphate buffered saline, pH 7.4 (PBS) which contained various amounts of solvent was incubated with antibody solution and immobilized antigen in the usual way. Wells which contained only PBS were used as the blanks. Replicate measurements for each set of conditions were made.

**Table 5.1.** Classification and solubility of compounds used in the specificity study (listed in alphabetical order). Structures of cross-reactants are shown in Appendix III.

Compound	Class	Rings	Position	Solvent
<i>l</i> -amphetamine sulfate	III	-	-	H <sub>2</sub> O
2-bromo-lysergic acid diethylamide hydrogen	I	ABCD	C2	H <sub>2</sub> O
coramine	III	-	-	H <sub>2</sub> O
dihydroergotamine tartarate	II	ABCD	C10 & C8	EtOH
<i>N, N</i> -dimethyltryptamine	III	AB	-	H <sub>2</sub> O
ergocornine	I	ABCD	C8 (amide)	EtOH
$\alpha$ -ergocryptine	I	ABCD	C8 (amide)	MeOH
ergocrystine	I	ABCD	C8 (amide)	EtOH
ergonovine maleate	I	ABCD	C8 amide	H <sub>2</sub> O
ergotamine tartarate	I	ABCD	C8 (amide)	H <sub>2</sub> O
gramine	III	AB	-	MeOH
hordenine hemisulfate	III	A	-	H <sub>2</sub> O
5-hydroxytryptamine (serotonin)	III	AB	-	H <sub>2</sub> O
<i>d</i> -lysergic acid	I	ABCD	C8	H <sub>2</sub> O
lysergic acid amide	I	ABCD	C8 (amide)	EtOH
<i>d</i> -lysergic acid diallylamide tartarate	I	ABCD	C8 (amide)	MeOH
<i>iso</i> -lysergic acid diethylamide	I	ABCD	C8	H <sub>2</sub> O
lysergic acid methylpropylamide (LAMPA)	I	ABCD	C8 (amide)	MeOH
lysergol	I	ABCD	C8	MeOH
mescaline	III	A	-	H <sub>2</sub> O
methylergonovine maleate	I	ABCD	C8 (amide)	H <sub>2</sub> O
methysergide maleate	II	ABCD	C8 & N1	MeOH
6-nor-6-allyl lysergic acid diethylamide tartarate	I	ABCD	C6	MeOH
6-nor-LSD ( <i>N</i> -demethyl lysergic acid diethylamide)	I	ABCD	C6	MeOH
2-oxo-3-hydroxylysergic acid diethylamide	II	ABCD	C2 & C3	MeCN
psilocin	III	AB	-	H <sub>2</sub> O
<i>l</i> -tryptophan	III	AB	-	H <sub>2</sub> O

### 5.2.1.2. Antibody specificity by ELISA.

The cross-reactivity of compounds of interest was measured using the optimized competitive binding ELISA (Appendix II). Derivatives were diluted in PBS which contained the minimum amount of solvent required for solubilization. Equal volumes of derivative and antibody in double strength blocking solution were added to antigen coated microtitre plates in the usual way. Duplicate measurements were made for each compound over a range of concentrations. LSD ( $1 \times 10^{-7}$  -  $1 \times 10^{-12}$  M) was used as the reference. The stoichiometry of each compound was taken into account so that molar concentration refers to the concentration of drug and not its salt. The amount of antibody which was bound at each inhibitor concentration was calculated as a percentage, relative to the measured absorbance when no drug was present. Inhibition curves were compared for each compound of interest, relative to LSD. The approximate % cross-reactivity was taken to be the amount of compound that produced a signal equivalent to 0.5 ng/mL LSD, which is the U.S. Department of Defense and U.S. Department of Health and Human Services cut-off concentration for a positive urine specimen (20). Four LSD antisera, which had been prepared from different immunogens were investigated by this method. Photolinked, Mannich, KIMS and CEDIA antibodies were used at the dilutions indicated in Table 5.2. A number of the rare drug derivatives were not available in sufficient quantity to allow all antibodies to be studied. The cross-reactivity of the Roche Abuscreen antibody was not investigated because it was produced using an immunogen prepared by the same chemical linkage as the Mannich antibody. Due to the nature of the immunogen, the Abuscreen and Mannich antibodies are expected to have similar specificity characteristics.

**Table 5.2** Source and description of five in-house and commercial antibodies to LSD used in characterization studies.

Name	Source	Immunogen	Dilution in ELISA	Host
photolinked	UBC	KLH-SASD-LSD	1:50	rabbit
Mannich	UBC	KLH-LSD	1:4000	rabbit
Abuscreen <sup>1</sup>	Roche Diagnostic Systems	BSA-LSD	1:9000	rabbit
KIMS <sup>2</sup>	Roche Diagnostic Systems	PTG-LSD	1:50000	goat
CEDIA <sup>3</sup>	Boehringer Mannheim Corp	KLH-LSD	1:30000	mouse

<sup>1</sup> Commercial polyclonal serum from the Abuscreen RIA for LSD. Bovine serum albumin is coupled to drug at the indole nitrogen by the Mannich reaction (21)

<sup>2</sup> Commercial polyclonal serum used in the KIMS test (Kinetic Interaction of Microparticles in Solution). Porcine thyroglobulin is coupled to drug at the indole nitrogen using an extended spacer arm (22).

<sup>3</sup> Commercial monoclonal antibody used in the CEDIA test (Cloned enzyme donor immunoassay). A proprietary chemical linkage of keyhole limpet hemocyanin to drug is used.

## 5.2.2. Calculation of the affinity constant.

### 5.2.2.1. Hapten inhibition ELISA.

The apparent association constants for LSD antisera was estimated by hapten inhibition enzyme immunoassay as previously described (10). Serial dilutions of BSA-LSD (12.5  $\mu\text{g}/\text{mL}$ ) and KLH-LSD (20  $\mu\text{g}/\text{mL}$ ) in PBS were used to coat polystyrene microtitre wells over a range of concentrations. After pre-blocking the wells for 30 minutes at 37 °C with blocking solution, hapten inhibition using a fixed concentration of antibody was performed for each immobilized antigen

concentration as follows. Appropriate dilutions of antibody and LSD in blocking solution ( $5 \times 10^{-8}$  -  $5 \times 10^{-11}$  g/mL) was incubated in the wells for 2.5 hours at 37 °C. After the plates were washed with PBS, either goat anti-rabbit IgG peroxidase or sheep anti-goat IgG peroxidase (1:1000) was incubated for 30 minutes at 37 °C. After the final washing step, the amount of peroxidase labelled antibody was detected using TMB in the usual way (Appendix II) after which the absorbance was measured at 450 nm using 620 nm as the reference.

Measurements for photolinked, Mannich, Abuscreen and KIMS antibodies (Table 5.2) were made in approximately the same OD range. None of the antibodies tested were affinity purified, so the absolute concentration of anti-LSD in each antiserum was not known. As such, the dilution used in each assay was chosen so that the OD was approximately equal for all antibodies tested (at 0% inhibition) using ELISA plates which were saturated with coating antigen.

#### 5.2.2.2. Radiolabelled study.

[ $^3\text{H}_3$ ]-LSD was selected for affinity analysis rather than  $^{125}\text{I}$ -LSD. This was partly due to the large size of iodine compared to tritium and the increased likelihood of its affect on antibody binding. It has been shown that incorporation of iodine can change affinity constant values by 25% or more (7). In addition, the anomalous behaviour of 2-bromo-LSD in the specificity study (Section 5.3.1), which is poorly understood, suggests that halide substitution in the 2 position of the drug has a pronounced effect on antibody recognition.

The intrinsic association constant of the photolinked antibody was measured using Protein A-coated agarose. Rabbit IgG was covalently attached to Protein A on the bead surface to give  $0.55 \pm 0.06$   $\mu\text{g/mL}$  specific drug antibody per mL gel (Section 6.2.3.1). After mixing a fixed

volume of gel with different amounts of [ $^3\text{H}_3$ ]-LSD, equilibrium concentrations of free drug were determined by scintillation counting of the supernatant layer as follows. [ $^3\text{H}_3$ ]-LSD was dissolved in PBS in the nM range and 500  $\mu\text{L}$  was added to a 1.5 mL eppendorf tube. The total activity of each solution was determined using a Phillips PW4700 liquid scintillation counter (Phillips, The Netherlands). Antibody coated agarose (100  $\mu\text{L}$ ) was added as a 50% slurry in PBS and gently rotated for 30 minutes at 21  $^\circ\text{C}$ . After centrifugation for 25 seconds at 6500 rpm, the activity of the supernatant layer which contained free LSD was measured. Duplicate analyses were performed for each concentration of drug. Total and free concentrations of LSD at equilibrium were calculated before and after the addition of antibody and the equilibrium concentration of bound LSD was calculated by difference. A Scatchard plot of bound/free against bound LSD at equilibrium was used to calculate the intrinsic association constant,  $K_a$  of the photolinked antibody.

### **5.2.3. Chaotropic elution with ELISA detection.**

#### **5.2.3.1. Thiocyanate elution at fixed antibody concentration.**

The strength of the Ab-Ag complex for four polyclonal LSD antisera (Table 5.2) was investigated with respect to both changing concentration of thiocyanate and antibody. Antibody affinity profiles were measured using thiocyanate elution followed by ELISA detection as previously described (13). Microtitre plates were coated overnight and treated with blocking solution as described in the optimized competitive binding ELISA (Appendix II). Anti-LSD was diluted in blocking solution so that all antisera produced the same OD in the absence of thiocyanate. The concentration of antibody was designed to be in the range in which there was a

linear relationship between OD and log antibody dilution. Each antibody (100  $\mu\text{L}$ /well) was incubated for 2.5 hours at 37 °C before washing twice with PBS. Ammonium thiocyanate (0, 2, 3, 4, 5, 6, 7, 8 M) in 100  $\mu\text{L}$  PBS was incubated for 15 minutes at room temperature. After 6 washes with PBS, 100  $\mu\text{L}$  of either goat anti-rabbit IgG peroxidase or sheep anti-goat IgG peroxidase (1:1000) was incubated for 30 minutes at 37 °C in blocking solution. Following the final PBS rinse, TMB was used to develop the plates in the usual way. The percent of the original absorbance which remained after treatment with different concentrations of thiocyanate was calculated, based on duplicate measurements.

#### **5.2.3.2. Thiocyanate elution over a range of antibody concentration.**

A modified thiocyanate elution ELISA was performed in which the antibody dilution was changed and the thiocyanate concentration held constant. Polystyrene plates were coated overnight with antigen and treated with blocking solution as described in Appendix II. Anti-LSD (100  $\mu\text{L}$ /well) was serially diluted across the plate in blocking solution and incubated for 2.5 hours at 37 °C. After washing the plate, 100  $\mu\text{L}$  of 8 M ammonium thiocyanate in PBS was incubated for 15 minutes at room temperature in parallel with wells containing PBS. After thorough washing, goat anti-rabbit IgG peroxidase or sheep anti-goat IgG peroxidase (100  $\mu\text{L}$ ) diluted 1:1000 in blocking solution was added and the plate was incubated for 30 minutes at 37 °C. After the final wash, the colour reaction was initiated with 100  $\mu\text{L}$  of TMB substrate solution and the absorbance was measured. The percentage of the original absorbance which remained after treatment with 8 M ammonium thiocyanate was calculated for each serum dilution, based on duplicate measurements.

### 5.3. Results and discussion.

#### 5.3.1. Antibody Specificity.

The only solvent which changed the average blank ELISA signal by more than 3 standard deviations (SD) was 7% acetonitrile. In all cases, 1% or less of ethanol, methanol or acetonitrile resulted in a change in OD of less than 1 SD (Table 5.3) which indicates that there was no significant effect on antibody binding. All compounds of interest could be solubilized up to  $1 \times 10^{-5}$  M using conditions which did not affect normal antibody binding.

**Table 5.3.** Effect of organic solvents on ELISA signal.

solvent	n	mean OD	SD	% CV	% binding
100% PBS	4	1.12	0.06	5.6	100
2% methanol	8	1.10	0.04	3.7	98
1% methanol	8	1.06	0.03	3.1	95
0.1% methanol	8	1.07	0.03	3.0	96
2% ethanol	8	1.18	0.03	2.8	106
1% ethanol	8	1.13	0.05	4.3	101
0.1% ethanol	8	1.05	0.05	4.3	94
7% acetonitrile	8	1.36	0.04	3.0	122
1% acetonitrile	8	1.09	0.06	5.2	98
0.1% acetonitrile	8	1.05	0.06	6.1	94

The cross-reactivity of 27 derivatives was investigated by measuring the degree to which each compound binds to the antibody (which results in decreased absorbance). The specificity of

photolinked, Mannich, KIMS and CEDIA antibodies to LSD are shown in Figures 5.1 (a) to (d) respectively. Compounds which resulted in less than 0.008% cross-reactivity are not shown for clarity. The cross-reactivity of each derivative was calculated from the concentration that produces a signal equivalent to 0.5 ng/mL LSD as shown in Table 5.4. A summary of the specificity of all antibodies investigated is given in Table 5.5.

**Figure 5.1.** Cross-reactivity of LSD antibodies with drug derivatives: a) photolinked, b) Mannich, c) KIMS, d) CEDIA.

**Figure 5.1 a)** photolinked

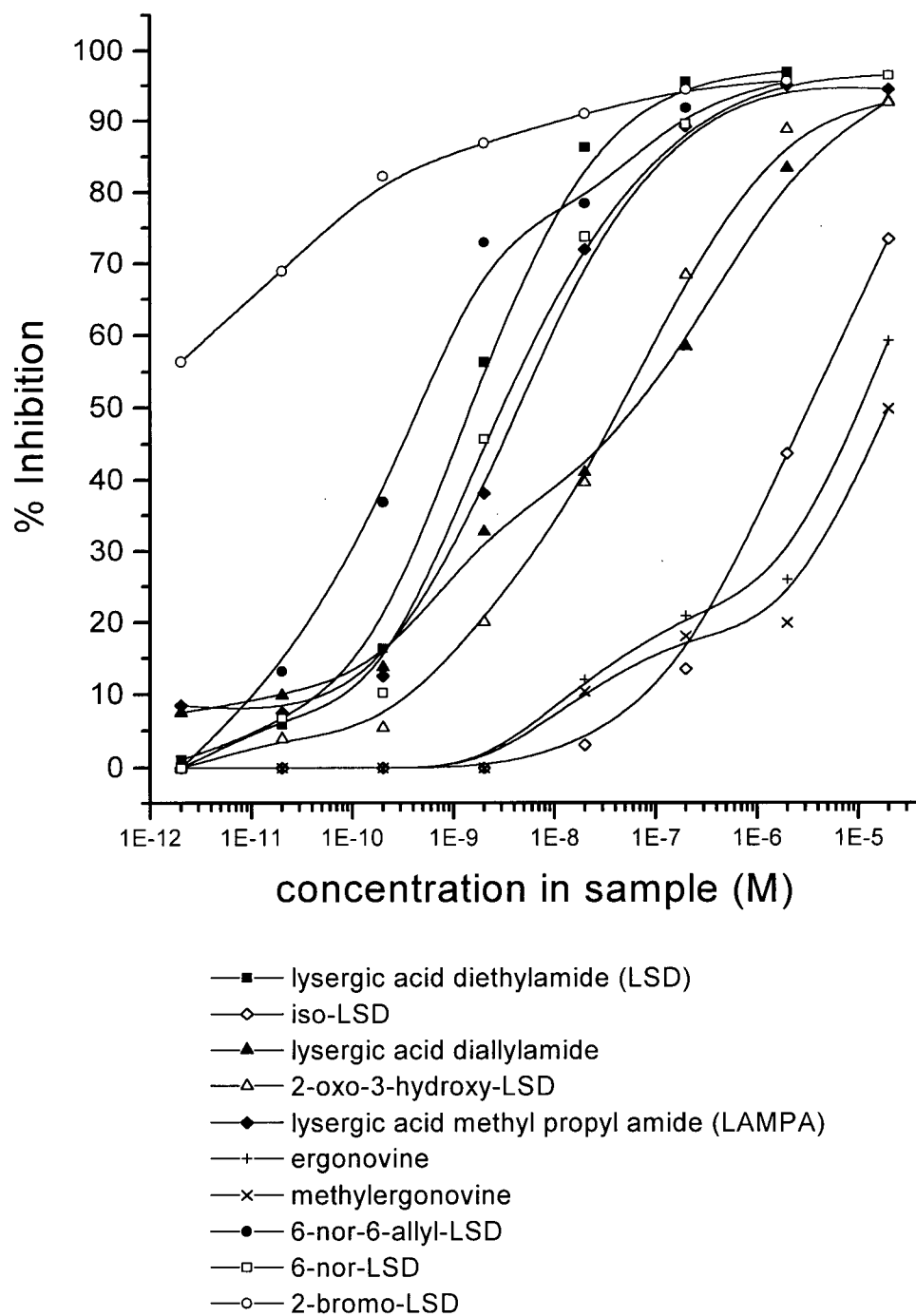
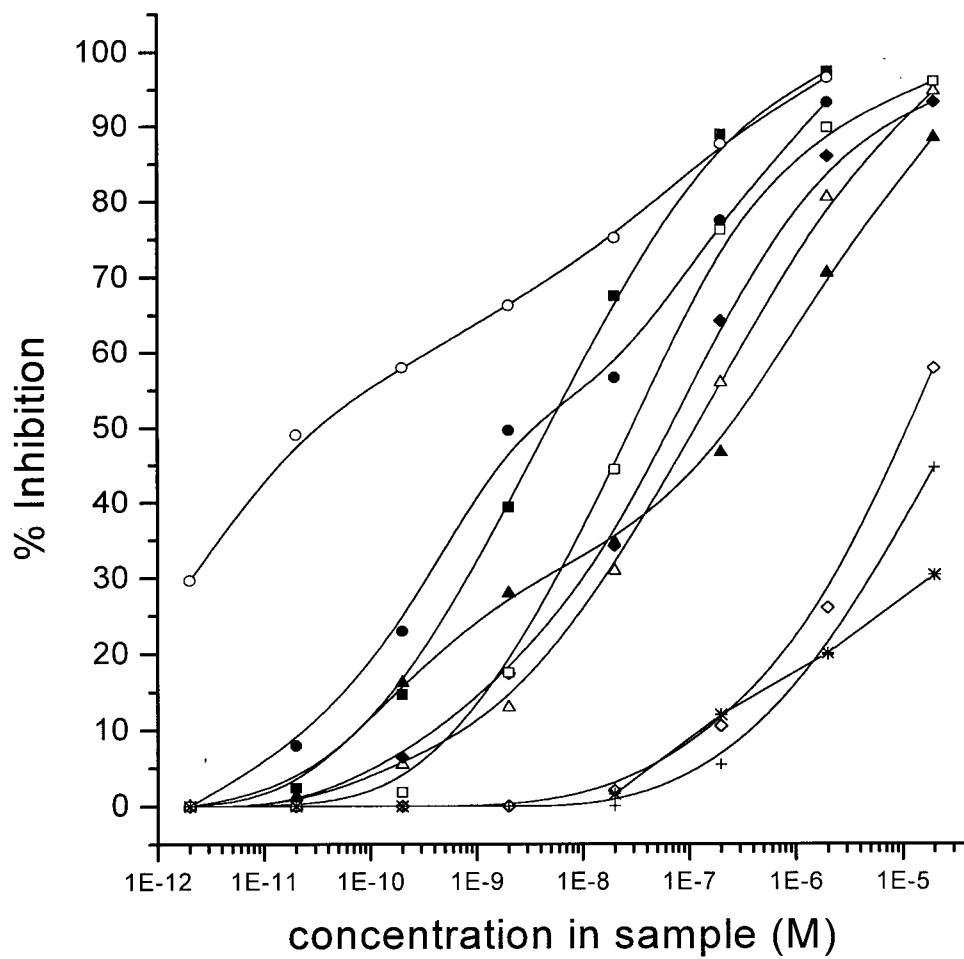


Figure 5.1 b) Mannich



- lysergic acid diethylamide (LSD)
- ◇— iso-LSD
- ▲— lysergic acid diallylamide
- △— 2-oxo-3-hydroxy-LSD
- ◆— lysergic acid methyl propyl amide (LAMPA)
- 6-nor-6-allyl-LSD
- 6-nor-LSD
- 2-bromo-LSD
- +— ergonovine
- \*— methysergide

Figure 5.1 c) KIMS

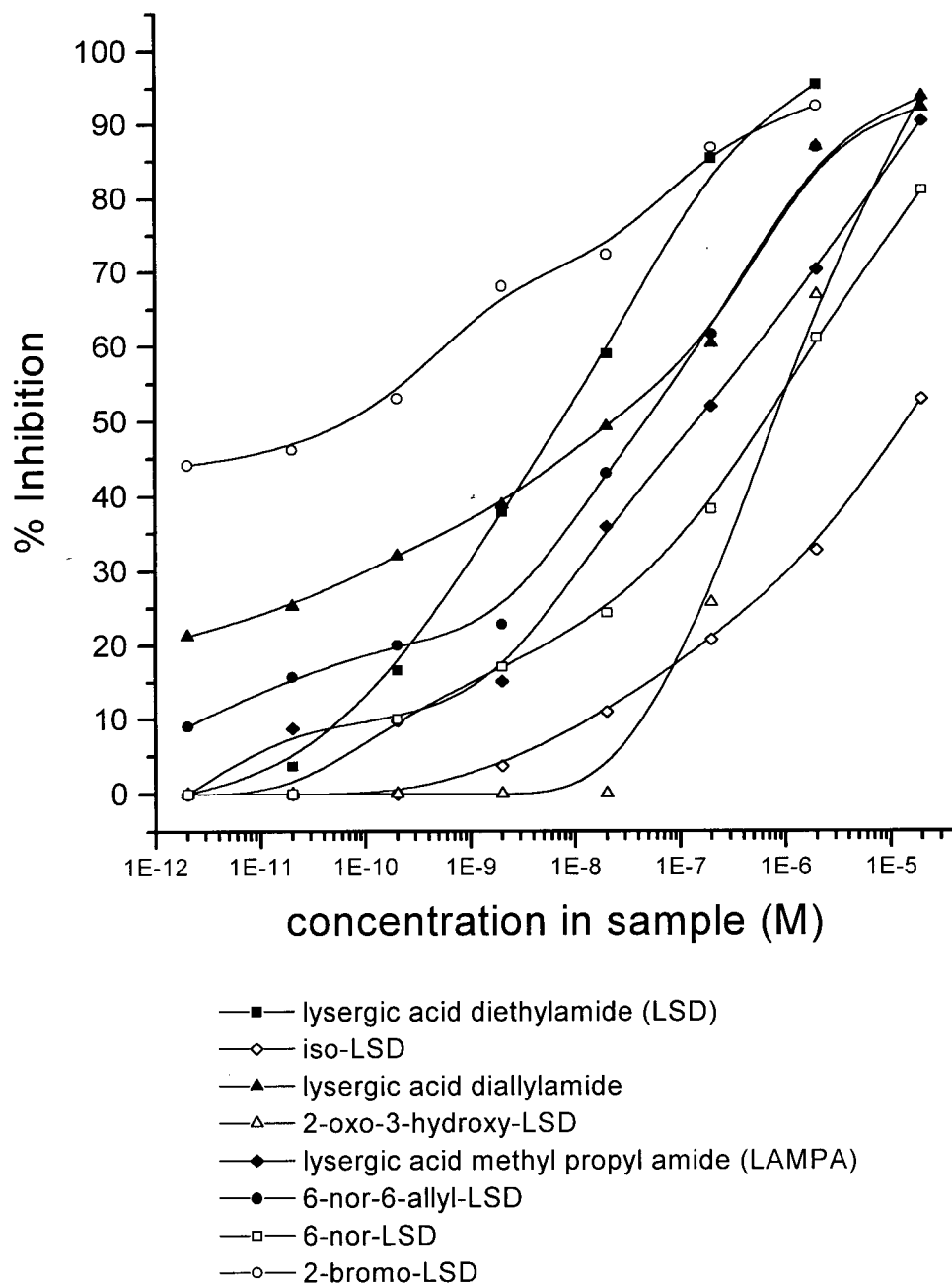
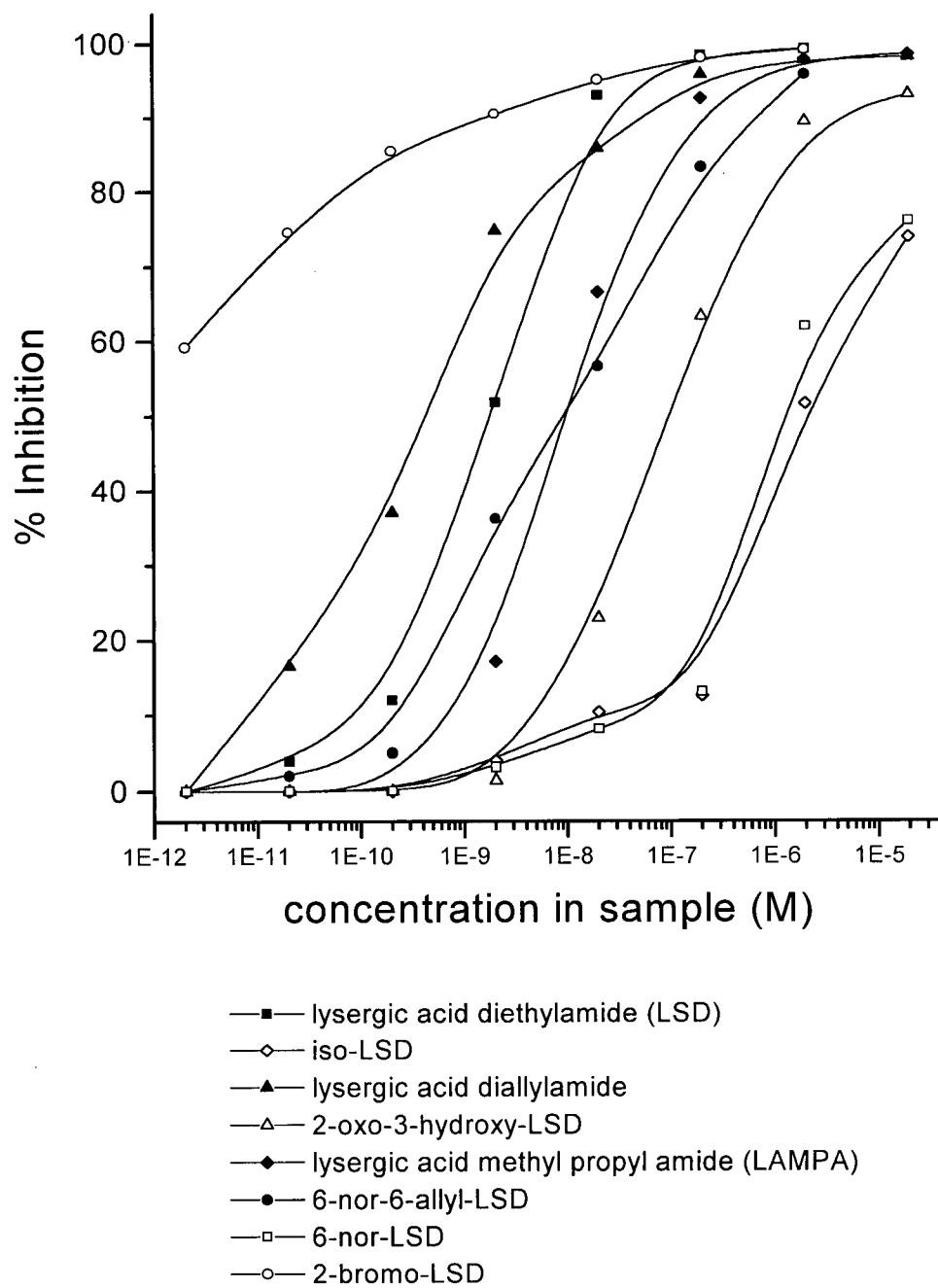


Figure 5.1 d) CEDIA



**Table 5.4.** Specificity of the photolinked antibody. Cross-reactivity was estimated from the amount of substance that produces a signal equivalent to 0.5 ng/mL (1.55 nM) LSD.

compound tested	nM equivalent to 0.5 ng/mL LSD	approximate % cross-reactivity
6-nor-6-allyl-LSD tartarate	0.005	344
6-nor-LSD	3	52
lysergic acid methyl-n-propyl amide (LAMPA)	4.5	34
2-oxo-3-hydroxy-LSD	45	3.4
lysergic acid diallylamide tartarate	60	2.6
<i>iso</i> -LSD	3000	0.05
ergonovine maleate	10000	0.016
methylergonovine maleate	20000	0.008
ergotamine tartarate	> 20,000	< 0.008
dihydroergotamine tartarate	> 20,000	< 0.008
methysergide maleate	> 20,000	< 0.008
<i>d</i> -lysergic acid	> 20,000	< 0.008
lysergic acid amide	> 20,000	< 0.008
lysergol	> 20,000	< 0.008
$\alpha$ -ergocryptine	> 20,000	< 0.008
ergocryptine	> 20,000	< 0.008
ergocornine	> 20,000	< 0.008
<i>N,N</i> -dimethyltryptamine	> 20,000	< 0.008
mescaline	> 20,000	< 0.008
psilocin	> 20,000	< 0.008
<i>l</i> -tryptophan	> 20,000	< 0.008
serotonin	> 20,000	< 0.008
hordenine hemisulfate	> 20,000	< 0.008
coramine	> 20,000	< 0.008
gramine	> 20,000	< 0.008
<i>l</i> -amphetamine sulfate	> 20,000	< 0.008
2-bromo-LSD hydrogen tartarate	nm	nm

nm = not measurable (see text).

**Table 5.5.** Specificity of commercial and in-house LSD antibodies by ELISA.

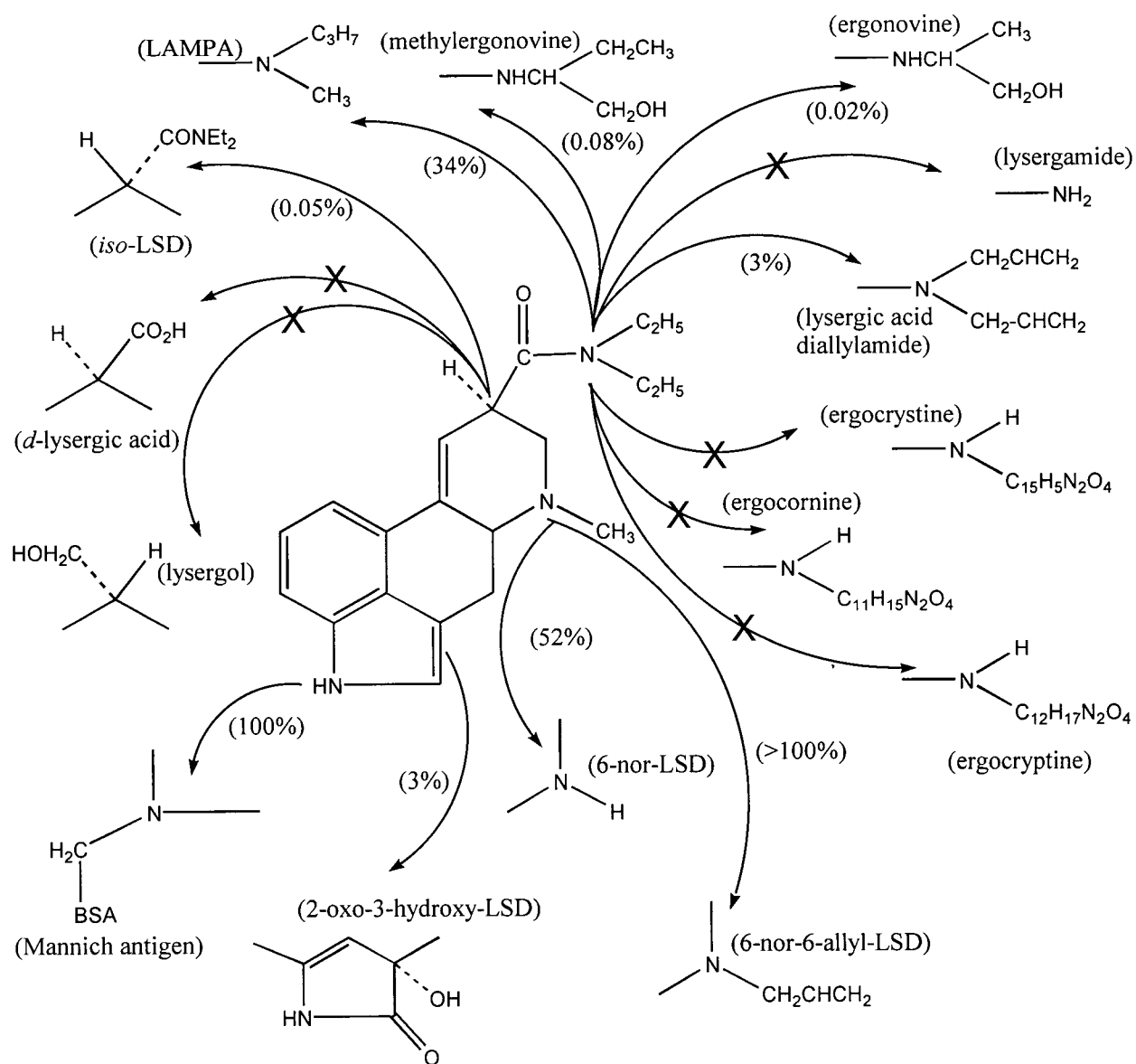
APPROXIMATE % CROSS REACTIVITY				
COMPOUND	Photolinked	Mannich	KIMS	CEDIA
6-nor-6-allyl-LSD tartarate	344	258	31	8
6-nor-LSD	52	16	0.16	1.6
lysergic acid methyl-n-propyl amide (LAMPA)	34	8	17	8
lysergic acid diallylamide tartarate	2.6	7.8	517	388
2-oxo-3-hydroxy-LSD	3.4	5.2	2.2	0.5
<i>iso</i> -LSD	0.05	0.04	0.09	0.08
ergonovine maleate	0.02	0.02	<0.08	<0.08
methylegonovine maleate	0.08	<0.08	<0.08	<0.08
ergotamine tartarate	<0.08	<0.08	<0.08	<0.08
dihydroergotamine tartarate	<0.08	<0.08	<0.08	<0.08
methysergide maleate	<0.08	<0.08	<0.08	<0.08
<i>d</i> -lysergic acid	<0.08	<0.08	<0.08	<0.08
lysergic acid amide	<0.08	<0.08	<0.08	<0.08
lysergol	<0.08	<0.08	<0.08	<0.08
$\alpha$ -ergocryptine	<0.08	<0.08	<0.08	<0.08
ergocryptine	<0.08	<0.08	<0.08	<0.08
ergocornine	<0.08	<0.08	<0.08	<0.08
<i>N,N</i> -dimethyltryptamine	<0.08	<0.08	<0.08	<0.08
mescaline	<0.08	<0.08	<0.08	<0.08
psilocin	<0.08	<0.08	<0.08	<0.08
<i>l</i> -tryptophan	<0.08	<0.08	<0.08	<0.08
serotonin	<0.08	<0.08	<0.08	<0.08
hordenine hemisulfate	<0.08	<0.08	<0.08	<0.08
coramine	<0.08	<0.08	<0.08	<0.08
gramine	<0.08	<0.08	<0.08	<0.08
<i>l</i> -amphetamine sulfate	<0.08	<0.08	<0.08	<0.08
2-bromo-LSD hydrogen tartarate	nm	nm	nm	nm

nm = not measurable (see text).

### 5.3.1.1. Photolinked antibody: structural insights.

Excluding 2-bromo-LSD, which will be discussed later, the highest cross-reactions involving the photolinked antibody occur with 6-nor-6-allyl LSD (344%), 6-nor-LSD (52%) and LAMPA (34%). Figure 5.2 illustrates the relationship between structure and specificity of a number of derivatives. In lysergic acid-*N*-methylpropylamide (LAMPA), the two ethyl substituents on the amide side chain of LSD are replaced with propyl and methyl groups which do not significantly change the electronic properties of the drug. It is therefore, no surprise that LAMPA cross-reacts with antibody to such an extent. Commercial LSD antisera report cross-reactivities of up to 60% with this derivative (23). A number of other compounds tested had structural differences at the amide position. Antibody was able to distinguish compounds having 2 ethyl groups on the amide from those which did not. When ethyl groups were replaced with hydrogen, in lysergic acid amide, no recognition occurs. In the same way,  $\alpha$ -ergocryptine, ergocornine, ergocryptine, ergonovine, ergotamine and methylegonovine, all of which are modified with large hydrocarbon groups at the amide position, do not significantly cross-react with antibody. When  $C_2H_5$  is replaced with  $CH_2-CH=CH_2$  in lysergic acid diallylamide, only minimal cross-reactivity is observed (<3%). The replacement of electron donating ethyl groups with electron withdrawing allyl groups makes the nitrogen less basic and significantly changes the properties of the molecule in such a way as to prevent effective antibody recognition.

**Figure 5.2** Effect of structural changes on photolinked antibody specificity. The approximate cross-reactivity of each derivative is shown in brackets and analogs which did not cross-react with the antibody are designated with an X.



Further insight is provided by cross-reactivity data of derivatives which differ from LSD at the C8 position. Replacement of the amide substituent with carboxylic acid or alcohol in lysergic acid and lysergol results in no cross-reaction and *iso*-LSD, which is a stereoisomer of LSD, has only 0.05% cross-reactivity. The antibody recognizes the change in spatial arrangement of diethylamide in *iso*-LSD, thus producing a poor fit between the antibody binding site and the drug. Overall, the photolinked antibody exhibits good specificity in the vicinity of the C8 and amide substituent, which suggests that an epitope exists in this region.

An antibody will not recognize a particular epitope if it has not been exposed to it during immunization. This sometimes occurs as a result of the chemical linkage between a reactive group on the target molecule and the carrier protein. Depending on the size of the carrier and the distance between it and the hapten, areas surrounding the point of attachment may be obscured from the immune system. Therefore, antibody specificity can provide valuable insights into the structural attachments in the immunogen.

Significant cross-reactivity was observed with both compounds which were derivatized in the N6 position. When  $\text{CH}_3$  is replaced with either H or  $\text{CH}_2\text{-CH}=\text{CH}_2$  in 6-nor or 6-nor-6-allyl LSD, the antibody cross-reactivity is 52% and 344% respectively. However, it has been shown that substitution of hydrogen and allyl groups in the vicinity of the amide group sufficiently changes the properties of the drug to prevent effective antibody recognition. Yet, this is not the case in the N6 region of the molecule. An explanation for this might be that LSD is covalently attached to carrier molecule at this position. During immunogen synthesis, the aryl azide in KLH-SASD inserts non-selectively into neighbouring molecules. However, the reactive nitrene produced during photolysis tends to be electrophilic in nature, thus having a preference for regions of high

electron density, such as double bonds or lone pairs (24). The nitrogen at the 6 position is a tertiary amine, with three electron donating groups. It is feasible that the electron deficient nitrene is attracted to the lone pair on this basic nitrogen which subsequently results in covalent attachment at this point. Further evidence for the proposed reactivity between the aryl azide and nitrogen is provided by the cross-reactivity of antibody with Mannich antigen (approximately 100%) in which LSD is derivatized at the indole nitrogen (see Chapter 3). The indole nitrogen is less basic than the tertiary amine in the 6 position because of the electron withdrawing double bonds of the indole ring. However, if the nitrene was attracted to the lone pair of electrons on the indole nitrogen, the subsequent chemical linkage would explain the failure of the antibody to distinguish the derivative from the parent drug. In addition to this, the hydrogen atom adjacent to the indole nitrogen is reactive. The removal of this acidic hydrogen results in a nucleophilic carbon in the 2 position which could also attract an electrophilic nitrene. The only compound which was derivatized in this position was 2-bromo LSD, which cross-reacted with antibody > 100%. As mentioned previously, the behaviour of 2-bromo-LSD is unusual because its interaction with antibody appears to be several orders of magnitude greater than parent drug itself. This phenomenon is not unique to the photolinked antibody but is also exhibited with other antisera (Figures 5.1 b to d).

As expected, none of the class III compounds cross-reacted with photolinked antibody. Interestingly, the same was true for class II compounds with the exception of 2-oxo-3-hydroxy LSD, which has a cross-reactivity of only 3%. This small cross-reaction could be the result of LSD attached to the carrier molecule at either the 1 or 2 position. It is feasible that even if protein is attached at the indole nitrogen of LSD, the large size of KLH and the spacer arm of SASD (19 Å) may not be sufficient to facilitate immune recognition of the drug at nearby positions.

Structural attachments within the immunogen are almost impossible to determine by conventional means due to the size and poor solubility of KLH-SASD-LSD. Therefore, derivatives which significantly cross-react with photolinked antibody provide a valuable insight into possible sites of attachment. This data likely suggests that LSD is attached to KLH at positions 1, 2 and 6 of the drug, which is plausible given the electrophilic nature of the nitrene.

#### **5.3.1.2. Other antibodies: general observations.**

Unusual antibody binding was observed with 2-bromo-LSD for which all four antisera tested had cross-reactivities greater than 100%. The tendency for antibody binding to approach a plateau at relatively high inhibition (Figures 5.1 c,d) raises some suspicion and suggests that there may be chemical interference between the 2-bromo-LSD and the macromolecule. The effect of 2-bromo-LSD on surface immobilized antigen was investigated by pre-treating antigen coated microtitre plates with derivative prior to LSD inhibition. No change in antibody binding was detected, which suggests that the apparent antibody inhibition is not due to an irreversible interaction or denaturation of BSA-LSD coating antigen. In a similar way, serum was incubated with 2-bromo-LSD, then thoroughly dialysed before it was used in an ELISA. No inhibition was observed which indicated that the derivative did not irreversibly interact with or modify the antibody molecule in such a way as to prevent it binding to surface antigen. Unfortunately, the quantity of 2-bromo-LSD available was very small (1 mg) which limited further investigation. It was not possible to rule out the presence of impurities in the sample and as such, the anomalous behaviour of 2-bromo-LSD is poorly understood. In some instances, inhibition with bromo-LSD did not decrease with decreasing concentration which is the case for true hapten inhibition. In

those cases, where a premature binding plateau is reached, cross-reactivity values were considered unreliable and not measurable.

Incorporation of allyl groups into LSD produced some interesting results. Lysergic acid diallylamide cross-reacted with KIMS and CEDIA antibodies > 100% but not with photolinked or Mannich antibodies. The opposite was true for 6-nor-6-allyl LSD, in which photolinked and Mannich cross-react > 100% whereas KIMS and CEDIA antibodies did not. The effect of allyl derivatives on coating antigen and antibody was measured by pre-treatment of BSA-LSD antigen and the antibody as described for 2-bromo-LSD. Once more, no irreversible modification of either macromolecule was detected. Neither 6-nor-6-allyl LSD nor lysergic acid diallylamide were detrimental to the cross-reactivity study because other compounds which were modified at the same positions were available. Therefore, in instances where > 100% cross-reactivity was observed, it was reasonable to exclude them from the structural attachment discussion due to the unusual "allyl effect".

It should be noted that binding studies involving structural analogs of LSD and certain serotonin receptor sub-types have reported unusual behaviour using both bromo and allyl derivative of LSD, as experienced here. The affinity of 6-nor-6-allyl LSD for serotonin receptor binding proteins was three times stronger than LSD itself (25). Additional studies showed that the antagonistic effect of 2-bromo-LSD on receptor binding, prevented subsequently administered LSD from binding to certain 5-HT receptors (25,26). The interaction between the small hapten and macromolecular antibody is analogous to the drug-receptor interaction. However, it is not fully understood whether the results obtained in the cross-reactivity study are related to similar properties in receptor binding studies or whether the results are coincidental.

This aside, the cross-reactivities of conventional antibodies towards the 25 other compounds tested were as expected. The derivative which cross-reacts with all antibodies the most is LAMPA, for reasons already discussed. The greatest cross-reaction with 2-oxo-3-hydroxy-LSD occurs with the Mannich antibody (5%) which is not unexpected. Its immunogen consists of a CH<sub>2</sub> bridge between a primary amine on the carrier protein and the indole nitrogen of LSD (Chapter 2). The close proximity of the drug to the protein results in reduced specificity in this region. Specificity should improve with increasing distance from the site of attachment, but cross-reactivity with 2-oxo-3-hydroxy LSD suggests that immune recognition is affected up to two carbon atoms away. The cross-reactivity of the Mannich antibody with 6-nor-LSD is slightly higher than expected (16%). This is not explained using the argument of point of attachment. The Mannich condensation is reported to take place primarily at the indole nitrogen, although the possibility exists that the tertiary amine in position 6 also reacts. The immunogen used for the production of the KIMS antibody consists of LSD coupled to carrier protein at the indole nitrogen. Therefore it is surprising that the greatest cross-reactivity occurs with 6-nor-6-allyl LSD (31%) although 6-nor-LSD cross-reacts to a lesser extent (<1%). It is possible that the cross-reaction with 6-nor-6-allyl LSD is an result of the anomalous "allyl effect". In general the specificity of this antibody in ELISA is good, probably the result of the extended spacer arm which is used between the drug and carrier protein (22). In general, monoclonal antibodies are more specific than their polyclonal counterparts because antibody is raised against only one epitope. It is therefore no surprise that the CEDIA monoclonal antibody has all round best specificity.

It should be noted that the estimated antibody specificities are applicable only to the competitive binding ELISA described here. Specificity can change from one assay to the next and

should be determined independently for each technique. For example, the reported cross-reactivity of the KIMS antibody with 2-oxo-3-hydroxy LSD is 40% in the Roche OnLine assay (27) and only 2.2% by ELISA. Boehringer Mannheim report the cross-reactivity of their monoclonal antibody to be 59% with LAMPA in the CEDIA test (23) compared with only 8% here. Even in a proven commercial assay, reported cross-reactivities vary from one batch to the next; for example, the cross-reactivity of the Roche OnLine test towards LAMPA is reported between 4.9% and 14% (22,27) and between 25% and 45% in the Roche Abuscreen radioimmunoassay (21,28).

#### **5.3.1.3. Clinical specificity.**

Aside from the structural implications of antibody specificity, it is important to recognize the clinical implications of drug detection in human urine, which is of paramount importance in the case of LSD. To date, the only confirmed metabolite in human subjects is 6-nor-LSD (29) although a number of other substances have been tentatively identified. Although LSD undergoes rapid biotransformation and excretion, the major metabolites remain unknown. Due to the small amount of drug ingested (50-100  $\mu\text{g}$ ), concentrations of parent drug in body fluids are extremely low, often undetected. As such, an effective screening immunoassay should employ an antibody of moderate specificity, which strikes a balance between clinical sensitivity (detection of drug and metabolites which indicate past use) and the false positive rate caused by unwanted cross-reactions with interfering substances. All commercial immunoassays for LSD to date report some cross-reactivity with metabolites and other derivatives which results in quantitative estimates which are often higher than parent drug concentrations which are confirmed by other methods. Therefore, the imperfect specificity dictates that although immunoassays are valuable screening tools, absolute

quantitative measurements are virtually unattainable by these methods and should only be used in combination with more rigorous techniques (30).

For present purposes antibody specificity should be viewed in the context of a clinical specimen and its contents. The indole group is common to many low molecular weight compounds which might be present in a biological specimen of a drug-free individual. For example, tryptophan, which is present in serum in the micro-molar range (31). However, specificity data clearly indicates that the immunodominant region of LSD resides in rings C and D rather than the indole rings (A and B), which is in agreement with the literature (32,33). *Iso*-LSD, which is a pharmacologically inactive stereoisomer, is usually present in illicit LSD. However, no significant cross-reactivity was observed for this compound or a number of other structurally related ergot alkaloids, which might also be present. Five of the twenty seven derivatives which were tested exhibited significant (>1%) cross-reactivity with the photolinked antiserum. Of these five compounds, it is unlikely that lysergic acid diallylamide or 6-nor-6-allyl LSD would be present in either an illicit LSD sample or a biological specimen. LAMPA, which cross-reacts 34%, is sometimes used as an internal standard for GC-MS analysis of LSD. However, it would not normally be added to a specimen prior to immunoassay. The two remaining derivatives, 6-nor-LSD and 2-oxo-3-hydroxy-LSD, which cross-react 52 and 3.4% respectively, could be present in the urine of someone who had taken LSD. A high cross-reactivity with the former of these, which is the major metabolite to date, is an advantage for drug screening purposes. On this basis, the photolinked antibody, which undergoes the highest cross-reaction with 6-nor-LSD, would be the best antibody for an ELISA drug screen.

### 5.3.2. Affinity constant measurements.

#### 5.3.2.1. ELISA method.

The hapten inhibition data shown in Figures 5.3 (a to d) was used to estimate the affinities of antibody subpopulations and their relative abundance in polyclonal antisera. Table 5.6 lists the results of apparent affinity constant ( $K_{app}$ ) estimates for anti-LSD antibodies according to the method of Nieto *et al.* (1984). The assumption that  $K_{app}$  is the reciprocal concentration of free hapten required for 50% binding is justified provided that the concentration of immobilized antigen is large with respect to the concentration of antibody. The range of  $\log K_{app}$  measurements illustrate the heterogeneous nature of the polyclonal antisera tested. When these individual values are weight-averaged, the highest overall apparent affinity constant is photolinked ( $4.1 \times 10^9 \text{ M}^{-1}$ ) followed by Abuscreen and Mannich ( $2.0 \times 10^9 \text{ M}^{-1}$  and  $1.7 \times 10^9 \text{ M}^{-1}$  respectively), and finally KIMS antibody ( $8.6 \times 10^8 \text{ M}^{-1}$ ). The last three represent roughly two to five fold reductions in  $K_{app}$  compared to the new photolinked antibody.

**Table 5.6.** Calculation of the apparent affinity constant ( $K_{app}$ ) from hapten inhibition data according to the method of Nieto (10). The 50% binding concentration (EC50) was calculated from inhibition curves (Figure 5.3 a,b,c,d) by interpolation.  $K_{app}$  was calculated from the inverse EC50 for each coating antigen concentration. The relative abundance of each antibody sub-population was estimated from the absorbance maximum for each coating antigen concentration, as a percent of the total (at saturation). A weight-averaged estimate of  $K_{app}$  was calculated by summing individual  $K_{app}$  values for each sub-population based on their relative abundance in the antiserum (% Ab). The error in estimating  $K_{app}$  was calculated assuming a 25% uncertainty in the interpolation of the EC50 concentration from calibration curves.

coating [Ag]	Photolinked			Mannich			Abuscreen			KIMS		
	EC50 (M)	log $K_{app}$	% Ab									
6.3	$9.5 \times 10^{-10}$	9.02	4.1	$2.0 \times 10^{-9}$	8.70	10.7	$2.5 \times 10^{-9}$	8.60	4.0	$6.5 \times 10^{-9}$	8.19	8.3
3.1	$7.0 \times 10^{-10}$	9.15	31.1	$1.3 \times 10^{-9}$	8.90	32.9	$3.0 \times 10^{-9}$	8.52	5.1	$3.5 \times 10^{-9}$	8.46	24.7
1.6	$4.2 \times 10^{-10}$	9.38	10.5	$6.0 \times 10^{-10}$	9.22	21.3	$1.3 \times 10^{-9}$	8.90	20.4	$2.5 \times 10^{-9}$	8.60	17.3
0.8	$2.5 \times 10^{-10}$	9.60	11.7	$3.5 \times 10^{-10}$	9.46	13.3	$5.5 \times 10^{-10}$	9.26	25.9	$1.3 \times 10^{-9}$	8.90	15.6
0.4	$1.3 \times 10^{-10}$	9.90	36.1	$3.0 \times 10^{-10}$	9.52	20.1	$3.3 \times 10^{-10}$	9.49	43.7	$5.8 \times 10^{-10}$	9.24	33.3
log $K_{app}$ range	9.0 - 9.9			8.7 - 9.5			8.5 - 9.5			8.2 - 9.2		
Average $K_{app}$ ( $M^{-1}$ )	$(4.1 \pm 1.0) \times 10^9$			$(1.7 \pm 0.4) \times 10^9$			$(2.0 \pm 0.5) \times 10^9$			$(8.6 \pm 2.1) \times 10^8$		

**Figure 5.3.** Estimation of  $K_{app}$  by hapten inhibition ELISA. Effect of immobilized antigen concentration on antibody binding, 12.5  $\mu\text{g}/\text{mL}$  (closed circles), 6.3  $\mu\text{g}/\text{mL}$  (open squares), 3.1  $\mu\text{g}/\text{mL}$  (closed triangles), 1.6  $\mu\text{g}/\text{mL}$  (open triangles), 0.8  $\mu\text{g}/\text{mL}$  (closed diamonds) and 0.4  $\mu\text{g}/\text{mL}$  (open circles). The four antibodies investigated were a) photolinked, b) Mannich, c) Abuscreen and d) KIMS.

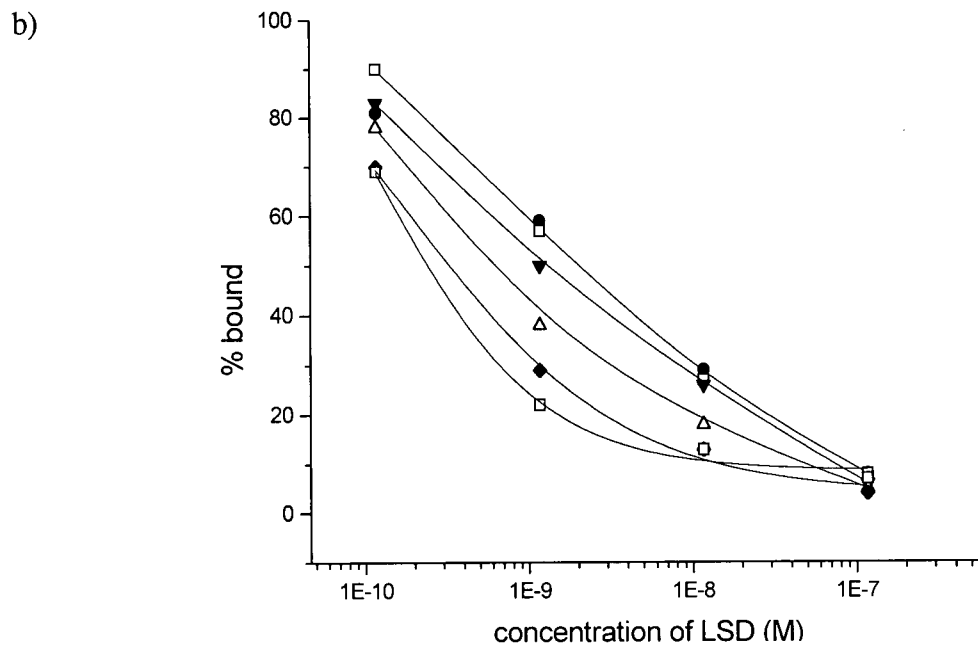
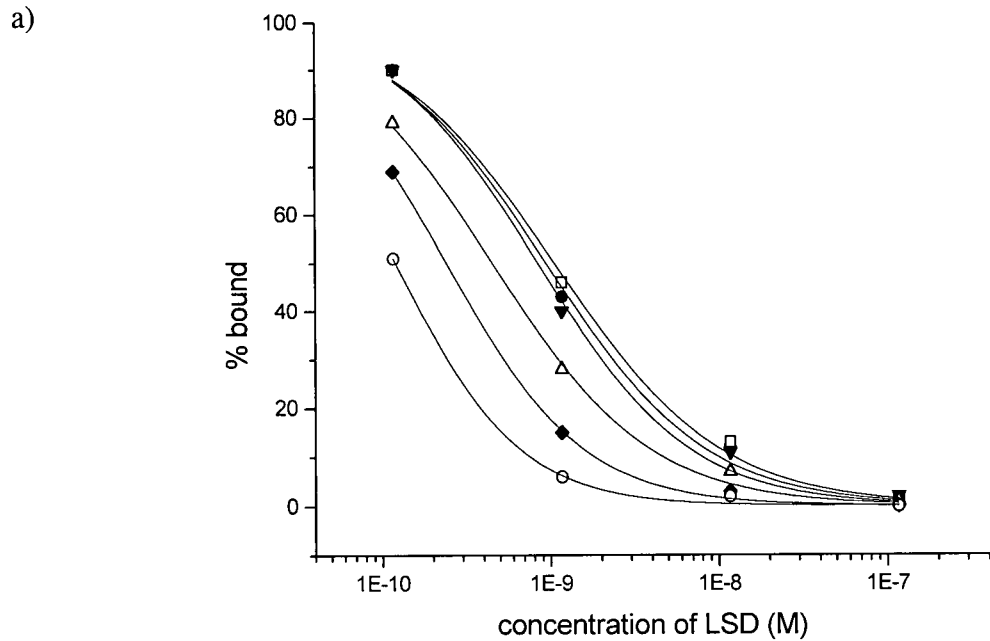
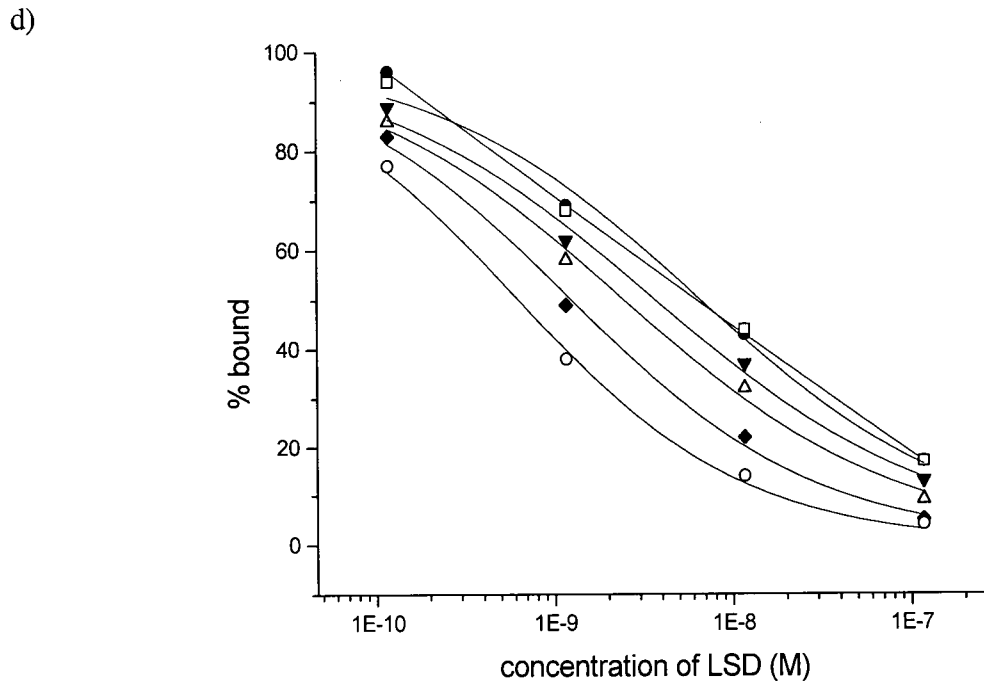
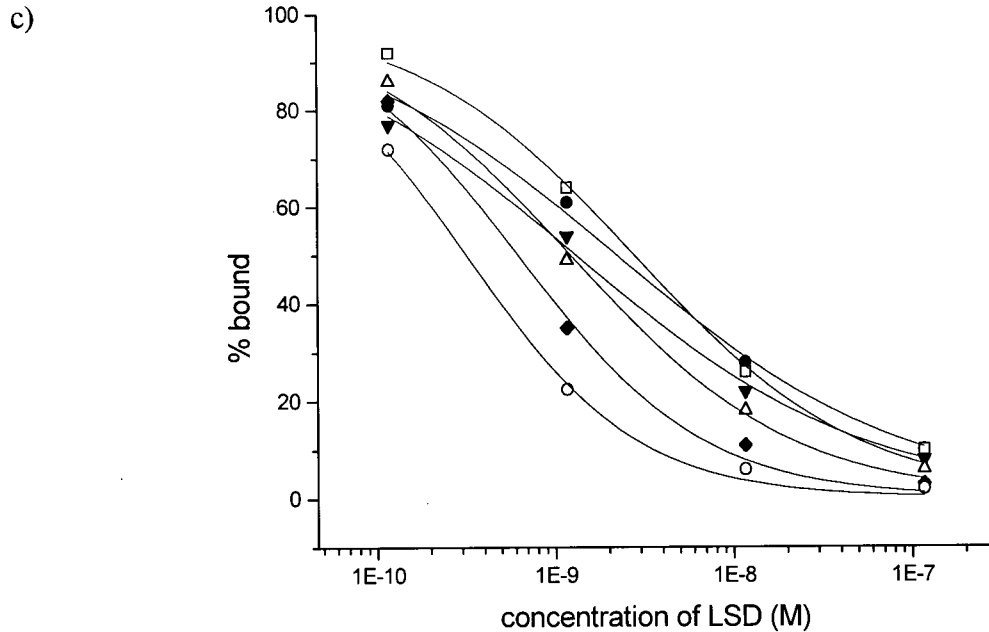


**Figure 5.3.** Estimation of  $K_{app}$  by hapten inhibition ELISA. Effect of immobilized antigen concentration on antibody binding, 12.5  $\mu\text{g}/\text{mL}$  (closed circles), 6.3  $\mu\text{g}/\text{mL}$  (open squares), 3.1  $\mu\text{g}/\text{mL}$  (closed triangles), 1.6  $\mu\text{g}/\text{mL}$  (open triangles), 0.8  $\mu\text{g}/\text{mL}$  (closed diamonds) and 0.4  $\mu\text{g}/\text{mL}$  (open circles). The four antibodies investigated were a) photolinked, b) Mannich, c) Abuscreen and d) KIMS.



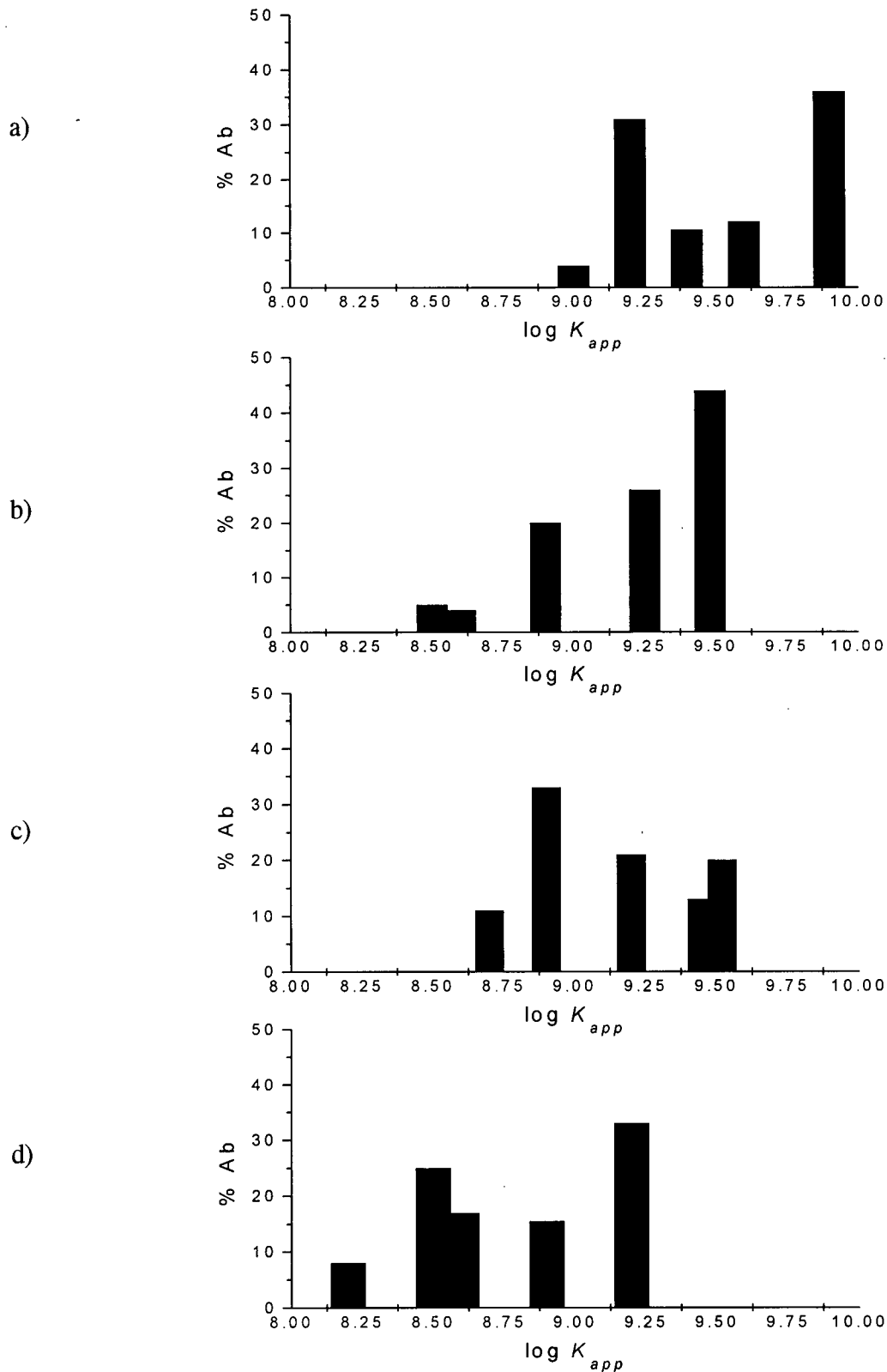
ELISA-based estimates of functional affinity measure the partition of antibody between solid and liquid phases. Estimates of the affinity are dependent on the surface density of the antigen as well as surface effects such as epitope orientation, diffusion effects and steric hindrance (34). Conditions for the calculation of a fluid phase affinity constant from inhibition of antibody binding to solid phase antigen are as follows:

- The fraction of surface adsorbed antigen which is bound by the antibody is much smaller than the total antigen which is adsorbed.
- Only a small fraction of the LSD added is bound by the antibody, such that the equilibrium concentration of LSD when 50% of the antibody is bound can be estimated from the total LSD added.
- The fraction of antibody bound to the solid phase is small compared to the total antibody.

Provided that the concentration of antibody used is small compared to the total LSD concentration for 50 % binding (EC50), it can be assumed that the concentration of free LSD is equivalent to total LSD concentration at 50% binding. The apparent affinity constant,  $K_{app}$  which is an estimate of the affinity constant, is equal to  $1/EC50$  under this assumption. Weight averaging  $K_{app}$  values by its fraction of the total antibody (Table 5.6) gives an average apparent affinity constant for the active subpopulations. Results show that EC50 values vary almost ten-fold with changing concentration of antigen on the surface (Table 5.6), implying that different antibody subpopulations are bound to the plate. Higher affinity subpopulations are inhibited at lower hapten concentrations than lower affinity subpopulations, which require higher concentrations of hapten to produce the same degree of inhibition. If enough surface antigen concentrations are used to

cover all subpopulations of antibody, this method can be used to determine relative concentrations of high and low affinity antibodies without the need for prior purification or fractionation. An advantage of this method is that it does not assume a normal distribution of affinities about an average value. Affinity distributions are constructed by plotting the relative abundance of the antibody population (%Ab) against the logarithm of its estimated affinity ( $K_{app}$ ). Figure 5.4 shows affinity distributions for different LSD antibodies which are displayed on the same scale for comparison. There is a definite change in average affinity from high to low, which is clearly indicated by the decrease in  $K_{app}$  of different subpopulations. The general trend from the affinity distribution in terms of decreasing affinity is photolinked (9.0 - 9.9) > Abuscreen (8.5 - 9.5)  $\approx$  Mannich (8.7 - 9.5) > KIMS (8.2 - 9.2), where numbers in brackets denote the range of  $\log K_{app}$  measurements. Although the range of the data changes from one antibody to the next, the overall spread (or heterogeneity) remains fairly constant. In other words, all  $K_{app}$  values calculated for a given antibody are within one order of magnitude of each other. However, the affinity distribution of  $K_{app}$  values varies from one antibody to the next, from binodal (photolinked) to skewed (Abuscreen) as would be expected for polyclonal antisera. Interestingly, the range of  $K_{app}$  for both Mannich and Abuscreen antibodies which were prepared using the same immunogen chemistry is almost identical, in contrast to photolinked and KIMS antibodies which were prepared using different methods.

**Figure 5.4.** Affinity distribution of LSD antibodies measured by hapten inhibition ELISA, a) photolinked, b) Abuscreen, c) Mannich and d) KIMS.



The concentration of specific anti-LSD which was used in the hapten inhibition ELISA was about  $8 \times 10^{-11}$  M for the photolinked antibody, which gave EC50 values between  $6.5 \times 10^{-9}$  and  $1.3 \times 10^{-10}$  over a range of coating antigen densities (Table 5.6). This implies that at 50% binding, the assumption that the concentration of antibody which is bound to LSD is negligible compared to the total concentration added may not be valid, particularly at low hapten inhibition concentrations. This assumption leads to a systematic error in which the equilibrium concentration of hapten at 50% binding is underestimated. This subsequently leads to an underestimation in the apparent affinity constant which is the reciprocal of the EC50. As such, although the ELISA method can be used to rank the antibodies with respect to affinity, the apparent affinity constants are likely to be underestimates of the true value, particularly in the case of the photolinked antibody. Therefore, the method described (10) has limited applicability for the measurement of high affinity interactions ( $K > 10^9 \text{ M}^{-1}$ ) in which the resultant 50% binding concentrations are prohibitively small, whereby assumptions inherent in the technique cannot be satisfied without introducing considerable systematic error.

Although the authors (10) report good agreement between ELISA and radiolabelled affinity measurements by this method, it should be noted that the affinity measurements made were of the order  $10^5 \text{ M}^{-1}$ , which is quite low. As the apparent affinity constant increases and the measured 50% inhibition concentrations approach the detection limit of the ELISA, one would expect there to be less concordance between the two methods. It has been suggested that the upper limit of affinity constant measurement is about  $10^9 - 10^{10} \text{ M}^{-1}$  by ELISA (3,10). The use of a fluorogenic detection system can increase assay sensitivity up to about  $10^{11} - 10^{12} \text{ M}^{-1}$ , whereas radiolabelled methods can measure even higher affinities (12). It was concluded that the affinity constant could be higher than the ELISA-based estimate, due to both systematic error inherent in the

mathematical assumptions and the detection limit of the technique.

The calculations used here assume monovalent binding of antibody in both solid and liquid phases. The calculation of affinity should take into account the bivalency of the IgG molecule. A mathematical correction can be applied using the binomial theorem in order to calculate affinity in terms of the antibody binding site rather than the antibody molecule (9). It has been shown that radiolabelled and ELISA based methods are in close agreement when the correction for bivalency is used (8). If  $f$  is the probability that one site is bound by hapten in solution, then the probability of both sites being bound is  $f^2$ . If only doubly liganded antibody is inhibited from binding to solid phase, as may be the case for a small target molecule, then the fraction of measured free antibody is  $1-f^2$ . The concentration of antigen at which  $f=0.5$  now occurs at 0.75 (or 75%) of the total antibody concentration added (4). If the apparent affinity constant is estimated from the inverse 75% binding concentration (EC75) at saturated immobilized antigen concentration, the trend in  $K_{app}$  ( $M^{-1}$ ) remains unchanged as follows: photolinked ( $1.8 \times 10^{10}$ ) > Mannich ( $1.1 \times 10^{10}$ )  $\approx$  Abuscreen ( $1.0 \times 10^{10}$ ) > KIMS ( $7.4 \times 10^9$ ).

This approach however is inadequate, because the total concentration of hapten which produces 75% binding is even smaller with respect to antibody concentration, thus increasing systematic error. It was therefore concluded that although ELISA-based estimates of functional affinity may not closely resemble intrinsic association constant, they may be useful for ranking antibodies in order of increasing affinity.

### 5.3.2.2. Radiolabelled study.

The equilibrium binding of radiolabelled LSD to antibody, which was coupled to agarose beads, was used to estimate the binding constant. The concentration of LSD which was not bound to antibody-coated agarose was measured at various times after the addition of antibody. Equilibrium was achieved within 30 minutes of sample mixing and this interval was routinely used for analysis. The association constant,  $K_a$ , can be determined from the Scatchard equation as follows,

$$v = n K_a L / (1 + K_a L)$$

where  $v$  is the molar concentration of bound ligand,  $L$  is the molar concentration of free ligand at equilibrium and  $n$  is the number of binding sites.

Measurement of  $v$  as a function of  $L$  allows both the association constant and the number of binding sites to be determined. Figure 5.5 shows the Scatchard plot of  $v/L$  vs  $v$ . It is clearly apparent from its non-linear nature, which is typical of a polyclonal antiserum, that more than one type of binding site is involved. If we assume 2 types of independent sites with association constants  $K_{1a}$ ,  $K_{2a}$  and numbers of binding sites  $n_1$  and  $n_2$  then,

$$v/L = [n_1 K_{1a} / (1 + K_{1a} L)] + [n_2 K_{2a} / (1 + K_{2a} L)]$$

Rearrangement gives,

$$v/L = -K_{1a} v + n_1 K_{1a} + n_2 K_{2a} [(1 + K_{1a} L) / (1 + K_{2a} L)]$$

When  $L \rightarrow 0$ ,  $v \rightarrow 0$  (none bound) then,  $(1 + K_{1a} L) / (1 + K_{2a} L) = 1$ , the initial slope is  $-K_{1a}$  and,

$$v/L = -K_{1a} v + n_1 K_{1a} + n_2 K_{2a}$$

When  $L \rightarrow \infty$ ,  $v \rightarrow \infty$  and  $v/L \rightarrow 0$

$$(1 + K_{1a} L) / (1 + K_{2a} L) \approx K_{1a} / K_{2a}$$

and  $v = n_1 + n_2$ .

The plot of  $v/L$  vs  $v$  provides  $K_{1a}$ ,  $n_1$  and  $(n_1 + n_2)$  from the initial slope and intercepts respectively. Given this,  $K_{2a}$  is guessed and re-substituted back in to the data to obtain the best fit for the non-linear equation (Figure 5.5). Assuming no cooperativity and 2 populations of binding sites with different affinities, antibody binding parameters were calculated as follows:

$$K_{1a} = 1.9 \times 10^{10} \text{ M}^{-1} \quad n_1 = 6.2 \times 10^{-10} \text{ M}$$

$$K_{2a} = 1.7 \times 10^8 \text{ M}^{-1} \quad n_2 = 3.1 \times 10^{-10} \text{ M}$$

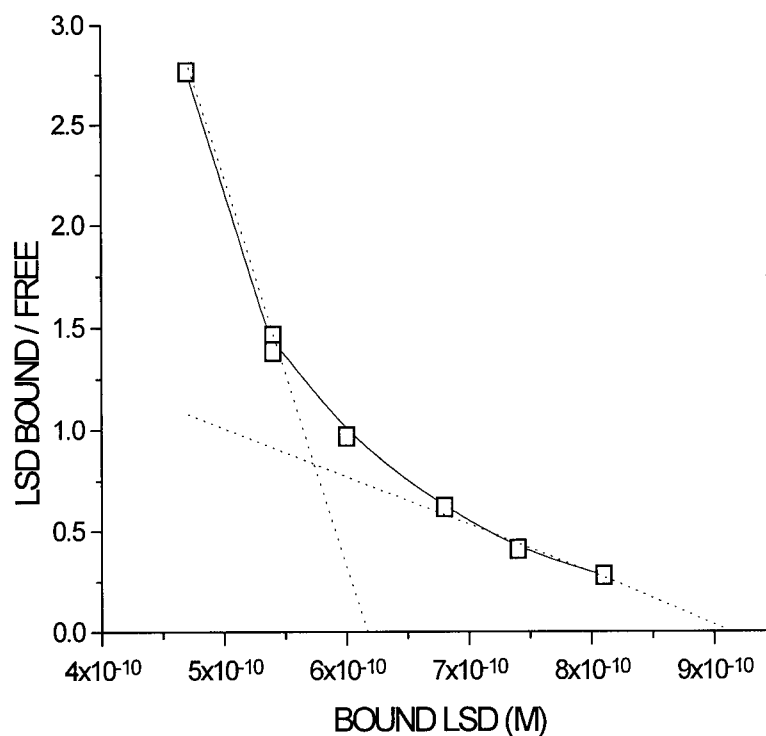
In which the high affinity interaction ( $K_{1a}$ ) accounts for 67% and low affinity ( $K_{2a}$ ) accounts for 33% of the total antibody population. The average equilibrium association constant,  $K_a$ , calculated from,

$$K_a = [K_{1a} \cdot n_1 / (n_1 + n_2)] + [K_{2a} \cdot n_2 / (n_1 + n_2)]$$

was  $(1.28 \pm 0.15) \times 10^{10} \text{ M}^{-1}$  and the total number of binding sites ( $n_1 + n_2$ ) was  $(9.3 \pm 1.2) \times 10^{-10} \text{ M}$ . The error analysis represents the uncertainty of the graphical analysis, which was greater than the uncertainty between duplicate samples (<10%). The total number of binding sites per antibody molecule was estimated from the amount of drug specific IgG used in the system ( $1.8 \times 10^{-13}$  moles) and the total number of binding sites. This number was  $2.8 \pm 0.8$  binding sites per molecule of IgG which is higher than expected. The maximum number of antibody binding sites on an IgG molecule is 2 which is within the calculated error limits (28.6%) given the uncertainties in both total antibody used and number of binding sites. However, a small underestimation in the concentration of drug specific antibody on agarose would account for a value of 2.8. The theoretical maximum of 2 binding sites can be used to calculate the concentration of antibody which was bound to agarose from the affinity data. This value suggests that the concentration of

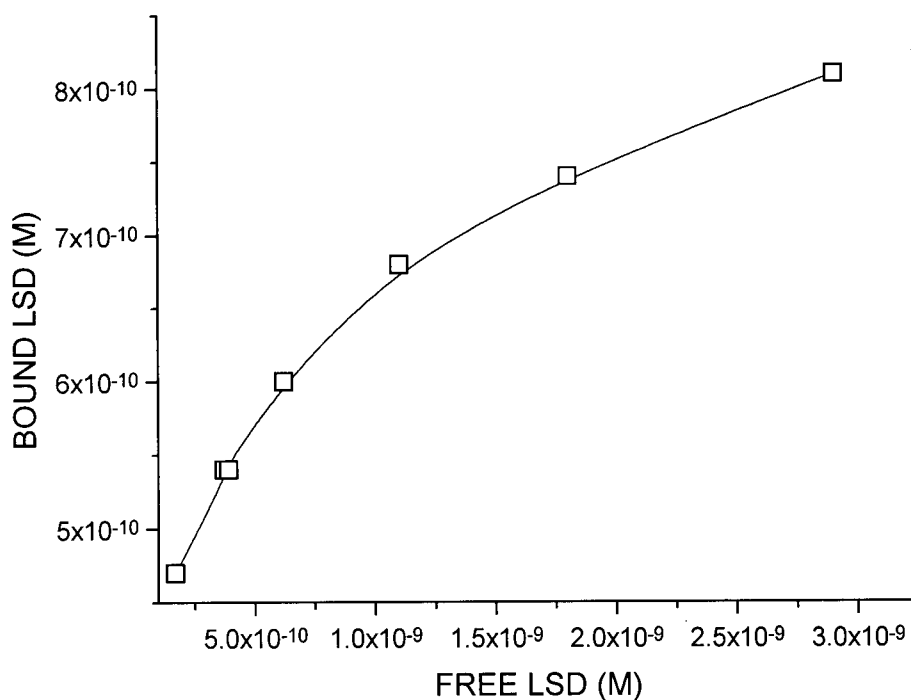
drug specific IgG bound on agarose gel is  $(0.79 \pm 0.10) \mu\text{g/mL}$  rather than  $(0.55 \pm 0.06) \mu\text{g/mL}$  as determined by capacity measurements (Section 6.3.3.1). Although these two estimates are not within experimental error, they are in moderately good agreement. It should be noted however that this uncertainty does not affect the equilibrium association constant, which is calculated independently of antibody concentration.

**Figure 5.5.** Scatchard plot which describes the binding of photolinked antibody to LSD. Assuming two sets of independent binding sites of high and low affinity, the equilibrium association constants were  $1.9 \times 10^{10}$  and  $1.7 \times 10^8 \text{ M}^{-1}$  respectively. The total number of binding sites was  $9.3 \times 10^{-10} \text{ M}$ .



Alternative representation of experimental data is shown in Figure 5.6 in which a direct plot of bound against free LSD at equilibrium clearly shows the near saturation of antibody binding sites at high concentrations of drug. It is possible to estimate both the association constant and the total number of binding sites from the initial slope (where  $L$  is infinitely small) and the saturation level. Estimates of  $K_a$  and  $n$  by this method are  $3.4 \times 10^9 \text{ M}^{-1}$  and  $8.25 \times 10^{-10} \text{ M}$  respectively. However, this approach is inferior to the Scatchard analysis given the difficulty in estimating the number of binding sites when saturation is not fully achieved.

**Fig 5.6** Direct plot of photolinked antibody binding to LSD. Estimated  $K_a = 3.4 \times 10^9 \text{ M}^{-1}$  and  $n = 8.25 \times 10^{-10} \text{ M}$  from the upper binding plateau ( $n$ ) and initial slope ( $nK_a$ ).



Affinity constant estimates for the photolinked antibody using radiolabelled and ELISA techniques were in closest agreement when the correction for divalent antibody binding was used. The approximate apparent affinity constant, estimated from the reciprocal concentration that produces 75% binding, was  $1.8 \times 10^{10} \text{ M}^{-1}$  compared with  $1.3 \times 10^{10} \text{ M}^{-1}$  by the radiochemical method. Despite reasonable agreement, the radiolabelled procedure provides the most reliable estimate of the intrinsic association constant for a number of reasons. The high specific activity of the labelled drug improves the sensitivity, which facilitates the measurement of high affinity antibody interactions, which take place at low hapten concentrations. Also, there are fewer inherent assumptions involved in the calculation. Finally, the Scatchard approach assumes not one but two sets of independent binding sites, which more realistically resembles a heterogeneous antibody population.

### 5.3.3. Antibody dissociability.

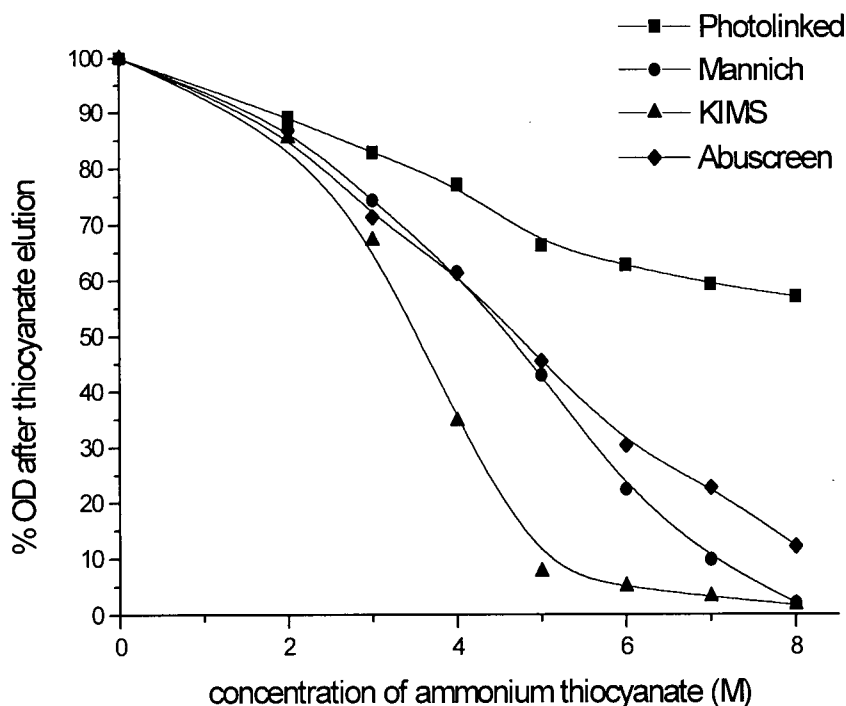
It has been reported that it is the rate of dissociation of antibody which largely determines the stability of a hapten-antihapten complex (35). This has a pronounced effect on immunoassay performance in terms of both sensitivity and reproducibility. Functional affinity can be quantified using indices which measure the degree of dissociability of antibody in the presence of an Ab-Ag disrupting agent. *Avidity indices* are defined as the ratio of antilog reciprocal serum dilutions at half maximum OD, which is a measure of the leftward shift in serum titration, before and after treatment with thiocyanate ions (13). The *Antibody dissociability* can be quantified by the length of the line drawn between data points at the same absorbance on antibody titration curves, in the presence and absence of denaturant (16). However, the most widely used parameter is *affinity*

*index*, which is the concentration of chaotropic agent required to reduce the initial OD by half (17,18,36,37). Although other quantitative estimates of functional affinity have been used for chaotropic elution (15,19), this remains the most popular. Antibody populations with the same average affinity may differ significantly with respect to their affinity distributions, which can be characterized by competitive binding ELISA and by chaotropic elution.

### 5.3.3.1 Antibody affinity profiles and distributions.

Affinity profiles shown in Figure 5.7 provide an effective qualitative representation of the strength of the antibody-antigen interaction. Antibodies which have the highest overall functional affinity, will have greater resistance towards thiocyanate ions than antisera of lower affinity. The photolinked antibody was by far the most resistant to dissociation, with more than 50% of the total OD remaining after treatment with 8 M ammonium thiocyanate. Mannich and Abuscreen antibodies prepared in-house and commercially by the same chemical linkage have strikingly similar profiles. The KIMS antibody appears to be the most vulnerable towards chaotropic eluent with a marked increase in dissociability over a range of thiocyanate concentrations. The average OD for all antibodies when no thiocyanate was present was  $0.33 \pm 0.01$  (n=4). *Affinity indices*, calculated from the concentration of thiocyanate which reduced the absorbance by half (Table 5.7), clearly indicated that resistance to chaotropic ion elution decreased in the order, photolinked > Abuscreen  $\approx$  Mannich > KIMS.

**Figure 5.7.** Antibody affinity profile measured by thiocyanate elution followed by ELISA detection. The affinity index (M) for antibodies raised against different immunogens was calculated from the concentration of ammonium thiocyanate that decreases the maximum OD by 50%.



As discussed earlier, although the exact mechanism of action of thiocyanate is unclear, it probably interferes with conformational changes which are necessary for the antibody to bind antigen (13). Pretreatment of BSA-LSD coated plates with thiocyanate prior to the antibody incubation did not affect binding. Hence, the result is unlikely to be due to denaturation of BSA-LSD.

A number of steps were taken to minimize the experimental error. Antisera were diluted to give approximately equal absorbance readings in the absence of thiocyanate, to minimize the effect of changing antibody concentration. In order to allow an approach to equilibrium, a 2.5 hour

antibody incubation period was used for all antisera tested. Finally, it is assumed that antibodies of a particular affinity are not preferentially measured. To reduce bias, BSA-LSD coating antigen was used at saturating concentrations throughout, as it is known that decreasing the amount of antigen which is immobilized, preferentially binds higher affinity sub-populations of antibody.

**Table 5.7.** *Affinity indices and Antibody dissociabilities of polyclonal antisera to LSD.*

Antibody	<i>Affinity index (M)</i>	<i>Antibody dissociability (mm)</i>
Photolinked	> 8	4
Abuscreen	4.2	17
Mannich	4.1	38
KIMS	3.5	> 78

### 5.3.3.2. Antibody titration curves.

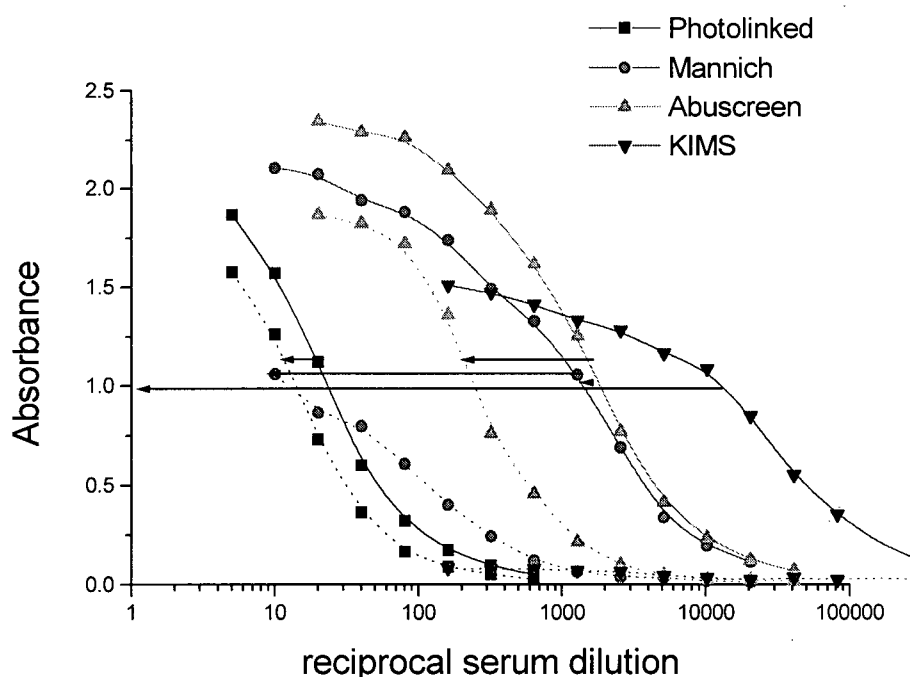
Antibody titration curves in the presence and absence of thiocyanate are shown in Figure 5.8. The dissociability of drug specific IgG bound to antigen over a range of concentrations is quantified using *antibody dissociability*, which is proportional to the leftward shift in titration data at OD=1 (Table 5.7). These values indicate that the functional affinity of the antisera tested decreased in the order photolinked > Abuscreen > Mannich > KIMS, which was in agreement with *affinity index* data.

Dissociability of the Ab-Ag complex varies over a range of antibody concentration. Under conditions of antibody excess, where the concentration of IgG in solution is greater than the concentration of surface immobilized antigen, the law of mass action predicts that the highest

affinity antibodies will bind first. Conversely, at low antibody concentrations where antigen is in excess, a mixture of both high and low affinity antibodies will bind. Therefore we expect greater resistance to chaotropic eluent at high antibody concentrations, which result in the strongest Ab-Ag complex formation due to preferential binding of high affinity subpopulations.

The *antibody dissociability* of the CEDIA monoclonal anti-LSD was measured in the same way. Its dissociability was comparable to the KIMS antibody, in which almost all of the antibody is eluted with thiocyanate regardless of antibody concentration. This is not surprising as it is known that monoclonal antibodies are more prone to dissociation than their polyclonal counterparts (38). It is interesting to note that there seems to be a trend between antibody titre and dissociability; as the antibody titre increases, so does its tendency to dissociate. This might suggest that a high titre response is not conducive to high affinity antibody production, which has been suggested elsewhere (16).

**Figure 5.8.** Antibody titration and thiocyanate elution. *Antibody dissociability* (mm) is defined as the length of the line drawn between titration curves in the presence and absence of thiocyanate.



The dissociation of surface immobilized antibody bound to antigen in the absence of any chaotropic eluent is reported to be minimal (39). Previous studies have shown that antibody binding was stable and no half time of dissociation could be measured within 69 hours. By comparison, Fab fragments of the same antibody dissociated with a half time of 16 hours which suggests that bivalence is important in maintaining stability of antibody bound to immobilized antigen.

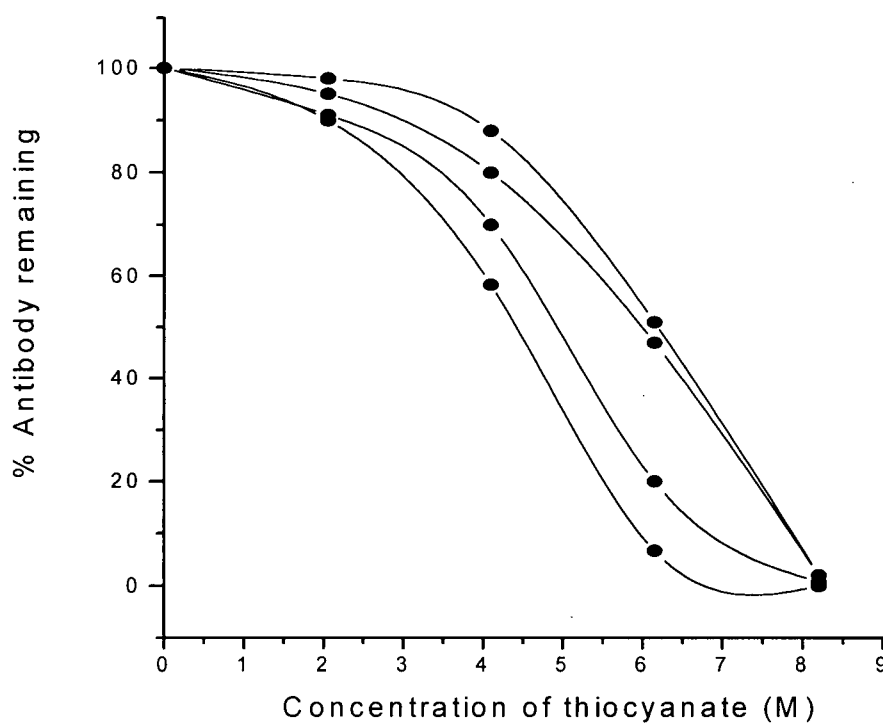
#### 5.3.4. Affinity maturation of antibodies.

Affinity maturation is characterized by a shift to the right, towards higher thiocyanate concentration, in the affinity distribution. This effect has been used to distinguish whether patients were acutely or chronically exposed to viral and microbial organisms (13). Affinity maturation of patients exposed to *Rubella* was illustrated by the increase in *affinity index* over time post vaccination (17) and by the decrease in *antibody dissociability* exhibited inpatients who were reinfected with the virus (16).

During the course of infection or immunization the immune response matures, which causes the average affinity of antibodies to increase. This is thought to be due to selection of high affinity clones. Antibodies which have a low affinity towards the antigen are considered to be the result of unwanted cross-reactions and are not selected for proliferation, which results in their production being secondary to that of the higher affinity clones. In clonal selection theory, it is assumed that cell-bound antibodies have a variety of affinities. A given cell is either stimulated or unresponsive to antigen. Early on in the immune response many cells are stimulated which results in a range of affinities but later on, as antigen becomes limiting, only the higher affinity clones are selected.

The affinity maturation process is illustrated in Figure 5.9. This antibody affinity profile obtained by thiocyanate elution and ELISA detection, clearly shows the strengthening of the Ab-Ag complex formation over time. This maturation process can change the antibody heterogeneity as well as the overall affinity of the antiserum.

**Figure 5.9.** Affinity maturation of antibodies over a period of four months. Affinity profiles were measured using thiocyanate elution and ELISA detection after successive immunizations.



Relative affinity measurements indicate that antibody heterogeneity is not normally distributed as once thought, as there may be a few restricted clones of B lymphocytes which secrete antibody. Affinity heterogeneity of polyclonal antisera in previous work has shown that symmetrical distributions of affinities are the exception, not the rule (40). Early after immunization (7 days) there is an approximately symmetrical distribution which becomes progressively skewed towards higher affinity. By day 90 there is usually an asymmetric

distribution of mostly high affinity antibody subpopulations. However, in some instances, low affinity antibodies persist throughout the entire immunization interval, which is usually attributed to genetic predisposition, malnutrition, immunosuppression, ageing or antigenic competition (41). Affinity maturation studies using fluorescein as the hapten have shown that affinity constant can increase from  $10^8$  to  $10^{11} \text{ M}^{-1}$  in the same rabbit (42). The immune response "matures" in the sense that the antibody changes during immunization towards a less heterogeneous mixture of higher affinity antibody.

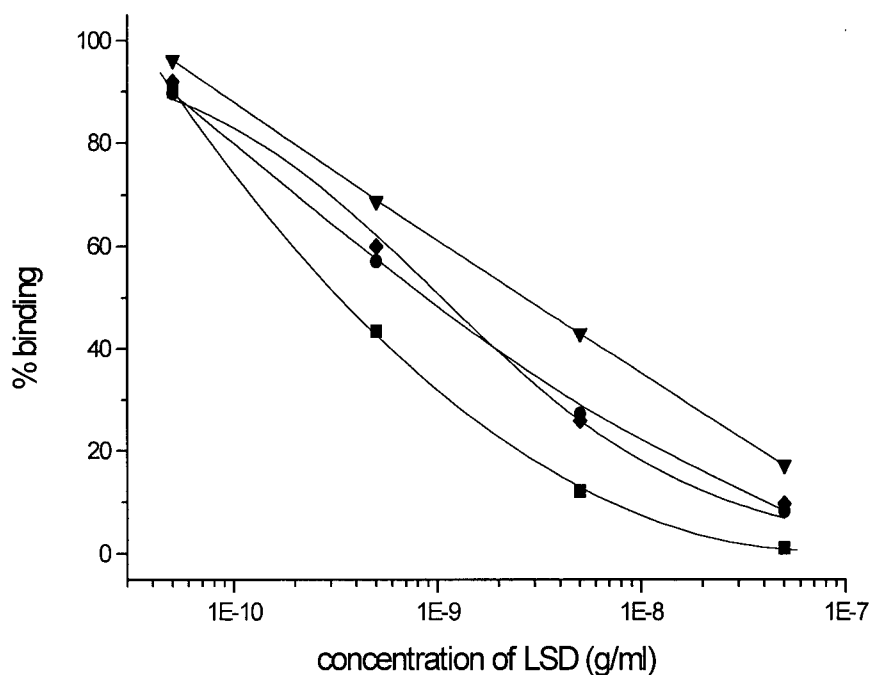
#### **5.3.5. Affinity, dissociability and sensitivity.**

It is well documented that the affinity of the Ab-Ag reaction largely determines the sensitivity of the immunoassay, although the exact nature of the interaction is poorly understood. Mechanistic studies of ligand binding show that the active site of the antibody reflects the nature of the hapten. Antibodies directed against negatively charged haptens frequently contain positively charged residues in the active site while those binding uncharged or polar haptens frequently bind through hydrophobic interactions (43). Both heavy and light chains are necessary for formation of the active site. Interaction of the variable domains of both chains provide the particular environment required to bind ligand. Specific interactions such as hydrogen bonding, protonation and ionic forces may contribute to the affinity of the non-covalent association. Thermodynamically, a single residue (eg. hydrogen bond, protonation) can contribute sufficient energy to affect the binding affinity. Therefore selective optimization of residues in the variable regions at the genetic level could in part account for an increase in affinity. Ionizable residues, such as lysine, arginine or histidine, can increase the binding energy between the hapten and the antibody, by creating a salt-type linkage which contributes a Coulombic energy to the Ab-Ag

interaction (44).

Some authors report significant correlation between affinity indices obtained from thiocyanate elution and affinity constants measured by equilibrium dialysis (36) whilst others have found no correlation (37). It is established however, that there is an inverse correlation between affinity constant and sensitivity, as measured by the EC<sub>50</sub> (14). Figure 5.10 shows dose-response data for different LSD antisera which were used in the competitive binding ELISA described in Appendix II. Although the concentration of LSD that results in 50% binding (EC<sub>50</sub>) changes with antigen density on the surface, the relative rank order remains unchanged (Table 5.6) (14).

**Figure 5.10.** Calibration of LSD using four different polyclonal antisera to LSD. Photolinked (squares), Mannich (circles), Abuscreen (diamonds) and KIMS (triangles).



In this chapter, quantitative estimates of affinity, dissociability and sensitivity of four polyclonal antibodies were investigated. Table 5.8 summarizes these results in terms of relative rank order, in which 1 is most favourable and 4 is least favourable. Kendall's coefficient,  $W$ , was used to measure the correlation between multiple sets of ranks (45) where,

$$W = \frac{12 \sum_{i=1}^N D_i^2}{m^2 (N) (N^2-1)}$$

The relative rank order of a number of antibodies ( $N$ ) with respect to different parameters ( $m$ ) is calculated and summed for each antibody. If there was no correlation among the ranks, the mean sum of the ranks for each antibody would be equal. Therefore the difference between the summed ranks and the mean sum is calculated ( $D$ ) and squared.

**Table 5.8.** Correlation between affinity, dissociability and sensitivity parameters. Calculation of Kendall's coefficient,  $W$ .

Antibody	Ranks					
	EC50	Affinity index	Antibody dissociability	$K_{app}$	sum of ranks	$D$
Photolinked	1	1	1	1	4	6
Abuscreen	3	2	2	2	9	1
Mannich	2	3	3	3	11	1
KIMS	4	4	4	4	16	6
					$\Sigma=40$	$\Sigma(D^2)=74$
$W=0.925$ which is significant ( $P < 0.001$ ) where $N=4$ and $m=4$						

Perfect agreement is indicated by  $W=1$  and no agreement by  $W=0$ . In this instance,  $W=0.925$ , which is highly significant ( $P<0.001$ ). Therefore we can conclude that there is a statistical correlation between antibody affinity (estimated from the apparent affinity constant,  $K_{app}$ ), dissociability (from thiocyanate elution) and sensitivity (EC50 by ELISA). As antibody affinity increases, dissociability decreases and overall assay sensitivity increases. It is clear from the results that the photolinked antibody ranked first and the KIMS antibody appeared last in each parameter tested.

In terms of affinity, dissociability and sensitivity, both Mannich and Abuscreen antibodies are strikingly similar, with EC50, *affinity indices* and  $K_{app}$  estimates within 20% of each other. The only common feature between Mannich and Abuscreen antibodies, which were produced in-house and commercially, is that they were both prepared from immunogens which utilized the same coupling chemistry. This data suggests that the antibody characteristics may be predetermined to some degree by the type of chemical linkage used to couple drug to carrier protein, which has been suggested elsewhere (46,47).

#### 5.4. Conclusion.

The specificity of the novel photolinked antibody was investigated using 27 structurally related compounds of interest. Significant cross-reactivity (34%) was observed with lysergic acid methylpropylamide (LAMPA) and 6-nor-LSD (52%). In general, the antibody exhibits good specificity in the vicinity of the C8 and amide substituent. This implies that an epitope exists in this region, which is in agreement with the literature which suggests that both C and D rings are immunodominant. Cross-reactivity of the photolinked antibody with LSD derivatized at either the N6 or the indole nitrogen could be the result of covalent attachment of KLH-SASD to LSD at these sites. Electron deficient nitrenes are attracted to regions of high electron density, and could preferentially react with the lone pairs of electrons on both these nitrogens. The small degree of cross-reactivity towards 2-oxo-3-hydroxy-LSD (3%) could well be the result of chemical linkage at the nearby indole nitrogen. In terms of forensic interest, cross-reactivity with 6-nor-LSD, which is the primary metabolite in man, is an advantage for screening purposes. Cross-reactivities towards this compound were found to decrease in the order photolinked (52%) > Mannich (16%) > CEDIA (1.6%) > KIMS (0.16%).

ELISA-based estimates could only be used to rank antibodies with respect to affinity, due to limitations in the mathematical assumptions which led to systematic errors. The general trend in order of decreasing affinity was photolinked > Abuscreen = Mannich > KIMS, whereby the photolinked antiserum gave the overall highest results. Affinity distributions varied between antisera from binodal (photolinked) to skewed (Abuscreen). Mannich and Abuscreen antibodies which were produced from immunogens utilizing the same chemical linkage were strikingly similar in terms of  $\log K_{app}$  ranges and affinity characteristics.

The equilibrium association constant of the photolinked antibody was measured using

tritiated LSD and IgG immobilized on agarose-Protein A. Assuming two sets of independent binding sites, a Scatchard plot was used to calculate the equilibrium association constants of high and low affinity interactions, which were found to be  $1.9 \times 10^{10} \text{ M}^{-1}$  and  $1.7 \times 10^8 \text{ M}^{-1}$  respectively. The high affinity interaction accounted for 67% of the total antibody binding sites which was estimated to be  $(9.3 \pm 1.2) \times 10^{-10} \text{ M}$ . The overall equilibrium association constant, obtained by weight averaging these measurements was  $(1.28 \pm 0.15) \times 10^{10} \text{ M}^{-1}$ .

Antibody dissociability was measured using chaotropic thiocyanate elution of antibody followed by ELISA detection. Quantitative estimates of the functional affinity of Ab-Ag interactions were obtained by titrating both antibody and thiocyanate. Antibody affinity profiles, *affinity indices* and *antibody dissociabilities* indicated that the strength of the immuno complex decreased in the order photolinked > Abuscreen = Mannich > KIMS. Thiocyanate elution methods were also used to illustrate the concept of affinity maturation which takes place in the rabbit during hyperimmunization.

Kendall's  $W$  was used to test the theory that there was a correlation between affinity, dissociability and sensitivity using 4 polyclonal LSD antisera. Quantifiable parameters which described these characteristics were ranked and tested statistically. Results showed that there was a highly significant correlation between these variables; as affinity increases, dissociability decreases and sensitivity increases.

In conclusion it was found that,

- 1.) Thiocyanate elution could be used for the rapid evaluation of affinity characteristics of different polyclonal antisera to LSD.

- 2.) The affinity of the antibody may be predetermined to some degree by the coupling chemistry which is used to attach the hapten to the carrier molecule.
- 3.) Photolinked antibody, which utilizes a novel approach to LSD immunogen synthesis, was found to be the highest affinity antibody tested. This suggests it would be a very effective antibody for the detection of LSD in forensic specimens where sensitivity is of crucial importance.
- 4.) Photolinked antibody also has the highest cross-reactivity towards the primary metabolite, 6-nor-LSD, by ELISA which is advantageous for drug screening purposes.
- 5.) Finally, characterization of four polyclonal antisera to LSD indicated a positive correlation between antibody affinity, dissociability and sensitivity by ELISA.

### 5.5. References.

1. Peterfy, F., Kusela, P., and Makela, O. 1983. *J. Immunol.* 130(4): 1809-1813.
2. Hoylaerts, M.F., Bollen, A., and Broe, M.E. 1990. *J. Immunol. Methods* 126: 253-261.
3. Friguet, B., Chaffotte, A.F., Djavadi-Ohanian, L., and Goldberg, M.E. 1985. *J. Immunol. Methods* 77: 305-319.
4. Hetherington, S. 1990. *J. Immunol. Methods* 131: 195-202.
5. Ballegaard, M., Hunding, A., and Rubin, I. 1995. *Journal of Immunoassay* 16(2): 123-136.
6. Kim, B.B., Dikova, E.B., Sheller, U., Dikov, M.M., Gavriola, E.M., and Egorov, A.M. 1990. *J. Immunol. Methods* 131: 213-222.
7. Fuchs, H., Orberger, G., Tauber, R., and Geesner, R. 1995. *J. Immunol. Methods* 188: 197-208.
8. Seligamn, S.J. 1994. *J. Immunol. Methods* 168: 101-110.
9. Stevens, F.J. 1987. *Mol. Immunol.* 24(10): 1055-1060.
10. Nieto, A., Gaya, A., Jansa, M., Moreno, C., and Vives, J. 1984. *Mol. Immunol.* 21(6): 537-543.
11. Schots, A., Van der Leede, B., De Jongh, E., and Egberts, E. 1988. *J. Immunol. Methods* 109: 225-253.
12. Goldberg, M.E. and Djavidi-Ohanian, L. 1993. *Current. Opin. Immunol.* 5: 278-281.
13. Ferreira, M.U. and Karzin, A.M. 1995. *J. Immunol. Methods* 187: 297-305.
14. Rath, S., Stanley, C.M., and Steward, M.W. 1988. *J. Immunol. Methods* 106: 245-249.
15. Luxton, R.W. and Thompson, E.J. 1990. *J. Immunol. Methods* 131: 277-282.
16. Inouye, S., Hasegawa, A., Matsuno, S., and Katow, S. 1984. *J. Clin. Microbiol* 20(3): 525-529.
17. Pullen, G.R., Fitzgerald, M.G., and Hosking, C.S. 1986. *J. Immunol. Methods* 86: 83-87.
18. Goldblatt, D., van Etten, L., van Milligen, F.J., Aalberse, R.C., and Turner, M.W. 1993. *J. Immunol. Methods* 166: 281-285.
19. Hedman, K., Lappalainen, M., Seppaia, I., and Makela, O. 1989. *The Journal of Infectious Diseases* 159(4): 736-740.

20. Liu, R.H. 1995. Handbook of Workplace Drug Testing. R.H. Liu and B.A. Goldberger, Eds., AACC Press, Washington, DC.
21. Roche Diagnostic Systems, Somerville, NJ, 1993. Abuscreen Radioimmunoassay for LSD *package insert*.
22. McNally, A.J., Goc-Szkutnicka, K., Li, Z., Pilcher, I., Polakowski, S., and Salamone, S.J. 1996. *J. Anal. Toxicol.* 20: 404-408.
23. Boehringer Mannheim Corp. 1996. CEDIA DAU LSD Assay, *product brochure*.
24. Patai, S. 1971. The Chemistry of the Azido Group, Interscience, New York.
25. Glennon, R.A. 1994. Hallucinogens: An Update. G.C. Lin and R.A. Glennon, Eds., pp. 4-73. National Institute on Drug Abuse, Rockville, MD.
26. Sankar, D.V.S. 1975. LSD - A Total Study, PJD Publications, Westbury, NY.
27. Goc-Szkutnicka, K., Bates, M.G., Honasoge, S., McNally, A.J., and Salamone, S.J. 1996. Society of Forensic Toxicologists Annual Meeting, Denver, CO (Abstract).
28. Roche Diagnostic Systems, Somerville, NJ 1996. Abuscreen OnLine for LSD, *specification sheet*.
29. Lim, H.K., Andrenyak, D., Francom, P., and Foltz, R.L. 1988. *Anal. Chem.* 60: 1420-1425.
30. Department of Health and Human Services 1986. Urine Testing for Drugs of Abuse. NIDA Research Monograph Series 73, National Institute on Drug Abuse, Rockville, MD.
31. Lopatin, D.E. and Voss, E.D. 1974. *Immunochemistry* 11: 285-293.
32. Huang, X., Marona-Lewicka, D., Pfaff, R.C., and Nichols, D.E. 1994. *Pharm. Biochem. Behaviour* 47(3): 667-673.
33. Berde, B. and Schild, H.O. 1978. Ergot Alkaloids and Related Compounds, Springer-Verlag, New York.
34. Underwood, P.A. 1993. *J. Immunol. Methods* 164: 119-130.
35. Levison, S.A., Hicks, A.N., Portmann, A.J., and Dandliker, W.B. 1975. *Biochem.* 14(17): 3778-3786.
36. Macdonald, R.A., Hosking, C.S., and Jones, C.L. 1988. *J. Immunol. Methods* 106: 191-194.

37. Hall, T. and Heckel, C. 1988. *J. Immunol. Methods* 115: 153-154.
38. Niwaguchi, T., Inoue, T., and Nakahara, Y. 1974. *Biochemical Pharmacology* 23: 1073-1078.
39. Nygren, H., Czerkinsky, C., and Stenberg, M. 1985. *J. Immunol. Methods* 85: 87-95.
40. Werblin, T.P. and Siskind, G.W. 1972. *Immunochemistry* 9: 987-1011.
41. Nimmo, G.R., Lew, A.M., Stanley, C.M., and Steward, M.W. 1984. *J. Immunol. Methods* 72: 177-187.
42. Portmann, A.J., Levison, S.A., and Dandliker, W.B. 1975. *Immunochemistry* 12: 461-466.
43. Kranz, D.M., Herron, J.N., and Voss, E.W. 1982. *J. Biol. Chem.* 257(12): 6987-6995.
44. Parker, C.W., Yoo, T.J., and Godt, S.M. 1967. *Biochemistry* 6(11): 3408-3416.
45. Downie, N.M. and Heath, R.W. 1965. *Basic Statistical Methods*. H.H. Remmers, Ed., Harper-Row, New York.
46. Adamczyk, M., Fishpaugh, J., Harrington, C., Hartter, D., Johnson, D., and Vanderbilt, A. 1993. *J. Immunol. Methods* 162: 47-58.
47. Adamczyk, M., Grote, J., Douglas, J., Dubler, R., and Harrington, C. 1997. *Bioconjugate Chem.* 8: 281-288.

## Chapter 6.

### **Analysis of Forensic Case Samples and Immunoaffinity Extraction of LSD from Blood and Urine.**

#### **6.1. Introduction.**

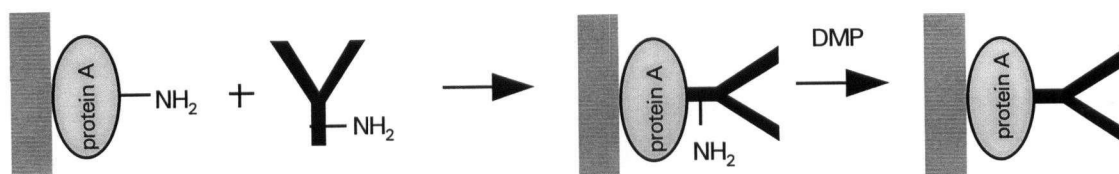
Commercial immunoassays for LSD which are designed for use with urine specimens are frequently used for non-urine matrices in forensic settings (1-5). There has been considerable interest in the detection of drugs of abuse from whole blood by immunoassay (6), particularly in the case of LSD (7,8). Some of the problems encountered are increased matrix effect, decreased precision and an overall decrease in sensitivity. The ELISA described in Chapter 4, which can be used to detect picogram quantities of LSD in urine, was used to detect LSD in whole blood specimens. The sensitivity and precision of the ELISA was compared for blood and urine analysis. Additionally, a number of forensic case samples were made available by the RCMP Forensic Laboratory in Vancouver, which included post-mortem samples of blood, urine, bile, liver and vitreous fluid. Quantitative estimates of LSD in these specimens were performed by ELISA.

The high affinity antibody, which is used for the detection of LSD by ELISA, can also be used to facilitate the extraction of drug from a biological matrix. Immunoaffinity extraction (IAE) of LSD can be performed by immobilizing antibody to the drug on a solid support. When a sample which contains LSD comes in contact with the support, the drug becomes immobilized on the surface. In this way, specific adsorption and subsequent release of drug using an eluent, provides a means of selectively extracting LSD and cross-reacting substances from a complex mixture, such

as a biological fluid.

Antibody immobilization techniques often result in some loss of antigen binding capacity due to the coupling process. Protein A, which has a high affinity for the Fc region of IgG, can be used to orient the immunoglobulin with its antigen binding sites directed away from the support. Covalent crosslinking of the oriented IgG molecule to Protein A-coated agarose creates a relatively stable immunoaffinity support, with antigen binding sites free to interact with the antigen. Dimethyl pimelimidate (DMP) is a homobifunctional crosslinker which contains two imidoester groups. These react rapidly with primary amines at alkaline pH to give amidine bonds. DMP is used extensively for protein-protein crosslinking and is used in this case to covalently attach Protein A-coated agarose to rabbit immunoglobulins raised against LSD (Figure 6.1).

**Figure 6.1.** Preparation of the immunoaffinity support. Covalent attachment of rabbit immunoglobulins raised against LSD to Protein A-coated agarose beads.

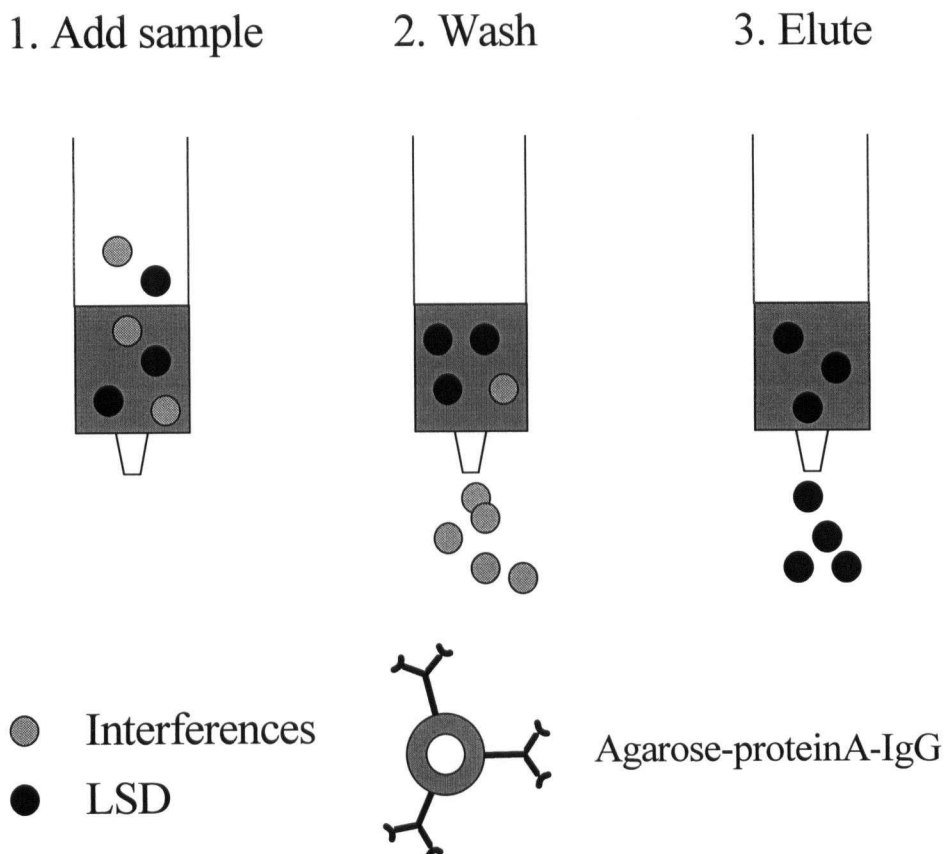


Immunoaffinity extraction is an alternative to liquid-liquid and solid phase extraction techniques which are currently used for small molecules of interest, such as LSD. Liquid-liquid extraction procedures are labour intensive and can result in sample loss during extraction, evaporation and reconstitution steps. Solid phase extraction (SPE) offers some improvement in terms of analyst time, but both methods can result in coextractive interferences which make drug detection difficult (1,4). In theory, immunoaffinity extraction should result in a much cleaner extract, which contains only the drug and closely related substances. The specificity of the extract

is largely determined by the cross-reactivity of the antibody which is immobilized on the support. This was demonstrated by a direct comparison of LSD extraction from urine using both immunoaffinity extraction and SPE techniques which were analysed using HPLC-FL (9). The improved specificity of the immunoaffinity extract can improve detection limits, which are compromised by the presence of coextractives and other interferences. In one report, immunoaffinity extraction coupled with LC-MS-MS analysis for the detection of LSD in urine, resulted in a 20-fold improvement in detection limit (10). IAE can also be used for trace enrichment of samples, which contain concentrations of drug that would not be detectable otherwise; by passing a large volume of sample through the column, it is possible to selectively enrich the LSD content of the extract. Using this technique, IAE-LC-MS-MS was used to detect LSD at 2.5 pg/mL from 100 mL sample (10).

The immunoaffinity extraction of LSD from a biological matrix such as urine is a 3 step process (Figure 6.2). First, sample is added to the column which contains immobilized anti-drug antibodies. Interferences are removed from the sample by thorough washing, after which the only species which remain bound are LSD and cross-reacting substances. Finally, an eluent is used to break the antibody-antigen bonds which are responsible for binding the drug to the column. The major disadvantage of this method is the cost of immunological reagents and the limited capacity of the affinity matrix, which is determined by the number of active antibody binding sites. Previous reports have indicated that the recovery of LSD by IAE was less quantitative than SPE. When LSD was spiked in urine between 0.3 and 5 ng/mL, the analytical recovery of drug was 86 - 100% using SPE, compared with 64 - 167% using IAE (11). There have been other reports of poor recoveries of LSD and other drugs from urine by immunoaffinity extraction, which is generally attributed to matrix interferences in the sample (12).

**Figure 6.2.** Immunoaffinity extraction of LSD. Sample containing LSD is added to the column in a liquid matrix. The column is washed to remove unwanted non-LSD interferences after which selectively bound drug is eluted.



The aim of this work was to show that the high affinity ( $1.3 \times 10^{10} \text{ M}^{-1}$ ) antibody to LSD could be used for extraction purposes. In theory, a high affinity interaction between the immobilized antibody and the LSD which is passed through the column should result in improved capture of the drug. Provided that the drug bound to the affinity matrix can be removed quantitatively, the use of a high affinity antibody should result in improved analytical recovery. Using LSD spiked in blood and urine, the feasibility of immunoaffinity extraction using the new LSD antibody is investigated.

## 6.2. Materials and methods.

Bovine blood and forensic specimens were kindly supplied by Wayne Jeffery (Head, Toxicology Section, RCMP Forensic Laboratory, Vancouver). Dimethyl pimelimidate (DMP) and Protein A agarose were purchased from Pierce (Rockford, IL) and ethanolamine, triethanolamine and triethylamine were from Sigma (St. Lois, MO). Inorganic salts (ACS grade), glycine (tissue culture grade), sodium dodecyl sulfate (SDS) and ammonium thiocyanate were obtained from Fisher Scientific (Edmonton, AB) as were the organic solvents methanol, ethanol, ethylene glycol and dioxane (HPLC grade). LSD tritiated in the *N*-methyl position ( $[^3\text{H}_3]$ -LSD, 0.25 mCi) and Atomlight scintillation fluid were purchased from DuPont NEN (Mississauga, ON). LSD and reagents used for ELISA are given in Chapter 4.

### 6.2.1. Detection of LSD in whole blood.

Bovine blood was used to assess the feasibility of whole blood analysis of LSD by enzyme linked immunosorbent assay. The ELISA described in Appendix II, originally intended for the detection of drug in urine was used for this study.

#### 6.2.1.1. Effect of blood on ELISA signal.

Bovine blood diluted in 150 mM phosphate buffered saline, pH 7.4 (PBS) was used in place of urine in the ELISA described in Appendix II. The total sample volume was made up to 50  $\mu\text{L}$  with PBS which was added to microtitre wells along with 50  $\mu\text{L}$  of diluted antibody reagent in 10% SM-PBS. Volumes of whole blood, between 8 and 50  $\mu\text{L}$  were used, which represent total matrix dilutions of 2 to 12-fold. The effect of dilution on absolute signal and precision was

measured using duplicate samples.

#### **6.2.1.2. Effect of blood dilution on sensitivity and precision.**

Whole blood was spiked with LSD at a relatively high concentration to assess the difference in signal between a positive and negative sample at different sample dilutions. Six negative (0 ng/mL) and six positive (5 ng/mL) blood samples were measured by ELISA using sample volumes of 25 and 12.5  $\mu\text{L}$ . In another assay, LSD calibrators prepared in blood and urine (5 - 0.04 ng/mL) were run in the ELISA described in Appendix II. Sample volumes were 50  $\mu\text{L}$  for urine and 25 or 12.5  $\mu\text{L}$  for blood. Normal rabbit serum was used to estimate the degree of non-specific signal using different matrices.

#### **6.2.1.3. Calibration of LSD in blood.**

Bovine blood was spiked with LSD between 5 and 0.04 ng/mL. Calibration data was obtained using 25  $\mu\text{L}$  blood and 25  $\mu\text{L}$  PBS in place of the 50  $\mu\text{L}$  urine used in the ELISA described in Appendix II. Replicate measurements of LSD calibrators (n=4) and the blank (n=12) were run in the same assay. The limit of detection was estimated from the mean response of the zero calibrator minus 3 standard deviations.

### **6.2.2. Analysis of forensic case samples.**

#### **6.2.2.1. Sample preparation and storage.**

Biological tissues and fluids from a homicide case, in which LSD use was suspected, were kindly supplied by Wayne Jeffery (Head, Toxicology Section, RCMP Forensic Laboratory,

Vancouver). Samples of urine, blood, bile, vitreous fluid and liver (as a 50% homogenate) from the victim and a blood sample from the accused were made available for analysis. Samples from the victim were obtained post-mortem and all specimens were stored for approximately 4 months at 4 °C prior to analysis.

Post-mortem urine was used directly in the ELISA described in Appendix II. However, post-mortem blood, bile, liver and vitreous fluid were pre-treated to minimize matrix interferences which might occur with post-mortem specimens. In the interest of treating all non-urine specimens equally, accused blood was also pre-treated. In forensic settings, methanolic extracts of blood and other complex biological matrices are frequently used for immunoassay drug screening (1,6). Based on this information, LSD in specimens of blood, bile, liver and vitreous fluid was extracted with methanol prior to ELISA.

#### **6.2.2.2. Analysis of post-mortem urine.**

LSD in normal human urine (5 - 0.04 ng/mL) was used in the ELISA described in Appendix II. Replicate measurements of each calibration standard (n=8) and the blank (n=14) were made. A sample of post-mortem urine (50  $\mu$ L) obtained from the victim was run in triplicate.

#### **6.2.2.3. Analysis of blood, bile, liver and vitreous fluid.**

Methanolic extracts were used to determine whether samples of liver, bile, blood or vitreous fluid contained LSD or cross-reacting substances. In an eppendorf tube, 50  $\mu$ L of methanol was vortex mixed with 25  $\mu$ L of specimen for 1 minute. After centrifugation for 2

minutes at 6500 rpm, the clear supernatant fraction was removed and evaporated. Dried extracts were redissolved in 54  $\mu\text{L}$  PBS of which 50  $\mu\text{L}$  was removed and used for the immunoassay. Bovine blood which was spiked with LSD (0.25 ng/mL) was treated in the same way, in order to estimate the recovery of drug from blood using the methanolic extraction procedure. A similar sample of bovine blood which did not contain LSD was also run in the assay to measure any interferences. All extracts were analysed in duplicate and LSD calibrators (5 - 0.04 ng/mL) in PBS (n=6) were used to construct a calibration curve, from which concentrations of LSD in forensic case samples were interpolated.

### **6.2.3. Immunoaffinity extraction of LSD from biological matrices.**

#### **6.2.3.1. Preparation of the affinity matrix.**

Rabbit anti-LSD was covalently attached to Protein A-agarose beads using dimethyl pimelimidate (DMP) as outlined previously (13). Immobilized Protein A (5 mL) was washed with deionized water followed by antibody binding buffer (50 mM sodium borate, pH 8.2). Gentle centrifugation was used to drain the gel to a wet cake. Neat serum (6 mL) from rabbits immunized with KLH-SASD-LSD was mixed with antibody binding buffer (5 mL). This solution, which contained about 60 mg rabbit IgG was added to the gel and allowed to equilibrate with gentle rocking for 30 minutes. Beads were then washed sequentially with 25 mL antibody binding buffer followed by 5 mL crosslinking buffer (0.2 M triethanolamine, pH 8.2) and drained to a wet cake. DMP (33 mg) dissolved in 5 mL crosslinking buffer was added immediately to the gel. The reaction was allowed to proceed for 1 hour with gentle rocking after which the beads were washed with 25 mL deionized water and drained to a wet cake. The remaining sites on the beads were

blocked with 5 mL 0.1 M ethanolamine, pH 8.2 for 10 minutes with gentle rocking. Beads were then washed sequentially with deionized water, 1 M sodium chloride, 0.1 M glycine (pH 2.8) and deionized water again. Finally, immobilized antibody was made up in PBS which contained 0.02% sodium azide as preservative. Beads were stored as a 50% slurry and kept at 4 °C until further use.

#### **6.2.3.2. Characterization of the affinity matrix.**

The concentration of drug specific antibody was calculated indirectly from the binding capacity of affinity matrix towards [<sup>3</sup>H<sub>3</sub>]-LSD. Affinity matrix (1 mL) was packed into a 3 mL polypropylene syringe which was stoppered with glass wool. PBS was used to rinse the column thoroughly, after which 0.5 mL aliquots of [<sup>3</sup>H<sub>3</sub>]-LSD (71.5 Ci/mmol) in PBS was sequentially added, each of which contained approximately 0.25 ng of labelled drug. The amount of tritiated LSD which passed through the column unretained was measured using a Phillips PW 4700 liquid scintillation counter (Phillips, The Netherlands). The column reached its maximum binding capacity when the number of radioactive counts which passed through the column was equal to the number of counts originally added. When all antigen binding sites on the affinity matrix were saturated, the column was washed with PBS (8 mL) after which [<sup>3</sup>H<sub>3</sub>]-LSD was eluted. More than a dozen eluents were investigated for the removal of drug from the affinity matrix. These included high and low pH, high salt, ionic detergents, chaotropic agents and organic solvents.

#### **6.2.3.3. Immunoaffinity extraction of LSD.**

The affinity matrix described in Section 6.2.3.1. was used to extract LSD from PBS buffer, urine and blood samples at concentrations which might be encountered in forensic case samples

(approximately 0.25 and 0.5 ng/mL). [ $^3\text{H}_3$ ]-LSD was used to determine the recovery of drug in different matrices. The basic procedure for all specimens was as follows. The column containing affinity matrix (1 mL) was washed with 6 - 8 mL PBS prior to use. Samples containing LSD, in a total volume of 1.0 mL, were added to the column and allowed to flow through under gravity into the fraction collector below. Non-drug components in the matrix and other interferences were rinsed from the column using 6 - 8 mL PBS, after which the LSD which remained bound was eluted with 6 - 8 mL 100 mM triethylamine in deionized water. Urine samples (1.0 mL) were spiked with concentrated neutral buffer at various ionic strengths and blood (0.1 mL) was diluted to 1 mL with buffer to reduce the sample viscosity prior to extraction.

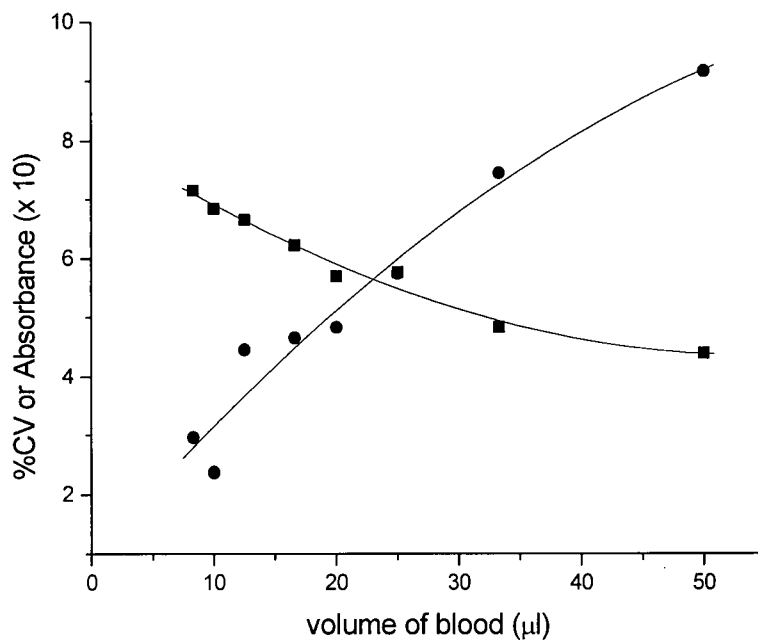
## 6.3. Results and discussion.

### 6.3.1. Detection of LSD in whole blood.

#### 6.3.1.1. Effect of blood on ELISA signal.

Decreasing the volume of blood used in the ELISA results in increased absorbance and precision (Figure 6.3). Ideal conditions, of optimum signal and precision of the blank, are achieved using small sample volumes ( $\sim 10 \mu\text{L}$ ), where matrix interferences are diluted out. However, excessive dilution of the sample will result in decreased overall sensitivity. The absorbance increased from 0.44 to 0.70 and the CV decreased from 6 to 2% when the volume of blood was decreased from 50 to 8  $\mu\text{L}$ . Complex matrices, such as blood or serum are often diluted to about 20% to reduce non-specific interferences in immunoassays. However, a dilution factor of more than 4 or 5 is undesirable in terms of sensitivity, as LSD is often present at very low concentrations to begin with.

**Figure 6.3.** Effect of whole blood on ELISA. Mean absorbance reading (x10) (squares) and % CV (circles) of duplicate measurements.



#### 6.3.1.2. Sample volume.

Decreasing the volume of blood used in the test decreases overall sensitivity, as expected. Maximum sensitivity is achieved when the difference between a positive and a negative sample is at a maximum. Table 6.1 shows that at 5 ng/mL LSD, twice as much antibody is bound using 12.5 µL compared with 25 µL blood.

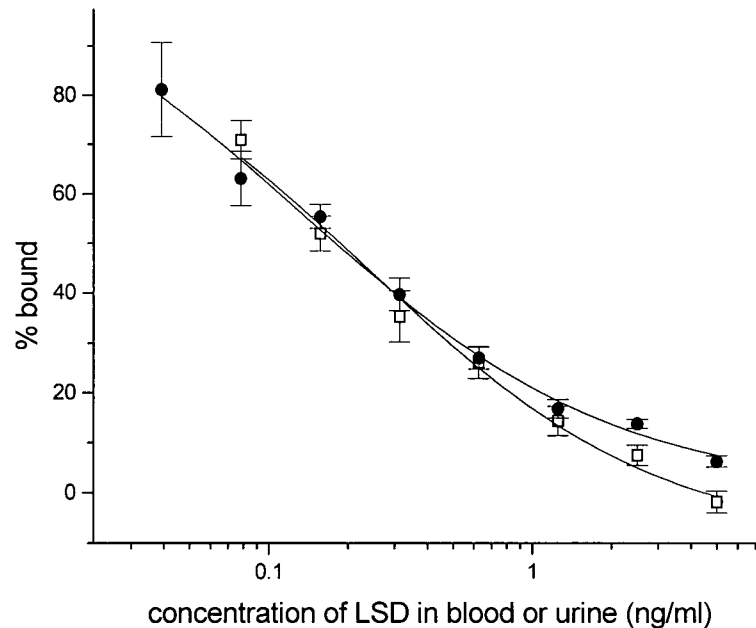
**Table 6.1.** Measurement of positive and negative blood specimens by ELISA. Decreasing the sample volume results in increased precision but decreased sensitivity. The non-specific signal remains unchanged.

	whole blood volume ( $\mu\text{L}$ )	
	25	12.5
% bound, negative blood (0 ng/mL)	100.0	100.0
% bound, positive blood (5 ng/mL)	$13.3 \pm 3.3$	$27.5 \pm 2.2$
Approximate EC50 (ng/mL)	0.25	0.6
CV <sub>blank</sub> (n=6)	5.7	1.9
Non-specific signal (OD)	0.02	0.02

Increased dilution of the blood matrix decreased the overall sensitivity by causing a displacement in the calibration curve towards higher concentration. When LSD calibration curves were generated using either 25 or 12.5  $\mu\text{L}$  blood, the concentration of LSD which results in 50% antibody binding (EC50) more than doubled. However, the increase in sensitivity is accompanied by an increase in the CV of the blank (n=6) from 1.9% (12.5  $\mu\text{L}$ ) to 5.7% (25  $\mu\text{L}$ ). The non-specific signal decreased four-fold when blood was used in place of urine. This was attributed to the presence of plasma proteins in the sample, which might behave as blocking agents during the 2.5 hour antibody-antigen incubation. Comparison of dose-response curves obtained using 25  $\mu\text{L}$  blood instead of 50  $\mu\text{L}$  urine were comparable. Calibrations performed in blood and urine on consecutive days are shown in Figure 6.4. Clearly, the error bars ( $\pm 1$  SD) of individual calibrators are larger in blood than in urine, particularly at low LSD concentrations. The CV of the zero calibrator in blood (n=6) and urine (n=6) was 5.5 and 4.5% respectively. Moreover, there was no decrease in signal of the zero calibrator when blood was used in place of urine. The absorbance of 25  $\mu\text{L}$  of drug-free blood was within one standard deviation of that obtained using

50  $\mu\text{L}$  of drug-free urine.

**Figure 6.4.** Comparison of calibration curves obtained using 25  $\mu\text{L}$  whole blood and 50  $\mu\text{L}$  urine. Data represents the mean response  $\pm$  1SD (n=4) of LSD calibrators in urine (open squares) and blood (closed circles).



### 6.3.1.3. Calibration of LSD in whole blood.

Whole blood specimens (25  $\mu\text{L}$ ) spiked with LSD were used to construct the calibration curve shown in Figure 6.5. The limit of detection was 39 pg/mL based on the mean response of the zero calibrator - 3 SD (n=12). When the same assay was used to detect LSD in urine (50  $\mu\text{L}$ ), the limit of detection was 10 pg/mL (Chapter 4). This decrease in sensitivity is the result of decreased sample volume and precision when blood is used instead of urine. Table 6.2 shows individual precision estimates for blood spiked with LSD between 5 and 0.04 ng/mL. The coefficient of variation for 1.25, 0.31 and 0.08 ng/mL LSD in blood was 5.6, 5.5 and 10.7%

respectively (n=4). This preliminary data suggests that whole blood samples can be run in the assay, with some decrease in sensitivity and precision compared to the analysis of urine.

**Figure 6.5.** Calibration of LSD in blood by ELISA. Whole blood (25  $\mu\text{L}$ ) was spiked with LSD between 5 - 0.04 ng/mL. Data represents the mean response (n=4) relative to the blank (n=12) and dotted lines show the 95% confidence limits. The limit of detection, based on the mean - 3 SD was 39 pg/mL LSD in blood.

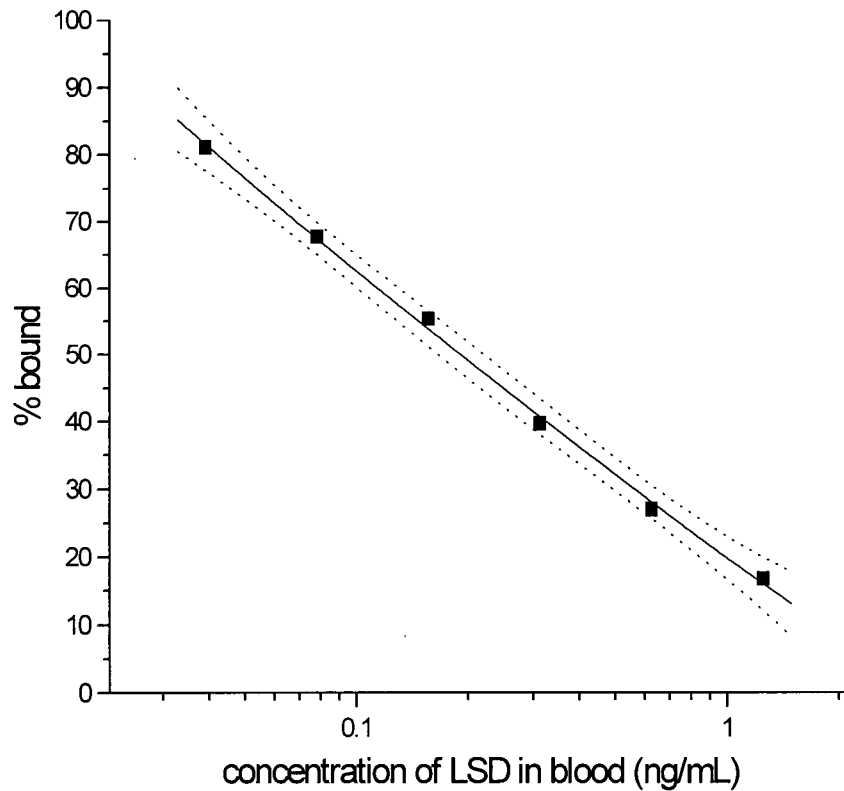


**Table 6.2.** Precision of LSD spiked in whole blood, run in the same assay (n=4).

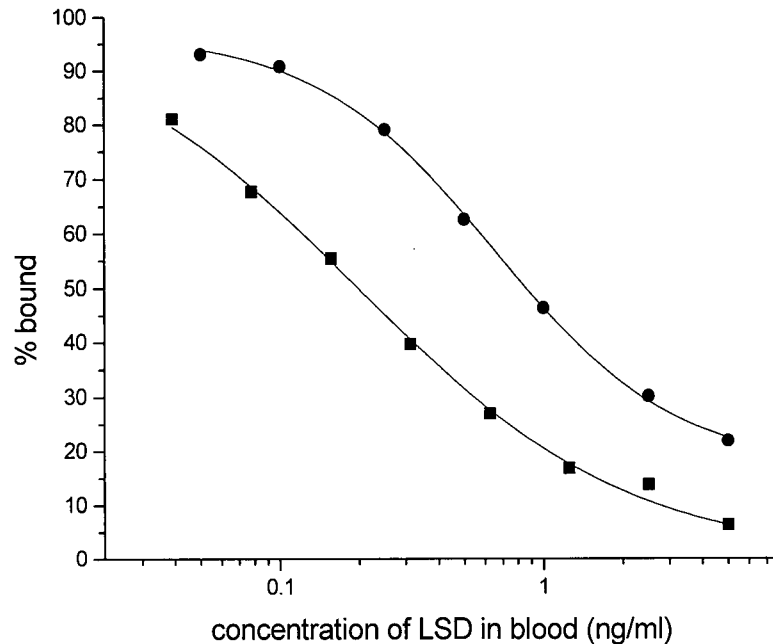
concentration of LSD in blood (ng/mL)	CV (n=4)
5.00	5.4
2.50	2.9
1.25	5.6
0.63	5.0
0.31	5.5
0.16	3.1
0.08	10.7
0.04	8.9

Comparison of whole blood LSD analysis by ELISA with the commercial STC assay indicates that the UBC assay is more sensitive. Table 6.3 compares calibration data reported in the literature (8) with the UBC assay, in which 25  $\mu\text{L}$  whole blood was used in each test. Graphical representation of this data in Figure 6.6. clearly indicates the increased sensitivity of the UBC ELISA, by the displacement of the calibration curve towards lower concentrations of LSD; the 50% binding concentrations (EC50) for UBC and STC calibration curves using blood were approximately 0.2 and 1.0 ng/mL respectively. This is consistent with the lower limit of detection for LSD in blood and urine using the UBC ELISA.

**Table 6.3.** Calibration data using UBC and STC immunoassays for the detection of LSD in 25  $\mu\text{L}$  whole blood.

UBC ELISA		STC ELISA (8)	
LSD (ng/mL)	% bound	LSD (ng/mL)	% bound
5.0	16.3	5.0	21.9
2.5	23.0	2.5	30.2
1.25	25.7	1.0	46.4
0.625	34.8	0.5	62.6
0.313	46.1	0.25	79.1
0.156	60.1	0.1	90.8
0.078	71.2	0.05	93.1

**Figure 6.6.** Calibration of LSD in blood (25  $\mu\text{L}$ ) using commercial and in-house immunoassays. Approximate 50% binding concentrations for UBC (squares) and STC (circles) calibrations are 0.2 and 1.0 ng/mL respectively.



### **6.3.2. Forensic case samples.**

#### **6.3.2.1. Quantification of LSD in post-mortem urine.**

LSD calibrators (5 - 0.04 ng/mL) in urine were used to estimate the concentration of LSD or cross-reacting species in the victim's urine. The mean absorbance and standard deviation of the zero calibrator was  $0.671 \pm 0.036$  (n=14) compared to  $0.681 \pm 0.026$  (n=3) for the post-mortem sample. ELISA results indicated that the victim urine, which was within one standard deviation of the zero calibrator, did not contain LSD or any cross-reacting metabolites.

#### **6.3.2.2. Quantification of LSD in blood, bile, liver and vitreous fluid.**

Quantitative estimates of LSD and cross-reacting species by ELISA was done using methanolic extracts of biological fluids and tissues. Results listed in Table 6.4 show the response (% bound) of each sample and the concentration of LSD in each sample calculated from the calibration curve (Figure 6.7). The cut-off concentration used to distinguish positive from negative samples was 0.05 ng/mL. The concentration of LSD in the sample was calculated from the interpolated concentration based on the volume of extract used in the assay (50 of 54  $\mu$ L) and the total sample volume (25  $\mu$ L). In the case of blood samples, a recovery factor of 56.1% was used to estimate the concentration of LSD in the blood sample obtained from the victim. This takes in to account that only 56.1% of the LSD spiked into bovine blood (0.25 ng/mL) was recovered during methanolic extraction.

The extraction efficiency in other matrices was not known. As such, reported concentrations for bile and liver samples assume 100% recovery of drug, which are therefore underestimates of the actual concentration in the specimen. It should be noted that the absorbance

using a methanolic bovine blood extract which contained no LSD, was within 1 SD of the zero calibrator, which was run in buffer. This suggests that there was no measurable matrix effect when a methanolic blood extract was used. However, the possibility of matrix interferences using bile and liver extracts is not known, as drug free specimens were not available at the time of analysis.

**Table 6.4.** Quantification of LSD and cross-reacting substances in forensic case samples. The methanolic blood extract (0 ng/mL) was within 1 SD of the blank, which was run in buffer. Interpolated concentrations less than 0.05 ng/mL were considered negative. Specimens of blood, bile and liver from the victim were analyzed in duplicate, on consecutive days.

Sample	% bound	interpolated concentration (ng/mL)	concentration in sample (ng/mL)
buffer	100.0	0.000	negative
blood (0 ng/mL)	102.2	0.000	negative
blood (0.25 ng/mL)	66.9	0.065	0.14 <sup>1</sup>
victim blood	69.4	0.062	0.24, 0.23 <sup>2</sup>
accused blood	93.5	0.000	negative
victim liver	54.9	0.092	0.42, 0.44 <sup>3</sup>
victim bile	9.23	0.924	2.05, 1.98
victim vitreous fluid	84.0	0.000	negative

<sup>1</sup> Total recovery of LSD from bovine blood was 56.1%.

<sup>2</sup> Assuming 56.1% recovery of LSD from the victim's blood sample.

<sup>3</sup> Based on the concentration of LSD in a 50% liver homogenate.

**Figure 6.7.** LSD calibration used for the quantification of LSD in blood, bile, liver and vitreous fluid. Data represents the mean response of LSD calibrators run in buffer ( $n=6$ )  $\pm$  1SD.

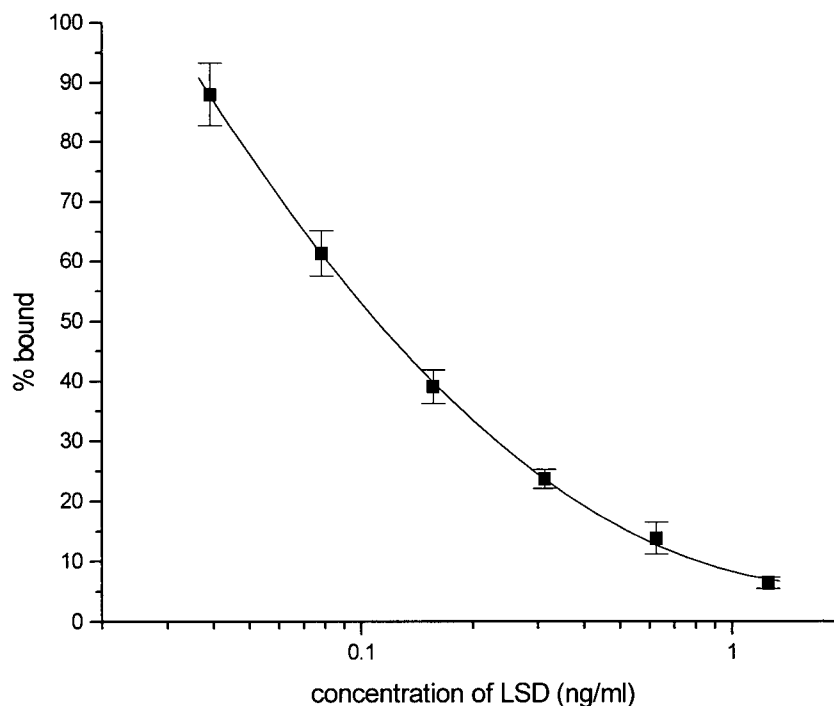


Table 6.5 summarizes the quantitative estimates of LSD and cross-reacting species in forensic case samples. Although the accused urine sample appears negative, the concentration of drug in the victim's blood, bile and liver, indicate recent drug use. Surprisingly, no LSD was detected in the victim's urine, despite detectable amounts of drug in both the bile (2 ng/mL) and liver (0.4 ng/mL), which might suggest that the time of death was soon after ingestion of the drug. Alternatively, the same result could be caused by dilution of LSD in the victim's urine by high intake of liquids or heavy drinking. Although the absence of LSD in the urine sample is unusual, other cases have been reported in which the urine is negative by immunoassay whilst blood and other specimens give positive results (14). Blood and urine samples were tested at the Central

Forensic Laboratory in Ottawa. No LSD was detected in the blood of the accused or the victim's urine.

**Table 6.5.** Summary of quantitative estimates of LSD and cross-reacting species in forensic case samples.

Sample	ELISA pre-treatment	Concentration of LSD $\pm$ 95% CL (ng/mL)
accused blood	methanolic extract	negative <sup>1</sup>
victim blood	methanolic extract	$0.24 \pm 0.06$ <sup>2</sup>
victim liver	methanolic extract of 50% homogenate	$0.43 \pm 0.13$
victim bile	methanolic extract	$2.02 \pm 0.45$
victim vitreous	methanolic extract	negative
victim urine	none	negative <sup>3</sup>

<sup>1</sup> negative by RIA

<sup>2</sup> 0.2 ng/mL by RIA

<sup>3</sup> negative by RIA

The victim's blood however, contained 0.2 ng/mL LSD by RIA, which could not be confirmed by GC-MS (Personal communication, Wayne Jeffery). This was in good agreement with results obtained using the UBC ELISA, which indicated 0.24 ng/mL LSD in the victim's blood. Unfortunately, no stomach contents were available. These typically contain much higher concentrations of LSD than other tissues or fluids. In one fatal poisoning by LSD, the concentrations of LSD in post-mortem blood, liver blood and stomach contents were 4.8, 7.2 and

55.2 ng/mL respectively by RIA (1).

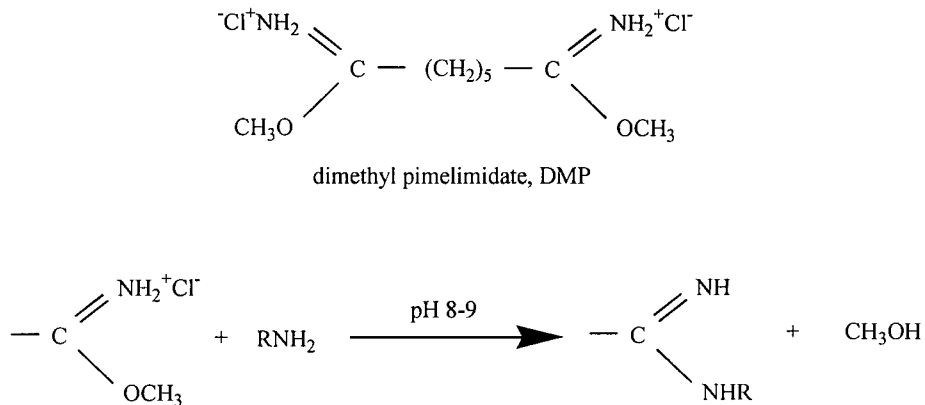
It is known that the concentration of drug and cross-reacting substances are present at high concentrations in the bile. LSD is reported to undergo almost complete metabolic change in the liver, which results in less than 1% of the parent drug excreted in the urine (15). Animal studies in which LSD was administered intravenously, revealed that the highest concentration of LSD was contained in the bile, followed by the plasma and liver, 90 minutes after administration (15). [<sup>14</sup>C]-LSD administered to rats, showed that 68% of the radiolabel was found in the bile after 5 hours, mostly as glucuronides of 13 and 14-hydroxy-LSD (16). Biliary excretion has been confirmed by other workers who have identified 2-oxo-LSD, lysergic acid monoethylamide, nor-LSD and the glucuronides of 13 and 14-hydroxy-LSD as metabolites in rats (17). Approximately 20% of the total radioactivity was found in the liver and 44% in the bile, primarily as glucuronides of hydroxylated LSD, with small amounts of 2-oxo-LSD (7%) and parent drug (1%) (17).

It is quite likely that LSD metabolites contribute to the quantitative estimate of LSD in the post-mortem bile sample. It has been established that the antibody cross-reacts with nor-LSD (52%) and 2-oxo-3-hydroxy-LSD (3.4%), the former of which is a confirmed metabolite in human urine (18). However, the specificity of the antibody towards 13 and 14-hydroxy-LSD is not known, due to the unavailability of these derivatives. Hypothetically, no cross-reactivity would be predicted between antibody and hydroxylated drug, particularly once it is conjugated to glucuronic acid. This is based on the structural argument that cross-reactivity occurs primarily at positions involved in, or nearby the site of attachment between the hapten and carrier protein in the immunogen. Previous results have indicated that conjugation of KLH likely occurs at positions 1, 2 and 6 of LSD (Chapter 6) rather than positions 13 or 14.

### 6.3.3. Immunoaffinity extraction of LSD.

#### 6.3.3.1. Characterization of the affinity matrix.

Rabbit IgG molecules were covalently attached to Protein A-agarose using dimethyl pimelimidate. Imidoester groups on the crosslinker react with amines on both proteins to form amidine bonds as shown below:



The concentration of specific drug antibody was estimated indirectly from column capacity measurements using [<sup>3</sup>H<sub>3</sub>]-LSD. After the addition of 2.35 ng of tritiated drug, the number of counts which pass through the column unretained, was equal to the total number of counts which were added. When 100 mM triethylamine was used to elute LSD from the column, 2.32 ng LSD was recovered (99%). An average of 2.33 ± 0.26 ng [<sup>3</sup>H<sub>3</sub>]-LSD was bound based on the uncertainty in measuring the column volume (± 100 μL) which was greater than the uncertainty of radioactive counting (±0.4%). Therefore, the total number of active antibody binding sites on 1 mL affinity matrix was 7.09 × 10<sup>-9</sup> M. If both Fab regions of the immunoglobulin molecule are still active, the concentration of IgG which is specific to LSD is about 3.55 × 10<sup>-9</sup> M (or 0.55 μg/mL). The low concentration of drug specific IgG relative to the total IgG bound is not surprising for three reasons.

Firstly, it has already been established that the antibody to LSD is present in a low titre antiserum (Chapter 3). Secondly, some of the antibody may have been denatured during coupling, or may be unavailable due to steric reasons. Finally, covalent coupling was performed using whole serum and not a purified antibody preparation. However, 1 mL of affinity matrix can still bind approximately 2.3 ng LSD, which is sufficient for the extraction of drug from small volumes of biological specimens.

A number of eluents were investigated for the removal of LSD from the affinity matrix. Disruption of antibody-antigen binding using low pH, high pH, high salt, detergents, chaotropic agents and organic solvents was performed according to the list below:

100 mM glycine, pH 2.7	100 mM triethylamine
1.5 M NaCl	50 - 100% ethanol
KCl (50 mM) - HCl pH 1.9	1% SDS
10 - 20 % dioxane	4M NH <sub>4</sub> SCN
50/50 (v/v) ethylene glycol, pH 8	100 mM triethylamine in 10% dioxane

Triethylamine (100 mM) in deionized water (pH 11.6) was the best aqueous eluent. Ideally the composition of the eluent should facilitate the sample preparation requirements of the detection technique. For example, an organic eluent may be preferable for subsequent analysis by GC-MS or other chromatographic method. The use of a volatile organic solvent, such as ethanol, for the elution of radiolabelled drug, was not routinely used for safety reasons. Our goal was merely to show that the high affinity LSD antibody could be used as an extractive tool, as well as for the detection of drug by enzyme-linked immunosorbent assay.

Imidoester crosslinking, which is used to couple the antibody to Protein A-agarose results in amidine bonds which are hydrolysable at high pH (13,19). Therefore, elution using high pH triethylamine may decrease the lifetime of the column. However, one column was re-used more than 20 times with no measurable decrease in column performance.

### 6.3.3.2. Immunoaffinity extraction of LSD from blood and urine.

LSD was extracted from buffer, urine and blood samples using a re-usable 1 mL affinity matrix column. The recovery of LSD from each sample was calculated using the radiolabelled tracer, [ $^3\text{H}_3$ ]-LSD. The recovery of 0.2 ng of LSD from 1.0 mL PBS using triethylamine and ethanol as eluents was not significantly different (78% and 81% respectively). However, elution profiles were much sharper when ethanol was used in place of triethylamine (Figure 6.8 a,b). When triethylamine was used, on average 70% of the total drug recovered was contained in two column volumes (SD=5%, n=8) and 84% was eluted in three column volumes (SD=5%, n=8). By comparison, ethanol eluted 83% of the total drug recovered in only one column volume (1 mL). Therefore, in the absence of radiolabelled species, ethanol was the superior eluent. Its use not only produces a more concentrated extract, but is also less likely to interfere with subsequent LSD analysis as it is readily removed by evaporation.

Both pH and ionic strength were shown to affect the recovery of LSD by immunoaffinity extraction. When 0.2 ng LSD was extracted from 1.0 mL urine in the absence of buffer (pH ~ 5) the recovery of drug was only 45%. When the pH of the sample was made neutral using PBS (150 mM) the recovery increased to 64%. However, when NaCl was omitted from the buffer and the ionic strength was lowered to 40 and 20 mM, the recoveries were 77 and 83% respectively (Table 6.6).

When 0.1 mL whole blood, containing 0.48 ng/mL LSD, was diluted in 50 mM phosphate buffer (pH 7), the recovery of drug was 88%. Elution profiles of LSD extracted from blood and urine using triethylamine as the eluent are shown in Figures 6.9 (a, b).

**Fig 6.8(a)** Immunoaffinity extraction of LSD (0.245 ng/mL) from PBS using ethanol as the eluent. Analytical recovery was 81% of which 83% of the total drug recovered was eluted in one column volume (1 mL).

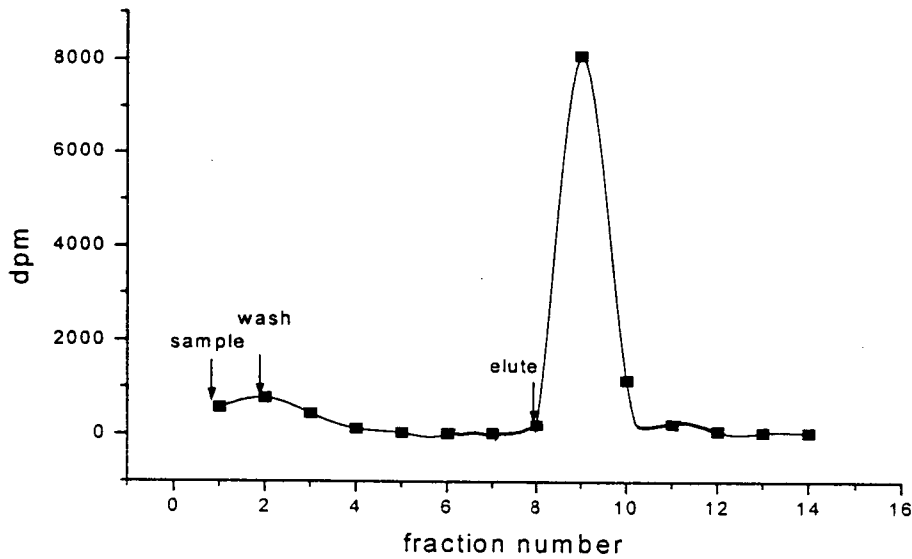


**Fig 6.8(b)** Immunoaffinity extraction of LSD (0.223 ng/mL) in PBS using 100 mM triethylamine as the eluent. Analytical recovery was 78% of which 88% of the total drug recovered was eluted in 3 column volumes (3 mL).

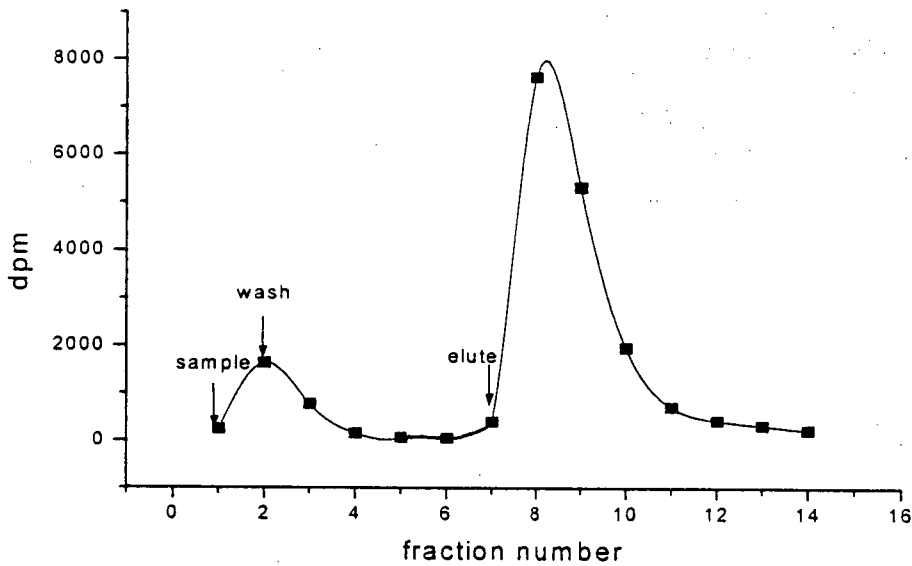


**Table 6.6.** Immunoaffinity extraction of LSD from blood, urine and buffer. Preliminary results show that extraction efficiencies greater than 80% are attainable in both blood and urine when low ionic strength buffer at neutral pH is used. Between 0.05 and 0.5 ng LSD was added to 1 mL affinity matrix in sample volumes between 0.1 and 1.0 mL.

sample	description	sample volume (mL)	total LSD in sample (ng)	total LSD recovered (ng)	recovery (%)
PBS	phosphate buffered saline 150 mM pH 7.4	1.0	0.223	0.174	78
urine, un-buffered	pH 5	1.0	0.222	0.100	45
urine, un-buffered	pH 5	1.0	0.471	0.265	56
urine, buffered	PBS	1.0	0.232	0.150	64
urine, buffered	PBS	1.0	0.470	0.290	62
urine, buffered	40 mM phosphate buffer, pH 7	1.0	0.223	0.172	77
urine, buffered	20 mM phosphate buffer, pH 7	1.0	0.230	0.191	83
whole blood, buffered	diluted in 50 mM phosphate buffer, pH 7	0.1	0.048	0.042	88

**Figure 6.9(a)** Immunoaffinity extraction of 48 pg total LSD in 0.1 mL whole blood. Blood was diluted to 1.0 mL in 50 mM phosphate buffer, pH 7. The total recovery of LSD was 88%.

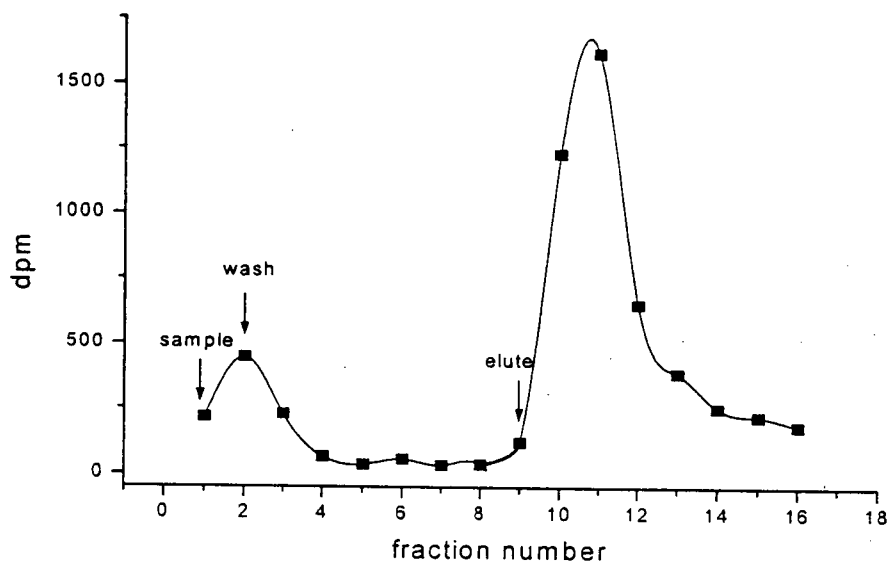
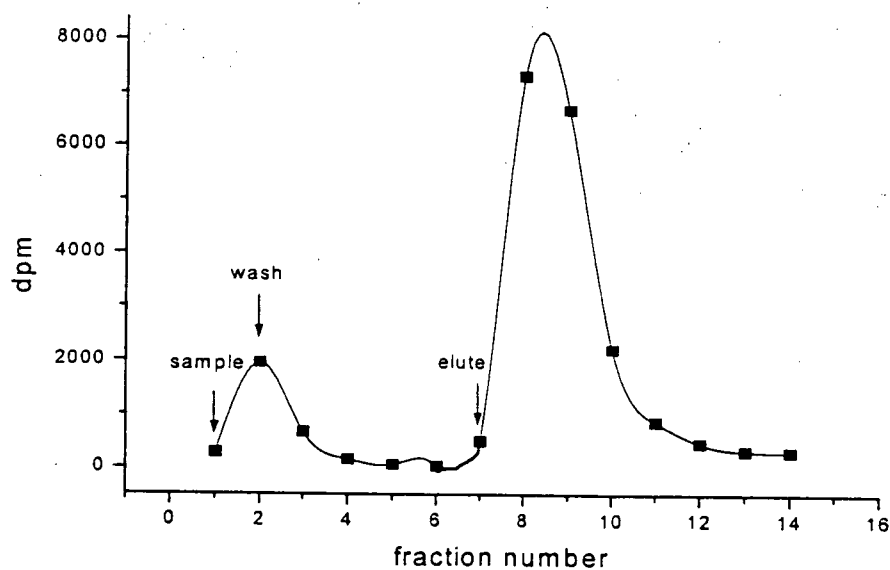


**Figure 6.9(b)** Immunoaffinity extraction of 0.22 ng LSD from 1 mL buffered urine (pH 7, 20 mM phosphate buffer). The total recovery of drug from urine was 83%.



The analytical recovery of LSD from blood and urine compares favourably with other methods recently described in the literature. Extraction efficiencies between 64 and 167% in urine are reported in one method in which the urine was mixed with the affinity matrix for half an hour prior to extraction (11). There are no known reports of immunoaffinity extraction of LSD from blood or other complex matrices in the literature to date. Preliminary results suggest that the extraction efficiency is affected by both pH and ionic strength of the matrix. When low ionic strength (50 mM or less) buffer at neutral pH was used in the present work, sub-ng quantities of LSD were successfully extracted from blood and urine with extraction efficiencies greater than 80%. None of the LSD added to the column was irreversibly bound. Studies using [ $^3\text{H}_3$ ]-LSD showed that  $99.1 \pm 6.7\%$  (SD,  $n = 8$ ) of the total drug added was recovered from the affinity matrix by washing and eluting procedures.

One advantage of this extraction method is its speed. Affinity isolation of LSD from blood and urine using this method was completed in about 10 minutes. This was due to the relatively high flow rate of approximately 1.5 mL / minute under gravity. Extraction of LSD from a complex biological matrix, such as blood is usually achieved by either liquid/liquid extraction with an organic solvent, or by solid phase extraction. The latter offers some improvement in terms of analyst time, but both methods are susceptible to coextractive interferences which can severely affect the results. Theoretically, immunoaffinity extraction should give superior results in terms of the specificity of the extract. The number of interferences in the sample are largely defined by the cross-reactivity of the antibody which is immobilized on the support. Substances other than the drug of interest and/or its metabolites, should pass through the column unretained. In this way, the final extract should be free of coextractives and chemical interferences.

The major disadvantage is the high cost of producing immunoaffinity media which are generally not re-usable. However, the affinity matrix described here was extremely robust. An assault of organic solvents, extreme pH (2 to 12), salts, chaotropic agents and detergents (Section 6.3.3.1) did not denature the antibody or decrease its capacity for LSD. The fact that the column is re-usable is a major advantage, given the relative cost of the affinity matrix relative to conventional chromatographic packing material used in solid phase extraction cartridges. One column, which was stored for 5 months at 4 °C, was used for more than 20 extractions with no decrease in column performance.

#### 6.4. Conclusion.

Preliminary data suggests that quantitative estimates of LSD in whole blood specimens can be determined by ELISA. The limit of detection was 39 pg/mL LSD, compared with 10 pg/mL in urine. This corresponds to less than 1 pg of total drug in a 25  $\mu$ L blood sample, which is required for analysis. Between run CVs for LSD spiked in blood at 1.25, 0.16 and 0.04 ng/mL were 5.6, 3.1 and 8.9% respectively (n = 4). An overall decrease in precision was observed when whole blood was used in place of urine due to the increased complexity of the matrix. However, the sensitivity of whole blood analysis compared favourably with the commercial STC ELISA (8).

The ELISA was also used to detect LSD in forensic case samples which included post-mortem blood, bile, liver and vitreous fluid. Using methanolic extracts, the concentrations of LSD and cross-reacting substances in blood, liver and bile were 0.24, 0.4 and 2.0 ng/mL respectively. This was in good agreement with RIA results obtained at the RCMP Central Forensic Laboratory in Ottawa which indicated 0.2 ng/mL LSD in the blood. No matrix effects were observed with either methanolic blood extracts or post-mortem urine analysis by ELISA.

The high affinity antibody to LSD was also used to extract drug from biological fluids. Antibody, which was covalently attached to Protein A-agarose, was used to selectively isolate LSD from blood and urine. No pre-treatment was required other than the addition of buffer to the sample, after which sub-nanogram quantities of LSD were extracted from blood and urine with greater than 80% efficiency. Immunoaffinity extraction offers an improvement over current liquid-liquid and solid phase extraction techniques in terms of analyst time and cleanliness of the extract. Preliminary evaluation indicates that the immunoaffinity isolation method could be used for the extraction of LSD from biological fluids, trace enrichment of samples which contain prohibitively low

concentrations of LSD, or drug metabolism studies.

### 6.5. References.

1. Fysh, R.R., Oon, M.C.H., Robinson, R.N., Smith, R.N., White, P.C., and Whitehouse, M.J. 1985. *Forens. Sci. Intl.* 28: 109-113.
2. Peel, H.W. and Boynton, A.L. 1980. *Can. Soc. Forens. Sci. J.* 13(3): 23-28.
3. McCarron, M.M., Walberg, C.B., and Baselt, R.C. 1990. *J. Anal. Toxicol.* 14: 165-167.
4. Twitchett, P.J., Fletcheer, S.M., Sullivan, A.T., and Moffat, A.C. 1978. *J. Chromatog.* 150: 73-84.
5. Ratcliffe, W.A., Fletcher, S.M., Moffat, A.C., Ratcliffe, J.G., Harland, W.A., and Levitt, T.E. 1977. *Clin. Chem.* 23(2): 169-174.
6. Perrigo, B.J. and Joynt, B.P. 1995. *Can. Soc. Forens. Sci. J.* 28(4): 261-269.
7. Champion, J.L. 1996. Society of forensic Toxicologists Annual Meeting, Denver, CO (Abstract).
8. Cassels, N.P., Craston, D.H., Hand, C.W., and Baldwin, D. 1996. *J. Anal. Toxicol.* 20: 409-415.
9. Francis, J.M. and Craston, D.H. 1996. *Analyst* 121: 177-182.
10. Cai, J. and Henion, J. 1996. *Anal. Chem.* 68: 72-78.
11. Webb, K.S., Baker, P.B., Cassels, N.P., Francis, J.M., Johnson, D.E., Lancaster, S.L., Minty, P.S., Reed, G.D., and White, S.A. 1996. *J. Forens. Sci.* 41(6): 938-946.
12. Rule, G.S. and Henion, J.D. 1992. *J. Chromatog.* 582: 103-112.
13. Hermanson, G.T., Mallia, A.K., and Smith, P.K. 1992. *Immobilized Affinity Ligand Techniques*, Academic Press, San Diego.
14. Smith, R.N. and Robinson, K. 1985. *Forens. Sci. Intl.* 28: 229-237.
15. Axelrod, J., Brady, R.O., Witkop, B., and Evarts, E.V. 1956. *Ann. NY. Acad. Sci.* 66: 435-444.
16. Siddik, Z.H., Barnes, R.D., Dring, L.G., Smith, R.L., and Williams, R.T. 1975. *Biochem. Soc. Trans.* 3(2): 290-292.
17. Siddik, Z.H., Barnes, R.D., Dring, L.G., Smith, R.L., and Williams, R.T. 1979. *Biochemical Pharmacology* 28: 3081-3091.
18. Lim, H.K., Andrenyak, D., Francom, P., and Foltz, R.L. 1988. *Anal. Chem.* 60: 1420-1425.

19. Mattson, G., Conklin, E., Desai, S., Nielander, G., Savage, M.D., and Morgensen, S. 1993. *Molecular Biology Reports* 17: 167-183.

## Chapter 7.

### Concluding Remarks and Further Study.

#### 7.1. Summary of findings.

A new lysergic acid diethylamide (LSD) immunogen was prepared, in which the drug was coupled to the carrier protein, keyhole limpet hemocyanin (KLH), using the heterobifunctional linker, sulfosuccinimidyl-2-(*p*-azidosalicylamido)ethyl-1,3'-dithiopropionate (SASD). A two-step conjugation procedure was used to covalently attach LSD to KLH using SASD, which has a spacer arm of approximately 19 Å. The amine reactive end of the linker was conjugated to lysine residues in KLH, after which the aryl azide group was photochemically coupled to LSD. Photochemically mediated linkage between the linker and the drug facilitates covalent attachment at a number of different sites on LSD, due to the high reactivity of the aryl nitrene which is produced. Presentation of LSD to the immune system depends on the site at which it is coupled to the carrier protein. Epitope recognition, which is sterically guided, should therefore take place at a number of different sites on the drug molecule. In this way, multi-site attachment facilitates epitope recognition, which should in theory, maximise antiserum sensitivity.

Using this approach, it was possible to attach an average of 35 molecules of LSD to each KLH molecule. The total efficiency of the reaction, estimated from the percent of lysine residues in KLH which were attached to LSD via SASD, was about 5%. Using this method, a favourable orientation of LSD on the carrier molecule is accompanied by a low coupling efficiency, which is typical for photoreactive conjugation methods (1).

An enzyme-linked immunosorbent assay (ELISA) was used to detect antibodies to LSD which were raised against the photochemically linked immunogen using rabbits. A heterologous assay system was employed, in which the chemical linkage between LSD and bovine serum albumin (BSA), which was used as the coating antigen, was different to that used in the immunogen.

Antibodies were characterized in terms of their affinity, dissociability, specificity and sensitivity towards LSD. A comparison of antibodies raised against the photochemically linked immunogen with other LSD antisera indicated the former to have the highest overall affinity. The equilibrium association constant,  $K_a$ , was determined to be  $1.3 \times 10^{10} \text{ M}^{-1}$  using radiochemical techniques. Chaotropic ion elution and ELISA detection were used to show that the increased strength of the antibody-antigen interaction using the photolinked antiserum, resulted in decreased dissociability relative to other antibody preparations which were tested. A statistical correlation was found between antibody affinity, dissociability and sensitivity using ELISA-based methods. Of the four polyclonal LSD antisera which were tested, which included two commercial preparations, the antiserum obtained using the photochemically linked immunogen ranked first. It is reported that the chemical modification of the target molecule during haptentation significantly influences the immune response at the T-cell level (2). Antibodies which were raised against immunogens which utilized the same chemical linkage had very similar characteristics relative to those which were prepared using different methods. These results support the suggestion that immunogen design plays a crucial role in predetermining the characteristics of the antiserum and its subsequent usefulness in an immunoassay (3,4).

Cross-reactivity studies, which were conducted using more than twenty structurally related analogs, provided some insight into the possible site of attachment of LSD in the immunogen. This

data indicated that LSD was probably attached to the carrier protein at positions N1 (indole nitrogen), C2 and N6, which is plausible, given the chemical nature of the electrophilic nitrene. A high cross-reactivity of the antibody with nor-LSD (52%), which is the major metabolite identified to date (5), is favourable for drug screening purposes. Other derivatives of interest which cross-react included lysergic acid methylpropylamide (34%) and 2-oxo-3-hydroxy-LSD (3%). Minimal cross-reactivity (0.05% or less) was observed with a number of other ergot alkaloids which could be present in a sample of illicit LSD eg. *iso*-LSD.

A low concentration of high affinity antibody was utilized in an ELISA to detect LSD in urine at concentrations typically encountered in forensic specimens. Evaluation of the UBC ELISA by comparison with the commercial ELISA from STC Diagnostics, indicated the former to be more sensitive and precise (6,7). The detection limit of the UBC ELISA was 10 pg/mL using 50  $\mu$ L urine. Analytical recoveries were reported in the range 98 - 106 % between 10 and 0.1 ng/mL LSD. Intra and inter-assay precision, estimated from the % CV of replicate measurements was 3.7 (n=4) and 6.7 (n=12) for a sample containing 0.2 ng/mL LSD in urine. The precision cut-off range, for which the intra-assay CV was < 5%, extended between 2 ng/mL and 10 pg/mL and the estimated upper and lower limits of quantitation of the assay were 7 ng/mL and 50 pg/mL respectively.

The feasibility of whole blood analysis by ELISA was demonstrated. The limit of detection was found to be 39 pg/mL when 25  $\mu$ L blood was used. The assay was also used to test for LSD in a number of complex biological matrices, including post-mortem specimens. LSD was detected in extracts of bile, liver and post-mortem blood using forensic case samples which were provided by the RCMP Forensic Laboratory in Vancouver. Quantitative estimates of LSD in post-mortem blood using the UBC ELISA were in good agreement with those obtained at the RCMP Central Forensic

Laboratory in Ottawa, using the Roche Abuscreen RIA (8).

The high affinity antibody was also used to extract LSD from biological fluids. An immunochromatographic support was prepared by covalently attaching anti-LSD to agarose beads. Analytical recoveries of greater than 80% were achieved using sub-ng/mL concentrations of LSD in blood and urine. Preliminary data suggested that the antibody used for immunoaffinity isolation of LSD from biological specimens in this study gave higher recoveries than a number of other reports (9-11). Theoretically, the immunoaffinity extraction (IAE) of LSD from biological matrices should give superior results in terms of the specificity of the extract, compared to conventional methods such as solid phase or liquid-liquid extraction procedures. The most cited disadvantage of IAE procedures is the high cost and limited lifetime of immunochromatographic media, which are usually not re-usable. The high affinity support described in this work was extremely robust; no drug was detected as being irreversibly bound to the beads and one column could be used more than twenty times without any detectable decrease in activity.

In summary, the new high affinity antibody was used for the detection and extraction of LSD from a number of biological matrices in the sub-ng/mL region of forensic interest. The unique characteristics of the antiserum, particularly its affinity for LSD, is believed to be the result of the approach to immunogen synthesis utilized, in which the drug molecules were attached to the carrier protein at a number of different sites.

## **7.2. Future work and applications.**

Immunochemical detection of LSD in a biological specimen necessitates the use of a highly sensitive antibody to reliably measure low concentrations of the drug that are frequently encountered.

Recent advances in analytical techniques, particularly mass spectrometry, have facilitated significant improvements in the detection of LSD, which has long remained an analytical challenge for drug detection agencies. Increasingly sophisticated techniques have been described, which allow picogram quantities of LSD to be detected using rigorous methods. Detection and quantification procedures have been described in the literature at concentrations which are below those of current screening techniques (12-14) and the detection of nor-LSD, in addition to the unmetabolized drug itself has also become common-place (5,15,16). Improvements in sensitivity now allow LSD and metabolites to be detected in unconventional samples, such as human hair (17). However, these advances in confirmatory detection techniques have not been paralleled by similar improvements in LSD screening technologies.

Although as many as three new immunoassays for LSD have become available in the last few months, none to date offer an improvement in sensitivity compared to existing radioimmunoassay procedures, which were first described over twenty years ago (18). Innovative approaches to immunochemical detection of LSD have taken place, such as CEDIA (Boehringer Mannheim, Concord, CA) (19) and OnLine (Roche Diagnostic Systems, Somerville, NJ) (20). However, these novel immunoassay methodologies have not enhanced the sensitivity of existing screening techniques.

The sensitivity of the aforementioned homogeneous immunoassays, which involve competitive antibody-antigen reactions, is largely dependent on the affinity of the antibody which is used. High affinity interactions can be of particular importance when the overall reaction time is short, as is the case for most homogeneous immunoassays, which are usually performed in a matter of minutes. The use of an antibody which is resistant to dissociation can improve the reproducibility

of the measurement and can reduce the non-specific binding. Significant improvements in immunochemical detection of LSD are likely to come about as a result of either enhanced detection techniques (21) or an improvement in the quality of the antibody. An appropriate use of the antibody raised against the photochemically linked immunogen would be in a competitive-type homogeneous immunoassay, where the benefits of high affinity and low dissociability would be realized to their full potential, to bring about an improvement in assay sensitivity.

The photochemical conjugation procedure has widespread application for the production of both polyclonal and monoclonal antibodies, due to the non-selective nature of the reaction. In theory, it could be used to couple any target molecule of interest to an immunogenic carrier protein. It is likely to be most useful for the detection of substances which are present at low concentrations, where multi-site attachment facilitates immune recognition (22) or for molecules which do not have reactive functional groups for effective haptentation. However, the full potential of the technique may not be realized unless higher titre responses are achieved.

The low titre immune response provided antibodies which, despite excellent quality, were present in prohibitively low concentrations from a commercial standpoint. This result was probably due to the very low hapten density of the immunogen, which was considerably lower than other LSD immunogens reported in the literature. Hapten densities for optimum immune response are reported to occur when the amount of LSD which is coupled to KLH is increased 7-fold (23). Such a large increase in the reaction efficiency is probably unattainable using the reagents described in this study. However, a number of approaches might be used to significantly improve the efficiency of the haptentation procedure and therefore maximise the potential of the technique.

Substitution of KLH with another carrier molecule which is richer in lysine residues would

provide an immediate advantage. For example, BSA, which has four times as many lysines per gram compared to KLH, would be a superior carrier in terms of reaction efficiency. In general, the attachment of more photoreactive linker arms to the carrier molecule should increase the hapten density. More importantly however, the use of a heterobifunctional linker which contains a polyfluorinated phenyl azide, is likely to offer a significant improvement in reaction efficiency (24,25). The recent introduction of these linkers has led to improved photochemical coupling efficiencies of between 20 - 80% (26,27). Therefore, the cumulative effect of changing the carrier molecule and the photoreactive crosslinker is likely to increase the yield of antibodies. Using this approach, it is more likely that larger quantities of high affinity antiserum would be produced, which would maximise the potential of the photochemical coupling technique.

### 7.3. References.

1. Thevenin, B.J.M., Shahrokh, Z., Williard, R.L., Fujimoto, E.K., Kang, J.J., Ikemoto, N., and Shoheit, S.B. 1992. *European Journal of Biochemistry* 206: 471-477.
2. Delmas, A., Brack, A., and Trudelle, Y. 1992. *Bioconjugate Chem.* 3: 80-84.
3. Adamczyk, M., Fishpaugh, J., Harrington, C., Hartter, D., Johnson, D., and Vanderbilt, A. 1993. *J. Immunol. Methods* 162: 47-58.
4. Adamczyk, M., Grote, J., Douglas, J., Dubler, R., and Harrington, C. 1997. *Bioconjugate Chem.* 8: 281-288.
5. Lim, H.K., Andrenyak, D., Francom, P., and Foltz, R.L. 1988. *Anal. Chem.* 60: 1420-1425.
6. Cassels, N.P., Craston, D.H., Hand, C.W., and Baldwin, D. 1996. *J. Anal. Toxicol.* 20: 409-415.
7. STC Diagnostics, Bethlehem, PA. 1995. STC LSD Micro-Plate EIA Kit, *package insert*.
8. Roche Diagnostic Systems, Somerville, NJ. Abuscren RIA for LSD, *specification sheet*.
9. Rule, G.S. and Henion, J.D. 1992. *J. Chromatog.* 582: 103-112.
10. Francis, J.M. and Craston, D.H. 1996. *Analyst* 121: 177-182.
11. Webb, K.S., Baker, P.B., Cassels, N.P., Francis, J.M., Johnson, D.E., Lancaster, S.L., Minty, P.S., Reed, G.D., and White, S.A. 1996. *J. Forens. Sci.* 41(6): 938-946.
12. Bukowski, N. and Eaton, A.N. 1993. *Rapid. Comm. Mass. Spectrom.* 7: 106-108.
13. Paul, B.D., Mitchel, J.M., Burbage, R., Moy, M., and Sroka, R. 1990. *J. Chromatog.* 529: 103-112.
14. Cai, J. and Henion, J. 1996. *Anal. Chem.* 68: 72-78.
15. Cai, J. and Henion, J. 1996. *J. Anal. Toxicol.* 20: 27-37.
16. Nelson, C.C. and Foltz, R.L. 1992. *Anal. Chem.* 64: 1578-1585.
17. Nakahara, Y., Kikura, R., Takahashi, K., Foltz, R.L., and Mieczkowski, T. 1996. *J. Anal. Toxicol.* 20: 323-329.
18. Taunton-Rigby, A., Sher, S.E., and Kelley, P.R. 1973. *Science* 181: 165-166.

19. Boehringer Mannheim Corp., Concord, CA. 1996. CEDIA DAU for LSD, *product brochure*.
20. Roche Diagnostic Systems, Somerville, NJ. 1996. Abuscreen OnLine for LSD, *specification sheet*.
21. Kricka, L.J. 1994. *Clin. Chem.* 40(3): 347-357.
22. Strahilevitz, M. 1986. *United States Patent, No. 4,620,977*
23. Malaitsev, V.V. and Azhipa, O.Y. 1993. *Bull. Exp. Biol. Med* 115(6): 726-728.
24. Keana, J.F.W. and Cai, S. 1990. *J. Org. Chem.* 55: 3640-3647.
25. Yan, M., Cai, S.X., Wybourne, M.N., and Keana, F.W. 1994. *Bioconjugate Chem.* 5: 151-157.
26. Kym, P.R., Carlson, K.E., and Katzenellenbogen, J.A. 1995. *Bioconjugate Chem.* 6: 115-122.
27. Pandurangi, R.S., Karra, S.R., Kuntz, R.R., and Volkert, W.A. 1995. *Bioconjugate Chem.* 6: 630-634.

## Appendix I.

### Reagent mixtures.

#### Bradford dye binding protein reagent.

Bradford dye binding reagent was prepared as follows (1). Coomassie Brilliant Blue G-250 (10 mg) was dissolved in 5 mL ethanol after which 10 mL phosphoric acid (85%) was added and the total volume made up to 100 mL with deionized water. The reagent was stored at 4 °C for up to 3 months prior to use.

#### Tetramethylbenzidine (TMB) substrate solution.

The TMB substrate solution (2) was prepared as follows. Deionized water (16 mL) was added to acetate/citrate buffer, pH 6 (4 mL). Immediately before use, 200 µL of 3,3',5,5'-tetramethylbenzidine in dimethyl sulfoxide (10 mg/mL) was added, followed by 20 µL hydrogen peroxide (3%). The acetate/citrate buffer was made by adding 200 mM citric acid to 200 mM sodium acetate to give a final pH of 6.0.

#### Van Urk reagent.

The Van Urk reagent (3) was prepared by mixing *p*-dimethylaminobenzaldehyde (0.5 g) with 5 mL concentrated hydrochloric acid and 50 mL ethanol. The reagent was stored for up to a month at -20 °C until required.

#### References.

1. Bradford, M.M. 1976. *Anal. Biochem.* 72: 248-254.
2. Bos, E.S., van der Doelen, A.A., van Rooy, N., and Schuur, A.H.W.M. 1981. *Journal of Immunoassay* 2: 187-204.
3. Look, J. 1967. *J. Pharm. Sci.* 56(11): 1526-1527.

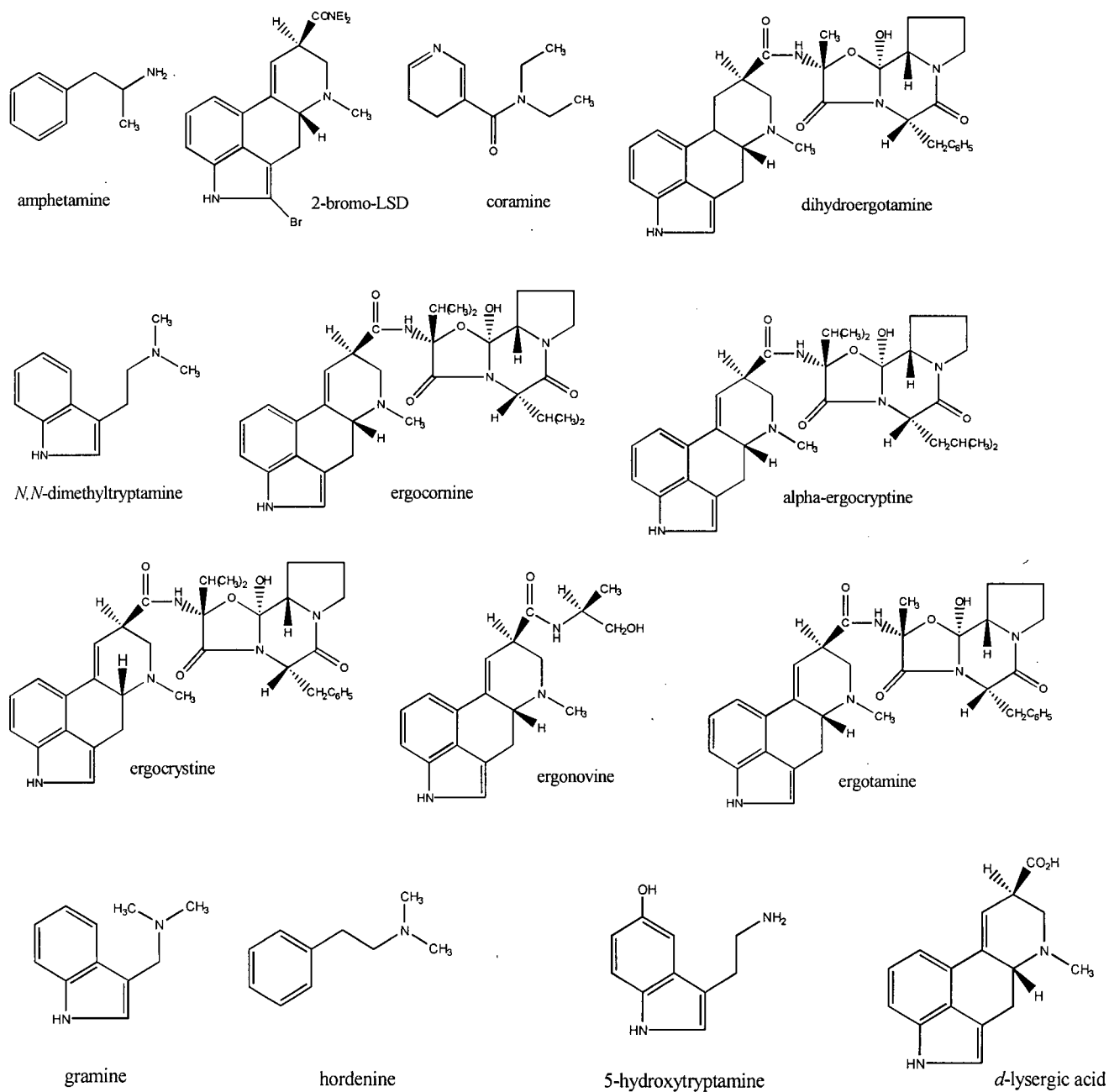
## Appendix II.

### Optimized competitive binding ELISA for LSD.

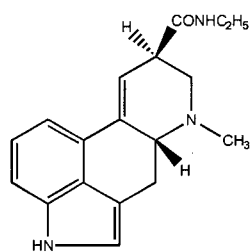
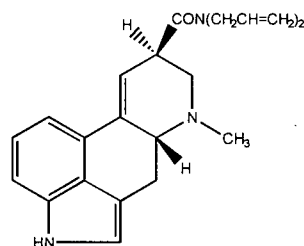
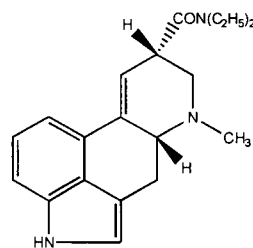
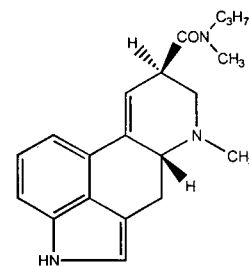
- 1.) Coat polystyrene plates overnight at 4 °C with 100 µL/well BSA-LSD (5 µg/mL) in 150 mM phosphate buffered saline, pH 7.4 (PBS).
- 2.) Coat microtitre plates with 175 µL/well of 5% Carnation non-fat dry skim milk powder in PBS (SM-PBS) for 30 minutes at 37 °C. Wash plates with PBS (250 µL/well) between steps 2 to 4 inclusive.
- 3.) Add 50 µL/well of test sample or LSD calibrator to microtitre plates. Add 50 µL/well of diluted rabbit serum in double strength SM-PBS (10% SM in PBS). The final dilution of immune rabbit serum after mixing with the sample should be 1:50. Incubate samples for 2.5 hours at 37 °C.
- 4.) Add 100 µL/well of goat anti-rabbit IgG peroxidase (1:1000) in SM-PBS. Incubate samples for 30 minutes at 37 °C.
- 5.) After the final plate wash, add 100 µL/well tetramethylbenzidine (TMB) substrate solution. After 5 minutes stop the colour reaction with 50 µL/well 1 M sulfuric acid. Read the absorbance at 450 nm using 620 nm as the reference.

## Appendix III.

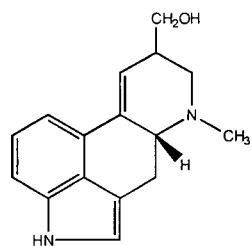
## Structures of compounds used in the cross-reactivity study.



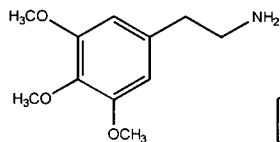
Appendix III: Structures of compounds used in the cross-reactivity study.

*d*-lysergic acid amide*d*-lysergic acid diallylamide*iso*-LSD

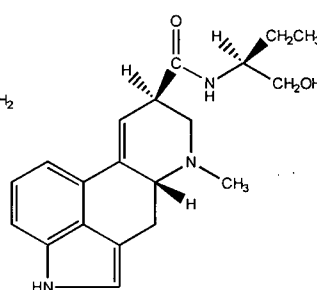
lysergic acid methylpropylamide



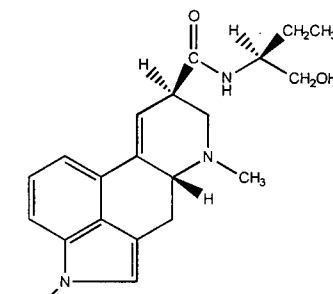
lysergol



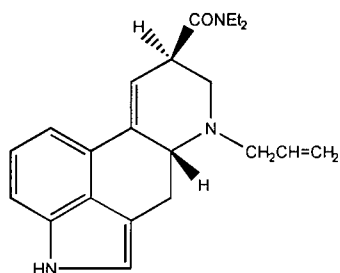
mescaline



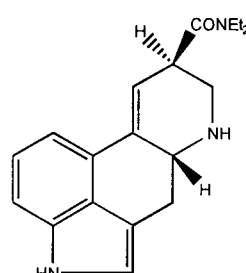
methylergonovine



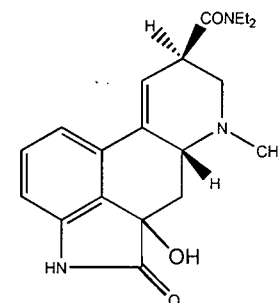
methysergide



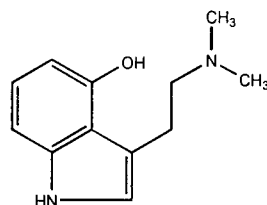
6-nor-6-allyl-LSD



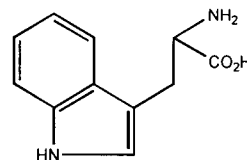
6-nor-LSD



2-oxo-3-hydroxy-LSD



psilocin



tryptophan